

University of Southampton Research Repository ePrints Soton

Copyright © and Moral Rights for this thesis are retained by the author and/or other copyright owners. A copy can be downloaded for personal non-commercial research or study, without prior permission or charge. This thesis cannot be reproduced or quoted extensively from without first obtaining permission in writing from the copyright holder/s. The content must not be changed in any way or sold commercially in any format or medium without the formal permission of the copyright holders.

When referring to this work, full bibliographic details including the author, title, awarding institution and date of the thesis must be given e.g.

AUTHOR (year of submission) "Full thesis title", University of Southampton, name of the University School or Department, PhD Thesis, pagination

University of Southampton

FACULTY OF NATURAL AND ENVIRONMENTAL
SCIENCES

Chemistry

**Some Novel Biological Applications of
Polymers Based on Poly(2-oxazoline)s**

By

Adam Lee Fisher

Thesis for the degree of Doctor of Philosophy

March 2015

This work is dedicated to my grandparents

Audrey, Bryan, Eileen and Fordham

If – Rudyard Kipling

If you can keep your head when all about you
Are losing theirs and blaming it on you,
If you can trust yourself when all men doubt you,
But make allowance for their doubting too;
If you can wait and not be tired by waiting,
Or being lied about, don't deal in lies,
Or being hated, don't give way to hating,
And yet don't look too good, nor talk too wise:

If you can dream—and not make dreams your master;
If you can think—and not make thoughts your aim;
If you can meet with Triumph and Disaster
And treat those two impostors just the same;
If you can bear to hear the truth you've spoken
Twisted by knaves to make a trap for fools,
Or watch the things you gave your life to, broken,
And stoop and build 'em up with worn-out tools:

If you can make one heap of all your winnings
And risk it on one turn of pitch-and-toss,
And lose, and start again at your beginnings
And never breathe a word about your loss;
If you can force your heart and nerve and sinew
To serve your turn long after they are gone,
And so hold on when there is nothing in you
Except the Will which says to them: 'Hold on!'

If you can talk with crowds and keep your virtue,
Or walk with Kings—nor lose the common touch,
If neither foes nor loving friends can hurt you,
If all men count with you, but none too much;
If you can fill the unforgiving minute
With sixty seconds' worth of distance run,
Yours is the Earth and everything that's in it,
And—which is more—you'll be a Man, my son!

UNIVERSITY OF SOUTHAMPTON

ABSTRACT

FACULTY OF NATURAL AND ENVIRONMENTAL SCIENCES

Chemistry

Doctor of Philosophy

SOME NOVEL BIOLOGICAL APPLICATIONS OF POLYMERS BASED ON POLY(2-
OXAZOLINE)S

By Adam Lee Fisher

Poly(2-oxazoline)s have attracted much attention in recent times due to their potential advantages over other similar polymers. They are easy to synthesise while maintaining control over length, polydispersity and functionality^{1, 2}. Furthermore the 2-methyl and 2-ethyl poly(2-oxazoline)s have both been shown to be 'stealth' biopolymers similar to that of poly(ethyleneglycol), (PEG)³ suitable for biological applications. Poly(2-isopropyl-2-oxazoline), poly(2-n-propyl-2-oxazoline) and poly(2-ethyl-2-oxazoline) have all been found to show thermoresponsive behaviour and are therefore potential alternatives to poly(N-isopropylacrylamide) (PNiPAAm)^{4, 5}.

We are interested in exploiting these properties of poly(2-oxazoline)s in novel applications particularly in the biological context.

We describe the synthesis and characterisation of poly(2-oxazoline) homo and co-polymers with particular attention paid to their cloud point temperature behaviour. We then developed a method to allow poly(2-oxazoline)s to be covalently attached to glass using a 'grafting-to' approach. We then successfully demonstrated their potential as cell selective surfaces.

Two different classes of thermogelling materials have also been synthesised, one based on a carboxymethylcellulose co-polymer and another poly(2-oxazoline) only co-polymer. Both of these materials have been characterised using rheology and their potential for tissue engineering applications has been demonstrated.

Finally the non-fouling properties of poly(2-methyl-2-oxazoline) coated surfaces has been explored. It has been shown that the non-fouling behaviour is dependent on the way in which bacteria are brought in contact with the surfaces.

Contents

| | |
|--|-------|
| Contents | viii |
| List of Figures | xiv |
| Declaration of Authorship..... | xviii |
| Acknowledgements..... | xx |
| Abbreviations..... | xxii |
| Chapter 1 Introduction | 1 |
| 1.1 Polymers | 1 |
| 1.1.1 History..... | 1 |
| 1.1.2 Polymer Nomenclature | 2 |
| 1.1.3 Polymer Architectures | 2 |
| 1.1.4 Polymer Morphology and Phase Behaviour | 5 |
| 1.1.5 Analytical Techniques | 6 |
| 1.2 Polymer Synthesis..... | 9 |
| 1.2.1 Synthesising a Polymer | 9 |
| 1.2.2 Step Growth Polymerisation | 10 |
| 1.2.3 Chain Growth Polymerisation | 11 |
| 1.3 Pseudo-Peptidic Polymers | 14 |
| 1.3.1 Overview | 14 |
| 1.3.2 Poly(acrylamide)s..... | 14 |
| 1.3.3 Poly(peptoid)s | 15 |
| 1.3.4 Poly(2-oxazoline)s | 16 |
| 1.4 Aim | 25 |
| Chapter 2 Synthesis and Cloud Point Temperature Control..... | 27 |
| 2.1 Introduction | 27 |
| 2.2 Monomer Synthesis | 28 |
| 2.2.1 Witte-Seeliger Synthesis of 2-Oxazolines | 28 |
| 2.2.2 Multi-step Route to Functionalised 2-Oxazolines..... | 29 |
| 2.3 Poly(2-oxazoline) Synthesis..... | 30 |
| 2.3.1 Polymer Synthesis | 30 |
| 2.3.2 Poly(2-isopropyl-2-oxazoline) | 31 |
| 2.3.3 Poly(2-isopropyl-2-oxazoline)-co-(2-butyl-2-oxazoline) | 32 |
| 2.3.4 Poly(2-isopropyl-2-oxazoline)-co-(5-(2-oxazoline)pentan-1-amine) | 33 |
| 2.3.5 End-Group Functionalization | 35 |
| 2.3.6 Summary | 37 |

| | | |
|-----------|--|----|
| 2.4 | Cloud Point Temperature Control..... | 37 |
| 2.4.1 | Introduction | 37 |
| 2.4.2 | Cloud Point Temperature Determination | 37 |
| 2.4.3 | Comparison of Methods | 41 |
| 2.4.4 | Effect of M_n | 41 |
| 2.4.5 | Effect of Media and Concentration..... | 42 |
| 2.4.6 | Co-polymerisation..... | 44 |
| 2.4.7 | Summary | 45 |
| 2.5 | Conclusions | 45 |
| Chapter 3 | Cell Selective Surfaces..... | 47 |
| 3.1 | Introduction | 47 |
| 3.1.1 | Polymer Surfaces..... | 47 |
| 3.1.2 | Thermoresponsive Surfaces..... | 47 |
| 3.1.3 | Cell Selective Surfaces..... | 49 |
| 3.2 | First Generation Cell Selective Surfaces | 49 |
| 3.2.1 | Overview | 49 |
| 3.2.2 | Method..... | 50 |
| 3.2.3 | Synthesis | 50 |
| 3.3 | Characterisation Techniques | 51 |
| 3.3.1 | Contact Angles | 51 |
| 3.3.2 | X-ray Photoelectron Spectroscopy | 52 |
| 3.4 | Cell Behaviour | 56 |
| 3.4.1 | Overview | 56 |
| 3.4.2 | Adhesion | 57 |
| 3.4.3 | 5 Day Growth and Staining | 58 |
| 3.4.4 | Cell Proliferation | 61 |
| 3.4.5 | Cell Motility | 62 |
| 3.4.6 | Co-cultures | 63 |
| 3.4.7 | Summary | 64 |
| 3.5 | Novel Second Generation Poly(2-oxazoline) Surfaces..... | 65 |
| 3.5.1 | Overview | 65 |
| 3.5.2 | Method..... | 65 |
| 3.5.3 | Aminolysis | 66 |
| 3.5.4 | Adamantane and β -Cyclodextrin Initiated Polymers..... | 70 |
| 3.5.5 | Summary | 74 |
| 3.6 | Conclusion..... | 74 |

| | | |
|-----------|---|-----|
| Chapter 4 | Antifouling Surfaces | 75 |
| 4.1 | Introduction | 75 |
| 4.2 | Synthesis | 75 |
| 4.3 | Surface Performance | 76 |
| 4.3.1 | Passive Antifouling Performance | 76 |
| 4.3.2 | Coating Performance after Ultrasound..... | 78 |
| 4.4 | Conclusion..... | 78 |
| Chapter 5 | Bacterial Capture Device | 79 |
| 5.1 | Introduction | 79 |
| 5.2 | Synthesis | 79 |
| 5.3 | Antibody Immobilisation and Performance..... | 80 |
| 5.4 | Capturing Bacteria | 84 |
| 5.5 | Conclusion..... | 85 |
| Chapter 6 | Thermogelling Poly(2-oxazoline)s | 87 |
| 6.1 | Overview | 87 |
| 6.2 | Applications of Thermoresponsive Polymers | 87 |
| 6.2.1 | Overview | 87 |
| 6.2.2 | Designing a Thermogelling Polymer | 87 |
| 6.2.3 | PNiPAAm Based Thermogels..... | 89 |
| 6.3 | First Generation Thermogelling Brush Polymers | 90 |
| 6.3.1 | Overview | 90 |
| 6.3.2 | Synthesis of Poly(2-oxazoline) Brush Polymers | 90 |
| 6.3.3 | Synthesis of Thermogelling Polymers | 91 |
| 6.3.4 | Molecular Weight Determination | 92 |
| 6.4 | Gelation Properties | 92 |
| 6.4.1 | Rheological Characterisation | 92 |
| 6.4.2 | Visual Confirmation..... | 93 |
| 6.4.3 | Thermoreversible Gelation | 93 |
| 6.4.4 | Tuning Gelation Temperature a Biologically Useful Temperature | 94 |
| 6.4.5 | Influence of Concentration on the Gelation Temperature | 96 |
| 6.4.6 | Stability | 98 |
| 6.5 | Application in Tissue Engineering | 99 |
| 6.5.1 | Overview | 99 |
| 6.5.2 | Modelling Tissue | 99 |
| 6.5.3 | Toxicity | 100 |
| 6.5.4 | Creating Tissue Models | 101 |

| | | |
|-----------|--|-----|
| 6.5.5 | Summary | 103 |
| 6.6 | Second Generation Triblock Poly(2-oxazoline) Thermogels | 103 |
| 6.6.1 | Overview | 103 |
| 6.6.2 | Proof of Principle | 104 |
| 6.6.3 | Development of Novel Thermogelling Poly(2-oxazoline)s..... | 105 |
| 6.6.4 | Visual Confirmation of Gelation..... | 108 |
| 6.7 | Gelation Properties | 108 |
| 6.7.1 | Reversible Gelation | 108 |
| 6.7.2 | Effect of Concentration..... | 109 |
| 6.7.3 | Influence of <i>PnBuOx</i> | 110 |
| 6.7.4 | Influence of the Relative Lengths of the A and B Blocks..... | 112 |
| 6.7.5 | Summary | 113 |
| 6.8 | Conclusion..... | 113 |
| Chapter 7 | Summary of Work | 115 |
| Chapter 8 | Future Work | 117 |
| Chapter 9 | Experimental Details | 119 |
| 9.1 | General Experimental Details | 119 |
| 9.1.1 | Lab book..... | 119 |
| 9.1.2 | Materials | 119 |
| 9.1.3 | Equipment..... | 119 |
| 9.1.4 | Cell methods | 120 |
| 9.2 | Synthesis and Cloud Point Control..... | 122 |
| 9.2.1 | Generic 2-alkyl-2-oxazoline Procedure | 122 |
| 9.2.2 | 2-BOC-2-Oxazoline Synthesis | 125 |
| 9.2.3 | 2-3-(Butenyl)-2-oxazoline | 128 |
| 9.2.4 | Generic Polymerisation Method | 129 |
| 9.2.5 | Poly(2-isopropyl-2-oxazoline) Lengths..... | 130 |
| 9.2.6 | Poly(2-isopropyl-2-oxazoline)-co-(2-butyl-2-oxazoline) | 131 |
| 9.2.7 | Poly(2-isopropyl-2-oxazoline)-co-(2-pentan-1-amine-2-oxazoline)..... | 132 |
| 9.3 | Cell Selective Surfaces..... | 133 |
| 9.3.1 | Generic method for (3-aminopropyl)triethoxysilane Coated Slides | 133 |
| 9.3.2 | Generic Methods for Poly(2-alkyl-2-oxazoline) Glass Coverslip Attachment | 133 |
| 9.3.3 | Aminolysis of Polycaprolactone (PCL) | 136 |
| 9.3.4 | Aminolysis of Polyethylene terephthalate (PET) | 136 |
| 9.3.5 | Carboxymethyl- β -cyclodextrin-Functionalization of Amine Surfaces..... | 136 |
| 9.3.6 | Adamantane-Functionalization of Amine Surface | 137 |

| | | |
|------------|---|-----|
| 9.3.7 | Synthesis of β -cyclodextrin Initiated Polymers..... | 138 |
| 9.3.8 | 2-(1-Adamantyl)ethyl p-toluenesulfonate initiator | 142 |
| 9.4 | Antifouling Surfaces | 144 |
| 9.4.1 | PMeOx-Silane Terminated Polymers | 144 |
| 9.4.2 | Surface Functionalization of PMeOx..... | 144 |
| 9.5 | Bacterial Capture Device..... | 145 |
| 9.5.1 | Amine Surface Synthesis | 145 |
| 9.5.2 | Chitosan Surface Synthesis | 145 |
| 9.5.3 | Carboxylated PEG Surface Synthesis..... | 145 |
| 9.5.4 | Carboxymethylcellulose Surface Synthesis..... | 145 |
| 9.5.5 | Glutaraldehyde Surface Synthesis | 146 |
| 9.5.6 | Antibody Functionalization | 146 |
| 9.5.7 | PEG Surfaces of Different Carboxylated PEG | 146 |
| 9.5.8 | Glutaraldehyde Modification of PEG Surface Attachment | 148 |
| 9.6 | Thermogelling Polymers | 149 |
| 9.6.1 | Thermoresponsive Polymer Arms..... | 149 |
| 9.6.2 | Thermogelling Polymers | 153 |
| 9.6.3 | Cell Work..... | 157 |
| 9.7 | Second Generation BAB Triblock Copolymers | 158 |
| 9.7.1 | Proof of Principle Polymers..... | 158 |
| 9.7.2 | Thermogelling BAB Triblock polymers | 160 |
| Chapter 10 | List of References..... | 167 |

List of Figures

| | |
|---|----|
| Figure 1: An example of linear, branched and network morphologies | 2 |
| Figure 2: Types of co-polymer structures | 4 |
| Figure 3: Typical features of a DSC trace | 7 |
| Figure 4: Typical TGA trace showing two areas of weight loss | 8 |
| Figure 5: Step growth polymerisation | 10 |
| Figure 6: Chain growth polymerisation..... | 11 |
| Figure 7: Poly(peptoid)s, Poly(acrylamide)s and Poly(2-oxazoline)s | 14 |
| Figure 8: Different acrylamide structures..... | 14 |
| Figure 9: Polymerisation of <i>N</i> -isopropylacrylamide..... | 15 |
| Figure 10: α , β and γ poly(peptoid)s | 16 |
| Figure 11: Number of patents including the word poly(2-oxazoline) since they were first reported | 16 |
| Figure 12: Dependence of the propagation rate constant on the side chain structure of 2-oxazolines..... | 18 |
| Figure 13: Poly(2-methyl-2-oxazoline) | 19 |
| Figure 14: Poly(2-ethyl-2-oxazoline) | 20 |
| Figure 15: Poly(2-isopropyl-2-oxazoline) | 22 |
| Figure 16: Binodal phase diagram demonstrating the determination of the LCST from a range of T_{cp} | 22 |
| Figure 17: Typical turbidimetry measurement of a thermoresponsive polymer. | 22 |
| Figure 18: Comparison of co-polymer T_{cp} found in literature ^{130, 132-135} | 24 |
| Figure 19: Structure comparison of PiPrOx and PNiPAAm | 24 |
| Figure 20: Strategies to introduce functionality into poly(2-oxazoline)s ¹³⁹ | 27 |
| Figure 21: Structure of a PiPrOx- <i>n</i> BuOx co-polymer | 32 |
| Figure 22: Representative NMR of PiPrOx- <i>n</i> BuOx. | 33 |
| Figure 23: Structure of a PiPrOx-BOC co-polymer | 33 |
| Figure 24: NMR of PiPrOx-NH ₂ -1. | 34 |
| Figure 25: NMR of PiPrOx-BOC-1 (red) and PiPrOx-NH ₂ -1 (blue) illustrating the loss of the BOC group..... | 34 |
| Figure 26: Different <i>p</i> -toluenesulphonate initiators used | 35 |
| Figure 27: Attempted synthesis of a BOC-protected amine initiator | 36 |
| Figure 28: Structures of different terminated PiPrOx..... | 37 |
| Figure 29: Set-up for measuring the cloud point temperature using a UV-Vis spectrometer | 38 |
| Figure 30: The change in transmission of PiPrOx-1 as it is heated | 38 |
| Figure 31: Fluorescence of rhodamine B and PiPrOx-2 as the samples are heated | 39 |
| Figure 32: Structure of Dansic acid | 40 |
| Figure 33: Fluorescence of dansic acid in solution with a thermoresponsive polymer..... | 40 |
| Figure 34: Temperature dependent fluorescence of 4mg ml ⁻¹ solutions of PiPrOx with different Mn..... | 41 |
| Figure 35: Comparison of the two T_{cp} determination methods..... | 42 |
| Figure 36: Effect of concentration on T_{cp} in two different solutions | 43 |
| Figure 37: T_{cp} dependence using either the same weight or concentration | 43 |
| Figure 38: T_{cp} dependence on hydrophobic butyl monomer percentage | 44 |
| Figure 39: T_{cp} change upon BOC-deprotection of PiPrOx-BOC-1 | 45 |
| Figure 40: Illustration of cell release via different methods..... | 47 |
| Figure 41: Contact angles for different coated glass slides | 51 |

| | |
|--|----|
| Figure 42: Contact angle variation for different batches of coated glass slides..... | 52 |
| Figure 43: Deconvoluted XPS spectra for PiPrOx coated surfaces | 53 |
| Figure 44: Assignment of PEtOx deconvoluted carbon XPS | 54 |
| Figure 45: Comparison of predicted vs calculated bond ratios from the carbon XPS | 55 |
| Figure 46: Simplified illustration of the cellular structure lining the air-liquid interface of a lung .. | 57 |
| Figure 47: Cell adhesion assays after 60 minutes | 57 |
| Figure 48: 16HBE cells stained after growing on different poly(2-oxazoline) surfaces | 59 |
| Figure 49: 16HBE cell area per cell on different poly(2-oxazoline) surfaces | 60 |
| Figure 50: Staining of MRC5 cells on different poly(2-oxazoline) surfaces | 60 |
| Figure 51: 16HBE proliferation on different polymer surfaces..... | 61 |
| Figure 52: MRC5 proliferation on different polymer surfaces..... | 62 |
| Figure 53: Cell motility on different poly(2-oxazoline) surfaces..... | 62 |
| Figure 54: Co-cultures on different poly(2-oxazoline) surfaces..... | 63 |
| Figure 55: Co-cultures after washing on different poly(2-oxazoline) surfaces..... | 64 |
| Figure 56: Co-culture with wash total cell number | 64 |
| Figure 57: Illustration of a transwell in use..... | 65 |
| Figure 58: Illustration of the two different adamantane/cyclodextrin coating methods..... | 66 |
| Figure 59: Aminolysis of poly(caprolactone) sheets using diaminopropane | 67 |
| Figure 60: Thickness profile of PCL coatings on Perspex slides before and after aminolysis | 68 |
| Figure 61: Aminolysis of a transwell insert | 68 |
| Figure 62: Degradation of PET transwell membranes over time characterised using SEM | 69 |
| Figure 63: Monitoring degradation of transwell inserts over time | 70 |
| Figure 64: Percentage of bound sites on functionalised PCL coatings | 73 |
| Figure 65: Number of poly(2-oxazoline)s per nm ⁻² at different time points | 73 |
| Figure 66: Bacterial concentration using an acoustic device | 75 |
| Figure 67: NMR spectrum showing PMeOx NMR resonances and the initiator CH ₃ resonance. | 76 |
| Figure 68: Bacterial adhesion from passive interaction with different coatings of the reflector after rinsing with different flow rates..... | 77 |
| Figure 69: Bacterial adhesion from passive interaction with different surfaces | 77 |
| Figure 70: Percentage of bacteria attached to different surfaces after introduction of ultrasound and after rinsing with several flow rates | 78 |
| Figure 71: Bacteria capturing device | 79 |
| Figure 72: Test of carboxylic acid surface using fluoresceinamine..... | 81 |
| Figure 73: Quantification of antibody compared to different functionalization methods..... | 81 |
| Figure 74: Comparison of the amount of antibody added to PEG surfaces with different amounts of carboxylic acid functionalised PEG content..... | 83 |
| Figure 75: Activity of antibodies attached to PEG surfaces with different numbers of available carboxylic acid sites | 83 |
| Figure 76: Assessing antibody activity using a sandwich assay | 84 |
| Figure 77: Number of bacteria coating antibody and control surfaces | 84 |
| Figure 78: Thermoreversible gelation of a 4% by weight solution of TG-I-A..... | 93 |
| Figure 79: Heating - cooling cycle for TG-33-A | 94 |
| Figure 80: Thermogelling behaviour of TG-I-A to TG-I-C | 95 |
| Figure 81: Thermogelation of TG-I-A, TG-27.5-A and TG-35-A..... | 96 |
| Figure 82: Relationship between gelation temperature and thermogel concentration | 97 |
| Figure 83: Complex viscosity of TG-33-A at different concentrations..... | 98 |
| Figure 84: Time dependent degradation of TG-33-A at two pH | 98 |

| | |
|--|-----|
| Figure 85: Graphic of the different methods of co-culturing cells currently used | 100 |
| Figure 86: Method of co-culture using a thermogel..... | 100 |
| Figure 87: Toxicity of poly(2-oxazoline) thermogel over time..... | 101 |
| Figure 88: Fluorescent microscopy of co-cultures..... | 102 |
| Figure 89: Confocal microscope image of co-cultured cell sheet..... | 102 |
| Figure 90: Thermothickening behaviour of $PnPrOx_{12}$ - $PMeOx_{109}$ - $PnPrOx_{12}$ and $PnPrOx_{14}$ - $PEtOx_{125}$ - $PnPrOx_{14}$ | 105 |
| Figure 91: BAB triblock copolymers with a butane core..... | 106 |
| Figure 92: Different co-polymers observed in the SEC trace for $PiPrOx_{61}/PnBuOx_{4.5}PMeOx_{62}PiPrOx_{61}/PnBuOx_{4.5}$ | 107 |
| Figure 93: Visual confirmation of thermogelation of $PnPrOx_{62}$ - $PMeOx_{64}$ - $PnPrOx_{62}$ | 108 |
| Figure 94: Heating and cooling cycle for $PnPrOx_{66}$ - $PMeOx_{82}$ - $PnPrOx_{66}$ | 108 |
| Figure 95: Dependence of the complex modulus at 37°C and onset of viscosity of $PnPrOx_{62}$ - $PMeOx_{64}$ - $PnPrOx_{62}$ | 109 |
| Figure 96: The dependence of the onset of the viscosity increase against the length of $PMeOx$ and the percentage of the $nBuOx$ included in the thermoresponsive B blocks | 110 |
| Figure 97: Influence of the length of the $PMeOx$ block and the percentage of $nBuOx$ in the thermoresponsive block on the complex viscosity at 37°C | 111 |
| Figure 98: Dependence of the onset of viscosity on the length of the A and B blocks | 112 |
| Figure 99: Dependence of the complex modulus on the length of the B and A blocks | 113 |

Declaration of Authorship

I, Adam Fisher declare that this thesis and the work presented in it are my own and has been generated by me as the result of my own original research.

Some Novel Biological Applications of Polymers Based on Poly(2-oxazoline)s

I confirm that:

1. This work was done wholly or mainly while in candidature for a research degree at this University;
2. Where any part of this thesis has previously been submitted for a degree or any other qualification at this University or any other institution, this has been clearly stated;
3. Where I have consulted the published work of others, this is always clearly attributed;
4. Where I have quoted from the work of others, the source is always given. With the exception of such quotations, this thesis is entirely my own work;
5. I have acknowledged all main sources of help;
6. Where the thesis is based on work done by myself jointly with others, I have made clear exactly what was done by others and what I have contributed myself;
7. None of this work has been published before submission

Signed:

Date:

Acknowledgements

Although acknowledgements usually begin with thanking colleagues and support staff I would like to begin by thanking my family. Their support has truly been invaluable not only during my PhD but throughout university. Words cannot express my gratitude and appreciation to them for all their help and support. Thank you Mum, Dad and Vicky.

A huge thank you must go to members of the Grossel group, past and present. Dom, Nick, Darren, Gareth, Richard, Andrew, Hassan, Francesco and Alya. All of them provided some form of help at one point or another. I'd like to thank Neil Wells for helping with my NMR issues. All the guys from stores and my friends and colleagues from other groups in the department which made my PhD so enjoyable.

I would also like to thank my collaborators, whom without their kind help and expertise I would not have had such a productive project.

Professor Dirk Aarts and Julia Schollick from Oxford University who helped characterising the gels, I will never forget sitting for hours in a hot cramped soundproof box.

At Southampton general hospital, Professor Donna Davies, Dr Angela Tait, Dr Emily Swindle and the rest of the Brooke laboratory provided immense help and support with the cell work. Angela requires a special mention for not only her hard work and help in training me to work with cells, but also for teaching me the importance of talking to them.

From the Engineering department Professor Martyn Hill, Dr Peter Glynne-Jones and Dr Dario Carugo also offered huge help with the bacterial devices. Our collaboration between them, ourselves and the hospital proved to be very fruitful.

From the University of Ghent I would like to thank Professor Richard Hoogenboom and Bart Verbraeken for their assistance and patience and for allowing me to play around in their lab and develop the second generation thermogels.

I would also like to thank my co-supervisor Jeremy Frey for his help and support throughout my PhD. The PNP work will get finished one day.

Finally my heartfelt thanks to Dr Martin Grossel for his advice and support. Martin allowed and encouraged me to develop my ideas and projects without any restrictions which is one of the reasons I believe we had such a successful project. His support in allowing myself and the group to go to conferences abroad and in the UK was also very much appreciated. Thank you for the opportunity and confidence you showed in me.

Abbreviations

| | |
|----------------------|---|
| 16HBE | Human bronchial epithelial cells |
| ABC | Accelerated blood clearance |
| ACN | Acetonitrile |
| ACS | American Chemical Society |
| ATRP | Atom transfer radical polymerisation |
| BOC | tert-butyloxycarbonyl |
| BOCOx | tert-butyl (5-(2-oxazoline)pentyl)carbamate |
| CMC | Carboxymethylcellulose |
| CROP | Cationic ring opening polymerisation |
| CRP | Controlled radical polymerisation |
| CRU | Constitutional repeat unit |
| DCC | <i>N,N'</i> -dicyclohexylcarbodiimide |
| DCM | Dichloromethane |
| DE | Degenerative exchange |
| DLS | Dynamic light scattering |
| D _p | Degree of polymerisation |
| DSC | Differential scanning calorimetry |
| ECM | Extracellular matrix |
| EDA | Ethylenediamine |
| EDAC | 1-ethyl-3-(3-dimethylaminopropyl)carbodiimide |
| EDTA | Ethylenediaminetetraacetic acid |
| EtOx | 2-ethyl-2-oxazoline |
| G _T | Gelation temperature |
| <i>i</i> PrOx | 2-isopropyl-2-oxazoline |
| IR | Infra-red spectroscopy |
| IUPAC | International Union of Pure and Applied Chemistry |
| <i>k_p</i> | Propagation rate constant |

| | |
|------------------|---|
| LCST | Lower critical solution temperature |
| Maldi-TOF | Matrix-assisted laser desorption/ionisation time-of-flight |
| MeOx | 2-methyl-2-oxazoline |
| M_n | Number average molecular weight |
| MRC5 | Human foetal lung fibroblast cells |
| M_w | Weight average molecular weight |
| <i>n</i> BuOx | 2- <i>n</i> -butyl-2-oxazoline |
| NCA | <i>N</i> -carboxyanhydride |
| NHS | <i>N</i> -hydroxysuccinimide |
| NMR | Nuclear magnetic resonance spectroscopy |
| NonOx | 2-nonyl-2-oxazoline |
| <i>n</i> PrOx | 2- <i>n</i> -propyl-2-oxazoline |
| PBS | Phosphate buffered saline |
| PCL | Poly(caprolactone) |
| PcPrOx | Poly(2-cyclopropyl-2-oxazoline) |
| PDI | Polydispersity Index |
| PEG | Poly(ethylene glycol) |
| PET | Poly(ethylene terephthalate) |
| PEtOx | Poly(2-ethyl-2-oxazoline) |
| PiPrOx | Poly(2-isopropyl-2-oxazoline) |
| PLL | Poly(L-lysine) |
| PMeOx | Poly(2-methyl-2-oxazoline) |
| P <i>n</i> BuOx | Poly(2- <i>n</i> -butyl-2-oxazoline) |
| P <i>Ni</i> PAAm | Poly(<i>N</i> -isopropyl-acrylamide) |
| P <i>n</i> PrOx | Poly(2- <i>n</i> -propyl-2-oxazoline) |
| PRE | Persistent radical effect |
| PZT | Piezoelectric transducer |
| RAFT | Reversible addition-fragmentation chain transfer polymerization |
| RP | Radical polymerisation |

| | |
|----------|--------------------------------------|
| RT | Retention time |
| SEC | Size exclusion chromatography |
| SEM | Scanning electron microscopy |
| T_{cp} | Cloud point temperature |
| TCPS | Tissue culture poly(styrene) |
| TFA | Trifluoroacetic acid |
| TGA | Thermogravimetric analysis |
| THF | Tetrahydrofuran |
| US | Ultrasound |
| UV-Vis | Ultraviolet and visible spectrometer |
| X | Persistent radical species |
| XPS | X-ray photoelectron spectroscopy |

Chapter 1 Introduction

1.1 Polymers

1.1.1 History

Many books will explain that the word polymer is derived from the Greek words 'poly' meaning many and 'meros' meaning parts. They then infer that the word polymer was coined to describe giant molecules of interconnecting monomer units. Historically however, this was not the case. The word polymer was originally used to describe compounds which had the same empirical formulae but different physical properties, for example benzene (C_6H_6 , empirical formula CH) and acetylene (C_2H_2 , empirical formula also CH). This means that up until the 1920's text books referring to polymers do not actually mean the modern day equivalent. In the 1920's Herman Staudinger⁶ used the word macromolecule (also from Greek) meaning literally, 'large molecule', though a macromolecule does not necessarily have to contain repeating structural units, generally it does. As with many concepts in chemistry it was initially received with some scepticism⁶. One chemist declared that it was like zoologists being told that "somewhere in Africa an elephant was found who was 1500 feet long and 300 feet high". By the 1930's Staudinger and others had accumulated much evidence in favour of the macromolecular hypothesis. In particular Wallace Carothers of the Du Pont Company who set out to prepare polymers of definite structure through the use of established organic reactions. He succeeded and by the end of the work had not only demonstrated the relationship between structure and properties but had also invented several materials of commercial importance, such as neoprene rubber and the nylons.⁷ During the following 20 years work on polymers increased enormously. This included the publication of the first journals devoted solely to polymer studies and the basic principles of polymer science being established. The work of Paul Flory was prominent during this period and he was awarded the Nobel Prize for Chemistry in 1974. Staudinger had also won this award in 1953⁸.

Nowadays industrial polymer production is big business with around 100 million tonnes of synthetic polymers being produced yearly, the largest contributor being America. From the early 70's to the late 90's polymer production in America trebled. However the variation of polymers produced has not increased by the same amount, with a similar proportion of the different types of polymers produced today as there was 30 years ago. This is a reflection of the cost of introducing and producing a new polymer, estimated to be around 3-5 billion US dollars. Recently there has been more interest in producing polymer blends of existing polymers as opposed to building new plants and developing manufacturing processes for new polymers⁹.

1.1.2 Polymer Nomenclature

A *polymer* is a macromolecule consisting of a *chain* of smaller molecules joined together with bonds to form the *backbone* of the polymer. Synthetic and some natural polymers contain a *constitutional repeat unit* (CRU), which is the simplest repeating structure of the polymer.

Monomers are the structural building blocks from which a polymer is synthesised. These contain a specific reactive moiety which is the site at which the growth process (*propagation*) occurs. Polymers grown from only one monomer are termed *homopolymers* while polymers grown from two or more types are called *co-polymers*⁹. With regard to naming polymers both the American Chemical Society (ACS) and the International Union of Pure and Applied Chemistry (IUPAC) have proposed similar but not identical naming conventions for polymers^{10, 11}. Generally polymers are known by a common name instead of their systematic name, for example nylon 6, instead of the ACS systematic name (poly[amino(1-oxo-1,6-hexanediyl)]) or the IUPAC systematic name (poly[amino(1-oxohexan-1,6-diyl)]). This thesis will follow the naming conventions which are found in the relevant literature instead of the systematic naming conventions which can often be overcomplicated.

1.1.3 Polymer Architectures

1.1.3.1 Macroscopic Structures

The implication so far is that polymers form linear chains. Although some polymers do have a linear skeletal structure there are often imperfections along the backbone, even in polymerisations in which side reactions are supposedly suppressed. These imperfections cause branched or networked structures to occur. Often these structures arise via design of the monomers or because of the inherent characteristics of the polymerisation conditions favouring the presence of side reactions, Figure 1 below illustrates three different morphologies⁸.

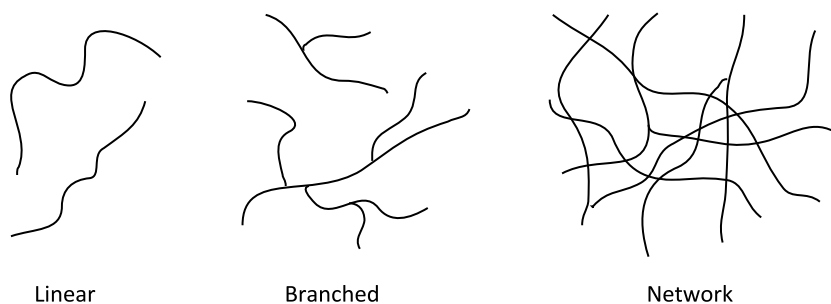


Figure 1: An example of linear, branched and network morphologies

Often the formation of these structures dictates the behaviour of the material and thus a thorough understanding of the polymerisation process and influencing factors is important to allow careful design and control over the properties of the resulting material.

Forming these structures after the polymerisation is often easier as it increases the level of control and functional tolerance which is not always possible in some polymerisation processes. An example of this is the use of sulphur to cross-link rubber which leads to an increase in toughness and rigidity¹², a process known as vulcanisation. These different structures also change the behaviour of the polymer in solution. If the three structures above were synthesised using the same monomer, each would have different features when solvated. Branched polymers entangle together much more than linear polymers. Thus, even with an equal mass of linear and branched polymers, the branched polymer solution would be much more viscous¹³. A networked structure creates a three dimensional interlinked polymer mesh which often traps solvent creating a gel material¹⁴.

1.1.3.2 Microscopic Structures

Co-polymers, which are polymers consisting of two or more monomers also have different structures depending on the orientation of the monomers on the polymer chain. Some common structures are: random, alternating, gradient, di-block, comb and brush co-polymers⁹. Random co-polymers consist of a random order of the two monomers along the polymer backbone. This is not always strictly random as several monomers could have slightly different reactivity; this causes a gradient to be created along the polymer. A higher proportion of the more reactive monomer will be at one end of the polymer and a higher proportion of the less reactive monomer at the opposite end. These are called gradient co-polymers. An alternating polymer consists of a repeating pattern of each monomer. Di-block polymers contain repeating blocks of the two monomers, a segment containing only one monomer followed by a segment containing only the other and so on. A brush polymer has arms coming off the backbone at spaced intervals while a comb having branches coming off every repeat unit. These structures are summarised in Figure 2.

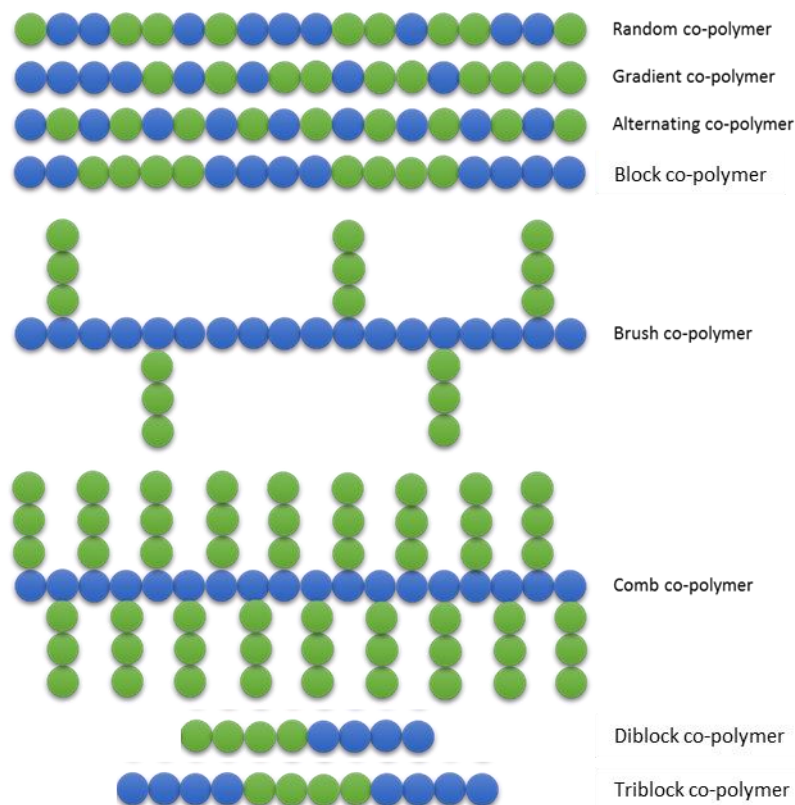


Figure 2: Types of co-polymer structures

These structures have an effect on the morphology and properties of the polymers even though they are built up of the same fundamental building blocks.

1.1.3.3 Polymer Mass

The polymerisation process nearly always creates a varied distribution of chain lengths. This means that a mass spectrum of a polymer will often display a range of masses separated by the mass of one repeating unit instead of one specific mass. One exception is that of dendrimers which are typically monodisperse¹⁵. This variation is often characteristic of the polymerisation process. A traditional radical polymerisation will have a much larger distribution of masses than that of a cationic ring opening polymerisation,^{16, 17} because the second polymerisation inherently has fewer terminating and branching side reactions, leading to a narrower weight distribution.

To help define the spread of the mass distribution, the quoted mass of a polymer comes with another parameter; the polydispersity index (PDI). The PDI of a polymer indicates the spread of molecular weights of the polymer, 1 being a monodisperse, single molecular weight polymer and higher numbers indicating a larger spread of molecular weights. To calculate the PDI, the number average molecular weight (M_n) and weight average molecular weight (M_w) must be calculated.

To calculate the number average molecular weight (M_n) we use the following equation. Effectively this calculates the mean value for the range of masses of the polymer sample.

$$M_n = \frac{\sum_i N_i M_i}{\sum_i N_i}$$

Equation 1: Number average molecular weight, where N_i is the number of molecules of molecular mass M_i

To calculate the weight average molecular weight (M_w) a slightly more complex equation is needed. This equation takes into account the fraction of the total weight represented by each polymer length.

$$M_w = \frac{\sum_i N_i M_i^2}{\sum_i N_i M_i}$$

Equation 2: Weight average molecular weight

The PDI is then calculated by dividing the weight average molecular mass by the number average molecular mass as shown below.

$$PDI = \frac{M_w}{M_n}$$

Equation 3: Polydispersity

Although polydispersity is a useful tool to characterise polymers care must be taken when quoting polymer molecular weights. If a polymer has an apparently low PDI (i.e. 1.5) then the distribution of molecular weight is still relatively large. A polymer with a calculated degree of polymerisation (D_p) of 100 repeating units for example would still have a large proportion of the material at a D_p of higher or lower than stated. Usually M_w is stated for the molecular weight as opposed to M_n as it takes into account the relative distribution of polymers among the different possible weights.

1.1.4 Polymer Morphology and Phase Behaviour

Polymer morphology describes the arrangement and small scale ordering of polymer chains in the solid state. Polymers can contain two different types of morphology; *amorphous* and *crystalline*. These domains can occur separately or together and influence the properties of the polymer when it is not in solution. Amorphous regions are regions in which the polymers are tangled together and have no order whereas crystalline areas do have some ordering and thus display crystalline-like behaviour.

The term crystalline is perhaps ambiguous when discussing polymers: it does not necessarily mean the same as the term used in crystallography. Instead it is more generically used to describe areas of three dimensional ordering on atomic scale, usually in the form of chain folding or stacking. A polymer with crystalline regions is often tougher and more impact resistant than a totally amorphous polymer.

These morphologies give rise to two distinct properties: the melting point and the glass transition temperature. The melting point (T_m) is where the crystalline phases in the polymer lose their order and become an amorphous phase. This is analogous to the melting point observed in crystallography.

The other property is the glass transition (T_g). This is the temperature at which the polymer goes from a brittle inflexible substance to a more fluid flexible material. This can be visualised by imagining a pen which is heated; when hot enough the pen can be bent and will re-harden into the bent form upon cooling. This process occurs simply by raising the temperature of the sample above the plastic's T_g and then lowering it below the T_g to harden again. Many polymers are flexible because their T_g is below room temperature. Far above and far below the T_g amorphous polymers behave like a brittle solid and a liquid respectively. Around the T_g more complex elastic or rubbery behaviour can be observed.

The T_m will always occur above the T_g and will have an accompanying crystallisation temperature upon cooling. Structural effects have a large influence over the T_g of a polymer. This is because the T_g is dependent on chain mobility i.e. how easily polymer chains can move around. Studying the glass transition and crystallisation behaviour of a polymer can be a powerful characterisation tool, particularly in relation to tuning the polymers solid-state behaviour.

1.1.5 Analytical Techniques

Macromolecules are, by definition, very large. Compared to small organic molecules they have many unique properties and characteristics. This means that they also have many unique problems when attempting to characterise and analyse a sample. This section discusses some polymer specific issues with standard organic chemistry techniques and some polymer-specific analytical methods.

1.1.5.1 Nuclear Magnetic Resonance

Nuclear magnetic resonance (NMR) is one of the most useful techniques for any organic chemist. It is also routinely used in polymer chemistry but there are several features of NMR spectra which are unique for polymers. The repeat units of a polymer chain look identical on paper; however in practice the electronic environment in which they find themselves is often subtly different. This causes broadening of peaks in the ^1H spectra and this often leads to peaks overlapping. Depending on the structure, picking out individual hydrogen environments may be difficult. This can also lead to issues when looking for a moiety attached to the polymer. This in itself may not suffer a broadening of the NMR signals but the peaks may be underneath the larger backbone hydrogen resonance for example. The same can be said for the ^{13}C spectra, with the main polymer chain carbons often not being able to be identified from the background noise of the

spectra. It is still a very useful way of identifying the hydrogen environments, proton ratios and also detecting defects within the structure.

1.1.5.2 Infra-red Spectroscopy

Infra-red spectroscopy (IR) is a very useful technique in polymer chemistry for identifying key functional groups attached to the polymer. The main problem can be that if the functional group is only a small percentage of the overall macromolecule then it will often be lost in the spectrum, especially if the peak has a weak absorption.

1.1.5.3 Elemental Analysis

Elemental analysis is used for polymers in much the same way as it is with conventional organic chemistry. Apart from confirming purity and the empirical formula of a polymer, it can also be used as a useful tool to quantify the number of functionalities introduced to a polymer alongside NMR data¹⁸.

1.1.5.4 Differential Scanning Calorimetry

Differential scanning calorimetry (DSC) is the method of choice for determining thermal transitions within polymer architectures, usually in the solid state. A sample is heated at a constant rate and compared with an inert sample. The input of heat required to continue heating at a constant rate is measured. This means any endothermic or exothermic transitions which take place in the polymer are measured as peaks or troughs in the spectra. This is how the glass transition and melting point are usually obtained. An example of a DSC and the key points is illustrated in Figure 3.

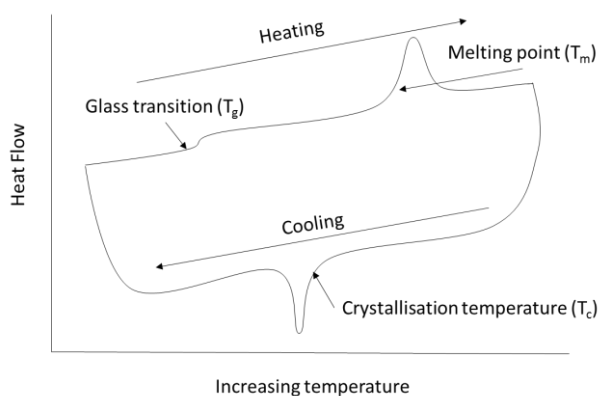


Figure 3: Typical features of a DSC trace

1.1.5.5 Thermogravimetric Analysis

Thermogravimetric analysis (TGA) is a simple technique which provides data on the thermal stability of the polymer. It involves heating a sample to a very high temperature, usually around 600°C and measuring the weight loss over this period. This can be a good indication of structure,

more stable structures having higher thermal stability. This can also be used to indicate the presence of impurities or solvents, which often are lost at lower temperatures. A typical TGA is shown in Figure 4.

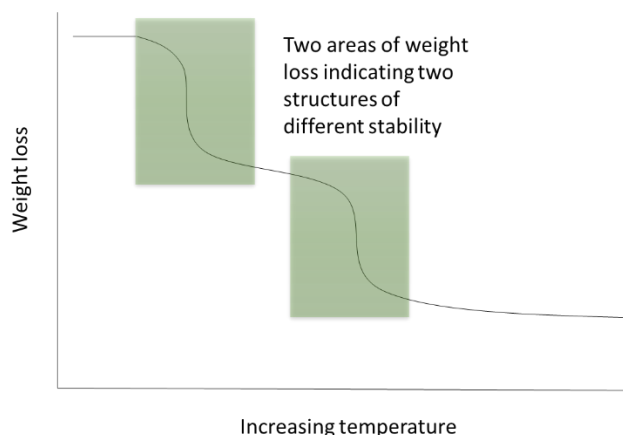


Figure 4: Typical TGA trace showing two areas of weight loss

1.1.5.6 Molecular Weight Determination

There are two common techniques to calculate the molecular weight of a polymer and the PDI.

Matrix-Assisted Laser Desorption/Ionisation Time-of-Flight

For smaller polymers matrix-assisted laser desorption/ionisation time-of-flight (MALDI-TOF) analysis can be performed. This method involves combining the polymer with a heavily UV absorbing matrix, often containing components used in sun-screen. Ultra-violet bombardment ablates the top layer of the matrix, causing a stream of fragmented matrix including the polymer to be ejected from the surface. The hot stream of molecules is then ionised and finally the time of flight is measured to resolve the masses of separate particles.

Size Exclusion Chromatography

The most popular method to determine molecular weight is size exclusion chromatography (SEC). This is where the polymer is injected into a stream of solvent as it is passed through a column containing porous beads. The size of the pores is important as it is this characteristic which will enable smaller polymers to be separated from larger polymers. The smaller polymers can fit into these pores, meaning that their retention time on the column is comparatively long compared to that of the larger polymers. The mass of the polymer can be obtained from comparison with a calibration curve which is often derived using mono-disperse poly(styrene) standards. Issues can arise from this if the calibration isn't an exact comparison for the material which is being measured. For example all of the SEC results for the poly(2-oxazoline) samples analysed in this thesis were scaled by a factor of 0.6 as the calibration does not provide the exact molecular weight of the samples.

1.2 Polymer Synthesis

1.2.1 Synthesising a Polymer

Polymers are synthesised from a process in which the monomers bearing a reactive moiety, join together in a repetitive way to form a macromolecule of large molecular weight. Understanding this process for all sorts of polymers has allowed scientists to control and design new materials with novel properties.

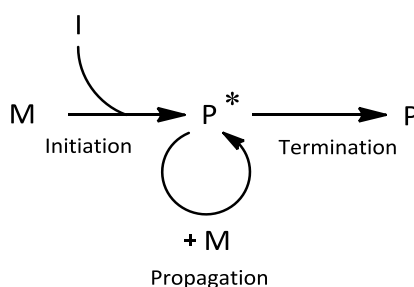
1.2.1.1 Mechanism

There are three distinct stages to a polymerisation

- Initiation
- Propagation
- Termination

Initiation involves adding a stimulus to the monomers to begin the polymerisation; this can be via a chemical or physical process such as the introduction of a catalyst or heat.

Once the polymerisation has been initiated the second stage is propagation, in which the active site on the newly formed polymer reacts with another monomer creating a new bonded monomer, which either bears or re-forms the active site. This process is repeated until the monomer is used up or the polymer terminates itself. Termination is the final stage of the polymerisation process and involves quenching the reactive end of the polymer so it can no longer grow, this process is often a characteristic of the polymerisation. Some mechanisms do not inherently terminate (termed living polymerisations) and a further addition of a termination reagent is required. These three steps are illustrated in Scheme 1.



Scheme 1: The three steps of a polymerisation

The process which occurs during propagation varies depending on the monomers. The following sections deal with some common polymerisation mechanisms.

1.2.2 Step Growth Polymerisation

Step growth polymerisation is the method used by nature to synthesise many natural polymers. Generally monomers involved in this type of polymerisation have two or more reactive sites. Initially the reaction mixture contains only monomer; these can react with each other to form dimers. Now both the monomer and the dimer can react, either with each other or with the same species. This complexity grows exponentially as the reaction proceeds until it comes to completion. Figure 5 illustrates this mechanism.¹⁹

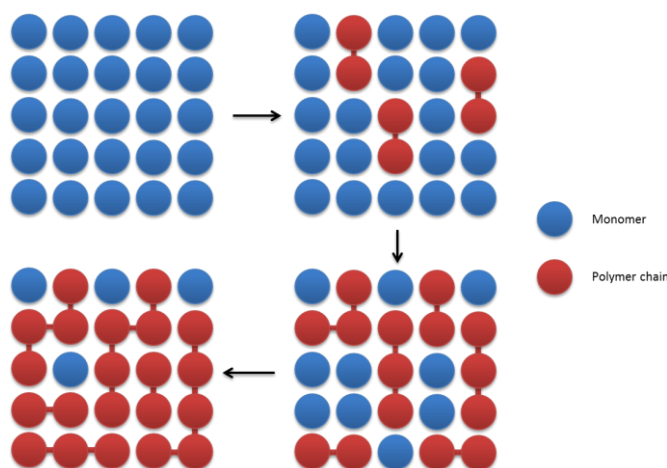
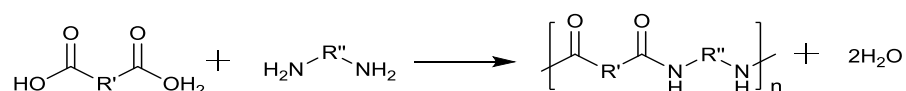


Figure 5: Step growth polymerisation

With this method structural control is often lost. This does not mean that the properties of the polymerised material cannot be controlled. This is still possible by carefully selecting the starting monomers. Step growth polymers are still of importance at a commercial level as they can sometimes be used to replace conventional building materials, especially some metals. This is because this class of polymers are often strong, lightweight and heat resistant.²⁰ The most common step-growth polymerisation is condensation polymerisation.

1.2.2.1 Condensation Polymerisation

Condensation polymers are polymers which are formed via a condensation reaction between the two monomers. The monomers react together losing a small molecule as a side product in the process. Scheme 2 below shows the general synthesis of a common class of polymers synthesised via condensation polymerisation, poly(amides).



Scheme 2: Synthesis of poly(amide)s

The R groups on the di-carboxylic acid and di-amine can be changed and this gives different properties depending on the group. For example Nylon 6,6 has $\text{R}':(\text{CH}_2)_4$ $\text{R}'':(\text{CH}_2)_6$ and in Kevlar

both R' and R'' are benzene rings. The useful applications of many of the polymers and the simple way to synthesise and adjust their properties have meant poly(amide)s have become important, industrially produced polymers.

1.2.3 Chain Growth Polymerisation

Chain growth polymerisation is the more common polymerisation method used in research. This mechanism proceeds by monomers adding to an active site on the polymer. There are usually only a small number of these active sites in proportion to the number monomers and these are normally constrained to one per growing polymer chain. More than two active sites lead to branched polymers instead of a linear polymer.²¹ The reactive site of these polymers can be one of several types of reactive moiety, some common types include;

- Free radical
- Ionic centre (cation or anion)
- Organometallic complex (such as ring-opening metathesis polymerisation²²)

Figure 6 illustrates how these polymerisations proceed. An example of this mechanism can be found in Section 1.3.4.2.

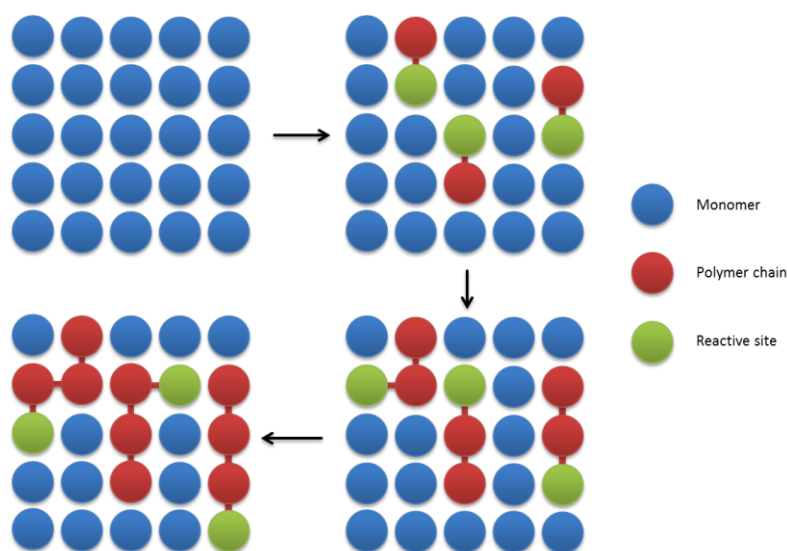


Figure 6: Chain growth polymerisation

1.2.3.1 Living Polymerisation

Some chain growth mechanisms are classed as a living polymerisations. These are polymerisation mechanisms in which the polymer has not got the ability to terminate. This living aspect was first discovered by Michael Szwarc in 1956 who was studying the polymerisation of styrene. He discovered that the viscosity of the polymerisation mixture would eventually plateau after the addition of the styrene monomer to the initiator. After adding more styrene however the viscosity would then begin to increase again²³. This living character of the polymerisation

mechanism has several advantages over traditional chain polymerisation such as a lower PDI and control over end groups.

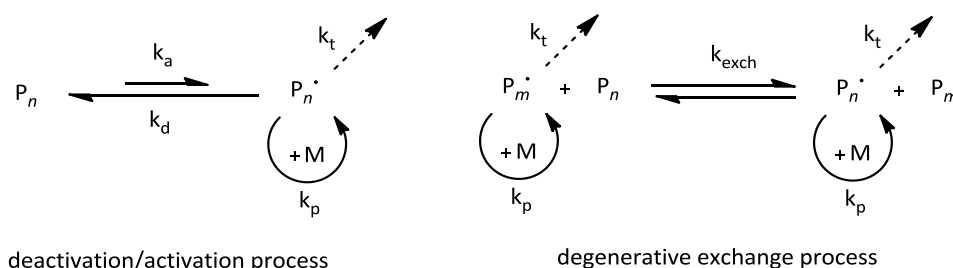
1.2.3.2 Radical Polymerisation and ‘Living’ Free Radical Polymerisation

History

By far the most thoroughly researched polymerisation is radical polymerisation. Although radical polymerisation has been important industrially since the 1950s and 1960s, controlling radical polymerisation has only become possible in the last 20 years²⁴. Conventional uncontrolled free radical polymerisation has an inherent lack of macromolecular control due to diffusion-controlled radical coupling and disproportionation²⁵. Controlling this process allows polymers to be synthesised with narrower weight distributions, predetermined degrees of polymerisation based on the monomer to initiator ratio, end group functionalities and structural features such as the control over branching co-polymers to be achieved. Often this process is called “living” radical polymerisation, however the polymerisation process is not strictly speaking a living polymerisation. A living polymerisation is a process which does not have chain breaking reactions such as chain transfer and termination²⁴. These chain breaking reactions are suppressed using controlled radical polymerisation (CRP) but not completely prevented, thus CRP is not strictly a “living” process²⁶.

Controlled Radical Polymerisation

Central to all CRP systems is the dynamic equilibrium between dormant and active radical polymer chains^{27, 28}. Fast exchange between the active and dormant species is needed to ensure control over the molecular weight, chain dispersity and molecular architecture. The growing species should only be active for a small amount of time (a few milliseconds) before deactivation (for several seconds). This means the lifetime of a growing chain is comparable to that of a propagating chain in radical polymerisation (RP). However the overall reaction can take at least several hours allowing several synthetic modifications to be introduced during the polymerisation²⁹. This equilibrium can be achieved either by trapping the radical in a deactivation/activation process or by the radical being involved in a reversible degenerative-exchange process as illustrated in Scheme 3 below.



Scheme 3: deactivation/activation process vs degenerative exchange process

In both cases other agents are used to stabilise the dormant species depending on the method involved. Deactivation/activation processes make use of the persistent radical effect (PRE) while the degenerative exchange (DE) process does not and has more in common with a RP³⁰.

The Persistent Radical Effect (PRE)

The persistent radical effect (PRE) is a kinetic feature which provides a self-regulating effect in several CRP processes^{28, 31, 32}. Propagating radicals are trapped or deactivated by species 'X' which is often a stable radical, one example being that of the nitroxide-mediated polymerisation (NMP) which uses a nitroxide radical as the 'X' species³³. This dormant species is then reactivated either spontaneously, using light, thermally or with a catalyst to form a growing radical. These growing radicals can propagate to form new polymers or terminate. Persistent radicals (X) cannot terminate with each other and only reversibly cross-couple with growing species. This means as the polymerisation progresses, any termination reactions between growing chains irreversibly increases the relative amount of 'X' species which in turn decreases the concentration of growing chains. This in turn reduces the number of termination reactions and so on.

1.2.3.3 Cationic Polymerisation

Overview

Cationic polymerisation is a class of chain growth polymerisation; it involves an initiator reacting with a monomer to create a positively charged monomer. This is then susceptible to attack from another monomer which in turn becomes cationic and this is repeated creating a polymer³⁴. This polymerisation only occurs with olefins which contain electron donating groups and heterocycles, the positive charge being stabilised by the electron donating groups and hetero-atoms respectively. Although olefins can be polymerised using this method, they are generally synthesised using controlled radical polymerisation.

Cationic ring opening polymerisation (CROP)

Cationic ring opening polymerisation (CROP) is a subclass of cationic polymerisations. CROP was investigated by Staudinger in the 1920's when he used it to establish the existence of covalently bonded macromolecules by modelling the formation of poly(ethylene oxide)⁶. Since then several other cyclic systems have been found to produce polymers via CROP such as tetrahydrofuran (THF)^{35, 36} and 2-oxazolines⁶⁰.

1.3 Pseudo-Peptidic Polymers

1.3.1 Overview

Pseudo-peptidic polymers are a class of polymers which closely resemble or mimic peptide polymers. These polymers include poly(acrylamide)s, poly(2-oxazoline)s and poly(peptoid)s as shown in Figure 7.

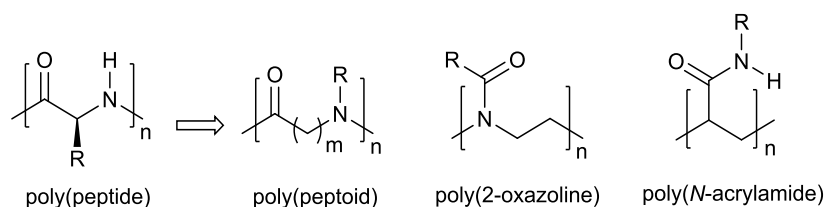


Figure 7: Poly(peptoid)s, Poly(acrylamide)s and Poly(2-oxazoline)s

Although these polymers appear similar and indeed display similar properties, i.e. thermoresponsive behaviour and biocompatibility, the synthetic method used to synthesise each polymer offers different control over the structure and functionality of them. The following section will discuss the differences between these three classes of polymers.

1.3.2 Poly(acrylamide)s

Poly(acrylamides) are a class of polymers which are synthesised from acrylamides using controlled radical polymerisation techniques as discussed previously. The simplest acrylamide is acrylamide itself, shown in Figure 8.

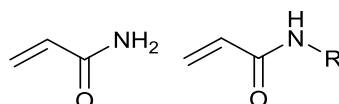


Figure 8: Different acrylamide structures
Acrylamide (left), and functionalised acrylamides (right)

One of the most commonly used acrylamide is the acrylamide with an isopropyl group attached to the amide bond, Poly(*N*-isopropyl-acrylamide). This polymer is thermoresponsive, meaning it displays a temperature dependant transition from soluble to insoluble in water. Due to this it has been widely investigated in research.

1.3.2.1 Poly(*N*-isopropyl-acrylamide) (PNiPAAm)

PNiPAAm was first reported to have a lower critical solution temperature (LCST) of 32°C in 1968³⁷ and because of this property it has found many uses in biochemistry. A few examples of these are: controlled drug and gene delivery systems³⁸⁻⁴¹; enzyme bioconjugates^{42, 43}; microfluidics⁴⁴ and microgels⁴⁵. PNiPAAm has carcinogenic monomers which has hampered the development of *in-vivo* applications. Recently thermoresponsive coatings and surfaces for tissue engineering have

become popular areas of interest. For reference several reviews have been published on the topic⁴⁶⁻⁴⁸.

Synthesis and characterization of PNiPAAm is summed up nicely in a review by Schild *et al*⁴⁹. Co-polymers of PNiPAAm are also of key importance when attempting to control and tune the LCST of the polymer; these have also been reviewed⁵⁰.

Figure 9 below illustrates the structure of *N*-isopropyl acrylamide and the corresponding polymer. The polymerization of *N*-isopropyl acrylamide is a well-known radical polymerization which is a versatile reaction allowing for easy co-polymerization and functionalization of substrates, for example glass. Apart from the conventional radical polymerization several other methods have been developed such as atom transfer radical polymerisation (ATRP)⁵¹ and reversible addition-fragmentation chain transfer polymerisation (RAFT), both of which have been used to create co-polymers. A review comparing the different methods of polymerization has been published⁵².

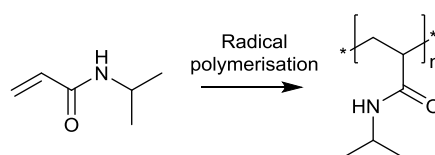
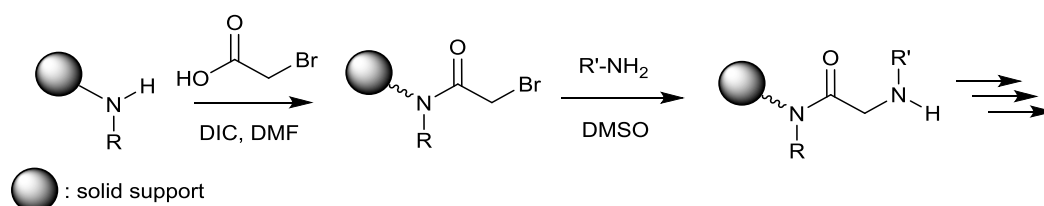


Figure 9: Polymerisation of *N*-isopropylacrylamide
N-isopropylacrylamide (left) and the corresponding polymer poly(*N*-isopropylacrylamide) (right)

1.3.3 Poly(peptoid)s

Poly(peptoid)s are the most analogous of the three pseudo-peptide polymers to peptides themselves. Not only is the structure similar but they can also be synthesised in a stepwise fashion much like peptides, according to Scheme 4 below⁵³.



Scheme 4: Stepwise synthesis of an α -poly(peptoid)

This method not only allows the synthesis to be automated, similar to that of conventional peptide synthesis⁵³ but allows a wide variety of commercially available R' groups to be introduced. A limitation of this method however is that it is only suitable to a relatively low chain length ($n < 30$) as longer sequences have low yields and are time-consuming.

Poly(peptoid)s not only allow functionalization via selection of the primary amide but they can also be adjusted via addition the addition of extra CH₂ groups on the backbone, so called α , β and γ poly(peptoid)s, show in Figure 10.

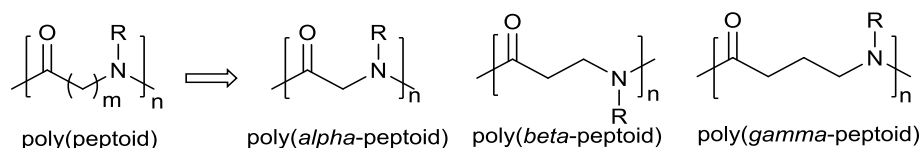


Figure 10: α , β and γ poly(peptoid)s

The stepwise method is the most commonly used synthesis but there are several other procedures which also allow poly(peptoid)s to be synthesised. These include nucleophilic ring-opening polymerisation of *N*-carboxyanhydride (NCA)^{54, 55} and metal-mediated polymerisation⁵⁶⁻⁵⁸. Poly(peptoid)s have found limited applications in biotechnology so far. This is mainly due to poly(peptide)s being cheaper to synthesise and have more established modes of action and applications⁵⁹.

1.3.4 Poly(2-oxazoline)s

1.3.4.1 History and Current Perspective

Although poly(2-oxazolines) were discovered in the 1960s not much research was published in the 1980s or 1990s mainly due to the long reaction times and limited applications of these systems². With the discovery of the 'biosteath' behaviour of methyl and ethyl poly(oxazoline)s^{60, 61} and the advent of microwave assisted polymerisation⁶² dramatically reducing reaction times, the field has been re-invigorated as illustrated with the number of patents published since poly(oxazoline)s were first reported, Figure 11.

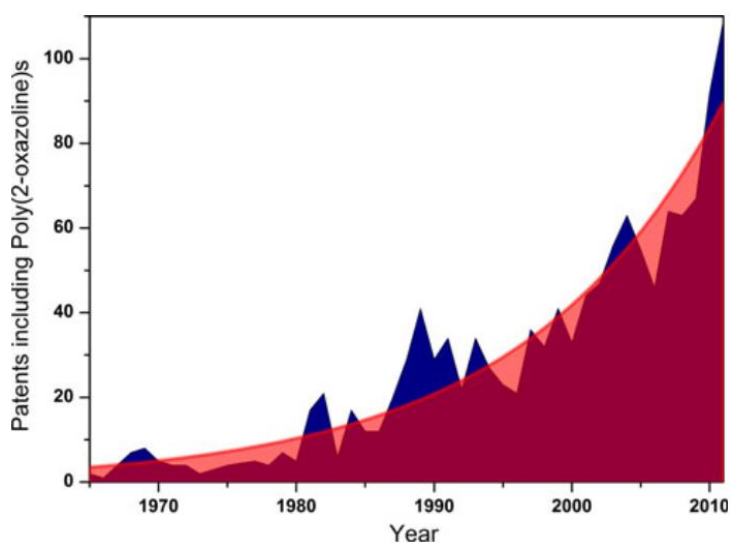


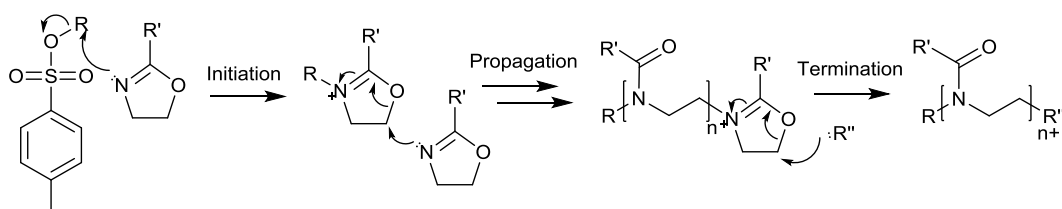
Figure 11: Number of patents including the word poly(2-oxazoline) since they were first reported Number of patents (blue) fitted with an exponential growth curve (red) taken from De la Rosa et. al⁶³

1.3.4.2 Structure, Mechanism and Control

The cationic ring opening polymerisation of 2-oxazolines is a well-known reaction and was discovered independently by four different research groups in 1966⁶⁴⁻⁶⁷. The cationic ring-opening process can be carried out using a microwave reactor. This leads to much shorter reaction times (tens of minutes rather than three days⁶²). Under the right conditions unwanted side reactions such as chain termination and chain transfer reactions are suppressed⁶⁸. This makes poly(oxazoline)s very desirable as good control over chain length and polydispersity can be achieved. It should be noted that although polymerisations are performed using microwave reactors, the microwave itself is not required. Comparable experiments using conventional pressure reactors have demonstrated that microwaves themselves have no influence on the polymerisation^{62, 69}.

Mechanism

Scheme 5 below shows the mechanism of formation of the poly(2-oxazoline)². Polymerisation is initiated using an electrophile to form the propagating cationic oxazolinium ion. The C-O bond in this species is now weakened and undergoes nucleophilic attack by the next monomer. Once the monomer has been used up the terminal cationic oxazolinium ion will remain until it is reacted with a nucleophile in the final step. This can also enable well-defined block co-polymers to be assembled via the addition of a different oxazoline monomer at this point which will continue the polymerisation from the terminal ion³⁶. This polymerisation method is shown in Scheme 5.

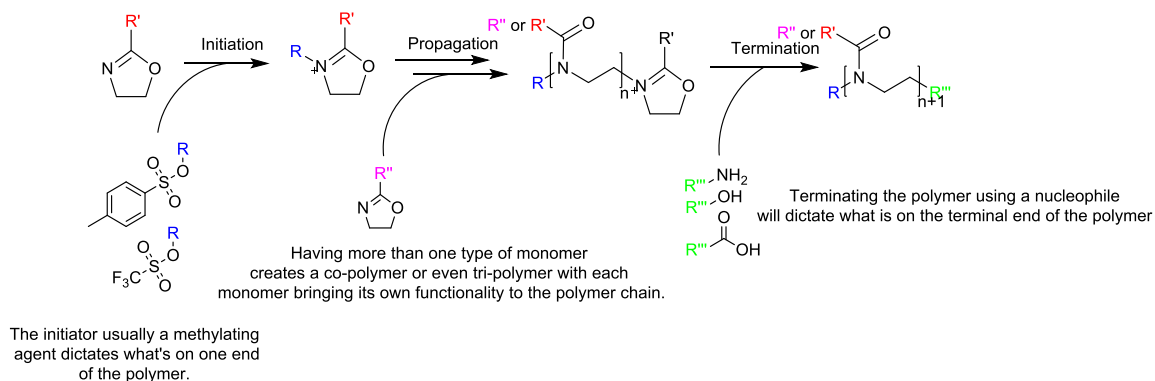


Scheme 5: Cationic ring opening of a 2-oxazoline using Methyl p-toluenesulphonate as an initiator

Functionalisation

This well-defined mechanism means a high degree of control can be achieved. Scheme 6 illustrates the different routes that can be exploited to functionalise the polymer. These three routes are;

- Functionalised 2-oxazoline monomers
- Functionalised initiators
- Nucleophilic terminators



Scheme 6: Illustration of the 3 routes of modification available during the polymerisation of 2-oxazolines

Combining two different 2-oxazoline monomers is a simple method to create co-polymers as this can be done *in situ* during the reaction producing either gradient or random co-polymers depending on the monomers used. The gradient nature is due to the different reactivity of the 2-oxazoline monomers causing a higher distribution of the more reactive 2-oxazoline at one end and the less reactive moiety at the other end^{7, 70}. The reactivity of the 2-oxazoline is highly dependent on the side chain at the 2 position of the 2-oxazoline. An example of this is the difference in the propagation rate constant (k_p) of *n*-propyl, *i*-propyl and *c*-propyl 2-oxazoline which is illustrated in Figure 12.

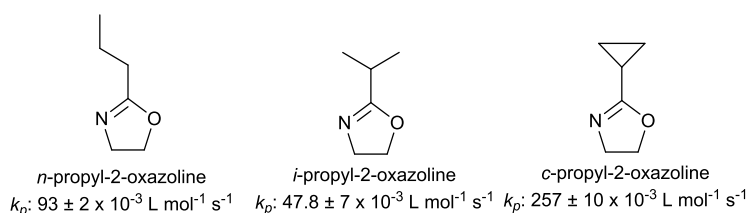


Figure 12: Dependence of the propagation rate constant on the side chain structure of 2-oxazolines

An alternative method is to add the two 2-oxazoline monomers separately, polymerising one monomer until it is used up then adding the second monomer, creating block co-polymers⁷.

This co-polymerisation is useful for two reasons; firstly it allows good control over the hydrophobic or hydrophilic nature of the polymer. Secondly it allows key functionalities to be built into the polymer via another monomer, for example an alkene moiety⁷¹. These can then be used to functionalise the backbone further.

As mentioned earlier end-capping poly(2-oxazolines) can be achieved via two methods, initiation and termination. Termination is the most popular method as this can be achieved using any nucleophile while choice of initiator is limited to a non-nucleophilic species to avoid interference with the polymerisation process. There are several examples of adding a hydrophobic group as either the initiator or terminator⁷²⁻⁷⁷ and the same using a hydrophilic group⁷⁸⁻⁸¹. More specifically there are a few examples of using this technique to add a fluorescent marker using a

fluorescent molecule as an initiator⁸² or a terminator⁸³. Although there is a lot of research in this area, each case employs the same method of termination with a nucleophilic group such as an amine or alcohol and the same method of initiation using either a triflate or toluenesulphonate.

Structure

Polymerisation of 2-oxazolines is known to proceed via a living polymerisation mechanism and under the correct conditions side and termination reactions are suppressed⁶⁸. This leads to a narrow polydispersity index of the final polymer. For a poly(oxazoline) a PDI of lower than 1.2 would be expected for a good sample⁶².

This mechanism in turn supplies an easy method to control of the polymer chain length via the adjustment of the molar ratio of initiator to monomer. This accurate control over chain length is another factor contributing to a low PDI.

1.3.4.3 2-Oxazoline Monomers

Several different routes for the synthesis of oxazolines have been reported in the literature using carboxylic acids⁸⁴⁻⁸⁶, nitriles^{4, 87, 88}, esters⁸⁹, and N-(2-hydroxyethyl)amides⁹⁰⁻⁹⁴. Not all of these routes are ideal as they often require a substituent attached to the ring at the 4 or 5 positions which hinders polymerisation⁹⁵. This will be discussed in more depth in Chapter 2.

1.3.4.4 Poly(2-methyl-2-oxazoline)

Poly(2-methyl-2-oxazoline) (PMeOx), (Figure 13) is one of the commonly studied poly(oxazoline)s. This is probably due to the commercial availability of the 2-methyl-2-oxazoline monomer.

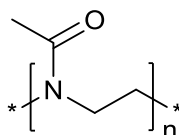


Figure 13: Poly(2-methyl-2-oxazoline)

Protein Repellent surfaces

The main reported application of PMeOx has been to synthesise protein repellent surfaces. The first report was by Textor and colleagues who synthesised a Poly(L-lysine) (PLL) backbone with PMeOx brushes. This was dip-coated onto Nb₂O₅ coated silicon wafers and its protein-repellent behaviour was characterised. They demonstrated that protein absorption was below that of the detection limit (2 ng/cm²) equalling poly(ethylene glycol) (PEG) surfaces⁹⁶⁻⁹⁸. In further work they also demonstrated the microbial anti-fouling properties of the co-polymers⁹⁸. Recently work by Pidhatika *et al.* reported a study comparing PEG with PMeOx brush coatings. They demonstrated that PMeOx-PLL films were far more stable than PEG films⁹⁹.

1.3.4.5 Poly(2-ethyl-2-oxazoline)

Poly(2-ethyl-2-oxazoline) (PEtOx), (Figure 14) is another of the commonly studied poly(oxazoline)s as it is also commercially available as a monomer. It has been investigated primarily as an alternative for poly(ethylene glycol) (PEG).

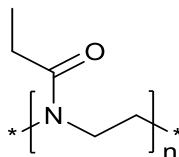


Figure 14: Poly(2-ethyl-2-oxazoline)

An alternative to PEG?

PEG has been used as a gold standard over the last 20 years for stealth behaviour in the body and is to date the only stealth polymer on the market. Recently several drawbacks to the use of PEG have been discovered and this has led to a search for suitable alternatives. Three excellent papers have been published highlighting the issues relating to PEG and the potential alternatives (PEtOx being one alternative) in the last few years^{3, 100, 101}. Some of the important points relating to issues with PEG and the use of PEtOx as an alternative will now be highlighted.

The increased use of PEG in a wide range of product has highlighted not only the beneficial properties of PEG but made it more likely to encounter issues with it. The main issues encountered coupled with a brief description are listed below¹⁰¹.

- **Immunological response**

Intravenous administration

It was shown in early studies that PEG can induce blood clotting and clumping of cells indicating nonspecific interactions with blood¹⁰². Since then it has been shown that PEG can induce specific and non-specific recognition by the immune system leading to a response by the body.

Oral administration

When orally administered PEG is not taken up via gastrointestinal adsorption in rats when the molecular weight is 4 kDa to 6 kDa. However when the molecular weight is 1 kDa around 2% is adsorbed¹⁰³. Two drugs, MoviPrep and GoLYTELY have reported angioedema¹⁰⁴ and anaphylactic reaction¹⁰⁵⁻¹⁰⁷ respectively in response to PEG.

Dermal administration

Application of PEG to the skin can also cause dermatitis for example dentifrice¹⁰⁸ and several patents by Fisher containing PEG also caused dermatitis due to hypersensitivity¹⁰⁹.

- **Changes in pharmacokinetics**

This issue relates to another potential immune response which involves accelerated blood clearance (ABC) of PEG. This was first reported by Dams et al¹¹⁰. and has subsequently been investigated in more depth¹¹¹. The issue arises when a second dose of PEG has drastically reduced circulation time compared with the initial dose indicating that the initial administration of PEG can alter the circulation of further doses.

- **Non-biodegradability**

This problem arises due to the non-biodegradability of PEG limiting the molecular weight possible for use of PEG. If the weight is below 400 Da PEG is metabolised into toxic compounds¹¹². While an upper limit of 20-60 kDa is imposed as this does not otherwise get excreted and can accumulate. There are no systematic studies that show if PEG is completely excreted and if accumulation occurs and its effects of accumulation¹¹³.

- **Degradation under stress**

PEG has been shown to degrade under a variation of stimuli including light and heating¹¹⁴⁻¹¹⁷, shear stress¹¹⁸ and mechanical stress (from flow, stirring and ultrasound)¹¹⁹. This will have an effect on the shelf life and activity of any drug containing PEG.

- **Toxicity of side-products**

There are three main toxic side products of PEG synthesis; 1,4-dioxane, ethylene oxide and formaldehyde¹⁰¹. The content of these in a pharmaceutical product are strictly limited and demonstrate the need for PEG to be used at a very high grade for any biological applications.

For these reasons suitable alternatives are in demand, PEtOx being one. There have only been some limited studies looking into the intravenous administration⁶⁰, prolonged blood circulation¹²⁰, tissue distribution^{61, 120} and biodegradability¹²¹ but they have all concluded that PEtOx behaves in a similar fashion to PEG. A few drug transport systems using PEtOx have also demonstrated similar behaviour to PEG¹²²⁻¹²⁴. A recent study by Bauer et al. directly compared PEtOx to PEG regarding cytotoxicity and hemocompatibility concluding that PEtOx is a promising candidate as an alternative to PEG³.

1.3.4.6 Poly(2-isopropyl-2-oxazoline)

Poly(2-isopropyl-2-oxazoline) (PiPrOx), (Figure 15) is one of the poly(2-oxazoline)s which display thermoresponsive behaviour. As it is not commercially available as a monomer, adoption of the polymer as a biologically relevant material has been slow.

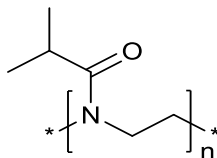


Figure 15: Poly(2-isopropyl-2-oxazoline)

Thermoresponsive Polymers

Thermoresponsive polymers are polymers that undergo a change in response to a thermal stimulus in solution, usually aqueous. These display a temperature induced phase transition called a cloud point temperature (T_{cp}). This is a transition from a one-phasic system to a bi-phasic system. The polymer in the bi-phasic system is not precipitated but the two phases contain a high polymer concentration and a low polymer concentration. This gives rise to the lower critical solution temperature (LCST) which corresponds to the T_{cp} at the lowest point of the binodal phase diagram (Figure 16).

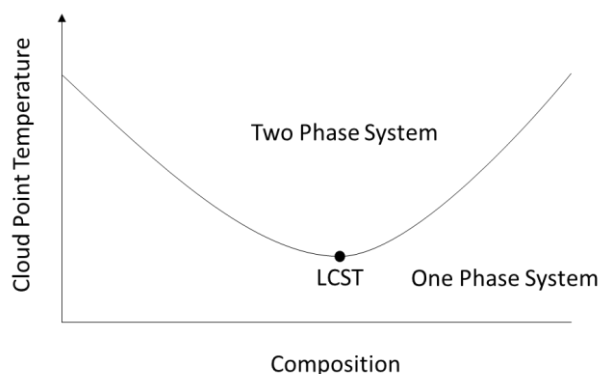


Figure 16: Binodal phase diagram demonstrating the determination of the LCST from a range of T_{cp} . The composition refers to the structural properties of the polymer investigated, usually this is a range in the degree of polymerisation.

The line shown on Figure 16 is the trend of T_{cp} measurements, a typical T_{cp} measurement is shown in Figure 17.

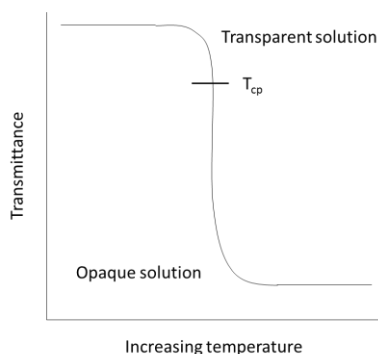


Figure 17: Typical turbidimetry measurement of a thermoresponsive polymer. T_{cp} was defined as a 20% change in transmittance.

At the T_{cp} the enthalpic contribution of the water hydrogen bonding to the polymer chain becomes less than the entropic gain of the system as a whole. This can be thought of as the dissolution enthalpy, ΔH , of the basic sites on the polymer favouring dissolution. Conversely, the entropic organisation ΔS of the solvent required to achieve this hydrogen bonding is unfavourable. This means that since the free energy of dissolution is equal to $\Delta H - T\Delta S$, as the temperature increases, the free energy of dissolution can change from negative (favourable) to positive (unfavourable) and thus cause the observed phase transition. This can only occur in strongly interacting solvents such as water¹²⁵.

Whilst PNiPAAm is the most studied thermoresponsive polymer, other thermoresponsive polymers have also been discovered such as poly(aminoacids)¹²⁶, Poly(L-lactide) and poly(ethylene glycol) or PEG co-polymers¹²⁷, poly(asparagine) derivatives¹²⁸ and poly(phosphoesters)¹²⁹. An excellent review of the field of thermoresponsive polymers was published by Dimitrov *et al* in 2007¹²⁵.

Thermoresponsive Behaviour of PiPrOx

The first report of the LCST transition of PiPrOx was by Uyama and Kobayashi in 1992¹³⁰ in the range 36–39°C depending on polymer concentration. Diab *et al* studied the phase transition in more detail using microcalorimetry¹³¹. They discovered that the phase transition is endothermic with the enthalpy of transition ranging from 1.51 kJ/mol to 5.64 kJ/mol depending on the molecular weight. They also found that the T_{cp} is dependent on salt concentration and is lower in D₂O by approximately 1.5°C than in H₂O. They argue that this is the result of the polymer chains may adopt a more extended structure due to the higher ordering of water in D₂O and thus a larger volume of solvated water. Secondly as D₂O is a more structured solvent, the solvent molecules which form the hydration layer around the polymer occupy a larger volume of space. The change in volume also increases as salts are added which indicates that the salts are also interacting with the solvation layer around the polymer in a manner similar to that of D₂O and thus also causing the T_{cp} to lower.

The most studied method to tune the T_{cp} is co-polymerisation. An excellent paper by Huber *et al*⁴ discusses the accurate control of the T_{cp} temperature using co-polymerisation with hydrophobic monomers. Figure 18 below summarises the co-polymers and their T_{cp} behaviour.

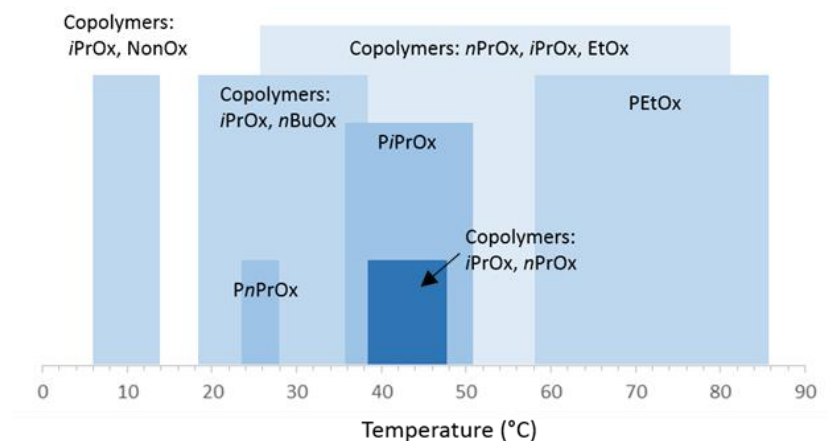


Figure 18: Comparison of co-polymer T_{cp} found in literature^{130, 132-135}

The T_{cp} is also dependent on the molecular weight¹³¹ and concentration¹³⁰ of the polymer.

1.3.4.7 Comparison Between PiPrOx and PNiPAAm

Polymerisation

Structurally PiPrOx and PNiPAAm can be thought of as structural isomers of each other¹, Figure 19.

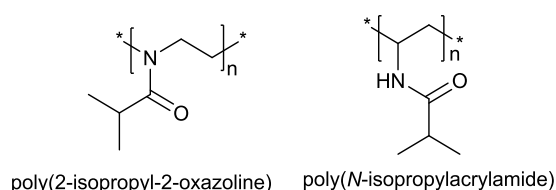


Figure 19: Structure comparison of PiPrOx and PNiPAAm

As discussed previously the mechanism of polymerisation for the two monomers is different. PiPrOx being synthesised via a cationic ring opening process and PNiPAAm via a radical polymerisation. These two mechanisms each carry inherent benefits along with several disadvantages. Cationic ring opening allows easy control over chain length, end group functionalization and suppresses side reactions preventing chain branching and termination. In traditional free-radical polymerisation these are all very difficult to control. As discussed above however, controlled radical polymerisation techniques have been developed which solve these problems although they do add complexity. CROP however does have limitations on functional groups on the monomers and is very sensitive to water and other contaminants which leads to the need for stringent purification requirements. Radical polymerisation is much more tolerant of functional groups and is less sensitive to other factors.

Radical polymerisation allows for the use of a wide range of commercially available starting materials, in contrast poly(2-oxazoline)s do not have many commercially available monomers and any functional 2-oxazolines must be synthesised. This can become an issue if quantities over 1-10g are required. Synthesising large batches of polymers is also difficult using poly(2-oxazoline)s since they require water-free conditions and long reaction times. This is not the case with radical polymerisation. However, modern synthetic methods are making this less of an issue through the use of microwave synthesis for example, which greatly reduces 2-oxazoline polymerisation times.

Applications

PNiPAAm has a serious limitation in that the monomers used are carcinogenic and teratogenic¹³⁶. This has meant that there has been a lack of development from the research stage to viable products for use in the body. PNiPAAm is not FDA approved which is a major stumbling block for future developments. Poly(2-oxazoline)s have several advantages in this area. Firstly poly(2-oxazolines) display low toxicity¹³⁷, indeed both the methyl and ethyl poly(2-oxazoline)s have already been FDA approved¹³⁸. These polymers also display a 'stealth' behaviour, which means they show reduced interactions with immune system proteins^{1,3}. These benefits combined with the accurate control over T_{cp} and functionalization makes poly(2-oxazoline)s exciting candidates for thermoresponsive biological applications.

1.4 Aim

The aim of this work is to develop poly(2-oxazoline)-based, functional biomaterials which have real applications in biological fields. This will be achieved by working with the current literature which describes in detail how to control and introduce functionality into poly(2-oxazoline)s, but which as yet contains very little relating to the application of this knowledge to develop functional materials. Particularly when combining the materials with biological systems. Potentially the comprehensive data on functionalising poly(2-oxazoline)s will allow accurate fine tuning of the behaviour and biocompatibility of these materials, something which is important when dealing with biological systems.

Chapter 2 Synthesis and Cloud Point Temperature Control

2.1 Introduction

In the past 20 years many different approaches have been developed to introduce functionality to poly(2-oxazoline)s.

Figure 20 below summarises some of the methods and strategies employed to introduce functionality into poly(2-oxazoline)s.

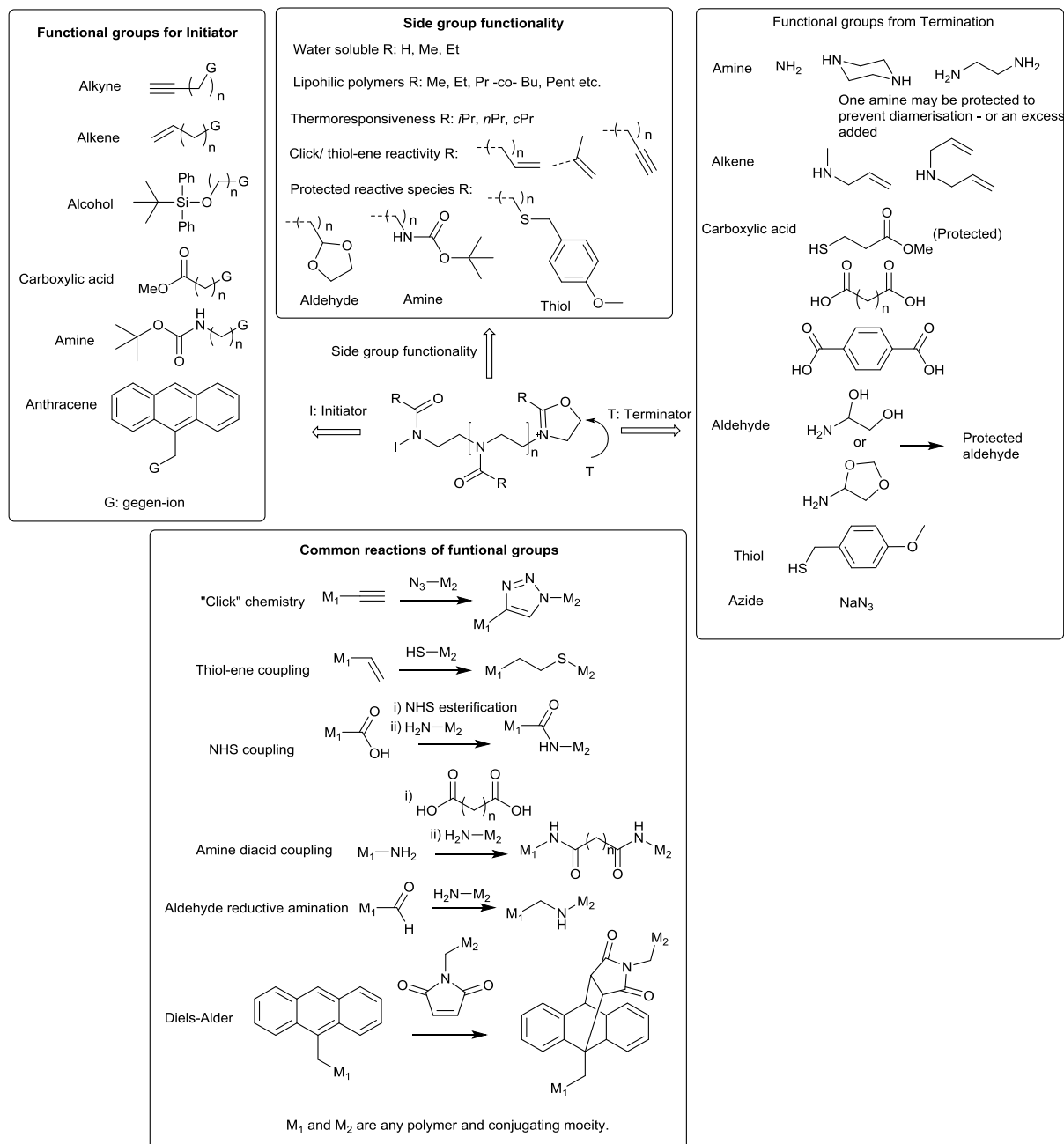


Figure 20: Strategies to introduce functionality into poly(2-oxazoline)s¹³⁹

A vast array of options are available to the synthetic chemist when designing materials which incorporate poly(2-oxazoline)s. One limitation however is the limited availability of poly(2-

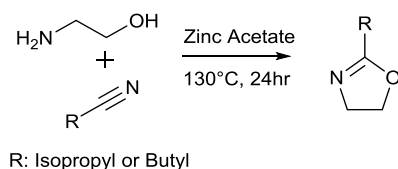
Synthesis and Cloud Point Temperature Control oxazoline) monomers. Only a few 2-oxazoline monomers are available commercially; 2-methyl-2-oxazoline and 2-ethyl-2-oxazoline (sigma-aldrich and fisher scientific). This suggests that commercially there is little interest currently in developing functional poly(2-oxazoline)s as it involves a large amount of synthetic work to make the precursors. By developing applications and demonstrating the potential of poly(2-oxazoline)s it is hoped that more interest will be generated and lead to further commercialisation of 2-oxazolines. The initial stage of this project was to synthesise some useful monomers to create a small 'tool-kit' of monomers which can be combined to create functional materials.

There are two synthetic procedures which have been exploited to synthesise 2-oxazoline monomers: a 'one pot' Witte-Seeliger method which is useful for synthesising a large amount of monomer but has a low tolerance of functional groups; and a multi-step method which allows more complex monomers to be synthesised⁸⁷.

2.2 Monomer Synthesis

2.2.1 Witte-Seeliger Synthesis of 2-Oxazolines

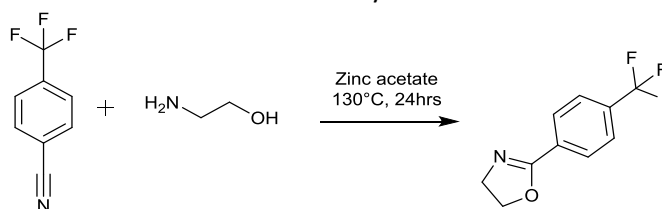
This method (Scheme 7), first reported by Witte and Seeliger allows 2-oxazolines to be easily synthesised using ethanolamine and the corresponding nitrile in the presence of a Lewis acid usually zinc or cadmium acetate^{4, 140}.



Scheme 7: Synthesis of 2-alkyl-2-oxazolines using the corresponding alkyl-nitrile

This method is an efficient and flexible reaction and has been shown to work for a wide range of nitriles⁸⁷. This reaction is useful as it allows large quantities (>100g) of monomer to be synthesised in one go.

In this project, 2-methyl-2-oxazoline and 2-ethyl-2-oxazoline were purchased commercially. 2-isopropyl-2-oxazoline (*i*PrOx) and 2-butyl-2-oxazoline (*n*BuOx) were synthesised in-house using the method illustrated in Scheme 7. A hydrophobic fluorinated monomer was also synthesised using this method according to Scheme 8, this monomer however was not used due to the very slow polymerisation times owing to the electron withdrawing effect of the fluorinated benzene ring.



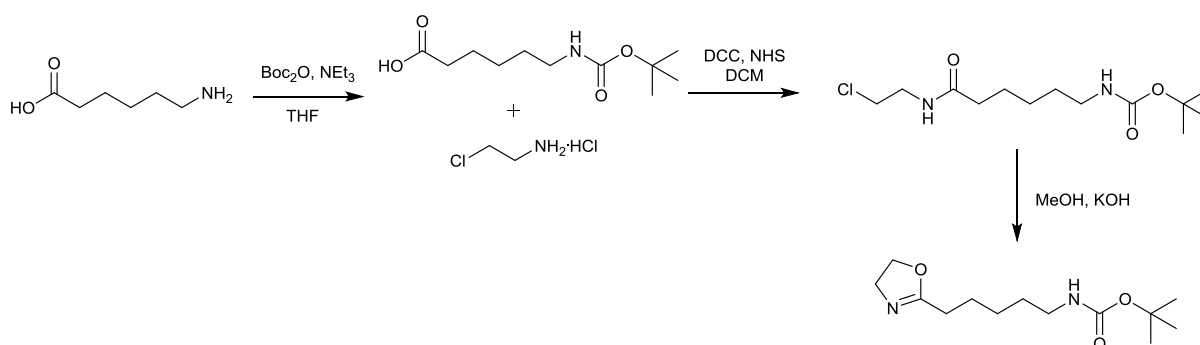
Scheme 8: Synthesis of a fluorinated 2-oxazoline

This 'one-pot' method has several limitations such as a low tolerance of functional groups, use of zinc or cadmium and associated toxicity of these elements and the release of ammonia during the reaction which can interfere in the polymerisation if it is not removed. Therefore the multistep route offers a convenient route to introduce functionality.

2.2.2 Multi-step Route to Functionalised 2-Oxazolines

Functional monomers are potentially useful for further modification of poly(2-oxazoline)s. As mentioned in the introduction, 2-oxazolines with a wide range of functional groups such as, amines¹⁴¹, carboxylic acids¹⁴², thiols¹⁴³ and alkenes¹⁴⁴ are possible to be synthesised. These are protected because nucleophilic heteroatoms interfere with the polymerisation and prematurely terminate it or induce side reactions.

An amine functionalised 2-oxazoline provides a convenient route for further functionalization of the polymer, particularly with regards to biological systems which often rely on amide coupling to introduce functionality. To synthesise an amine 2-oxazoline; a tert-butyloxycarbonyl (BOC) protected 5-(2-oxazoline)pentane-1-amine was prepared from an adapted published procedure according to Scheme 9¹⁴¹.

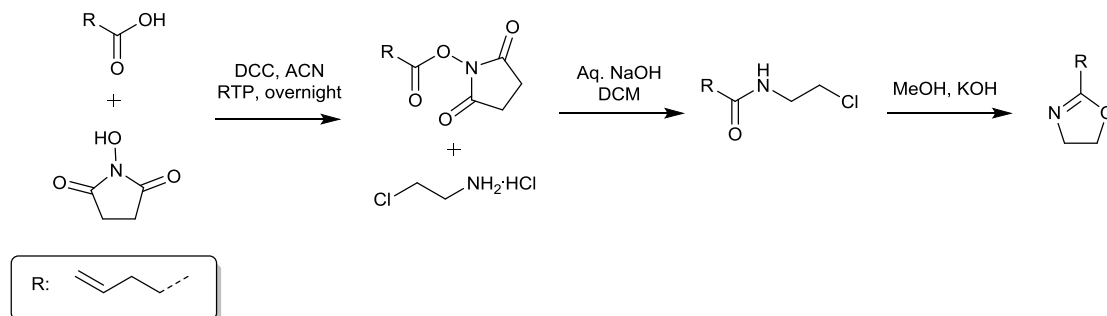


Scheme 9: Synthesis of BOC-protected 2-oxazoline

The amine was first protected according to a different procedure¹⁴⁵. The carboxylic acid was activated in the form of an *N*-hydroxysuccinimide (NHS) ester using *N,N'*-dicyclohexylcarbodiimide (DCC) instead of 1-ethyl-3-(3-dimethylaminopropyl)carbodiimide (EDAC) the latter having been reported previously in oxazoline synthesis¹⁴⁴. The succinimide ester was then reacted with 2-chloroethylamine (neutralised from 2-chloroethylammonium chloride)

Synthesis and Cloud Point Temperature Control to form the peptide bond. This was then subjected to a ring closure reaction in the presence of KOH to yield the BOC-protected amine in gram quantity.

This method was used to synthesise another potentially useful monomer functionalised with an alkene according to Scheme 10¹⁴⁴.



Scheme 10: Synthesis of an alkene and alkyne functionalised 2-oxazoline monomer

Poly(2-oxazoline)s with pendant alkene groups have been shown to be useful for utilising a thiol-alkene click reaction^{146, 147}.

2.3 Poly(2-oxazoline) Synthesis

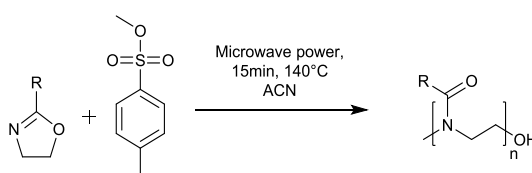
2.3.1 Polymer Synthesis

The method of choice for 2-oxazoline polymerisation utilises microwave irradiation instead of conventional heating. There are several benefits to using microwave irradiation^{148, 149}. These are;

- Fast reaction times, 10-15 minutes compared to 3 or 4 days.
- High concentration, 4M solutions.
- Suppression of undesired side products and hence lower polydispersity.
- Auto-loading system enabling up to 24 polymerisations in sequence.
- Accurate control over polymer length via initiator/monomer ratio.

The temperature was set to 135°C as over 140°C side reactions can occur⁶². The reaction time as 15 minutes.

The polymers were synthesized according to Scheme 11. The length was adjusted by varying the ratio of initiator to monomer.



Scheme 11: Synthesis of poly(2-oxazoline)

The standard method used to purify poly(2-isopropyl-2-oxazoline) (PiPrOx) is via dialysis in water followed by freeze-drying. The methyl and ethyl poly(2-oxazoline)s are precipitated in ether^{79, 150, 151}. It was desirable to develop a method to precipitate PiPrOx. Unlike Poly(2-methyl-2-oxazoline) (PMeOx) and poly(2-methyl-2-oxazoline) (PEtOx) precipitation in diethyl ether affords a sticky gum instead of a powdery precipitate, presumably the reason for PiPrOx to be purified via dialysis. It was found that precipitation of PiPrOx in a 3:1 mix of ether:hexane at 0°C creates the preferred white powder. The same was found for the PiPrOx co-polymers.

PiPrOx was initially focussed on due to the thermoresponsive behaviour it exhibits. Initial investigations centred around the dependence of the T_{cp} on composition and concentration. This knowledge enables functional thermoresponsive materials to be developed with a good understanding and prediction of the thermoresponsive behaviour.

Several different polymer samples were synthesised and are described in the next section.

2.3.2 Poly(2-isopropyl-2-oxazoline)

A range of different length PiPrOx were prepared.

2.3.2.1 Characterisation

The PiPrOx polymers of different lengths were characterised using SEC, Table 1.

| Polymer | M_w | M_n | PDI | repeating units [†] |
|----------|-------|-------|------|------------------------------|
| PiPrOx-1 | 13559 | 15469 | 1.14 | 137 |
| PiPrOx-2 | 24888 | 28027 | 1.13 | 248 |
| PiPrOx-3 | 30604 | 33110 | 1.08 | 293 |
| PiPrOx-4 | 36346 | 39454 | 1.09 | 349 |
| PiPrOx-5 | 39947 | 48138 | 1.21 | 425 |
| PiPrOx-6 | 53818 | 60948 | 1.13 | 539 |

[†]Based on M_n

Table 1: Characterisation of PiPrOx of different lengths

The polymers display the characteristic low PDI which can be expected from poly(2-oxazoline)s.⁶² The number of repeat units is calculated from the number average molecular weight (M_n) as opposed to the weight average molecular weight (M_w) because the M_n describes the overall molecular weight of population better than the M_w which is only the mean of the weights. This is an important consideration when analysing the T_{cp} as this could have a bearing on the temperature at which it displays the phase transition.

2.3.3 Poly(2-isopropyl-2-oxazoline)-co-(2-butyl-2-oxazoline)

2.3.3.1 Synthesis

Using the same method outlined previously, co-polymers can also be synthesised. To investigate the modulation of the T_{cp} of *PiPrOx* we synthesised a co-polymer using the more hydrophobic *nBuOx* monomer, Figure 21.

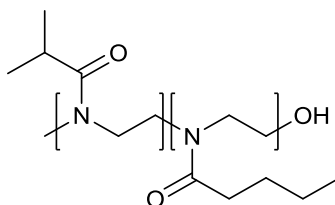


Figure 21: Structure of a *PiPrOx-nBuOx* co-polymer

To ascertain the effect of co-polymerisation with a more hydrophobic monomer on the T_{cp} , a range of polymers having different percentage composition but with the same molecular weight were synthesised. These are tabulated below in Table 2.

| Polymer | molar % butyl* | M_w | M_n | PDI | Repeat units [†] |
|------------------------|----------------|-------|-------|------|---------------------------|
| <i>PiPrOx-nBuOx</i> -1 | 6.2 | 25256 | 14649 | 1.72 | 128 |
| <i>PiPrOx-nBuOx</i> -2 | 11.9 | 24026 | 14788 | 1.62 | 129 |
| <i>PiPrOx-nBuOx</i> -3 | 21.4 | 23735 | 13587 | 1.74 | 117 |
| <i>PiPrOx-nBuOx</i> -4 | 31.8 | 22950 | 13466 | 1.7 | 114 |
| <i>PiPrOx-nBuOx</i> -5 | 41.1 | 20282 | 12298 | 1.64 | 103 |

[†]Based on M_n . *Calculated from ¹H NMR

Table 2: poly(2-isopropyl-2-oxazoline)-co-(2-butyl-2-oxazoline)

The PDI was slightly higher for these samples than for the *PiPrOx* samples. This is possibly due to slightly more impurities getting into the vessel because of the use of two separate monomers. The PDI value is sufficiently low that it should not affect the T_{cp} measurement's accuracy. As with *PiPrOx*, the number of repeat units is calculated from the M_n for the reasons outlined earlier.

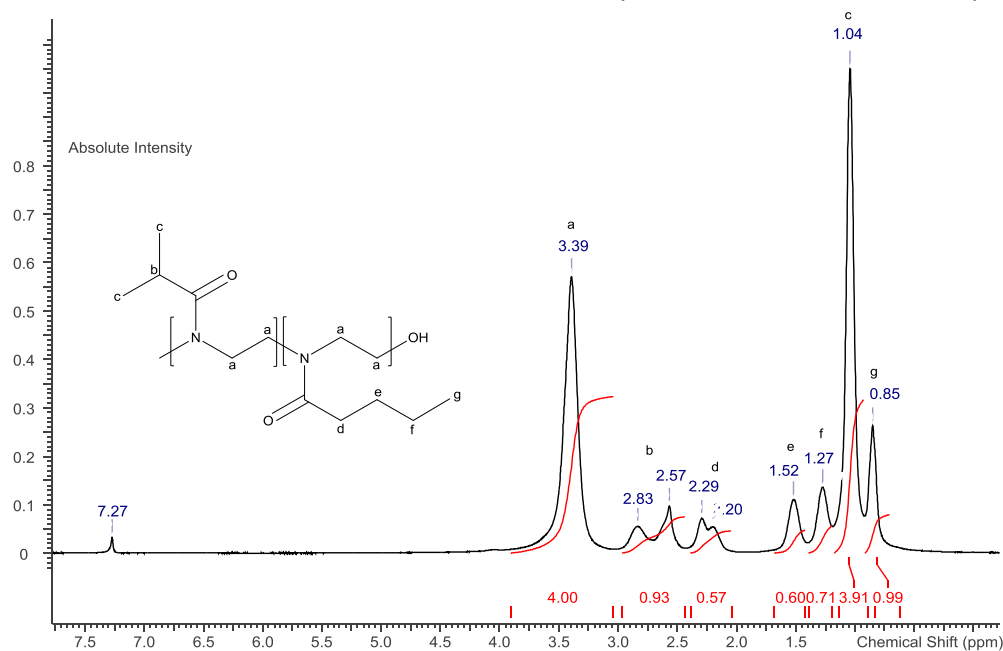


Figure 22: Representative NMR of PiPrOx-PnBuOx.

Figure 22 shows a representative NMR of a PiPrOx-*n*BuOx co-polymer. The relative proportion of PiPrOx and PnBuOx was calculated by comparing the CH₂ backbone resonance (*a*) to the CH peak of the isopropyl peak (*b*) and the CH₂ of the butyl chain (*e*). The peaks *a* and *e* were selected as they have no overlap with the corresponding co-monomer.

2.3.4 Poly(2-isopropyl-2-oxazoline)-co-(5-(2-oxazoline)pentan-1-amine)

The co-polymer poly(2-isopropyl-2-oxazoline)-co-(5-(2-oxazoline)pentan-1-amine) PiPrOx-NH₂ was synthesised via a BOC-protected intermediate (PiPrOx-BOC), Figure 23.

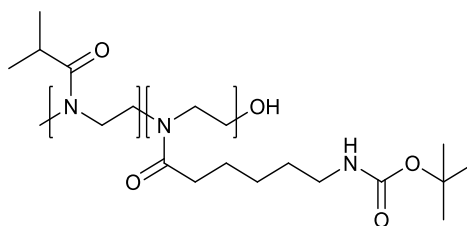


Figure 23: Structure of a PiPrOx-BOC co-polymer

Several polymers were synthesised and the percentage of BOC calculated, Table 3.

| Polymer | molar % BOC* | Terminal group |
|--------------|--------------|----------------|
| PiPrOx-BOC-1 | 11.9 | OH |
| PiPrOx-BOC-2 | 2.4 | OH |
| PiPrOx-BOC-3 | 2.7 | Rhodamine B |

*Calculated from ¹H NMR

 Table 3: ¹H NMR analysis of poly(2-isopropyl-2-oxazoline)-co-(2-pentan-1-amine-2-oxazoline)

The percentage of Boc-co-monomer was calculated by comparing the integrals of the two respective co-monomers in the NMR, Figure 24.

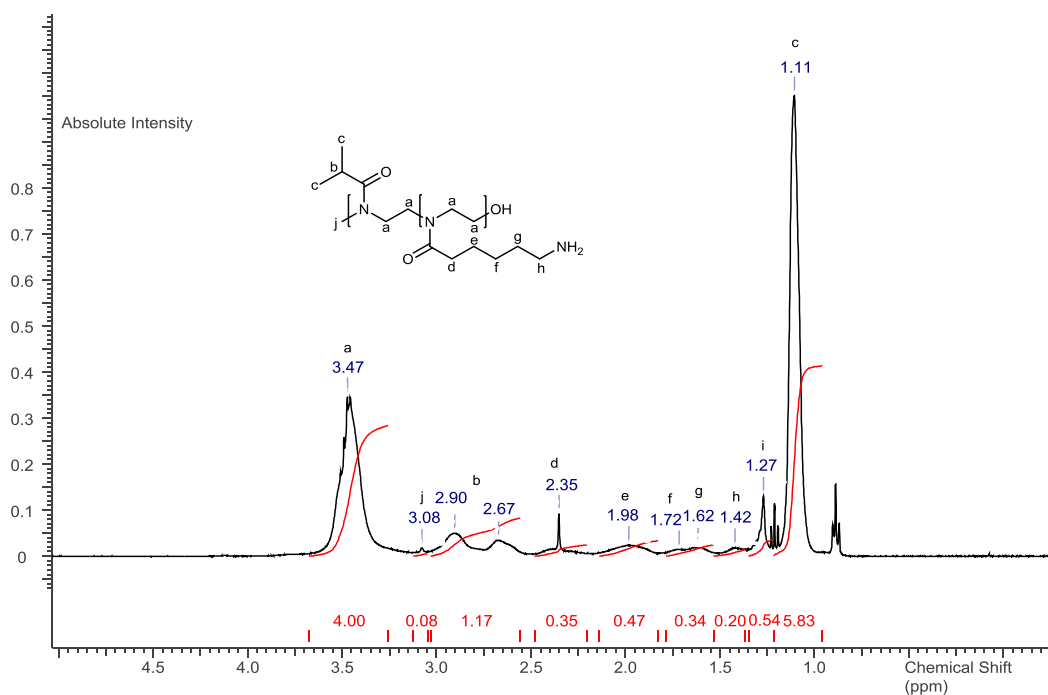
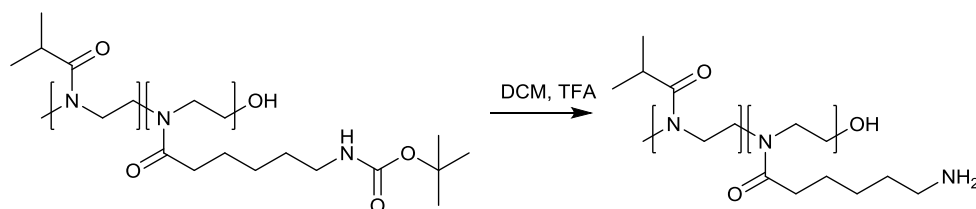


Figure 24: NMR of PiPrOx-NH₂-1.

The BOC protecting groups were then deprotected using trifluoroacetic acid (TFA) as has been reported for similar polymers¹⁴¹, Scheme 12.



Scheme 12: Deprotection of PiPrOx-BOC using TFA

The product was characterised using NMR to determine if deprotection had occurred.

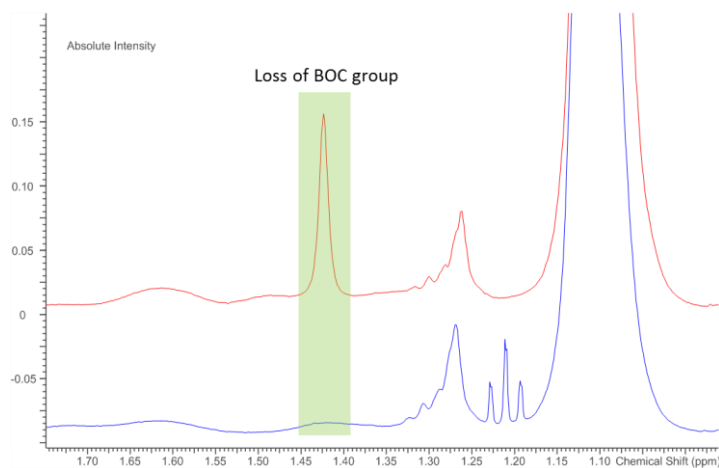


Figure 25: NMR of PiPrOx-BOC-1 (red) and PiPrOx-NH₂-1 (blue) illustrating the loss of the BOC group

Figure 25 shows the loss of the *tert*-butyl peaks after deprotection, this loss of BOC resonance after deprotection has been reported elsewhere¹⁴¹. Characterisation of these polymers is shown in Table 4.

| Polymer | molar % amine * | Terminal group |
|---------------------------|-----------------|----------------|
| PiPrOx-NH ₂ -1 | 11.9 | OH |
| PiPrOx-NH ₂ -2 | 2.4 | OH |
| PiPrOx-NH ₂ -3 | 2.7 | Rhodamine B |

*calculated assuming 100% deprotection

Table 4: Polymers after BOC deprotection

2.3.5 End-Group Functionalization

2.3.5.1 Initiation

Several initiators have been used to add functionality to the initiating end of the polymer. These are shown in Figure 26.

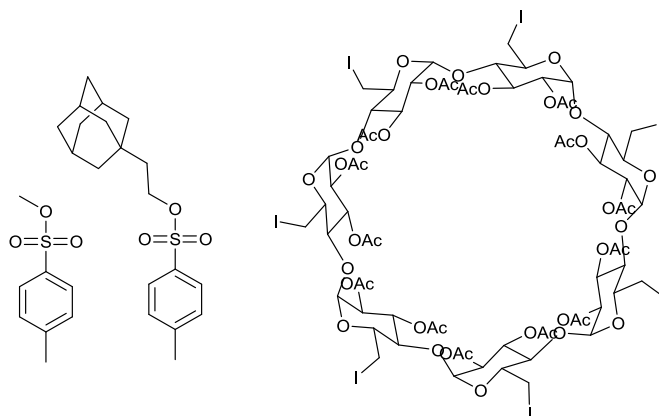


Figure 26: Different *p*-toluenesulphonate initiators used

The adamantane moiety at the end of a polymer was chosen as adamantane moieties display a well-characterised host-guest interaction with β -cyclodextrins¹⁵². The β -cyclodextrin initiator it was hoped would provide the same host-guest binding as with the adamantane initiator but offering the reverse¹⁵³. This could be useful for developing interesting self-assembling supramolecular architectures which will be discussed later.

Work was carried out to try and introduce an amine group via initiation. This was based on previously published work which used a BOC-protected aromatic amine¹⁵⁴. An aromatic amine would be less reactive than an aliphatic amine so two more reactive initiators were attempted to be synthesised, both were unsuccessful for different reasons as illustrated in Figure 27 below.

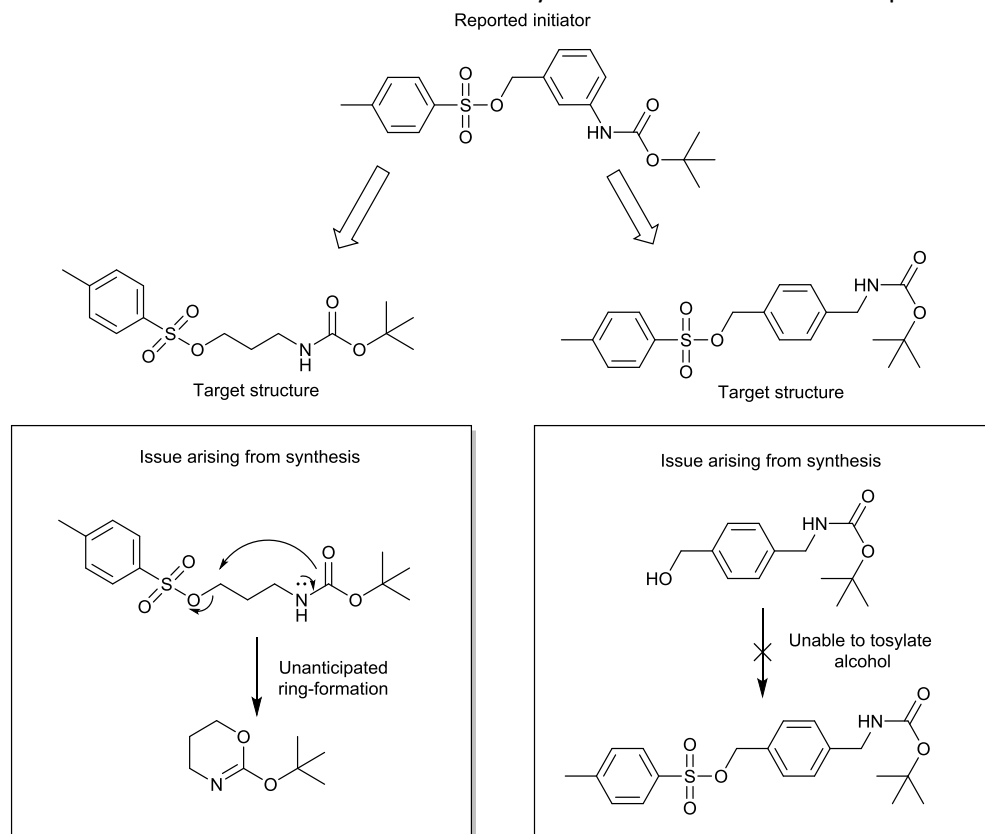


Figure 27: Attempted synthesis of a BOC-protected amine initiator

Our initial attempt to replace the benzene ring was successful however the initiator wasn't stable as an unanticipated ring formation occurred. The intramolecular ring formation could be followed via NMR on a purified sample of the initiator. To prevent this we inserted a benzene ring to prevent folding of the initiator however the tosylation of the alcohol was unsuccessful after attempting several different conditions. It is suggested that this same process occurred in the second initiator except the reaction was an intermolecular substitution. Only starting material was ever recovered from the reaction. It is worth noting neither of the target structures were known molecules.

2.3.5.2 Termination

The nucleophilic termination of poly(2-oxazolines) is another avenue which has been exploited to help expand functionality. Two useful terminators have been used; rhodamine B and diaminopropane, Figure 28. Rhodamine B is a fluorescent dye which can be used to tag the polymer allowing it to be imaged using fluorescence spectroscopy; this can be useful for biological applications. The use of rhodamine B was inspired by the published use of fluorescein⁸³. rhodamine B was chosen over fluorescein as it is soluble in ether so removal of excess rhodamine B can be done in the same step as precipitation. Fluorescein is not soluble in ether making purification more difficult.

The diamine was used to add a terminal amine onto the end of the polymer. A large excess of amine prevented coupling of polymer chains. The precedent for this was the use of a dicarboxylic acid to add a terminal carboxylic acid to the end of the polymer⁸¹.

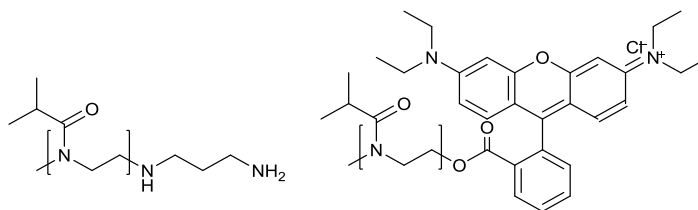


Figure 28: Structures of different terminated PiPrOx
Amine terminated PiPrOx (left), rhodamine B terminated PiPrOx (Right)

Proving the attachment of the two end groups is difficult as they could not be detected in the NMR as the long length of the polymer meant the small signals were lost in the noise of the spectra. Rhodamine B has characteristic aromatic peaks which can be seen in the NMR but this does not actually prove attachment. For the rhodamine B-terminated polymers the attachment can be inferred from the bright pink colour that, after several precipitations, is no longer apparent in the ether filtrate but stays with the precipitated polymer.

As the amine terminal group is not coloured it is more difficult to prove attachment. The only evidence that the amine group was present is that when the polymers were used (Chapter 6) they were successfully reacted. The rhodamine B terminated polymers are listed and discussed in more depth in Section 3.5 and the amine terminated polymers can be found in Section 6.3.

2.3.6 Summary

Synthesis of different poly(2-oxazoline)s has been demonstrated, effectively controlling length and structure. Several potentially useful monomers were synthesised, some of which were incorporated into co-polymers. Functionality was also introduced using different initiators and terminators.

2.4 Cloud Point Temperature Control

2.4.1 Introduction

Using the polymers synthesised in the previous section we can begin to characterise the T_{cp} behaviour of poly(2-oxazoline)s.

2.4.2 Cloud Point Temperature Determination

Conventionally T_{cp} determination of poly(2-oxazolines) is carried out using dynamic light scattering (DLS)^{147, 155-158} or turbidimetry^{71, 158-160}. We have used two methods to determine the T_{cp} the first of these is conventional turbidimetry which involves monitoring transmission of light

Synthesis and Cloud Point Temperature Control through a sample. When the temperature is increased the transmission decreases as the solution becomes opaque above the T_{cp} of a polymer. The second method uses fluorescence spectroscopy to determine the T_{cp} of a polymer.

2.4.2.1 Turbidimetry

Turbidimetry measurements involved the use of an ultraviolet and visible spectrometer (UV-Vis) to measure the transmission of a sample at 550nm. The spectrometer is fitted with water circulation around the sample to allow the temperature to be controlled. Using a pump and a heater/stirrer plate the temperature in the chamber can be increased or decreased. A thermocouple is then inserted into the sample so an accurate temperature can be obtained. This set-up is illustrated in Figure 29.

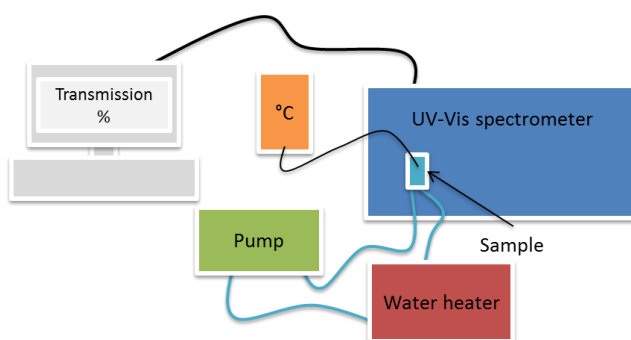


Figure 29: Set-up for measuring the cloud point temperature using a UV-Vis spectrometer

An example of the change in transmission against temperature for PiPrOx is shown in Figure 30.

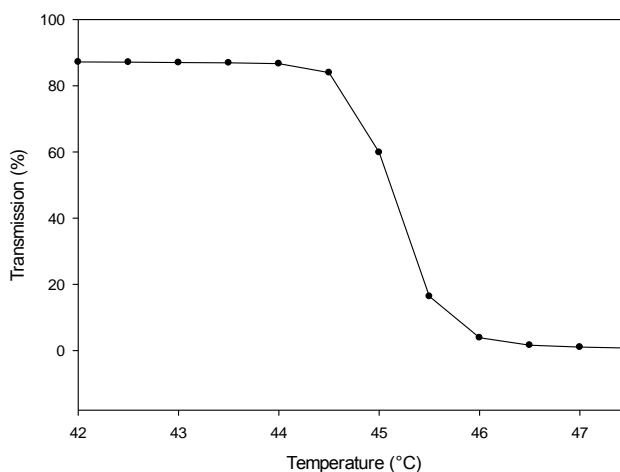


Figure 30: The change in transmission of PiPrOx-1 as it is heated

2.4.2.2 Fluorescence

Rhodamine B

Monitoring fluorescence of a sample as a function of temperature offers an alternative approach to T_{cp} determination. Four samples can be analysed simultaneously and the spectrometer is equipped with a temperature-controlled stage. Fluorescence has been used before in poly(2-

Synthesis and Cloud Point Temperature Control oxazoline) analysis, mainly to analyse micelle formation with thermoresponsive block co-polymers, specifically using pyrene as a fluorescent probe^{74, 150, 151, 161, 162}. By monitoring the peak emission of rhodamine B (581nm) over a temperature range we can detect changes in the intensity of the emission peak, these changes are due to the thermoresponsive transition of the polymer.

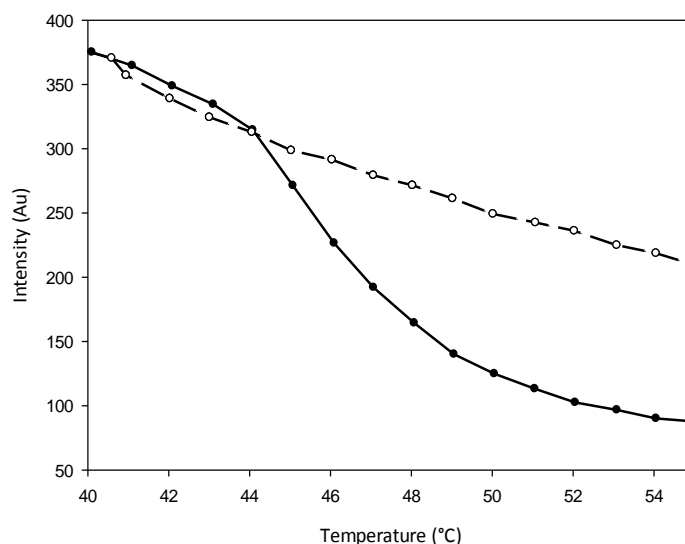


Figure 31: Fluorescence of rhodamine B and PiPrOx-2 as the samples are heated
PiPrOx-2 and rhodamine B (●), rhodamine B only (o)

Figure 31 illustrates the change in fluorescence for PiPrOx-2. When the polymer undergoes the phase transition the solution becomes opaque and therefore less light passes through and the fluorescence decreases. It should be noted that rhodamine B fluorescence is temperature dependent, explaining the decrease in intensity over the observed range for the rhodamine B control.¹⁶³

Dansic acid

Although the majority of work has been using rhodamine B as the dye, we also looked into using dansic acid as the fluorescent T_{cp} indicator. Dansic acid is derived from dansyl chloride which undergoes hydrolysis in water to make the sulphonic acid. Whilst dansyl chloride is often used as an amine reactive fluorescent tag; the use of the acid derivative has not been investigated in any great depth. The acid did not have a published crystal structure so it was initially characterised by single crystal X-ray diffraction (see Figure 32).

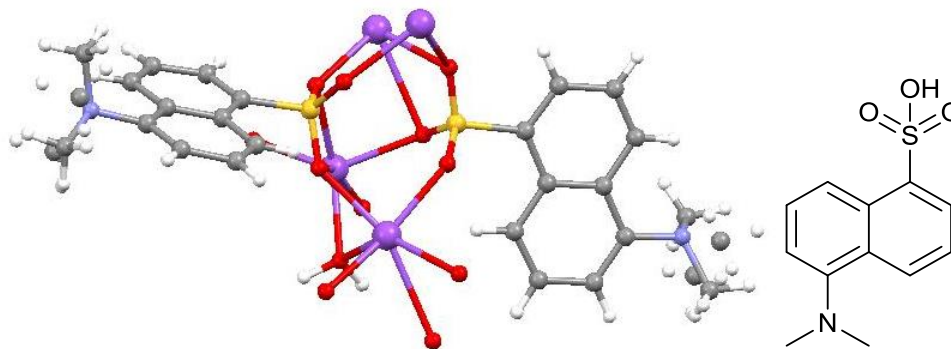


Figure 32: Structure of Dansic acid
 Dansic acid (right), crystal structure of dansic acid with bridging sodium (left)

We investigated the fluorescent properties of dansic acid and found that it displays unusual fluorescent behaviour, in particular when used to monitor the T_{cp} transition of poly(2-oxazoline)s, Figure 33.

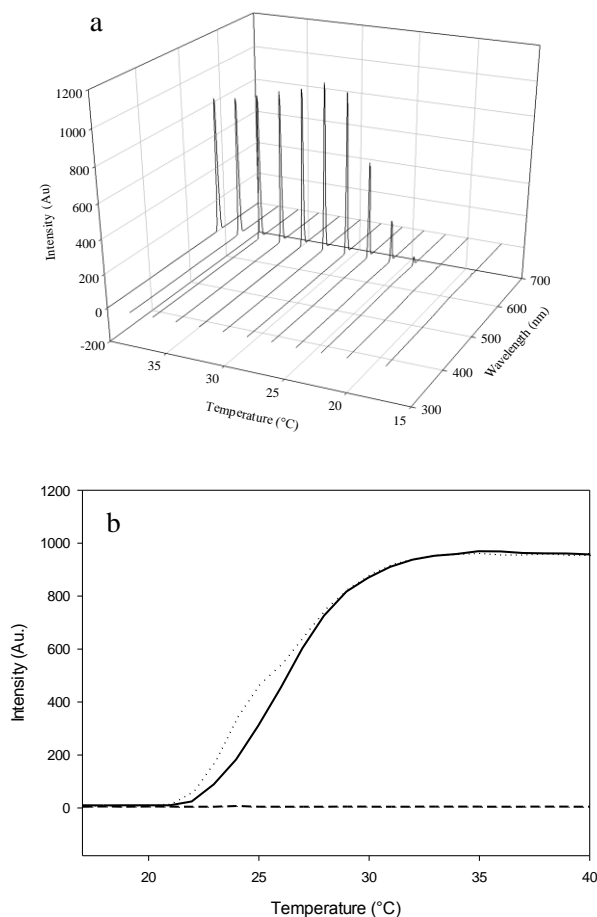


Figure 33: Fluorescence of dansic acid in solution with a thermoresponsive polymer
 A 4mg ml⁻¹ solution of *PiPrOx-nBuOx-3* in water was used. The two graphs show; a) narrow emission of dansic acid above the T_{cp} of *PiPrOx-nBuOx-3*, b) Heating cooling cycle of *PiPrOx-nBuOx-3* monitoring the emission at 582nm, heating (solid line), cooling (dotted line), dansic acid without *PiPrOx-nBuOx-3* (dashed line)

The major absorption of the dye was found to occur at 292nm with the corresponding emission at 582nm, this is an unusual large wavelength shift of almost 300nm. Furthermore, it only

Synthesis and Cloud Point Temperature Control displays fluorescence in water when the polymer is above the T_{cp} . Such a solvatochromatic response is observed for other dyes such as pyrene as was mentioned previously. What makes dansic acid unusual is that it displays negligible fluorescence in water despite being soluble and the presence of a narrow and well-defined emission peak above the T_{cp} .

2.4.3 Comparison of Methods

We can then compare the T_{cp} values obtained from turbidimetry and fluorescence methods. Both the transmission and fluorescence T_{cp} values are calculated from a 10% change as opposed to a 20% as is usual. This is due to the turbidimetry measurements being taken at a 10% change.

Both methods were found to give consistent results and are shown when relevant in the following sections.

2.4.4 Effect of M_n

The effect of molecular weight on the T_{cp} transition was investigated. Using the PiPrOx samples synthesised previously the T_{cp} transition was characterised using the turbidimetry and fluorescence techniques. The fluorescence data is shown in Figure 34. This allows a comparison to be drawn between the two techniques, Figure 35.

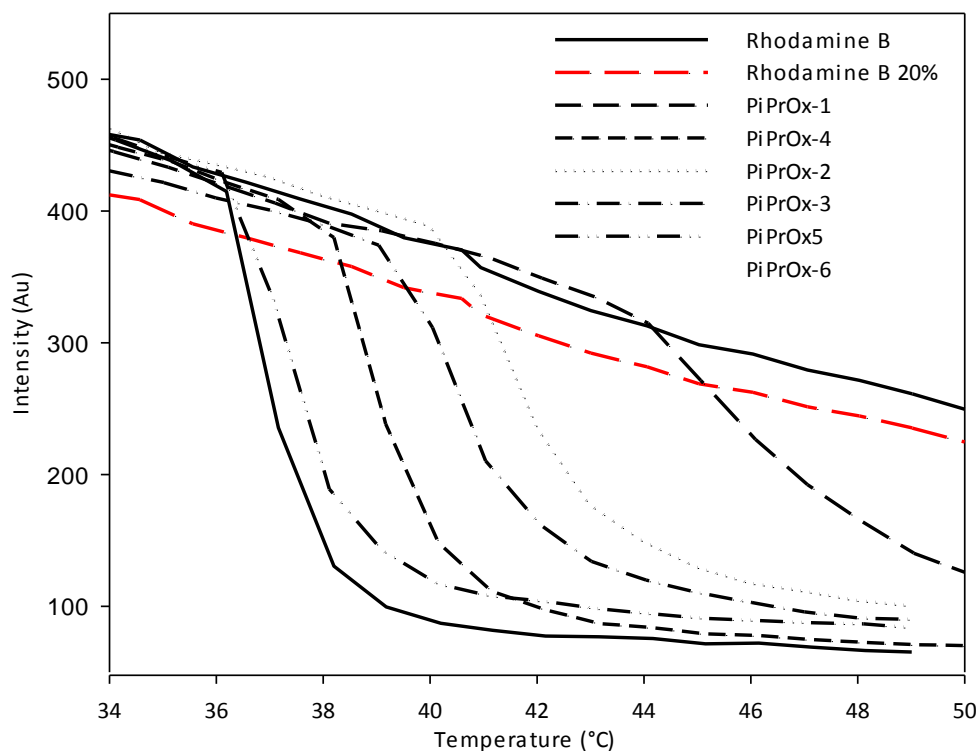


Figure 34: Temperature dependent fluorescence of 4mg ml⁻¹ solutions of PiPrOx with different M_n

By defining the T_{cp} temperature as the temperature at which the fluorescence has dropped by 20% [indicated by the rhodamine B 20% line (red)] we can plot the T_{cp} temperature against molecular weight.

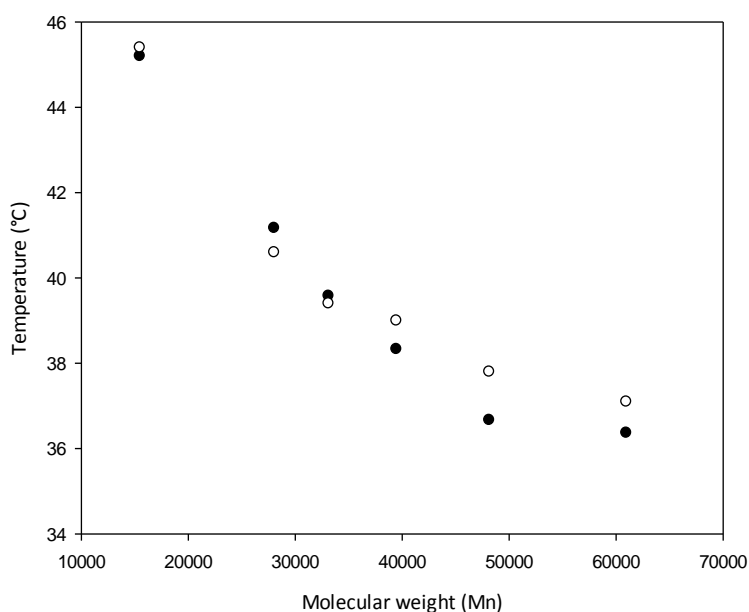


Figure 35: Comparison of the two T_{cp} determination methods Fluorescence (●) and turbidimetry (○) with 4mg ml^{-1} solutions of P/PrOx with different M_n

The T_{cp} weight dependence of poly(2-isopropyl-2-oxazoline) is apparent from this plot, displaying a difference of almost 10°C over the molecular weight range considered. There has been several investigations into the molecular weight dependence of T_{cp} for poly(2-isopropyl-2-oxazoline) and our results are consistent with that reported^{79, 131, 133}. The explanation behind the M_n dependence is that as the polymers increase in length they become more entangled. This entanglement contributes to a reduced amount of water solvated around the polymer, or less ordering. This means that less energy is required to reach the T_{cp} and with a consequent decrease in T_{cp} .

2.4.5 Effect of Media and Concentration

So far all the samples were analysed using solutions containing a concentration of 4mg ml^{-1} . The effect of concentration however must also be considered, especially for any applications which involve higher concentrations of materials. Another consideration is that biological materials have to function with other additives such as enzymes and salts. These could also have an effect on the T_{cp} . Two sets of samples were analysed using turbidimetry, both sets having a range of concentrations and the solvents used were deionised water and cell media to compare the effect of using cell media on the T_{cp} , Figure 36.

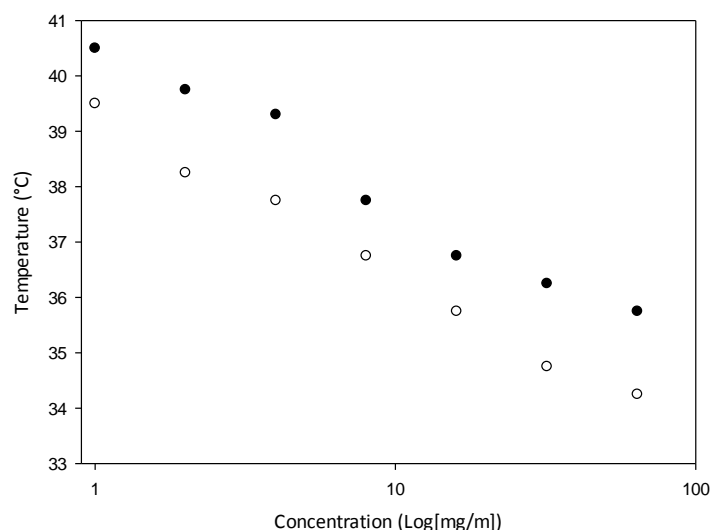


Figure 36: Effect of concentration on T_{cp} in two different solutions
Water (●), cell media (○)

Increasing the concentration causes the T_{cp} to decrease logarithmically. This can be explained by thinking in terms of entanglement. The more polymer in a sample the more entangled it is and thus the less water which needs to be de-solvated hence the lower the T_{cp} .

The concentration dependence raised an interesting problem. If the polymer's T_{cp} is concentration dependent and the polymers T_{cp} is also molecular weight dependent then the T_{cp} change upon changing the molecular weight is inaccurate. This was investigated for the different molecular weight polymers, Figure 37.

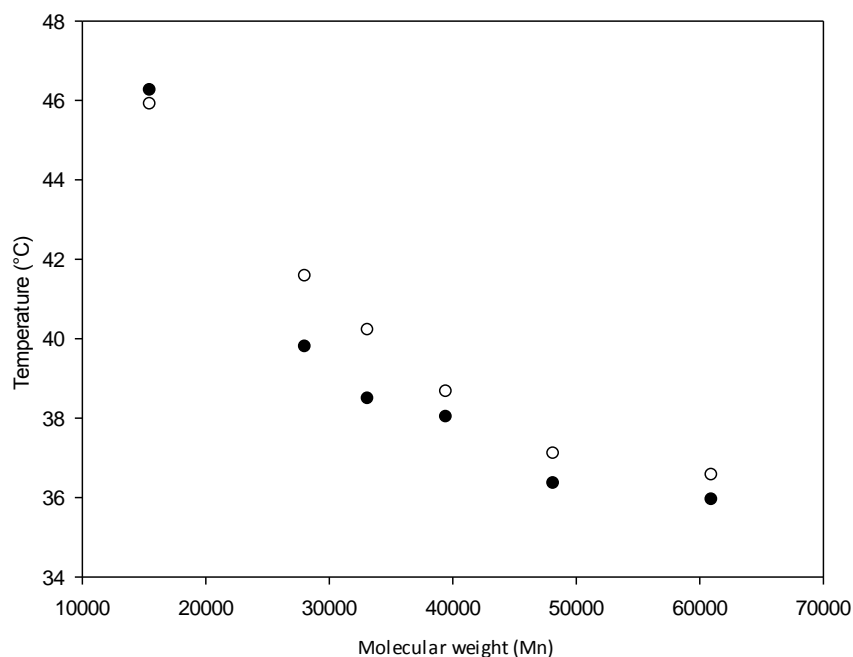


Figure 37: T_{cp} dependence using either the same weight or concentration
4mg ml⁻¹ (○), 258μM (●)

A similar concentration was chosen to that used for the 4mg ml⁻¹ samples. The samples T_{cp} values are reasonably similar and do not seem to change by a large amount. This is important to know as when using these polymers for an application they won't necessarily have the same concentration or weight but hopefully the T_{cp} should be reasonably comparable nonetheless.

2.4.6 Co-polymerisation

2.4.6.1 Poly(2-isopropyl-2-oxazoline)-co-(2-butyl-2-oxazoline)

The 2-butyl-2-oxazoline (*n*BuOx) co-polymers were also investigated to see how co-polymerisation with a more hydrophobic monomer would affect the T_{cp} . Previously published work showed that this would decrease the T_{cp} ⁴, something which would be desirable if the T_{cp} is over 37°C. Using both T_{cp} determination methods the T_{cp} for each co-polymer was analysed. Figure 38 below compares the T_{cp} for the two methods.

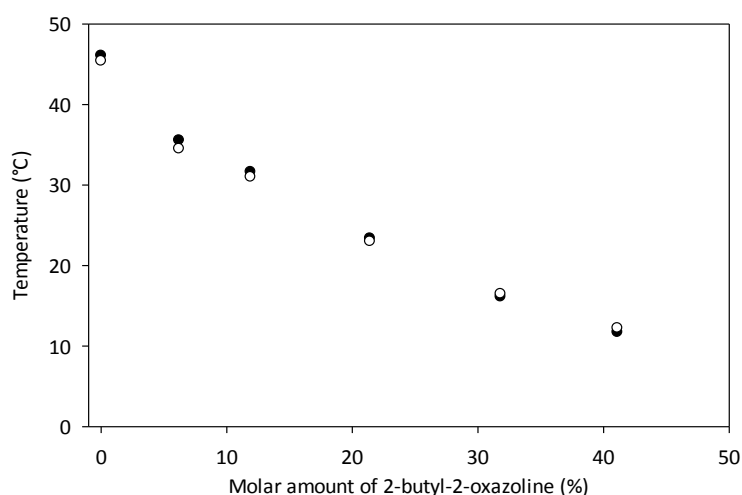


Figure 38: T_{cp} dependence on hydrophobic butyl monomer percentage
All solutions were 4mg ml⁻¹, fluorescence method (●) transmission method (○)

By co-polymerising *i*PrOx with the more hydrophobic *n*BuOx the T_{cp} can be decreased by a considerable amount. For biological applications a range of 20-30°C would be the most applicable. Again the two methods seem comparable. The zero percentage butyl oxazoline (*Pi*PrOx-2) has been included as it has a similar M_n to that of the butyl co-polymers.

2.4.6.2 Poly(2-isopropyl-2-oxazoline)-co-(2-pentan-1-amine-2-oxazoline)

For the amine co-polymers the BOC-protected amine and deprotected amine are different in terms of polarity. The BOC-protected oxazoline should have a much lower T_{cp} than the deprotected amine which will be much more polar. Dansic acid was used to monitor the T_{cp} change (see Figure 399).

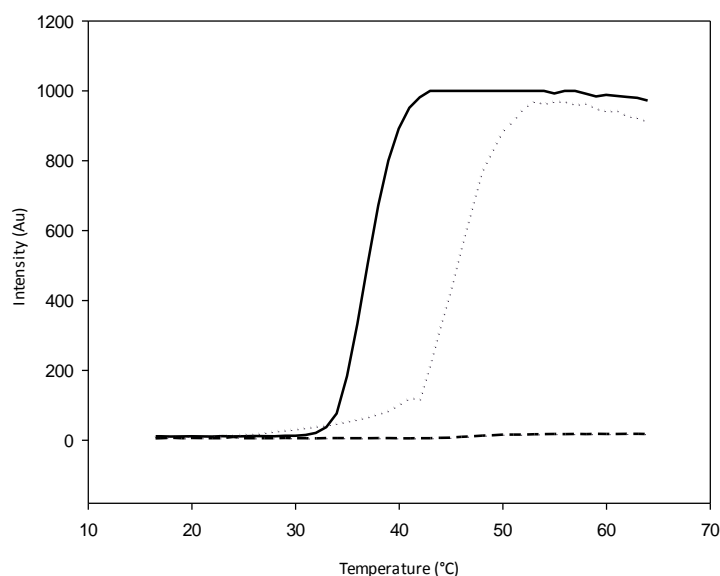


Figure 39: T_{cp} change upon BOC-deprotection of PiPrOx-BOC-1
 Dansic acid was used to indicate the T_{cp} . Heating curves only. PiPrOx-BOC-1 (solid line), PiPrOx-NH₂-1 (dotted line),
 dansic acid only (dashed line)

As expected the deprotection of the amine causes a shift of around 10°C indicating that the polymer is more polar which is consisted with deprotection having occurred.

2.4.7 Summary

The cloud point behaviour of poly(2-oxazoline)s has been investigated varying functionality and co-polymer composition. Control has been demonstrated and biologically relevant temperatures have been achieved.

2.5 Conclusions

In conclusion, we have successfully demonstrated the synthesis and control of various poly(2-oxazoline) polymers and their corresponding monomers. This includes the investigation of several useful functional moieties such as fluorescent tags and reactive groups. We have demonstrated control over the T_{cp} of these polymers using two techniques to characterise this phase transition.

Chapter 3 Cell Selective Surfaces

3.1 Introduction

3.1.1 Polymer Surfaces

As mentioned in the introduction PN/PAAm surfaces have become popular areas of research. A potentially interesting application would be to develop poly(2-oxazoline) surfaces which display thermoresponsive behaviour similar to that of PN/PAAm based systems. Several published papers have documented various ways to attach poly(2-oxazoline)s to surfaces such as glass¹⁶⁴, silicon^{165, 166} and gold¹⁶⁷. These also claimed that such surfaces have thermoresponsive properties. Before thermoresponsive surfaces can be developed it would be important to establish the nature of cellular behaviour on poly(2-oxazoline) surfaces.

3.1.2 Thermoresponsive Surfaces

Cell-sheet technology is an emerging field which relates to tissue engineering. Traditionally cells which are grown on conventional materials in the laboratory are harvested by disaggregating the extra cellular matrix (ECM)¹⁶⁸. The extra cellular matrix is the part of tissue that provides support for the cells and fulfils other important functions such as providing adhesion to surfaces and giving the cells a sense of orientation when anchoring themselves. When the ECM is disaggregated, using an enzyme called trypsin, a proteolytic enzyme which breaks down proteins into polypeptides or amino acids, and ethylenediaminetetraacetic acid (EDTA) which chelates Ca^{2+} and Mg^{2+} ions, key surface proteins and structures will be damaged. From a tissue engineering perspective the loss of structure is counterproductive, Figure 40.

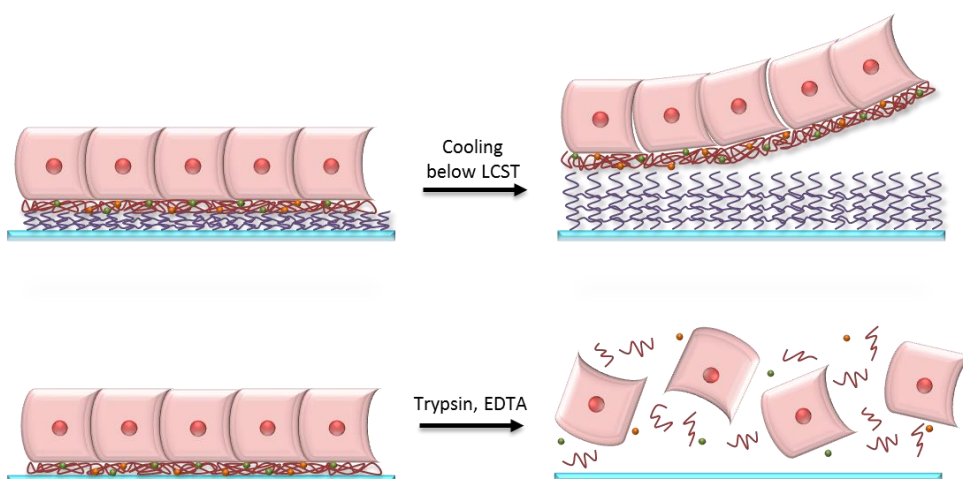


Figure 40: Illustration of cell release via different methods
A thermoresponsive surface (top) or a conventional method (bottom)

Thermoresponsive surfaces offer a method for removing the cell-sheet without having to use trypsin or EDTA. This is achieved by changing the temperature in order that a surface which is cell

adherent at 37°C becomes a non-adherent surface below the T_{cp} . There are two strategies which have been used. The more popular method is to attach the thermoresponsive polymer covalently to the surface¹⁶⁹. The other involves coating the tissue culture plate with a thermoresponsive layer on which the cells grow but which can be dissolved by lowering the temperature, thus releasing the cells¹⁷⁰.

The covalent approach has proved to be more popular as it is simple and avoids the issue of polymer removal which is the problem with the coating method. Nearly all the research to date has involved PNIPAAm-functionalised surfaces.

3.1.2.1 Fabrication Methods of Thermoresponsive PNIPAAm Surfaces

There are four methods for attaching PNIPAAm to surfaces covalently.

- Radiation induced graft polymerisation
- “Grafting to” approach
- “Grafting from” approach
- Surface-initiated living radical polymerisation (using ATRP)

Radiation-induced polymerisation involves irradiating a solution of monomers to create a covalently bound layer of polymer on the surface. The types of radiation can include UV¹⁷¹; electron beam¹⁷²; plasma activation and plasma polymerisation¹⁷³⁻¹⁷⁵. “Grafting to” the surface involves synthesising a polymer with a functional group and reacting this with an appropriately functionalised surface^{176, 177}. This has a limitation in that the density of the grafted polymer on the surface is low because of the sterically limited reactivity of the surface groups⁴⁸. “Grafting from” is the reverse; a surface is functionalised with an initiator as a result of which the polymer is grown from the surface¹⁷⁸⁻¹⁸⁰. This has the benefit of allowing the formation of denser layers than the “grafting to” approach. Surface-initiated ATRP has attracted attention recently as it allows for the formation of brush surfaces^{181, 182}. The polymer brush layers show properties which are different from the “grafting from” and “to” approaches⁴⁸.

3.1.2.2 Cell Detachment and Control

When the cells are confluent (i.e. the cells have come together to form an interlinked sheet) on a thermoresponsive surface and are ready to be harvested, the temperature is lowered, usually by washing the coated surface with cold cell media, and incubating the cells at a lower temperature for a defined period of time. As the cells detach their cellular contractile forces are no longer supported by the adhesion to the surface and they begin to contract, eventually forming multi-cellular spheroids⁴⁶. To prevent this, a membrane is placed on top of the cells to which they adhere. This allows the cell sheet to be removed and the cells to be transferred. The cells are

then placed wherever they are required and the transfer membrane usually spontaneously detaches from the cells when media is added to it. The mechanism of detachment has been the subject of several papers since if this can be understood, the thermoresponsive coatings can then be fine-tuned to improve adhesion and detachment^{181, 183-185}.

3.1.2.3 Important Factors

There are some important parameters which have to be taken into account when developing thermoresponsive surfaces.

There is an optimal density of polymer chains on the surface of approximately $1.4 \mu\text{g cm}^{-1}$. Any surface with a density lower or higher than $0.8\text{-}2.2 \mu\text{g cm}^{-1}$ will probably not be thermoresponsive which will prevent any harvesting of cells¹⁸¹. This density is directly related to the thickness of the layer, and means that an optimal thickness of around 20nm is also important, otherwise the polymer can be too hydrated or not hydrated enough¹⁸¹.

The substrate on which the polymer is grafted also makes a difference. For example PNiPAAm has been shown to have different behaviour on glass surfaces than on tissue culture poly(styrene) (TCPS)¹⁸⁶.

3.1.3 Cell Selective Surfaces

Very little work has been reported investigating the behaviour of cells on poly(2-oxazoline) surfaces. Two papers have been published, one of which explored endothelial cell adhesion on PEOx¹⁶⁴, demonstrating that PEOx surfaces are cell compatible substrates. The second investigated PMeOx bottle-brush brush surfaces, concluding that the protein-repellent surface of PMeOx effectively prevents cell adhesion and growth¹⁸⁷. To study poly(2-oxazoline) surfaces further, it was desirable to develop a method which allows a range of poly(2-oxazoline)s to be covalently immobilised on a glass surface in a simple and reproducible way. These were then characterised based on cell behaviour when interacting with these surfaces.

It was anticipated that by comparing the behaviour of different cells on the different polymer coatings, a polymer surface could be chosen which will encourage one cell type to grow over another.

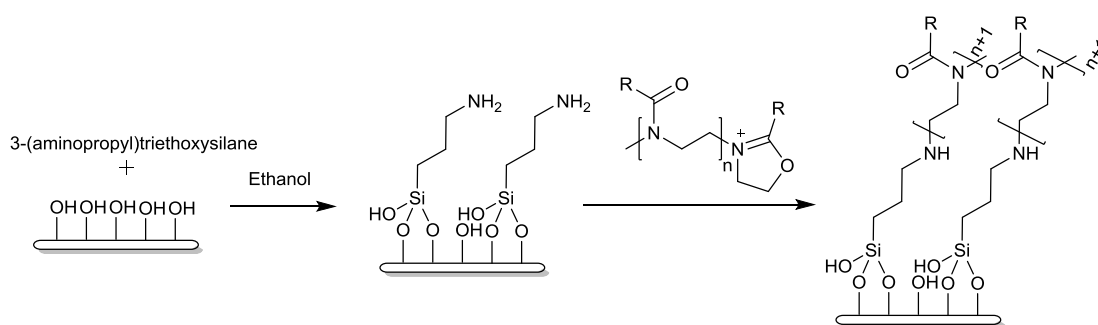
3.2 First Generation Cell Selective Surfaces

3.2.1 Overview

The polymer surfaces had several requirements which needed to be met. The method must be versatile and simple allowing a large number of surfaces to be synthesised affording a series of different poly(2-oxazoline) coatings.

3.2.2 Method

Several approaches were attempted initially. These were based on a 'grafting to' methodology whereby the poly(2-oxazoline)s were first synthesised with a glass-reactive functional group and then attached to the surface. This retained the control over the poly(2-oxazoline) polymerisation and then allowed surface attachment. An amine-functionalised silane has been used previously^{166, 188} to terminate the polymer. When the method was being developed P*i*PrOx and P*n*BuOx could not be precipitated so the method was adjusted to skip the purification step. The surface was first coated with an amine. The amine surface was then used to terminate the polymer growth, resulting in a covalent attachment to the surface according to the Scheme 13.



Scheme 13: Synthesis of poly(2-oxazoline) 'grafted to' surfaces

3.2.3 Synthesis

Four types of polymer surface were synthesised; these were the methyl, ethyl, isopropyl and butyl poly(2-oxazoline)s. To characterise the cell behaviour on each surface at least 3 batches of surface were required for each polymer type. Each batch had to cover all the tests which were required to characterise the cells. Table 5 summarises the batches and number of slides synthesised.

| Polymer | Batch number | Number of slides | Total | Overall total |
|---------|--------------|------------------|-------|---------------|
| PMeOx | 1 | 38 | 117 | 491 |
| | 2 | 37 | | |
| | 3 | 42 | | |
| PEtOx | 1 | 36 | 121 | |
| | 2 | 42 | | |
| | 3 | 43 | | |
| PiPrOx | 1 | 42 | 123 | |
| | 2 | 40 | | |
| | 3 | 41 | | |
| PnBuOx | 1 | 42 | 130 | |
| | 2 | 46 | | |
| | 3 | 42 | | |

Table 5: Number of glass slides synthesised

3.3 Characterisation Techniques

The surfaces were characterised using a range of techniques, the quickest and easiest of which involved contact angle measurements. X-ray photoelectron spectroscopy (XPS) provided a more quantitative method of characterising the polymer surfaces. Reflective infra-red spectroscopy was attempted but no useful spectra could be acquired, possibly because of the low surface-density of polymer coverage.

3.3.1 Contact Angles

Contact angle measurements are the quickest way to check that a surface coating has been applied. This method measures the surface wettability and gives an approximated angle which is dependent on the topology and the chemical properties of the coating. Ten samples of each of the polymer coated slides were characterised to give an average contact angle value for each of the surfaces, as shown in Figure 41.

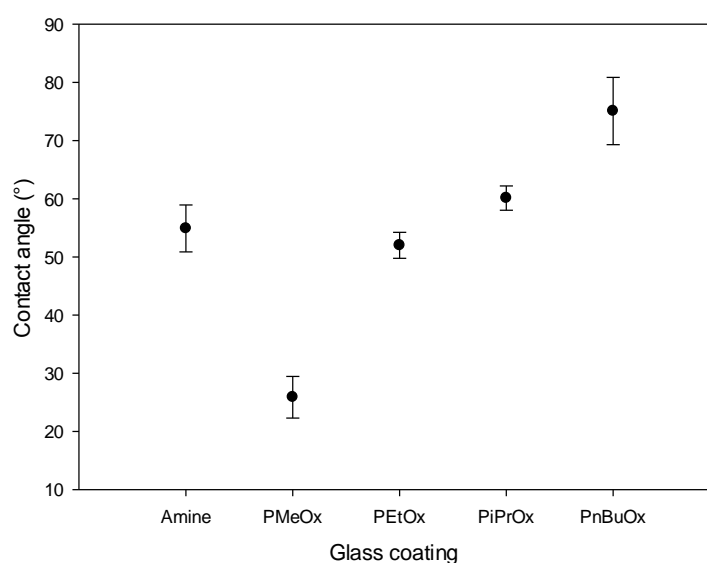


Figure 41: Contact angles for different coated glass slides

Piranha cleaned glass slides have an angle of typically 10-16°, however as the surface is so hydrophilic it is difficult to get a reliable figure.

It was found that, as the carbon chain length was increased, the polymer became more hydrophobic and the surface also became more hydrophobic. The amine-coated slides had contact angles in the range of 50-60° which is consistent with literature¹⁸⁹.

To illustrate reproducibility, the contact angle was measured over the three batches of coatings; these results are shown in Figure 42.

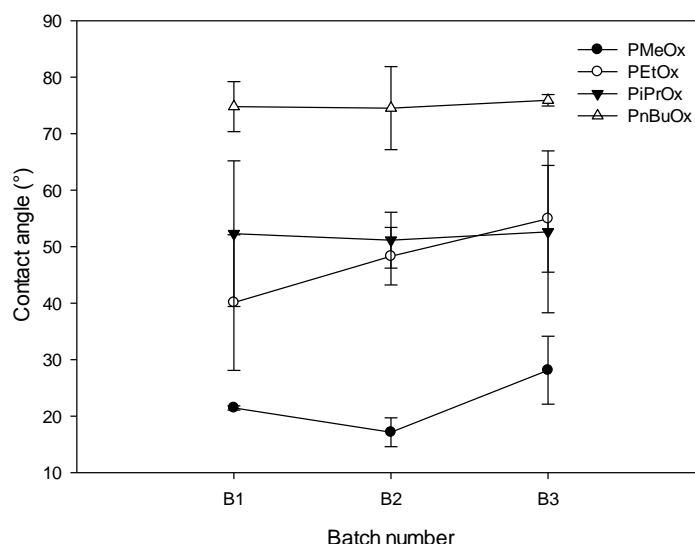


Figure 42: Contact angle variation for different batches of coated glass slides

The behaviour of the batches stayed reasonably consistent. The PEtOx batches showed the largest variation but with a large standard deviation for the samples it is difficult to draw any conclusions from the data. This illustrates that this method was reasonably robust and reproducible.

3.3.2 X-ray Photoelectron Spectroscopy

3.3.2.1 Overview

A more qualitative study of the polymer coatings was undertaken using X-ray Photoelectron Spectroscopy (XPS). XPS uses X-ray irradiation to measure photo-emitted electrons which have been emitted from the top 1-10nm of the surface. Each element has a characteristic peak corresponding to a characteristic binding energy for the element; this peak corresponds to electrons within the atoms in different orbitals, i.e. 1s, 2s, 2p, etc. Thus we can analyse and quantify the extent of bonding of an element on the surface of the sample. This technique also allows comparison of the relative amounts of the elements on the surface.

3.3.2.2 Deconvolution of Carbon and Nitrogen Peaks

To analyse the elemental peaks using XPS the spectra are deconvoluted to calculate the relative ratio of the different bonding energies present. Nitrogen and carbon are the two bonding elements which are of most use for the polymer coatings. Oxygen energies are often more difficult to deconvolute as they contain mainly bare silicon oxygen bonds from the surface.

An example of a deconvoluted nitrogen and carbon XPS spectrum for the PiPrOx coated surfaces is shown in Figure 43.

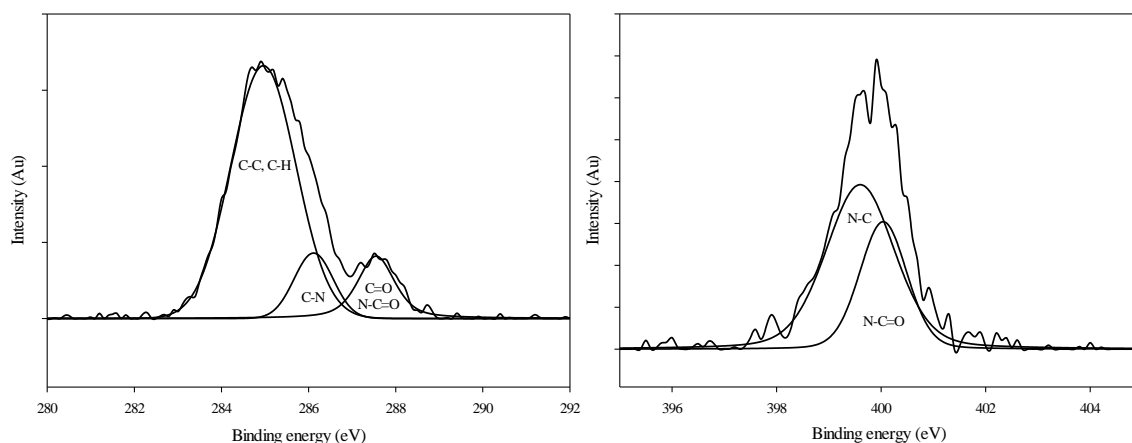


Figure 43: Deconvoluted XPS spectra for PiPrOx coated surfaces
Carbon bonding energies (left) and nitrogen bonding energies (right)

Charging was observed on the polymer surfaces, this means that the peaks were shifted from their expected binding energies. To standardise this the C-C bonding peak was used as a reference peak with a binding energy 285.0 eV¹⁹⁰ as has been done previously.

The carbon bonding peaks can be deconvoluted into C-C bonds, C-N bonds and C=O and N-C=O bonds which correspond with published literature¹⁹⁰. The nitrogen peak is deconvoluted into N-C and N-C=O environments which are also in agreement with literature¹⁹¹. XPS data was kindly collected by Dr Nick Alderman at the University of Southampton.

3.3.2.3 Silane Attachment

XPS was initially used to demonstrate the (3-aminopropyl)triethoxysilane attachment. This is the coating which preceded the poly(2-oxazoline) attachment.

Carbon-nitrogen ratio

The carbon nitrogen ratio was found to be 1:6 (N:C). This is higher than the expected 1:3 and suggests that the silane may not be completely attaching to the surface leaving free ethoxy-arms. It could also arise from hydrocarbon contaminants.

Carbon

The carbon XPS corroborates the unbalanced ratio, Table 6.

| Bond | Bond % | |
|------|--------|-------|
| | Calc. | Act. |
| Si-C | 25 | 4.64 |
| C-C | 50 | 76.55 |
| C-N | 25 | 18.80 |

Table 6: Carbon bond characterisation for amine surface

Nitrogen

The nitrogen deconvoluted peak provides information on the terminal amine group. The calculated-to-actual ratios of the bonds are comparable, Table 7.

| Bond | Bond % | |
|------|--------|-------|
| | Calc. | Act. |
| C-N | 33.3 | 37.00 |
| N-H | 66.6 | 63.00 |

Table 7: Nitrogen bond characterisation for amine surface

This confirms the presence of free amines on the surface.

3.3.2.4 Polymer characterisation

Carbon

Carbon XPS of each of the surfaces confirms the presence of the poly(2-alkyl-2-oxazoline) coatings. Each of the spectra deconvolutes to produce three peaks. The assignments of these peaks for are shown in Figure 44 below.

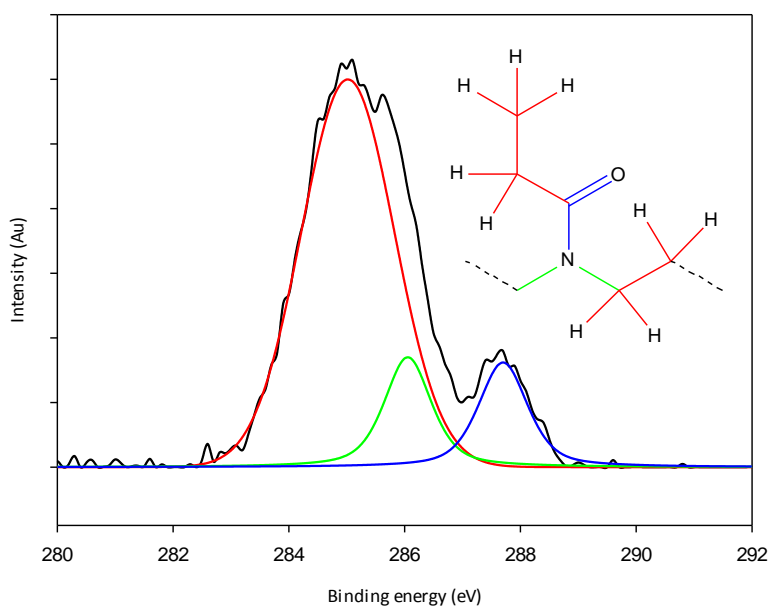


Figure 44: Assignment of PEtOx deconvoluted carbon XPS

The relative areas of these peaks correspond to the ratio of bonds present; for PEtOx the ratio should be, 6:1:1, (red:green:blue). Experimentally we find the ratio to be 5.8:1:1 which is in close agreement with the predicted ratio. The analysis of the carbon-bond deconvolution for each of the four surfaces is shown in Table 8

| | | Bond | | |
|--------|----------------|-----------|--------|-------------|
| | | C-C / C-H | C-N | C=O / N-C=O |
| PMeOx | Peak Pos (eV) | 285.00 | 285.65 | 287.58 |
| | Calculated (%) | 69.23 | 15.38 | 15.38 |
| | Actual (%) | 68.47 | 14.26 | 17.28 |
| PEtOx | Peak Pos (eV) | 285.00 | 286.00 | 287.60 |
| | Calculated (%) | 75.00 | 12.50 | 12.50 |
| | Actual (%) | 74.26 | 13.00 | 12.75 |
| PiPrOx | Peak Pos (eV) | 285.00 | 286.10 | 287.50 |
| | Calculated (%) | 78.95 | 10.53 | 10.53 |
| | Actual (%) | 75.55 | 11.70 | 12.76 |
| PnBuOx | Peak Pos (eV) | 285.00 | 286.00 | - |
| | Calculated (%) | 81.82 | 9.09 | 9.09 |
| | Actual (%) | 82.44 | 8.78 | 8.78* |

*estimated based on C-C and C-N peaks.

Table 8: Deconvoluted carbon XPS data for the four polymer coatings

The PnBuOx sample suffered from charging and as a result the C=O peak was outside the binding energy range analysed. The main peak was still present however so the smaller peak was calculated based on the two other peaks.

The increase in C-C and C-N peaks is clear as the polymer alkyl chains increase in size. The ratios of the peaks can be calculated from the percentages, this gives a clearer overview of the four surfaces, Figure 45.

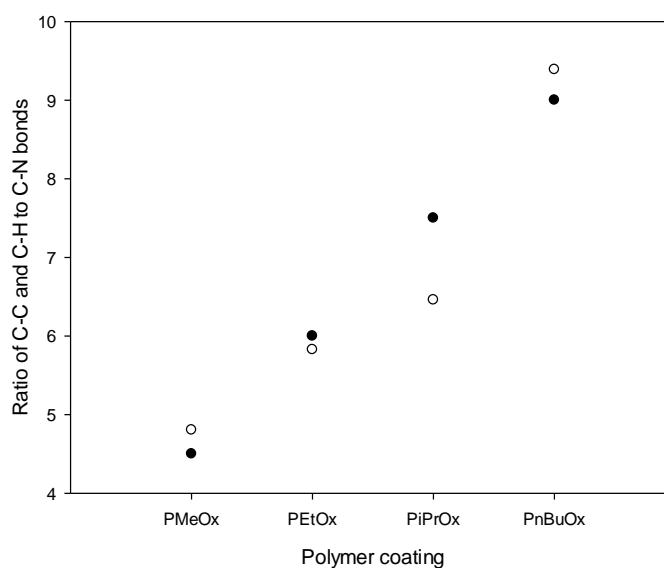


Figure 45: Comparison of predicted vs calculated bond ratios from the carbon XPS
Calculated ratio (○), predicted ratio (●)

The comparison is reasonably similar with the exception of the *PiPrOx* which has a slightly lower ratio of 6.5 instead of 7.5. This is possibly the result of contamination on the surface.

Nitrogen

The same analysis was performed for nitrogen on the surface as shown in Table 9. This deconvolution consists of two peaks, the N-C bond and the N-C=O bond. The N-C peak is slightly higher energy than expected as a result of the presence of the carbonyl bond.

| | | Bond | |
|---------------|-----------------------|--------|--------|
| | | N-C | N-C=O |
| PMeOx | Peak Pos (eV) | 399.51 | 399.91 |
| | Calculated (%) | 66.67 | 33.33 |
| | Actual (%) | 66.11 | 33.89 |
| PEtOx | Peak Pos (eV) | 399.89 | 400.16 |
| | Calculated (%) | 66.67 | 33.33 |
| | Actual (%) | 66.89 | 33.11 |
| PiPrOx | Peak Pos (eV) | 399.59 | 400.03 |
| | Calculated (%) | 66.67 | 33.33 |
| | Actual (%) | 66.22 | 33.78 |

Table 9: Deconvoluted nitrogen XPS data for three of the polymer coatings

We can also analyse the expected ratio of N-C to N-C=O bonds; for each of these samples it should be 2:1. In each case this ratio correlates closely with that of the predicted. Due to charging on the *PnBuOx* sample the nitrogen peak was shifted out of the range analysed for the nitrogen component so analysis of the nitrogen bonding could not be performed.

3.4 Cell Behaviour

3.4.1 Overview

The four poly(2-oxazoline) surfaces were studied to see how cells behave when seeded on them. As mentioned previously, the aim of this was to establish how the cells behave on poly(2-oxazoline) surfaces. This is important as there has not been a systematic investigation on these surfaces. This work was undertaken by Angela Tait assisted by myself at Southampton General Hospital. For a potential application it was hoped that one of the poly(2-oxazoline) surfaces would display some cell specific behaviour. If a cell-specific substrate can be developed it would be a potentially useful clinical material. A sample from a patient could be taken, broken down into its constituent cells and, using the cell-specific substrate, one cell type could be selectively and simply cultured. To this end, two cell types were investigated. The experimental details contains a section describing the methodology used for all the cell experiments.

Two cell types were studied; human bronchial epithelial cells (16HBE); and human foetal lung fibroblast cells (MRC5). These are both involved in the lining tissue of our lungs as shown in Figure 46.

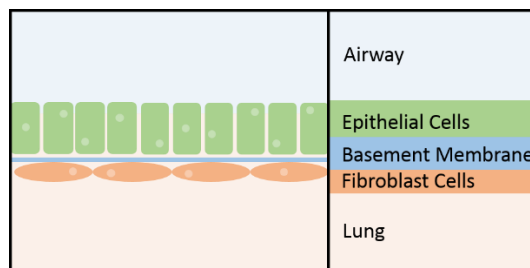


Figure 46: Simplified illustration of the cellular structure lining the air-liquid interface of a lung

All of the results shown in the following sections are from 3 combined batches of each surface, details of each method are described in the methods section of the experimental details chapter.

3.4.2 Adhesion

Both of the cell types have been analysed for cell adhesion for each of the four polymer coatings, three batches of each coating. This gives a measure of how “cell-friendly” the surfaces are, Figure 47. See section 9.1.4.1 for the adhesion assay method.

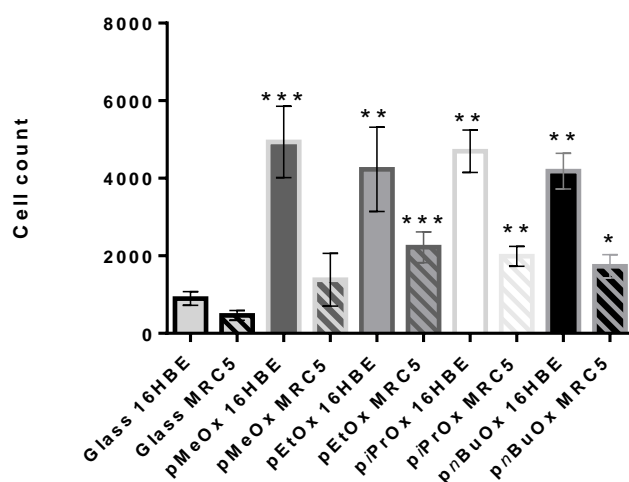


Figure 47: Cell adhesion assays after 60 minutes
16HBE (solid fill) and MRC5 (dashed fill)

Whilst cells adhere to all of the surfaces, glass on its own is not particularly adhesive. The addition of the polymer improves the adhesive nature of these surfaces.

However, the MRC5 cells are less adhesive to the poly(2-oxazoline) surfaces, the most adhesive surface for these cells being the PEtOx surface. The 16HBE cells did not show a preference of one surface over another. All of the surfaces were significantly more cell-adhesive than glass.

3.4.3 5 Day Growth and Staining

3.4.3.1 16HBE

The cells were then grown for 5 days and then fixed and stained. On all the surfaces the cells grew to confluence. The PMeOx surface was the slowest to reach confluence. They were stained to see if they were creating tight junctions and for the cytoskeleton. These images are shown in figure 48. See section 9.1.4.4 for staining protocols.

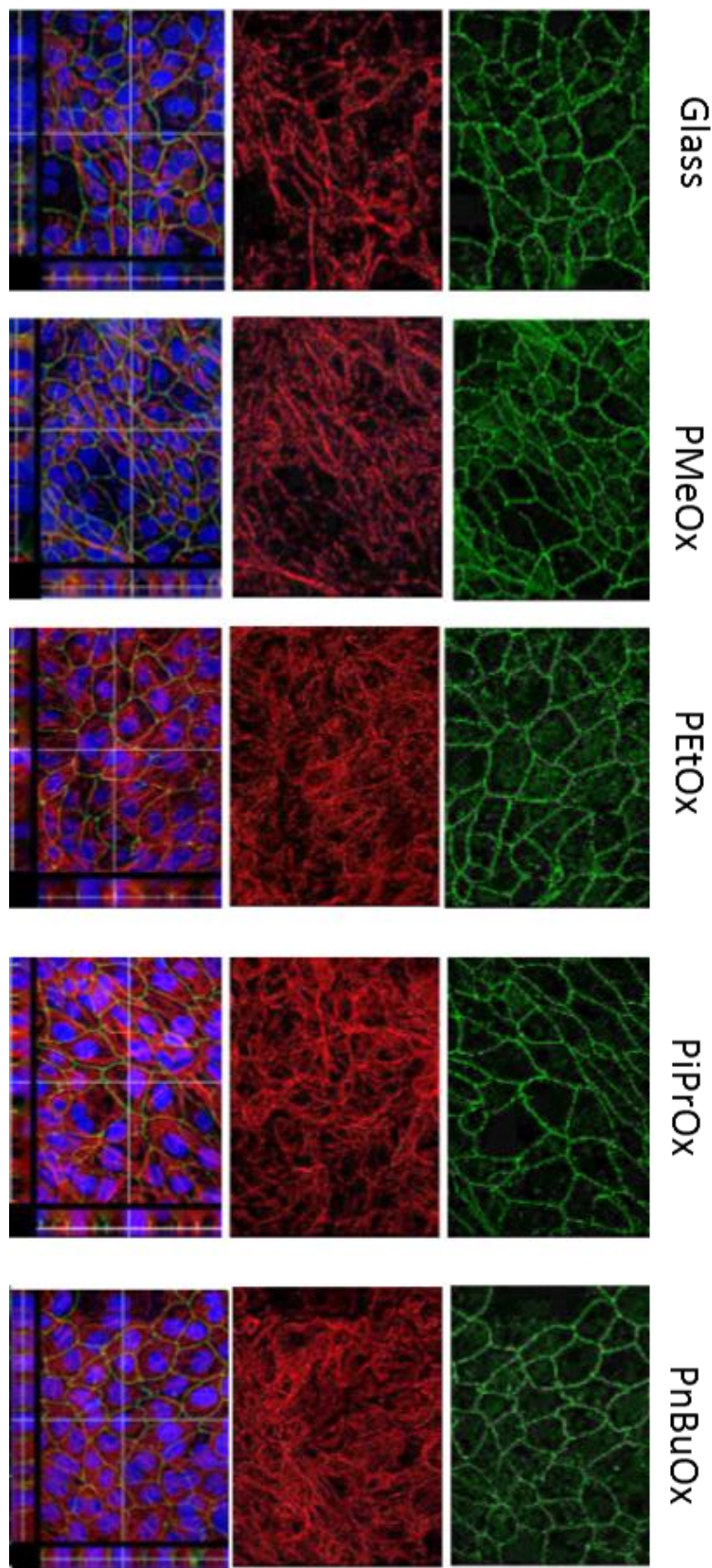


Figure 48: 16HBE cells stained after growing on different poly(2-oxazoline) surfaces
 Imaged using a fluorescent light microscope at 20x magnification. Stains used were ZO-1 mouse IgG1 (Invitrogen) conjugated alexa647 (1 in 1000; 0.77 μ g/ml) and F-actin Acti-stainTM 555 phalloidin or Acti-stainTM 670 phalloidin, (cytoskeleton, Inc, Denver, USA) (1 in 500), E-cadherin mouse IgG1-k (Invitrogen) conjugated Alexa488 (1 in 500). Tight junctions (green, right) cytoskeleton (red, middle) and nuclei (blue, left, *includes overlay of tight junction and cytoskeleton images*)

All of the cells created tight junctions, meaning that they are connecting with the cells next to them and binding together; this is important for creating confluent sheets of the correct structure. The area of the cells can be calculated allowing a comparison to be drawn between the surfaces, Figure 49.

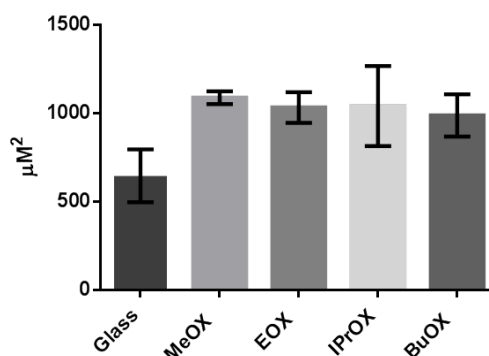


Figure 49: 16HBE cell area per cell on different poly(2-oxazoline) surfaces

The cells appeared to behave similarly on all four polymer surfaces. They also appeared to be larger than the 16HBE cells on the amine surface.

3.4.3.2 MRC5

The MRC5 cells were grown and imaged for 5 days. Rounding of the cells was observed for the glass surface indicating that the cells were not happy sitting on bare glass. On the polymer surfaces however all of the cells began to form fibrous structures indicating that they are happier on polymer surfaces. These surfaces were then stained for cytoskeleton, Figure 50. Tight junctions were not stained for as these cells don't make them in the same sense as 16HBE cells. These cells have a different function and create more of a fibrous mat for the 16HBE cells to sit on.

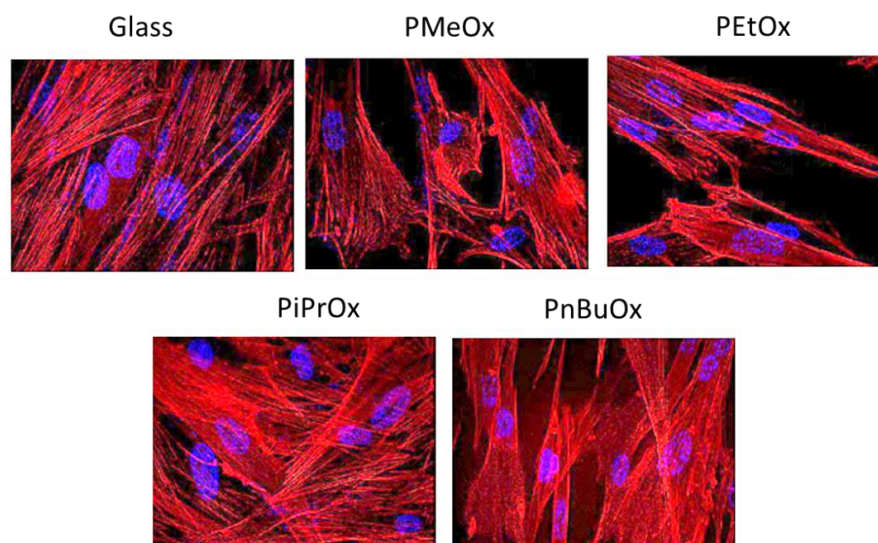


Figure 50: Staining of MRC5 cells on different poly(2-oxazoline) surfaces
Imaged using a fluorescent light microscope at 20x magnification. Stains used were ZO-1 mouse IgG1 (Invitrogen) conjugated alexa647 (1 in 1000; 0.77μg/ml) and Dapi for the nuclei. Cytoskeleton (red) and nucleus (blue)

Again these cells are becoming confluent on all the polymer surfaces and seem to be creating fibrous structures. An important structural feature of note is that the cells seem to be orientating themselves in one direction, behaviour which we would expect to be seeing from these cells.

3.4.4 Cell Proliferation

Cell proliferation, the increase in cell numbers by division, can be measured by monitoring the number of cells over time. This has been analysed for each of the surfaces at 3 days and 5 days.

3.4.4.1 16HBE proliferation

16HBE proliferation was observed for each of the polymer surfaces. The results are summed up in Figure 51.

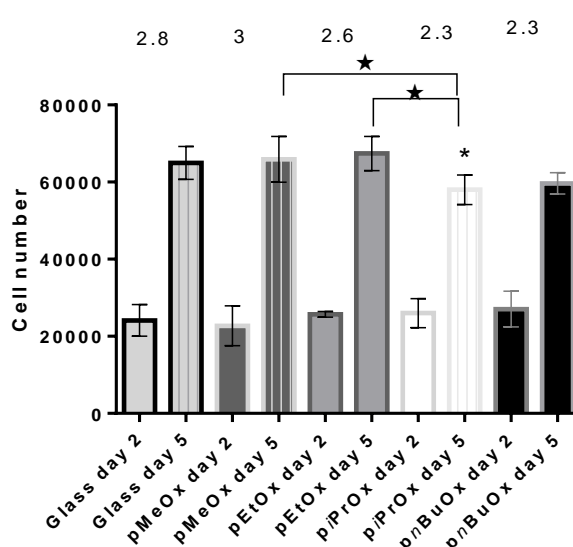


Figure 51: 16HBE proliferation on different polymer surfaces
Day 2 (solid fill) and 5 (lined pattern)

16HBE cells spread out to form an interlinked membrane. Once this has occurred proliferation will slow down as the cells have no space to grow into. The lower proliferation rate on PiPrOx and PnBuOx indicates that the cell sheets form with a lower number of cells while on PMeOx more cells are required to form the same sheet.

3.4.4.2 MRC5 proliferation

MRC5 proliferation was observed for each of the polymer surfaces as shown in Figure 52.

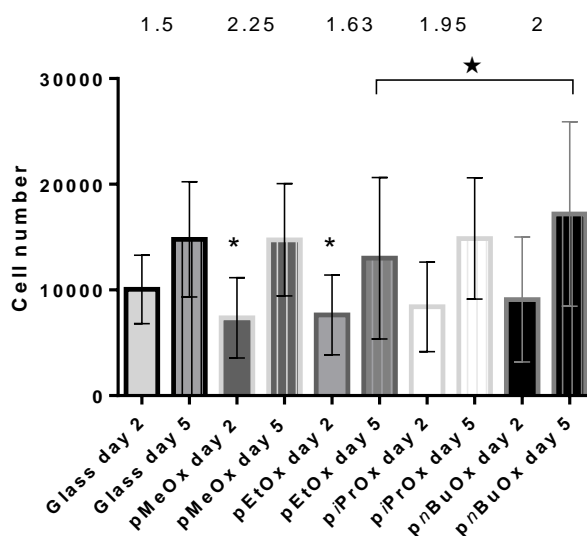


Figure 52: MRC5 proliferation on different polymer surfaces
Day 2 (solid fill) and day 5 (lined fill)

The MRC5 cells appear to behave similarly on all of the polymer surfaces.

3.4.5 Cell Motility

Cell motility was observed for the two cell types. This assay measures how much the cells move on a surface and indicates how happy the cells are on a surface, Figure 53.

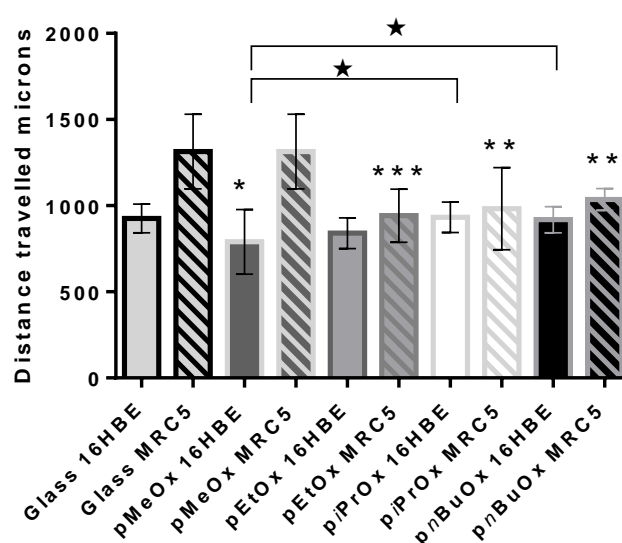


Figure 53: Cell motility on different poly(2-oxazoline) surfaces
16HBE (solid fill) and MRC5 (dashed fill)

On the PMeOx surfaces the 16HBE cells move the least; this is perhaps why the cells take longer to reach confluence on the PMeOx surface. The other polymer surfaces are comparable to glass. The MRC5 cells however, display significantly reduced movement on the PEtOx, PiPrOx and PnBuOx surfaces indicating that the cells are happier to be on these surfaces. PMeOx displays similar behaviour to the glass surfaces indicating that the cells are not so happy on PMeOx.

3.4.6 Co-cultures

To investigate the selectivity of the surfaces towards MRC5 and 16HBE cells co-cultures were investigated. This involved adding both cell types together and analysing the cell growth behaviour. To distinguish between the 16HBE cells and the MRC5 cells when seeded together on the poly(2-oxazoline) coated glass coverslips, the MRC5 cells were stained with cell tracker orange and the 16HBE cells were transfected with green fluorescent protein (GFP). See section 9.1.4.5 for the co-culture methodology.

3.4.6.1 Co-culture without wash

Initially the two cells were added together and after 24 hours the cell surfaces were analysed, Figure 54.

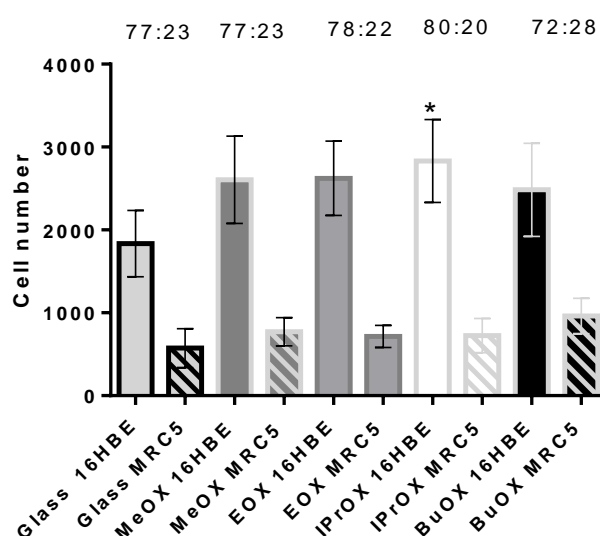


Figure 54: Co-cultures on different poly(2-oxazoline) surfaces
Number at the top is the ratio between MRC5 (dashed fill) and 16HBE (solid fill)

All the polymer-coated slides show an increase in cell numbers over the glass slides. Furthermore an increase in selectivity of the 16HBE cells over the MR5 cells compared to glass is observed for the PiPrOx surface.

To enhance this further a wash step was included to take advantage of the increase adhesion of the 16HBE cells to the polymer surfaces compared with the MRC5 cells. This was anticipated to increase the selectivity of the surfaces.

3.4.6.2 Co-culture with wash

When the wash step was included a bigger difference between the slides was observed. PiPrOx was clearly the better performing slide however the selectivity was actually decreased, Figure 55.

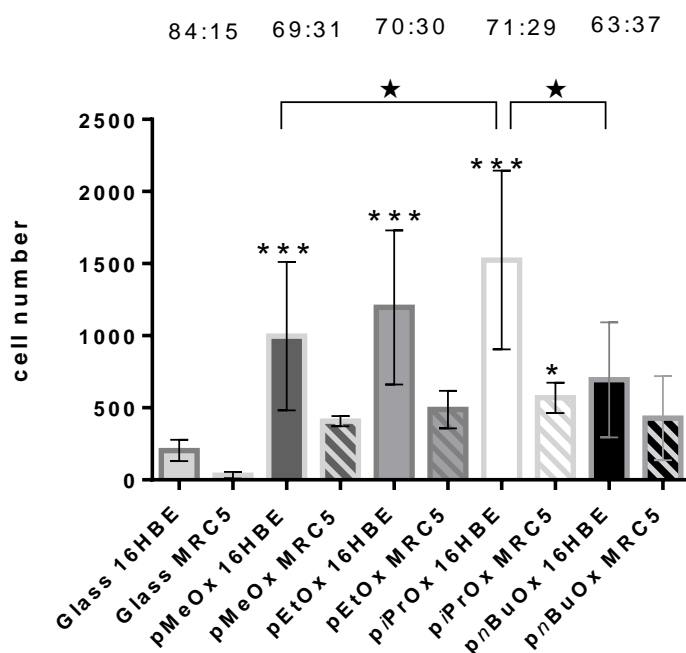


Figure 55: Co-cultures after washing on different poly(2-oxazoline) surfaces
Number at the top is the ratio between MRC5 (dashed fill) and 16HBE (solid fill)

The total number of cells for each surface demonstrates the same trend, Figure 56.

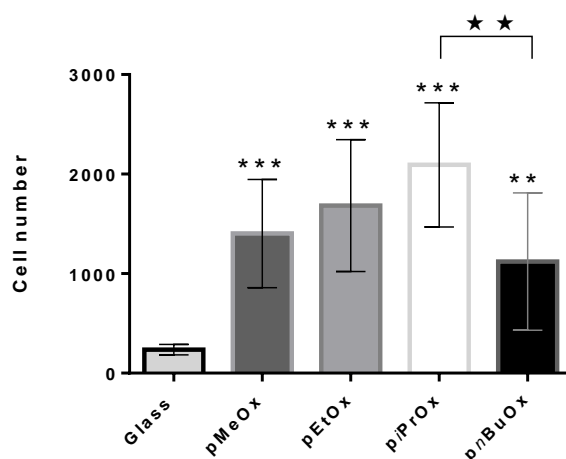


Figure 56: Co-culture with wash total cell number

For further selectivity this method could be repeated in order to further increase the ratio of 16HBE to MRC5 cells.

3.4.7 Summary

In summary all of the polymer types are non-toxic and facilitate cell growth. This is unsurprising as poly(2-oxazoline)s have already been shown to be non-toxic. Another factor is that these polymers are not too structurally dissimilar; for these cells the key structural features required are present on all the surfaces regardless of whether one is more polar than another. The best surface for cell selectivity appears to be PiPrOx which gives the greatest selectivity and highest

number of cells. PMeOx appears to be the worst surface for cell growth and adhesion which agrees published literature¹⁸⁷.

3.5 Novel Second Generation Poly(2-oxazoline) Surfaces

3.5.1 Overview

A good understanding of how cells behave on poly(2-oxazoline) surfaces gives us a basis for trying to improve cell adhesion and developing a thermoresponsive surface. The ideal substrate for a thermoresponsive surface would be a transwell. A transwell is an insert which is put into a cell dish and allows cells to be grown at an interface, Figure 57. The cells are supported at the bottom on a material which has pores to allow diffusion of nutrients through it. The transwell is made of a polyester, poly(ethylene terephthalate) (PET). The goal of this work was to develop a method which would allow a transwell to be functionalised with the thermoresponsive coating

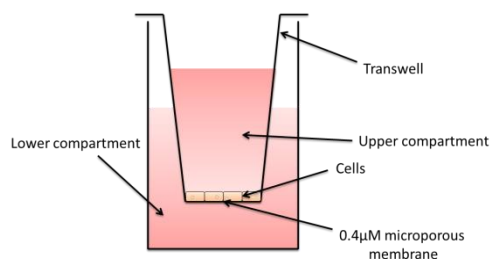


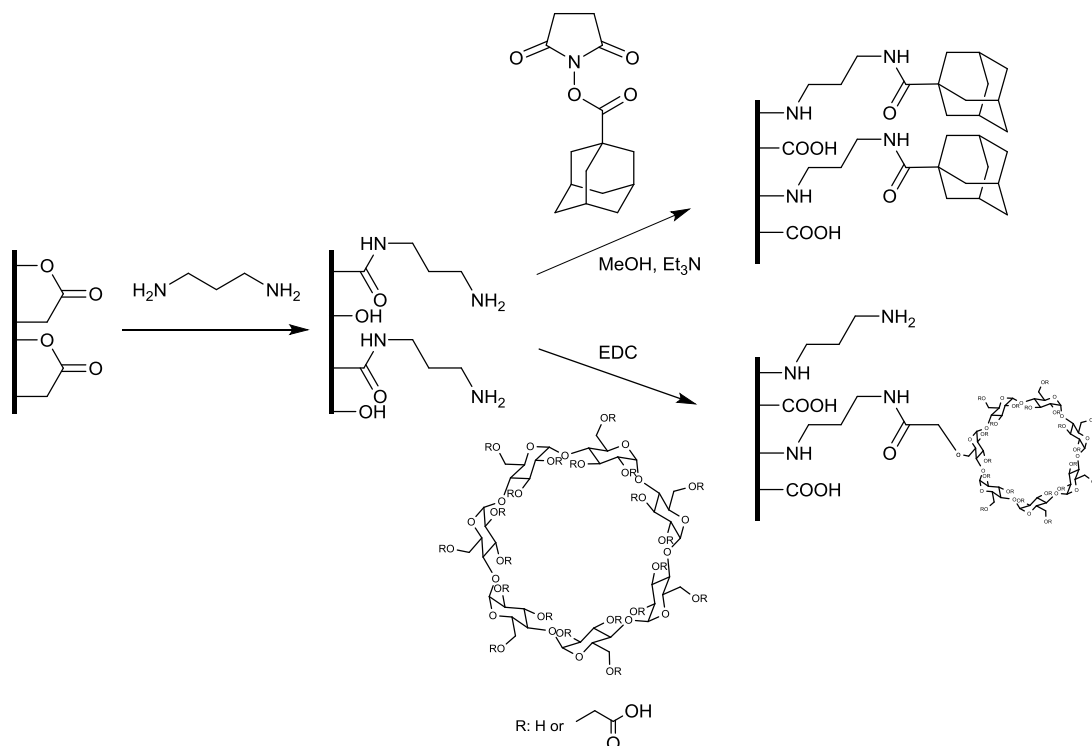
Figure 57: Illustration of a transwell in use

To develop a thermoresponsive transwell, a polyester sheet using poly(caprolactone) (PCL) was used as a model. Once this had been shown to work the method could be applied to the PET transwells which are much more expensive.

3.5.2 Method

A method has been developed which should provide a dense poly(2-oxazoline) surface. The steps involved: (i) Subjecting the PCL surface to aminolysis to create amine group on the it; (ii) coupling these with β -cyclodextrin or an adamantane group to create a β -cyclodextrin- or adamantane-functionalised surface; (iii) Preparing a novel adamantine-initiated or β -cyclodextrin-initiated polymer which should attach to the surface via the adamantane- β -cyclodextrin binding¹⁹².

Scheme 14 below illustrates the surface-functionalization method.



Scheme 14: Synthesis of adamantane and cyclodextrin polyester surface

Once the surfaces had been functionalised, the polymers could then simply be added in solution to create a polymer surface via adamantane- β -cyclodextrin complex formation. In order to synthesise the polymers an adamantane initiator and a β -cyclodextrin initiator were used. By combining the surfaces with the initiated polymers, poly(2-oxazoline) surfaces could then be created according to Figure 588.

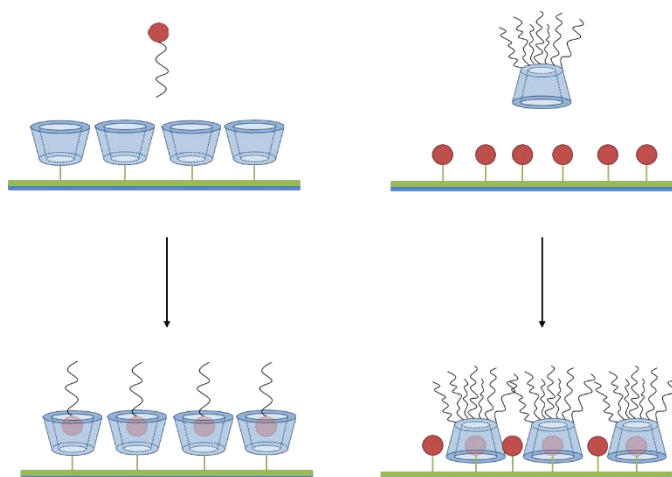


Figure 58: Illustration of the two different adamantane/cyclodextrin coating methods
 Adamantane initiated polymers with a β -cyclodextrin surface (left) and β -cyclodextrin initiated polymers with an adamantane surface (right)

3.5.3 Aminolysis

As mentioned above, aminolysis was to be modelled first on PCL sheets and coated slides and, once the method of aminolysis was better understood, it would be applied to PET membranes.

3.5.3.1 Aminolysis of PCL

Aminolysis of poly(esters) is a well-characterised surface modification technique. It introduces amines to the surface of poly(esters) by cleaving the ester bonds with a diamine leaving a peptide bond and a primary amine¹⁹³. Three different solutions of diaminopropane at a concentration of 0.5M in various alcohols was used to characterise the aminolysis process, shown in Figure 59.

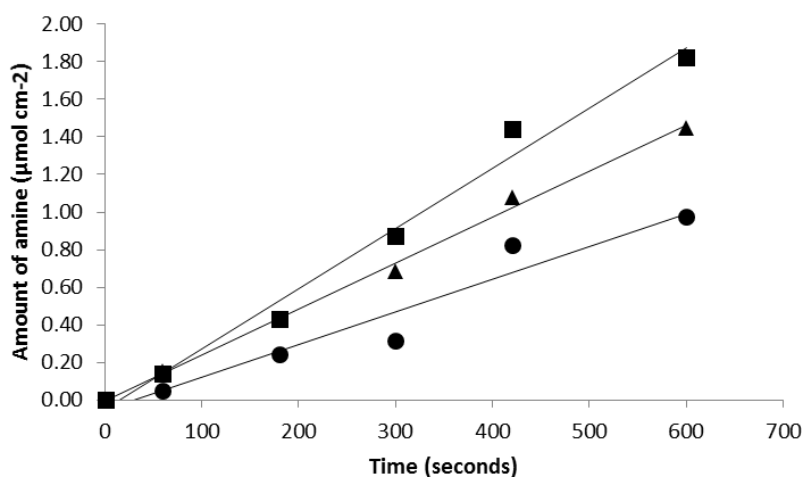


Figure 59: Aminolysis of poly(caprolactone) sheets using diaminopropane
A 0.5M solution of diaminopropane was used in different alcohol solutions, (methanol: ■), (ethanol: ▲), (isopropanol: ●)

The amount of amine on the surface was characterised using a ninhydrin assay¹⁹⁴. As expected the alcohol influences the rate of aminolysis with methanol being the quickest and isopropanol being the slowest¹⁹³. The aminolysis shown above was measured using a PCL sheet. However PCL-coated slides would provide a more accurate method for comparison with a transwell. It was found that using a coated slide gave a reduced amount of amine on the surface. To assess the ninhydrin assay it was compared with an alternative characterisation method based on orange II; this has been shown to be comparable with the ninhydrin method¹⁹⁰. The results are shown in Table 10 below.

| | Quantification Method | Amine in top 0.1μm [μMol cm ⁻²] | Number of NH ₂ groups [nm ⁻²] |
|-------------|-----------------------|--|---|
| PCL sheet | Orange II | 8.92E-03 | 53.74 |
| | Ninhydrin | 7.34E-03 | 44.19 |
| PCL coating | Ninhydrin | 1.52E-03 | 9.18 ± 2.92 |

Table 10: Quantification of the aminolysis of PCL sheets and coatings

By calculating the moles of amine per cm² it allows the number of NH₂ groups per nm² to be estimated. The values calculated for the number of amines are higher than would be expected from a perfectly smooth surface indicating that the surfaces are quite rough and have a much higher surface area than, for example, a glass surface.

Further analysis of the PCL coating was undertaken using height profiles kindly acquired by Gareth Ward with a Zscope, Figure 60. By comparing the PCL coating before and after aminolysis, a decrease in the thickness in the PCL and in increase of the surface roughness is observed. This is consistent with aminolysis occurring which causes degradation of the PCL surface¹⁹³.

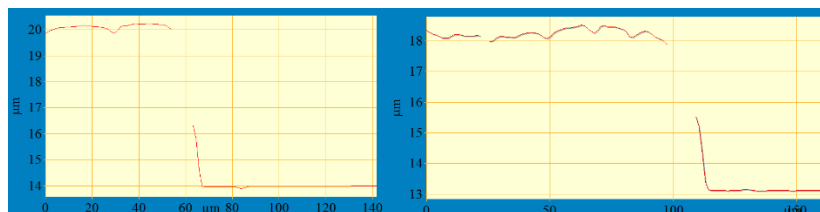


Figure 60: Thickness profile of PCL coatings on Perspex slides before and after aminolysis
Before aminolysis (left) and after aminolysis (right)

3.5.3.2 Aminolysis of PET Transwell Membranes

Once the aminolysis was established for PCL, aminolysis of PET was attempted. PET is much more stable than PCL and hence required much harsher conditions. Using a 35% by weight solution of ethylenediamine (EDA) in methanol the transwell inserts were characterised at different time points. It was anticipated that these more aggressive conditions would create an aminolysed surface according to previously reported work¹⁹⁵. The results are shown in Figure 61.

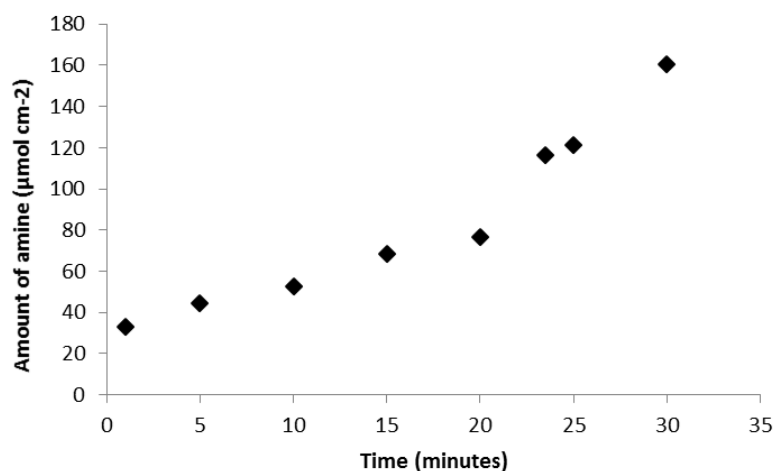


Figure 61: Aminolysis of a transwell insert
Amine concentration characterised using an orange II assay at different time points

In comparison to the PCL sheets, a similar increase in amount of amine over time was observed, however much larger values were obtained for the amount of amine present than that seen for the PCL sheets. This was attributed to the porosity of the transwells and hence the presence of a much larger surface area than the non-porous PCL sheets. It was observed that this porosity combined with longer aminolysis times caused the transwells to degrade to the point at which they fell apart. This degradation was observed using scanning electron microscopy (SEM) (Figure 62).

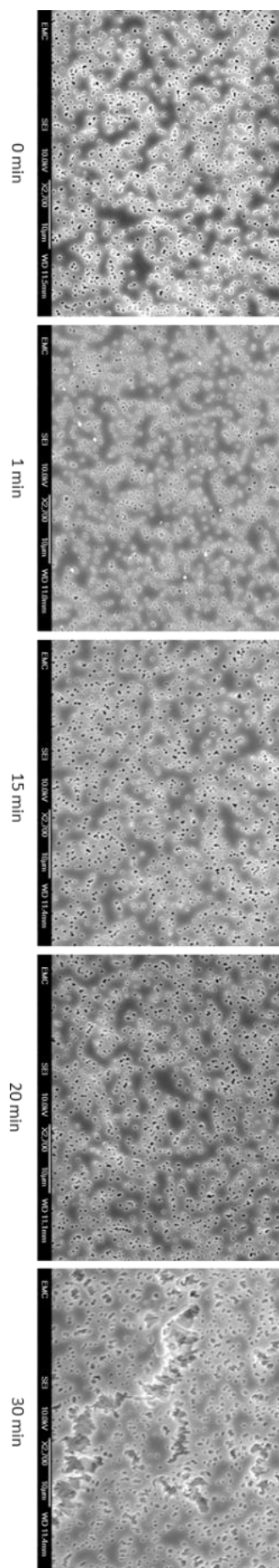


Figure 62: Degradation of PET transwell membranes over time characterised using SEM

The degradation and porosity of the membranes is clearly visible after 30 minutes (Figure 63). To attempt to quantify the degradation further the number and size of the pores was analysed. If degradation is occurring within the membrane not only would the overall surface area increase and mechanical strength decrease, but the pore size should also increase. This would be a more subtle effect than the increase in surface area but it would be easier to measure visually.

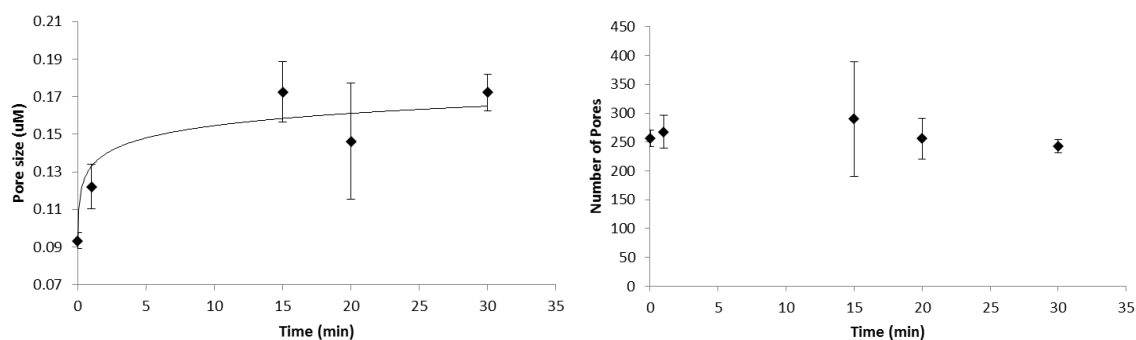


Figure 63: Monitoring degradation of transwell inserts over time
Pore size (left) and number of Pores (right) over time

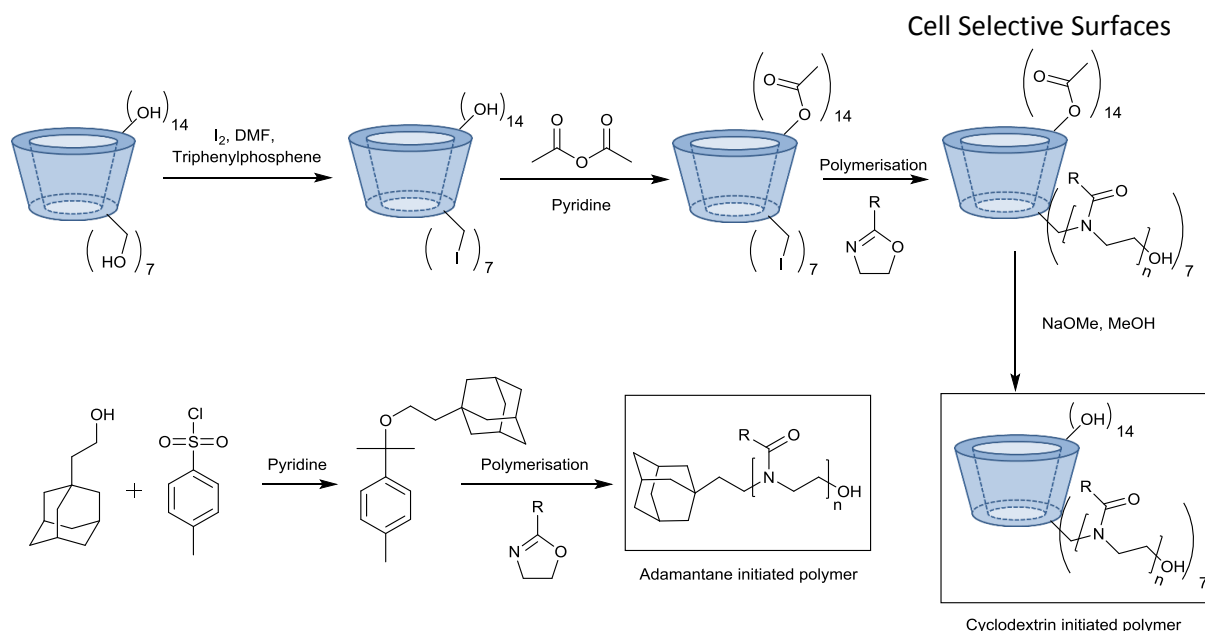
The data (Figure 63) indicates that the pore sizes are increasing with longer aminolysis times while the number of pores stays constant. The time for aminolysis is therefore very important to retaining functionality of the membrane. It is important not to carry out the aminolysis for too long otherwise the membrane could be susceptible to tearing.

3.5.4 Adamantane and β -Cyclodextrin Initiated Polymers

To functionalise the aminated surface, carboxymethyl- β -cyclodextrin and 1-adamantanecarboxylic acid was used. Coupling between the acid and amine was achieved using NHS and EDAC in water. After functionalization the amount of amine was measured using the orange II method. No amine was detected implying a quantitative yield.

3.5.4.1 Polymer Synthesis

To synthesise the polymers two initiators were used. The synthesis of the initiators and polymerisation are shown in Scheme 15.



Scheme 15: Synthesis of a β -cyclodextrin star polymer and adamantane-initiated polymer

The adamantane initiation of poly(2-oxazoline)s has not been reported in literature but was predicted to work by virtue of the initiator containing only alkyl group. The adamantane tosylate would be less reactive than the methyl tosylate which should lead to a larger PDI, but for surface applications this is not such an issue. The alcohol was tosylated according to a published procedure to yield the adamantane initiator¹⁹⁶.

In contrast the synthesis of the β -cyclodextrin initiator followed a more complex synthetic pathway. Instead of a tosylate leaving group, an alkyl halide was used. Synthesis of the initiator was taken from published literature¹⁵³. The final deacetylation was achieved using sodium methoxide¹⁹⁷. It was expected that, as the cyclodextrin-initiated polymer has seven oxazoline arms to each β -cyclodextrin, once bound to an adamantane surface it would produce the densest coating.

To quantify the polymer coating, rhodamine-terminated polymers were used. Several adamantane-initiated polymers were synthesised and one polymer was terminated with rhodamine for later coating quantification as summarised in Table 11.

| Polymer | Terminated with | Mw | Mn | PDI | Repeat units |
|------------|-----------------|-------|-------|------|--------------|
| Ad-PMeOx | OH | 32229 | 25381 | 1.26 | 298 |
| Ad-PEtOx | OH | 32257 | 26007 | 1.24 | 262 |
| Ad-PEtOx-R | Rhodamine | 38012 | 32577 | 1.16 | 329 |
| Ad-PiPrOx | OH | 33730 | 30158 | 1.19 | 267 |

Table 11: Characterisation of adamantane initiated poly(2-oxazoline)s

The β -cyclodextrin initiated polymers were also characterised. Instead of SEC these were characterised using NMR. By comparing the acetate ester CH_3 resonance present in the NMR

Cell Selective Surfaces
before deacetylation with the poly(2-oxazoline) NMR resonance, the length of the poly(2-oxazoline) chains can be estimated. This is summarised in Table 12.

| Polymer | Terminated with | Estimated Dp of poly(2-oxazoline) arms | Estimated Mw |
|------------|-----------------|--|--------------|
| CD-PMeOx | OH | 89 | 55105 |
| CD-PMeOx-R | Rhodamine | 73 | 45294 |
| CD-PEtOx | OH | 66 | 45537 |
| CD-PiPrOx | OH | 45 | 37476 |

Table 12: Characterisation of cyclodextrin initiated poly(2-oxazoline)s

Both initiators were successful at causing polymerisation as evidenced by the presence of polymer. It is worth noting that the β -cyclodextrin polymers will have a higher polydispersity than the adamantane-initiated polymers because of the multiple polymer chains per initiator.

3.5.4.2 Polycaprolactone Sheet Surface Functionalisation

To test and characterise the polymer coatings, adamantane and β -cyclodextrin coated PCL slides were incubated with the rhodamine-terminated polymers for different amounts of time. Non-specific absorption of the polymers on unfunctionalised PCL was observed, so a non-treated aminolysed PCL coating was used as background fluorescence for each time point. To quantify the amount of polymer present the PCL coating was rinsed and soaked in water to remove excess unbound polymer. The PCL coating was then dissolved, the rhodamine content was analysed by UV-Visible spectroscopy and the concentration of rhodamine was calculated from a known calibration. The results presented in Figure 644 and Figure 65 have taken into account any non-specific absorption by using the fluorescence of a non-treated PCL coating dipped in the polymer solution as a baseline from which the fluorescence from a treated PCL coating was subtracted. It was hoped that this would discount any non-specific absorption and only consider adamantane- β -cyclodextrin bound polymers.

The results are shown as a percentage of the total number of available binding sites complexed with by the corresponding polymer. The total number of available sites was calculated by dividing the number of detected polymers, either the star β -cyclodextrin polymer or adamantane polymer, per nm by the number of estimated available binding sites per nm. The numbers of available binding sites was assumed to be $9.18 \text{ sites nm}^{-2}$. This value was obtained from measuring the number of amines before and after surface functionalization with adamantane and β -cyclodextrin. No amines could be detected after functionalization, therefore it was assumed that 100% of sites were functionalised. One limitation of this analysis is the assumption that the carboxymethyl- β -cyclodextrin will react with only one amine while in reality there is the potential for it to react with multiple amines on the surface. This may lead to it appearing that less binding is occurring than anticipated in the β -cyclodextrin surface case. Another limitation is

that the detection limit of the ninhydrin assay used to determine the amount of amine available to react with is unknown.

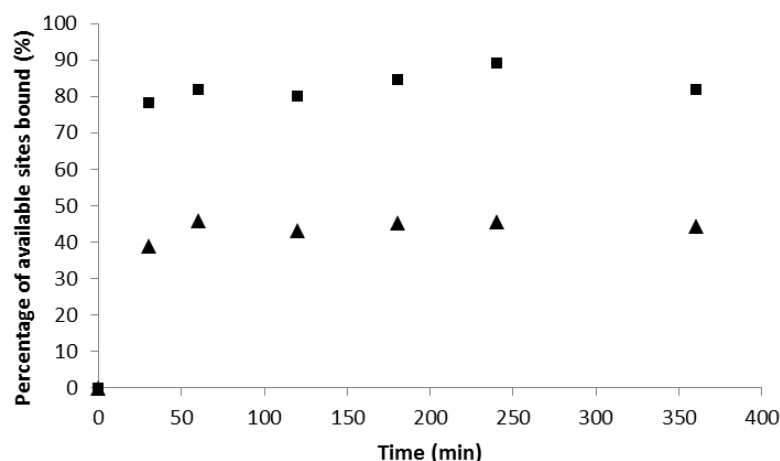


Figure 64: Percentage of bound sites on functionalised PCL coatings
Ad-PEtOx-R bound to a cyclodextrin surface (■), CD-PMEOx-R bound to an adamantane surface (▲)

Both the coatings bind at the same rate and within an hour do not show an appreciable increase in binding. The rate would be expected to be similar for the two methods as the binding kinetics should be unaffected by any groups attached. It would appear that the β -cyclodextrin star polymer produced worse coatings as only ca. 40% of sites are bound compared with ca. 80% of sites binding for the adamantane-initiated polymers.

However, the β -cyclodextrin star polymer has seven poly(2-oxazoline) chains stretching from the β -cyclodextrin core so a plot of the number of poly(2-oxazoline) polymer chains per nm^2 demonstrates that the coverage of the β -cyclodextrin star polymer leads to ca. 4 times as many poly(2-oxazoline) chains per nm^2 as the adamantane initiated polymer does.

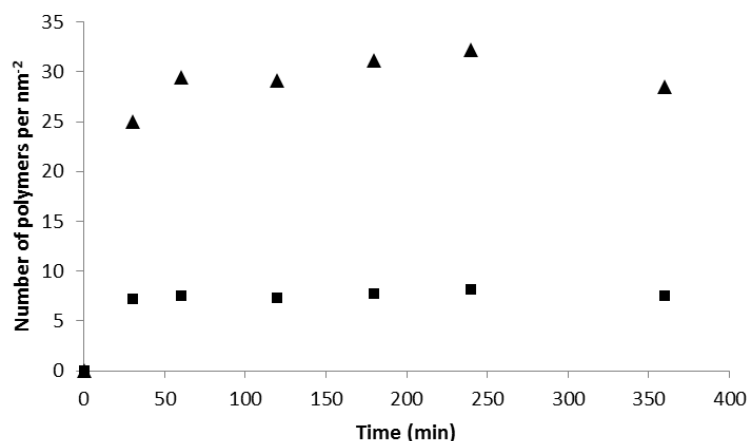


Figure 65: Number of poly(2-oxazoline)s per nm^2 at different time points
PEtOx-R bound to a cyclodextrin surface (■), PMEOx-R bound to an adamantane surface (▲)

In an ideal situation every possible binding site on the surface should be bound to one polymer. In this case we would expect to see around seven times as many poly(2-oxazoline)s present on the adamantane surface than the cyclodextrin surface. Two main factors influence the reality of the binding observed. Firstly the estimation of the number of β -cyclodextrins available for the adamantane-initiated polymers to complex with are most likely lower than the anticipated value as it is perhaps not reasonable to assume 100% of the available sites would react, particularly considering the β -cyclodextrins reacted with the surface contain more than one reactive site. This on its own however would increase the difference between the numbers of polymers on the two surfaces which is the opposite of what we observe. It is suggested that due to the relatively high concentration of β -cyclodextrin used when coating the aminolysed PCL surface, the ratio of β -cyclodextrins binding to amines approaches close to one to one. This is indicated by the high percentage of adamantane initiated polymers present after binding with the surface β -cyclodextrins (approx. 80%). Instead the lower ratio between the two methods could be due to the number of polymers present on the adamantane surface being lower. This could be due to the bulky nature of the β -cyclodextrin initiated polymers. This could lead to the relatively small adamantane sites located nearby to the bound adamantane to become blocked from further binding leading to a lower number of poly(2-oxazoline) chains than in an ideal situation.

Even though there are potentially less available sites for the β -cyclodextrin initiated polymers to bind to, this is overcome by the fact that every site which is bound has seven poly(2-oxazoline)s bound to it leading to a denser polymer coating.

3.5.5 Summary

A novel poly(2-oxazoline) surface functionalization method has been successfully demonstrated which depends on the complexation between cyclodextrin and adamantane moieties. This method has a wide range of potential applications due to the method being applicable for any poly(ester) material and any water-soluble poly(2-oxazoline) derivative. Further work needs to be undertaken to demonstrate cell compatibility and potentially thermoresponsive behaviour.

3.6 Conclusion

To conclude, a method was developed to allow poly(2-oxazoline)s to be grafted to glass. The behaviour of two types of cells were then investigated on these surfaces. This led to a method being developed which allows one cell to be selectively grown from a mixture of cells on the poly(2-oxazoline) surface. A new method was then developed which should allow transwells to be functionalised with poly(2-oxazoline)s using β -cyclodextrin and adamantane complexation. These surfaces have a large potential for easy surface coatings which display thermoresponsive behaviour.

Chapter 4 Antifouling Surfaces

4.1 Introduction

This work was carried out in collaboration with Dr Peter Glynne-Jones, Dr Dario Carugo and Professor Martyn Hill from the department of Engineering at the University of Southampton as part of the AQUALITY 'Online industrial water quality analysis system for rapid and accurate detection of pathogens project'. They had designed a device which concentrates bacteria using acoustic manipulation of particles. The device uses an acoustic field to push particles (in this case bacteria) onto a reflector. The acoustic field is ultrasound. The reflector was made out of a glass microscope slide and a piezoelectric transducer (PZT) was used to produce the acoustic field. This allows bacteria to be concentrated using an online constant flow system as opposed to removing a sample and centrifuging it back in the laboratory, Figure 66.

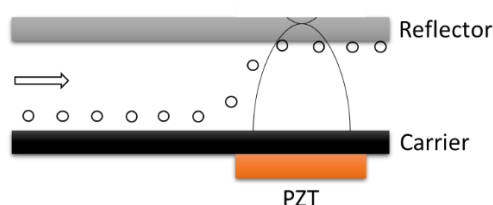


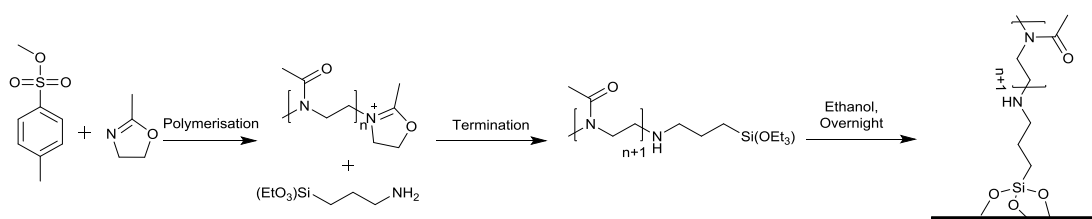
Figure 66: Bacterial concentration using an acoustic device

Figure 66 illustrates how the bacteria are concentrated as they are flowed into the device. The acoustic field pushes the bacterial flux to the reflector surface where it can be separated from the rest of the flow leading to a much more concentrated solution of bacteria.

The issue that arose from this process however was that the bacteria would stick to the reflector surface. Over time this meant that the efficiency of the device dropped and it became unusable. As discussed in the Introduction, PMeOx has shown potential as an antifouling surface⁹⁶⁻⁹⁹ and it was anticipated that using a PMeOx-coated glass slide would help to prevent the bacterial adhesion.

4.2 Synthesis

Synthesis of the PMeOx coated slides was undertaken using a modified published procedure according to Scheme 16¹⁸⁸.



Scheme 16: Synthesis of a PMeOx coated reflector for an acoustic device

PMeOx was polymerised and terminated using (3-aminopropyl)triethoxysilane. Precipitation was used to remove any excess terminating agent. Finally the polymer was incubated with the glass slide to functionalise it with polymer.

Comparison of the terminal methyl group resonances with that of the PMeOx methyl peak in the NMR spectrum (Figure 67) allowed an estimation of the polymer length to be calculated. This came to approx. 52 repeating units.

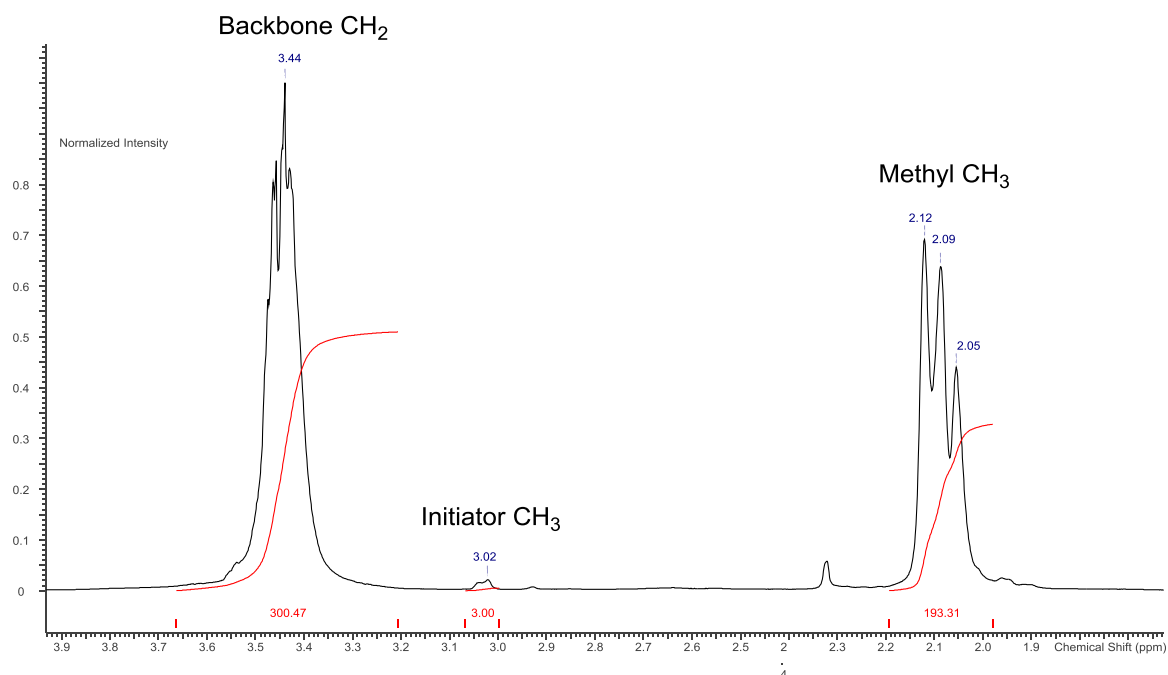


Figure 67: NMR spectrum showing PMeOx NMR resonances and the initiator CH₃ resonance.

4.3 Surface Performance

This work was performed in collaboration with Dr Dario Carugo and Dr Peter Glynne-Jones at the University of Southampton. The PMeOx surface performance was characterised in comparison with that of several other coatings, a fluorinated surface (1H,1H,2H,2H-Perfluorooctyltriethoxysilane), a commercially available Duxcoat™ glass slide, and a clean glass slide as a control.

Two experiments were performed to characterise the antifouling properties of the four surfaces.

4.3.1 Passive Antifouling Performance

Firstly a passive measurement of the antifouling properties of the surfaces was made. This involved incubating the bacteria within the device chamber and allowing the bacteria to interact with the surface with no external influence (*i.e.* no acoustic manipulation) for 30 minutes. Solution was then flowed through the chamber for 5min to remove non-bound bacteria. Images

were taken on the reflector surface before and after the flow to determine the percentage of bacteria attached, Figure 68.

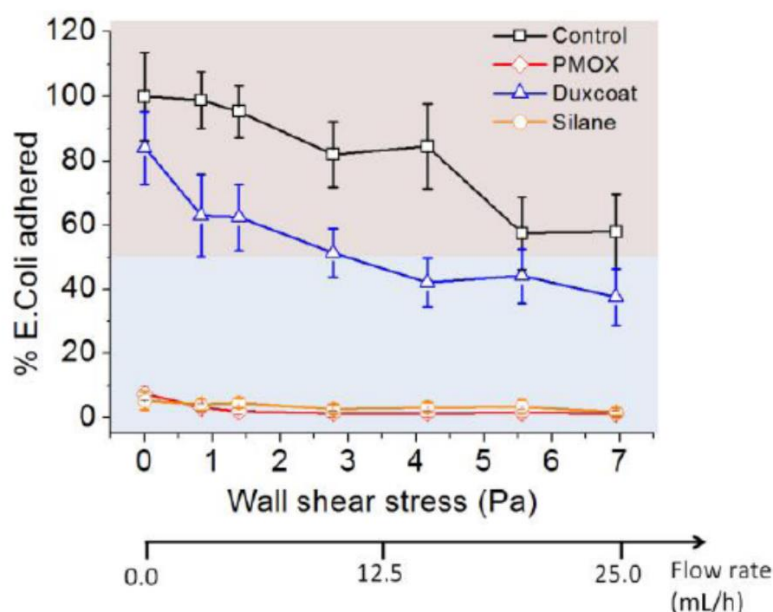


Figure 68: Bacterial adhesion from passive interaction with different coatings of the reflector after rinsing with different flow rates

Figure 688 shows the results from the passive experiment. The glass and the Duxcoat surfaces do not perform particularly well even at high flow rates. The fluorinated silane and PMeOx coatings however appear to be very non-fouling, a result which would be anticipated due to the high hydrophobicity of the fluorinated silane and the published literature surrounding the antifouling properties of PMeOx. A zoomed in region for the silane and PMeOx coatings can be found in Figure 69.

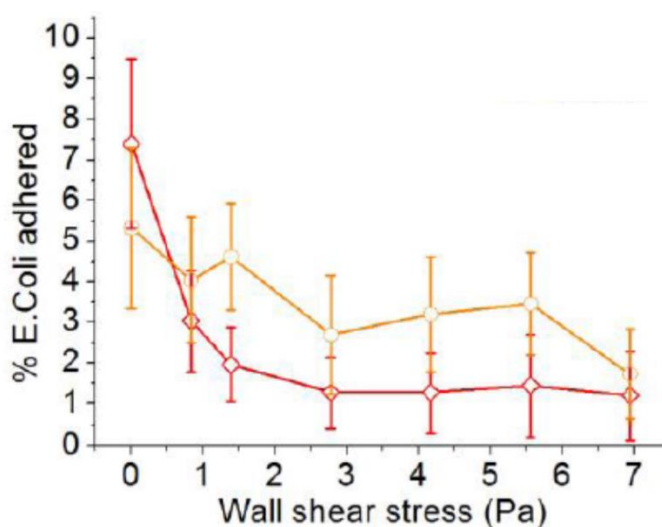


Figure 69: Bacterial adhesion from passive interaction with different surfaces PMeOx (red) and fluorinated silane (orange) surfaces, after rinsing with different flow rates

From this it can be concluded that for a passive interaction the PMeOx coating appears to be the best coating with only a small percentage of bacteria remaining even at low flow rates.

4.3.2 Coating Performance after Ultrasound.

The second experiment involved characterising the surfaces after the ultrasound was applied to the bacteria. The difference in this experiment is that the bacteria are forced into contact with the reflector, unlike the passive experiment where the bacteria are allowed to move independently. The results are shown in Figure 70.

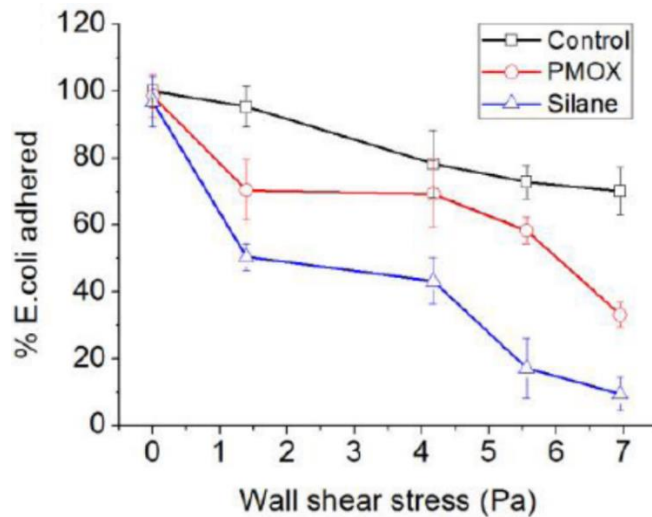


Figure 70: Percentage of bacteria attached to different surfaces after introduction of ultrasound and after rinsing with several flow rates
PMeOx (red) and fluorinated silane (blue) against a clean glass control (black)

The results demonstrate that by introducing the ultrasound and physically forcing the cells onto the reflectors significantly more attachment is observed than in the passive experiments. In this case the fluorinated surface displays much better antifouling properties than PMeOx, possibly this is due to the highly hydrophobic nature of the fluorinated surface.

These results demonstrate that developing antifouling behaviour is not a straightforward procedure. Obviously there is more to learn about bacterial adhesion and behaviour particularly in that case of shear stress being applied.

4.4 Conclusion

To conclude we have demonstrated that PMeOx surfaces are indeed non-fouling in the case of passive bacterial adhesion and they outperform a commercially available coating and are comparable with a fluorinated surface. When ultrasound is applied the behaviour of the surfaces changes dramatically and the PMeOx coating no longer performs in the same manner as the fluorinated surface. This has implications for antibacterial surfaces particularly in situations where there is the potential for shear stress to be applied to bacteria.

Chapter 5 Bacterial Capture Device

5.1 Introduction

Bacterial detection and quantification is an important field, particularly in a medical context. As antibiotic resistance increasingly becomes an issue, detecting if a patient has a bacterial infection and being able to quantify which type of bacterium it is, is one of the big challenges in medicine.

One of the issues facing rapid detection and quantification is sensitivity. It was anticipated that using the device described in Chapter 4 will have an increased the sensitivity by concentrating bacteria. When concentrating bacteria the devices pushes bacteria against the glass reflector. It was hoped that having a particular antibody array on the glass would allow bacteria to be selectively captured. Optical detection would allow quantification of which bacteria are present. As illustrated in Figure 71.

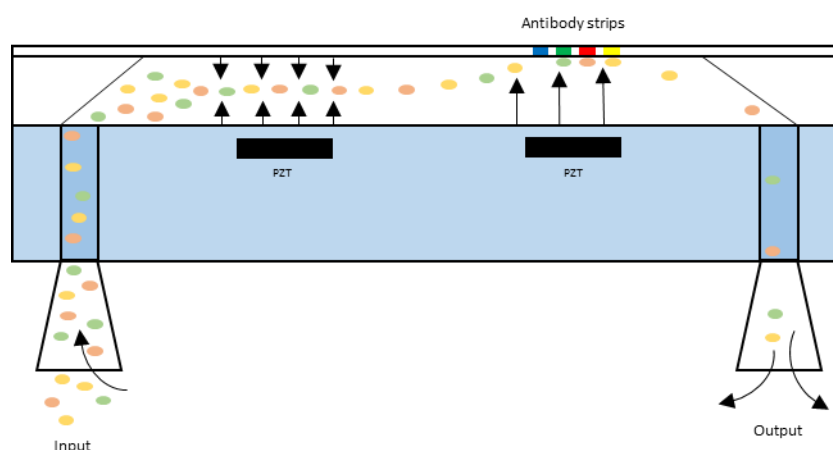


Figure 71: Bacteria capturing device

5.2 Synthesis

The first stage was to test antibody functionalization methods. Five methods were explored, two of which were based on physical absorption and three being based on covalent absorption. These methods have been summarised in Table 13.

| Physical absorption | |
|-----------------------------------|--|
| Amine surface ^{198, 199} | |
| Chitosan surface ¹⁹⁸ | |

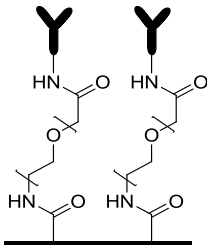
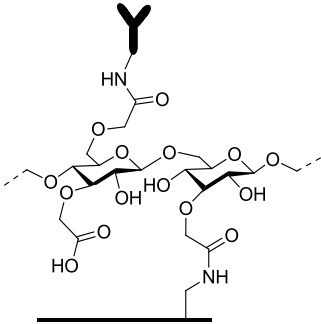
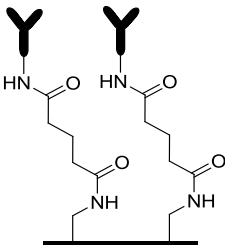
| Covalent absorption | |
|-------------------------------|--|
| Carboxylated PEG |  |
| Carboxymethylcellulose |  |
| Glutaraldehyde ²⁰⁰ |  |

Table 13: Summary of different antibody functionalization methods

The physical absorption method is based on an amine surface. The antibody interacts non-covalently with the amines to absorb onto the surface.

The covalent attachment methods are all based on the coupling of an amine to a carboxylic acid surface. To quantify the amount of antibody on the surface, a fluorescently tagged antibody was used. Using the resultant fluorescence, the amount of antibody could be calculated based on a known calibration sample.

5.3 Antibody Immobilisation and Performance

Initially to test the availability of carboxylic acids on the surfaces fluoresceinamine was used as a model antibody. Antibodies are expensive and were only used once the presence of carboxylic acids was confirmed.

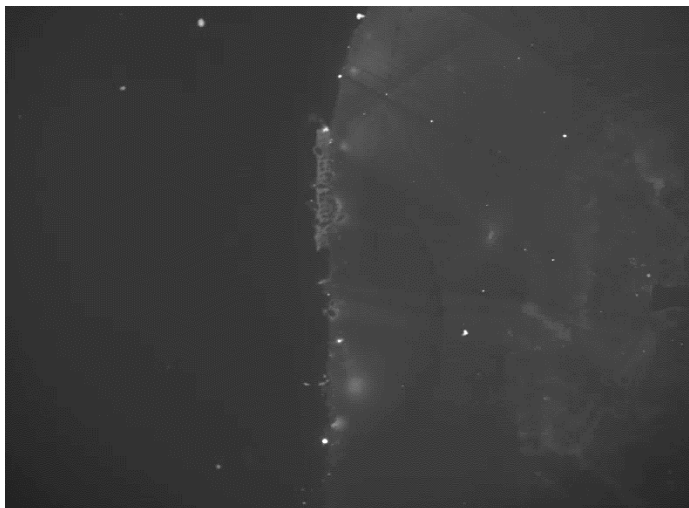


Figure 72: Test of carboxylic acid surface using fluoresceinamine
After EDC/NHS-sulpho coupling with fluoresceinamine. No carboxylic acid (left). Carboxylic acid surface (right)

The test demonstrated that the method should work for antibody attachment, Figure 72. The five surfaces were then coated and the amount of amine attached to them was quantified by recording the fluorescence per pixel compared with the fluorescence per pixel of a known solution of antibody, Figure 73.

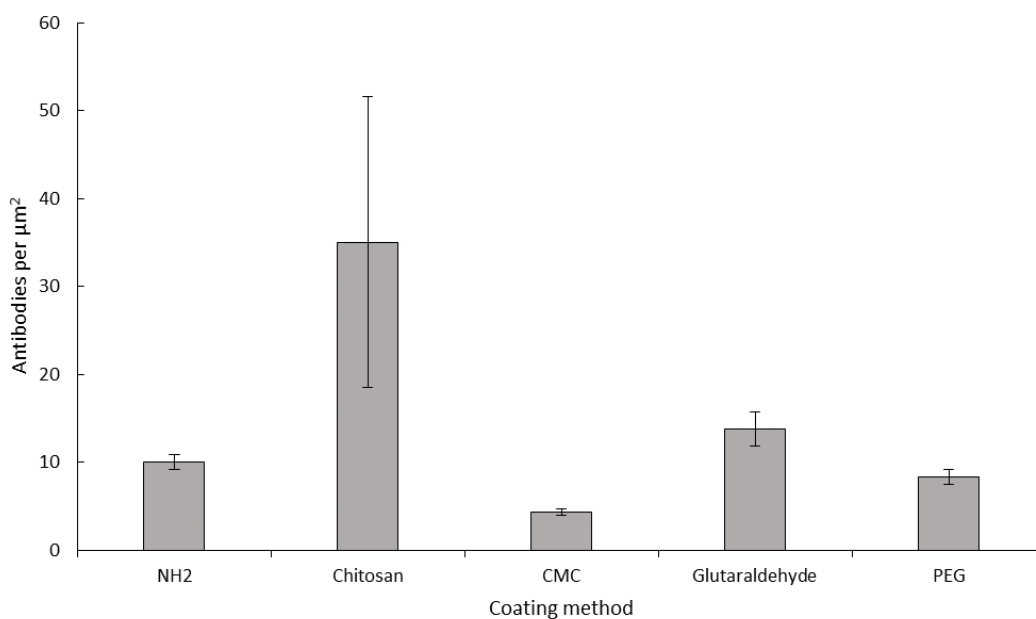
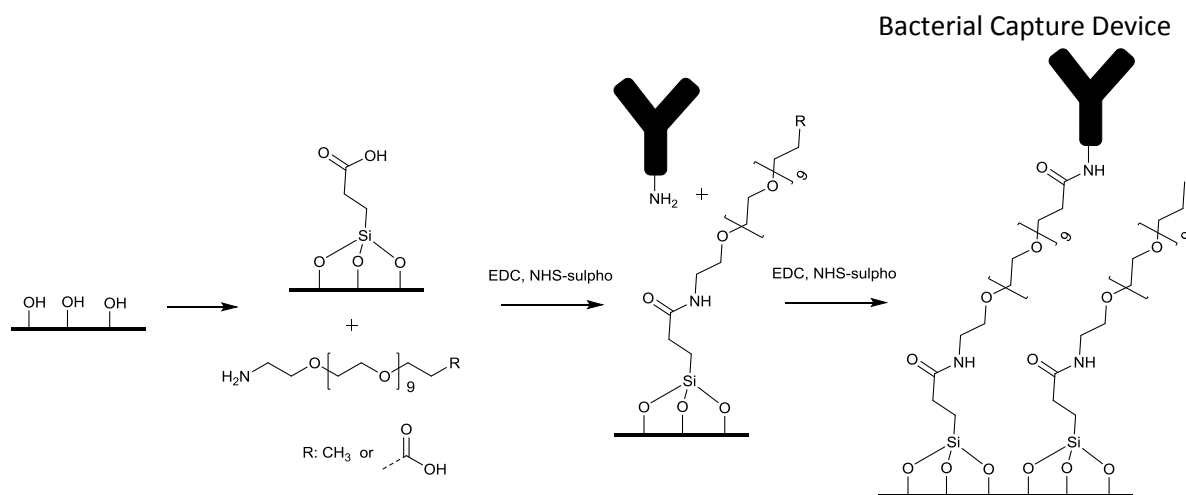


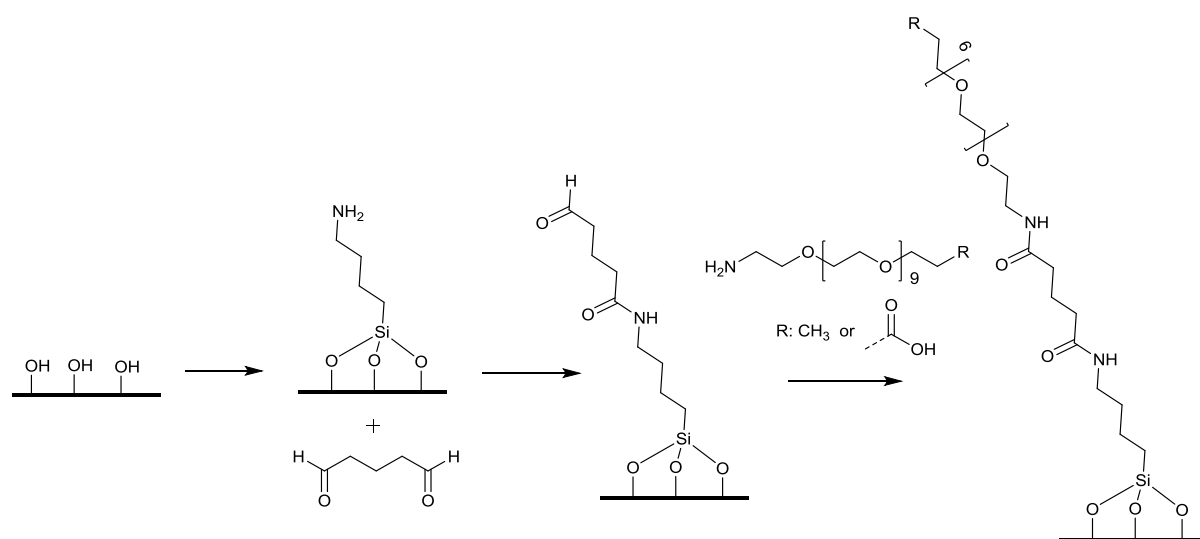
Figure 73: Quantification of antibody compared to different functionalization methods

Antibodies were successfully attached to all five surfaces. The highest functionalization occurred on the chitosan surface, however this surface had also the highest error and most inconsistent coating of antibody. The PEG method was chosen to take further as further tuning of surface coverage could potentially be achieved by adjusting the ratios of PEG functionalised with carboxylic acid groups and PEG functionalised with a methyl group. This is illustrated in Scheme 17.



Scheme 17: Synthesis of Antibody-PEG functionalised glass surfaces

Based on this method a range of different percentages of carboxylic acid surfaces were synthesised. The method illustrated in Scheme 17 was compared with a glutaraldehyde adapted method in which the carboxylic acid silane step was replaced with an amine silane followed by glutaraldehyde step which was used to link the amine surface with the PEG. This is shown in Scheme 18



Scheme 18: Glutaraldehyde modification of PEG surface

The modified PEG attachment and the original method were compared to see which allowed the most antibody to be functionalised. The results are shown in Figure 7474 which compares the amount of antibody added to PEG surfaces with different amounts of carboxylic acid and functionalised PEG content.

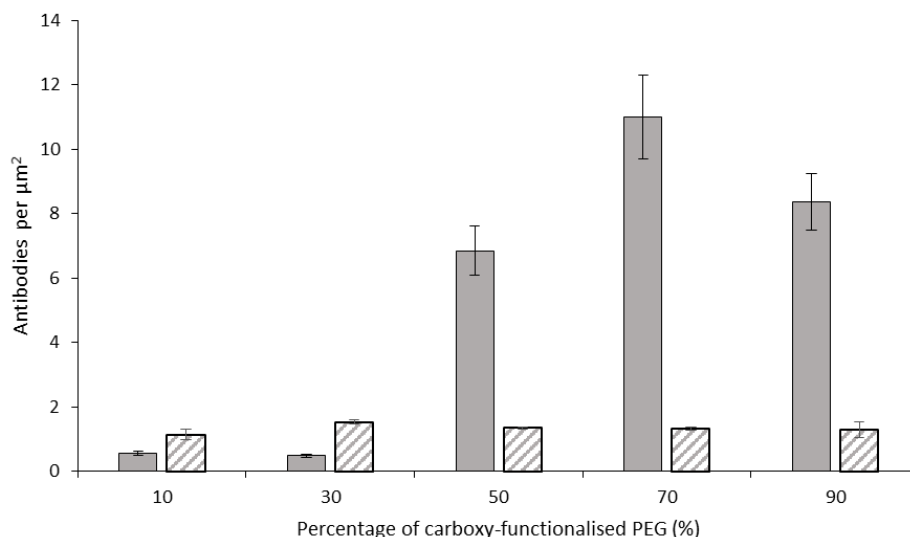


Figure 74: Comparison of the amount of antibody added to PEG surfaces with different amounts of carboxylic acid functionalised PEG content
Original PEG method (solid fill). Modified glutaraldehyde PEG method (dashed fill)

It was found that the original PEG method worked the best. It allowed a larger amount of antibody to be attached for higher percentages of carboxylic acid-functionalised PEG. The results indicated a plateauing of the level of antibodies attached to the surface presumably as a result of saturation of antibodies on the surface preventing reactive sites to be accessed. The original PEG coating method was adopted and the activity of the antibodies was then assessed as a function of the amount of carboxylic acid PEG. The results are shown in Figure 75.

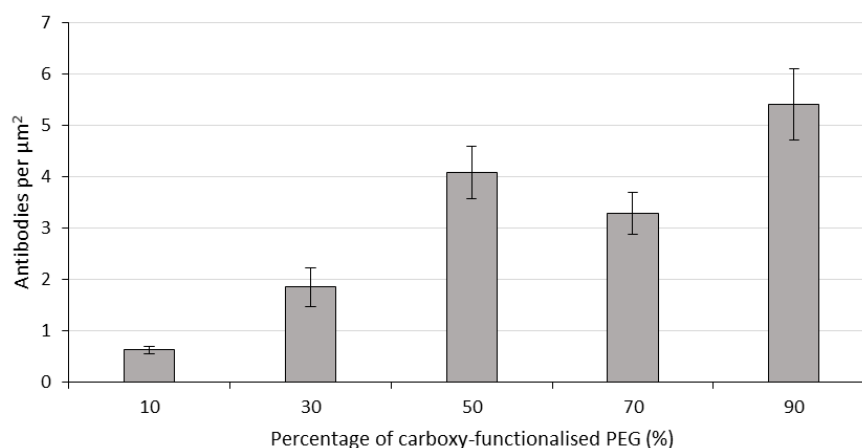


Figure 75: Activity of antibodies attached to PEG surfaces with different numbers of available carboxylic acid sites

The activity of the antibodies was assessed using a 'sandwich' assay. This involved functionalising the surface with non-fluorescent antibody and incubating this with bacterial broth. This broth is a solution in which bacteria can be cultivated. It contains all the necessary nutrients required for bacterial growth. Once the bacteria have been cultured and removed this broth contains many proteins and pieces of dead bacteria which will bind to the antibody-coated surfaces. After the antibody surface has been coated it is rinsed to remove unbound protein and broth and

Bacterial Capture Device
incubated again with the fluorescent antibody. The fluorescent antibody will bind to proteins on the surface and enables the surfaces to be quantified for activity. This method is illustrated in Figure 76 76.

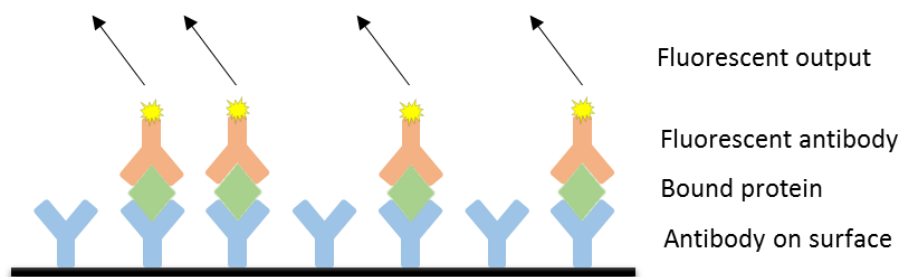


Figure 76: Assessing antibody activity using a sandwich assay

It was found that the activity of the antibody followed a similar trend to that of the amount of antibody as anticipated.

5.4 Capturing Bacteria

An attempt was made to capture bacteria using the device discussed in the Introduction. The bacteria were introduced into the device for different periods of time and the antibody-coated area was compared with the non-antibody coated area, Figure 77.

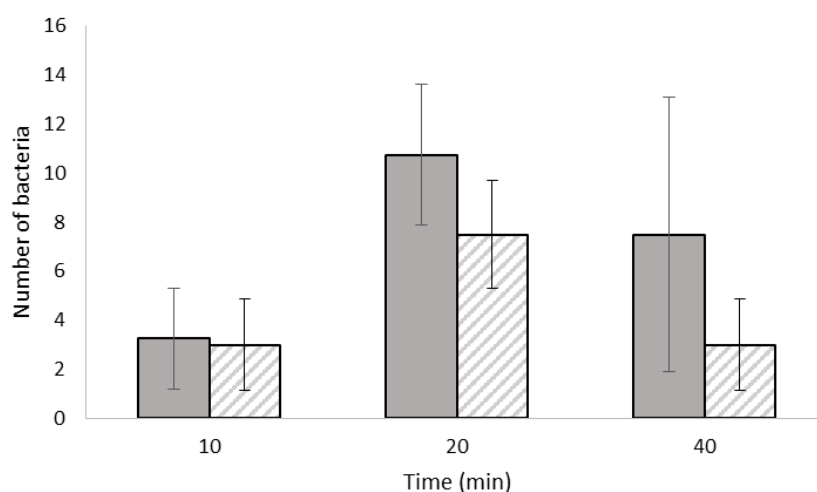


Figure 77: Number of bacteria coating antibody and control surfaces
Antibody coated surface (solid fill) and PEG surface (dashed fill)

It was anticipated that significantly more bacteria should be captured by the antibody. There could be several reasons why this was not successful. The device itself could be inhibiting the bacteria sticking to the antibodies or the time bacteria have to attach to the surface could be too short. Further work will be needed to optimise the bacterial adhesion.

5.5 Conclusion

In conclusion, several antibody coating methods have been tested and compared. One method was developed further and the behaviour of the antibodies was investigated. Further work needs to be undertaken to develop a method which allows bacteria to be captured on the device.

Chapter 6 Thermogelling Poly(2-oxazoline)s

6.1 Overview

Thermoreversible gelation is an interesting behaviour which could lead to a useful material for biological applications. We report here the synthesis of the first poly(2-oxazoline)-based thermogelling polymers. It is hoped that these polymers offer more flexible and tuneable properties than their PNiPAAm-based counterparts leading to useful applications.

6.2 Applications of Thermoresponsive Polymers

6.2.1 Overview

A gel is defined as a three-dimensional network which is swollen by a large amount of solvent. It is typically characterised by²⁰¹:

- The absence of an equilibrium modulus
- The presence of a storage modulus, $G'(\omega)$, that exhibits a pronounced plateau extending to times at least of the order of seconds.
- The presence of a loss modulus, $G''(\omega)$, that is considerably smaller than the storage modulus in the plateau region.

Such materials are classified as either chemical or physical gels depending on the nature of the cross-linking within the structure. Chemical gels are gels which are covalently cross-linked forming a three-dimensional network. Physical gels however are gels which are formed via the growth of physically cross-linked aggregates such as hydrogen-bonded domains, ionic clusters, crystalline regions or phase-separated microdomains.²⁰² Physical gels are of interest mainly because they can be useful in biological applications. Many natural proteins and polysaccharides form these physical gels upon cooling in aqueous solutions, a few examples of which are gelatin, pectin, agarose, agar and carrageenan²⁰³. These bio-polymers gel upon cooling. However, several polymers have been synthesised which gel upon heating. These offer interesting opportunities in drug delivery and tissue engineering as these polymers can be tuned to gel at body temperature and become aqueous when cooled.²⁰⁴⁻²⁰⁷ We aim to use this reversible gelation to create a gelled polymer surface upon which cells can be grown. It is hoped that once the cells have grown into a confluent sheet, cooling of the polymer gel will dissolve the gel network leaving a free cell sheet for further manipulation.

6.2.2 Designing a Thermogelling Polymer

A thermoreversible hydrogel must be made up of two components, a hydrophilic component and a thermoresponsive component which reversibly links the network together.

Crystalline and hydrogen-bonded regions are not suitable for a thermogelling polymer which gels upon heating as these both link at lower temperatures and become disrupted as the temperature is increased. Therefore only hydrophobic interactions can be used to create the linkages within a polymer network upon heating. This is the case with several thermoresponsive polymers making them ideal candidates for the cross-linking component of the thermogelling polymer.

A thermogelling polymer must be a block co-polymer. This can be explained by considering the free energy of the system. We can assume that in water three types of contacts exist: segment-segment interactions, segment-solvent interactions and solvent-solvent interactions. The free energy change (ΔG) when a segment-solvent interaction (E_{12}) is replaced with a segment-segment interaction (E_{11}) and a solvent-solvent interaction (E_{22}) is:²⁰⁸

$$\Delta G = E_{11} + E_{22} - 2E_{12}$$

Equation 4: Energy change of solvent-segment interactions

The Flory-Huggins parameter (χ) which describes how a polymer interacts with a solvent, is related to ΔG :²⁰⁹

$$\chi = \text{const.} \times \left(-\frac{\Delta G}{K_B T} \right)$$

Equation 5: Flory-Huggins parameter (χ). K_B is the Boltzmann constant and T is the temperature

In the case of good solubility, $\Delta G < 0$ and $\chi < \frac{1}{2}$. Phase separation is dependent on the Dp of the polymer chain and occurs when:

$$\chi \geq \frac{1}{2} \left[\frac{1}{(1 + N^2)} \right]$$

Equation 6: Phase separation. N is the Dp of the polymer chain

Strong segment-segment interactions require negative E_{11} values which are large in absolute terms as ΔG needs to be negative. Strong segment-segment interactions are required to form the associative cross-links. These large values lead to a large Flory-Huggins parameter (χ) which in turn makes the polymer insoluble. Therefore, in order for the system to form a reversible gel, it has to be a co-polymer comprising of a segment which reversibly cross-links and a segment which allows the polymer to stay in solution²¹⁰.

These two segments must balance their respective hydrophobic and hydrophilic characteristics to allow the polymer to gel and for this gelation to occur at a suitable temperature. An example of this delicate balance can be illustrated when poly(ethylene glycol) (PEG) and poly(propylene glycol) (PPG) are considered. PEG has an LCST of 100-150°C and this temperature decreases as

Thermogelling Poly(2-oxazoline)s the molecular weight increases²¹¹. An increase in the monomer length by 1 carbon (PPG) lowers the LCST to 10-30°C which also decreases as the polymer weight increases²¹². The inclusion of just an extra methyl group causes the LCST of these polymers to dramatically shift by at least 70°C.

6.2.3 PNiPAAm Based Thermogels

PNiPAAm has been shown to gel using several different systems based on PEG, methacrylates and several different biodegradable systems. These are discussed in the following sections.

6.2.3.1 PEG

PEG-methacrylate of 200-1000 Daltons were copolymerised with PNiPAAm. It was found that as the amount of PEG content increased from 2 – 18 mol% the stability of the gel increased²¹³. A pentablock copolymer of poly(4-styrenesulfonic acid sodium)-PEG-NiPAAm-PEG-poly(4-styrenesulfonic acid sodium) also produced a gel at higher concentrations²¹⁴.

6.2.3.2 Methacrylates

Attempts to combine thermoresponsive characteristics with methacrylate monomers is the most common avenue investigated to produce thermogels. Methacrylate monomers are readily available with a wide range of products, and simple radical co-polymerisation with NiPAAm can create a range of thermogelling polymers.

Poly(NiPAAm-co-methacrylic acid) has been investigated by several groups²¹⁵⁻²¹⁷. Adding an acidic moiety can also add pH sensitivity to the gelling polymers. In fact by comparing copolymers of acrylic acid, methacrylic acid and propylacrylic acid, it was found that due to the nature of the polymer's different hydrophobicity, their pK_a values were 4.3, 5 and 6. It was also found that the methacrylic polymers formed significantly weaker gels than their propylacrylic acid counterparts. This was enhanced further by incorporating a butyl-acrylate monomer and thus increasing the hydrophobic nature of the polymer.

Another popular monomer investigated is poly(*N,N*-dimethyl aminoethyl methacrylate), specifically the quaternized, methylated amine^{218, 219}. It has been found that the gelation not only depends on hydrophobic interactions as with the previous acidic examples but also on minimising cation-repulsion. Addition of NaNO_3 helps to reduce this repulsion by bridging cationic groups and leads to an increase in the strength of the gels formed. By combining these cationic thermogelling polymers with the acidic thermogelling polymers it was found that no pH dependency occurs when the molar ratio is even. This was attributed to the formation of neutral ion pairs²¹⁵.

6.2.3.3 Biodegradable Systems

Broadly speaking the PNiPAAm-based biodegradable systems are based on either a polyacrylate/methacrylate polymer or a polyacrylate/methacrylamide polymer. The principle

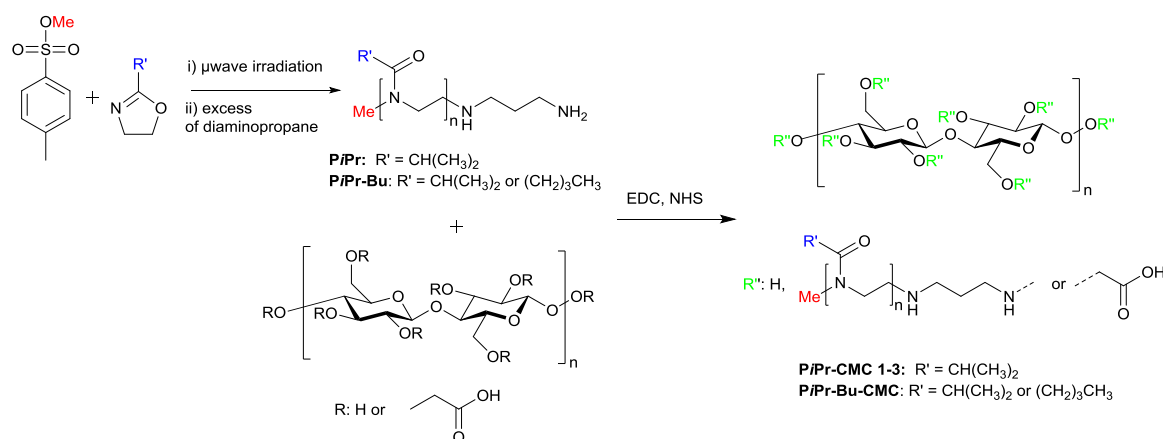
behind the degradation was the incorporation of degradable pendant arms which would be susceptible to hydrolysis. This causes the polymer to become more hydrophilic and thus become soluble at 37°C. Some of the systems investigated were: lactate-dilactate block co-polymer²²⁰; dimethyl- γ -butyrolactone acetate co-polymers^{221, 222}; hydrophobic polypeptide segments²²³; poly actylmethacrylate moiety's²²⁴; and poly(trimethylenecarbonate) co-polymers²²⁵.

6.3 First Generation Thermogelling Brush Polymers

6.3.1 Overview

The first attempt at designing and synthesising a thermogelling polymer followed the principles laid out in the Introduction. A similar paper which used PNiPAAm was used as a basis for synthesising the first poly(2-oxazoline) thermogelling polymers. Carboxymethylcellulose (CMC) was used as the polar backbone with poly(2-oxazoline)s providing the thermoresponsive arms.

The amine-functionalised end groups of the poly(2-oxazolines) mentioned in the Synthesis section seemed to provide a good choice for linking poly(2-oxazoline)s to the CMC backbone following the method outlined in Scheme 19 below.



Scheme 19: Synthesis of thermogelling poly(2-oxazoline)s

6.3.2 Synthesis of Poly(2-oxazoline) Brush Polymers

Several amine-terminated polymers were synthesised using the procedure outlined in section 2.3.5.2 and these are tabulated in Table 14.

| Polymer | % Butyl | M_w | M_n | PDI | T_{cp} (°C) |
|--|---------|-------|-------|------|-------------------|
| PiPrOx-NH ₂ -1 | 0 | 44555 | 39854 | 1.11 | 38.5 [†] |
| PiPrOx- <i>n</i> BuOx-NH ₂ -1 | 27.5 | 26631 | 16066 | 1.65 | 23 |
| PiPrOx- <i>n</i> BuOx-NH ₂ -2 | 35 | 28115 | 17182 | 1.63 | 13.12 |
| PiPrOx- <i>n</i> BuOx-NH ₂ -3 | 33 | 35212 | 42243 | 1.19 | 14.17 |

[†]calculated from plot of M_n vs T_{cp} , T_{cp} calculated using a 4mg ml⁻¹ solution in water.

Table 14: Amine terminated poly(2-alkyl-2-oxazoline)s

Initially PiPrOx-NH₂-1 was synthesised to test the synthetic method for producing thermogelling polymers. The co-polymers were synthesised to lower the T_{cp} sufficiently to allow the gelation temperature to be in the region useful for biological applications. The T_{cp} for the co-polymers is well below 37°C, however it was anticipated coupling the poly(2-oxazoline)s with a polar backbone would increase the T_{cp} , similar to the effect observed when a more hydrophilic monomer is incorporated into thermoresponsive poly(2-oxazoline)s⁴.

6.3.3 Synthesis of Thermogelling Polymers

The thermogelling polymers were synthesised according to the method discussed above. To gain insight into how the gelation temperature (G_T) can be adjusted, the thermogelling polymers were synthesised with varying numbers of arms on each backbone. It was hypothesised that this should change the properties of the gel and the gelation temperature. The results are summarised in Table 15.

| Oxazoline polymer | Thermogelling polymer | μ Moles of Oxazoline | μ Moles of CMC (COOH) | Ratio COOH:Oxazoline | Number of arms per backbone | Average Mw of Polymer† (kDa) |
|---------------------------------|-----------------------|--------------------------|---------------------------|----------------------|-----------------------------|------------------------------|
| PiPrOx-NH ₂ -1 | TG-I-A | 2.48 | 1.24 | 2.00 | - | - |
| | TG-I-B | 1.24 | 1.24 | 1.00 | - | - |
| | TG-I-C | 0.41 | 1.24 | 0.33 | - | - |
| PiPrOx-nBuOx-NH ₂ -1 | TG-27.5-A | 7.07 | 1.24 | 5.68 | 7.7 | 214.22 |
| | TG-27.5-B | 3.53 | 1.24 | 2.84 | 4.8 | 166.92 |
| | TG-27.5-C | 1.77 | 1.24 | 1.42 | 5.5 | 178.11 |
| | TG-27.5-D | 1.18 | 1.24 | 0.95 | 5.5 | 178.13 |
| PiPrOx-nBuOx-NH ₂ -2 | TG-35-A | 6.64 | 1.24 | 5.34 | 8.6 | 331.80 |
| | TG-35-B | 3.32 | 1.24 | 2.67 | 4.5 | 217.35 |
| | TG-35-C | 1.66 | 1.24 | 1.33 | 3.1 | 176.76 |
| | TG-35-D | 1.11 | 1.24 | 0.89 | 2.9 | 170.65 |
| PiPrOx-nBuOx-NH ₂ -3 | TG-33-A | 34.08 | 9.96 | 3.42 | 4.3 | 240.83 |

†Calculated from elemental analysis

Table 15: Thermogelling polymers synthesised

Poly(2-oxazoline) arms were observed from the elemental analysis for all of the thermogelling polymers by measuring nitrogen content. Control over the extent of side-arm addition was poor and yields were low. This method appears to have several problems which are listed below;

- The end termination using the amine polymers could be low yielding, resulting in a reduced number of reactive end-functionalised polymers than calculated. Characterisation of the number of amine terminal groups is difficult due to the relatively low concentration of these compared to the rest of the poly(2-oxazoline) present.
- The number of polymers attaching to the backbone could be inhibited because of slower reaction rates due to the temperature used in the coupling reaction (approx. 2°C) and

high viscosity. Steric hindrance could also be an issue causing a limited amount of polymer to be able to reach the backbone.

- The purification method may remove the polymers which have a higher number of poly(2-oxazoline) chains. Purification is achieved via precipitation in methanol. The poly(2-oxazoline) arms may solubilise the high density grafted polymers in methanol leaving only the low density grafted polymers to precipitate.
- To obtain a reasonable yield which could be used in a practical application 20 or 30g of poly(2-oxazoline) needs to be synthesised for just half a gram of thermogelling polymer therefore the reaction is not particularly efficient. Any excess polymer can be removed by precipitation in the workup.

Issues aside, this method does successfully provide thermogelling polymers in high enough quantity that we can begin to analyse some of their properties.

6.3.4 Molecular Weight Determination

To calculate the molecular weight elemental analysis can be used. The poly(2-oxazoline) brushes contain nitrogen and the CMC backbone does not, this can be used to determine the number of poly(2-oxazoline) arms per backbone and thus give an estimate of the molecular weight.

The calculated molecular weight is only a guideline, both the backbone and the arms have a statistical distribution of molecular weights, this means although the elemental analysis and subsequent molecular weight determination could give a certain number of arms per backbone there is a wide distribution of possible structures.

6.4 Gelation Properties

To characterise the gelation of these polymers rheology was used. Rheology is the study of the flow of liquids and is used to monitor properties of a liquid or gel while subjecting it to external forces. The two parameters which are of most importance are the storage modulus (G') and the loss modulus (G'')²²⁶.

6.4.1 Rheological Characterisation

The storage modulus measures the deformation energy stored by a sample. This energy is stored by the sample and then released completely or partially to recover the original structure of the sample. This means that if a sample has a high G' then it is storing any deformation energy and using most of it to revert back to its original structure, behaving like an elastic material. Therefore G' represents the elastic behaviour of the material.

The loss modulus measures the amount of energy lost by a sample as it is deformed. This energy is lost due to the flow of the material. The molecules physically move and flow over each other as

Thermogelling Poly(2-oxazoline)s
the sample is put under load; this causes frictional contact to occur between these molecules. This generates heat and it is via this route that the energy is lost. The energy loss is therefore irreversible and the deformation cannot be recovered. Accordingly G'' represents the viscous behaviour of the samples.

From these two values we can calculate the complex viscosity of the material. This is related to both G' and G'' and gives a value for the viscosity of the solution.

By monitoring these two parameters the behaviour of the material can be monitored as gelation is induced via a controlled variation of temperature. The gelation temperature (G_T) is defined as the crossover point between G' and G'' . Above this point the material is behaving like a solid and below this it is behaving like a liquid.

6.4.2 Visual Confirmation

Initially PiPrOx-NH₂-1 was used to synthesise TG-I-A – TG-I-C (see Table 15, page 91). Each of these samples demonstrated the thermogelation behaviour. Gelation was confirmed visually using TG-I-A, Figure 78. When the thermogel solution was heated in water gelation was observed to occur very rapidly.

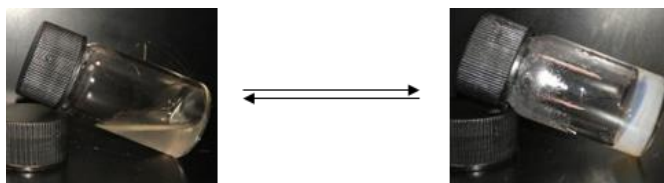


Figure 78: Thermoreversible gelation of a 4% by weight solution of TG-I-A
At 20°C (left) and 50°C (right)

The solution was observed to become cloudy upon heating, this is possibly due to the cross-linking microdomains forming and scattering light.

6.4.3 Thermoreversible Gelation

The first factor to consider was whether the gels displayed *thermoreversible* gelation. For the gels to be applicable for a biological application they had to re-liquefy at a useful temperature. The heating and cooling cycle for TG-33-A is shown in Figure 799. The gel was dissolved in phosphate buffered saline (PBS) as the polymer without buffer is quite acidic in solution owing to the acidic side chains on the cellulose. The buffer kept the pH to a biologically relevant pH 7 while also containing similar salts and concentrations used in cell media.

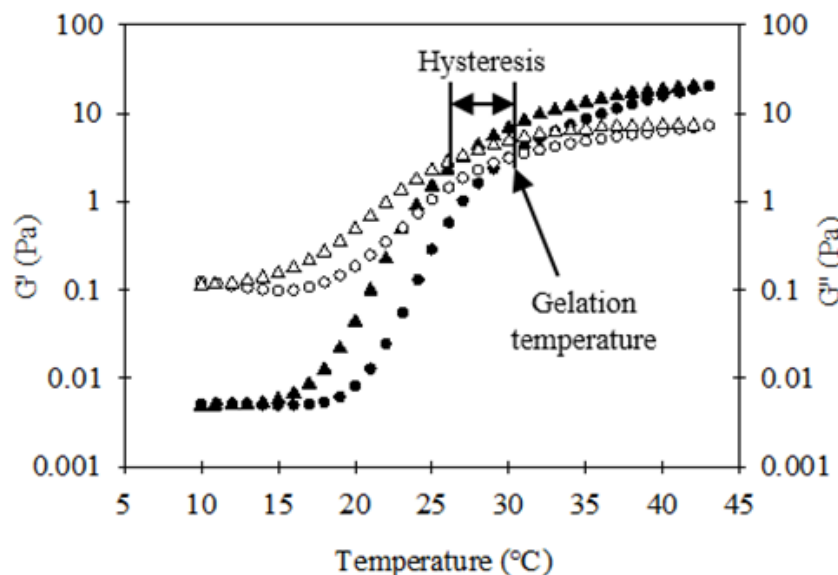


Figure 79: Heating - cooling cycle for TG-33-A
4% w/w solution in PBS, Heating ● (open G'' , closed G'), Cooling ▲ (open G'' , closed G')

Figure 79 shows the classic features of a thermogelling polymer. Both G' and G'' increase as the polymer approaches the G_T ; this is accompanied by a crossover point where G' becomes larger than G'' which is the gelation temperature.

A hysteresis between heating and cooling is observed. This is possibly due to a kinetic phenomenon in which the polymers resist the disentanglement of the polymer chains creating a hysteresis. This is something observed in the analogous PN/PAAm thermogelling polymers²²⁷. The hysteresis observed for these polymers appears to be much smaller due to poly(2-oxazoline)s containing only hydrogen bond accepting moieties while PN/PAAm contains both hydrogen bond accepting and donating sites.

6.4.4 Tuning Gelation Temperature a Biologically Useful Temperature

For these polymers to be biologically useful we need to be able to control the gelation temperature to within a region suitable for biological applications (i.e. below 37°C).

6.4.4.1 Influence of Poly(2-oxazoline) Brush Concentration

By observing the gelation of the three samples which are functionalised with different amounts of poly(2-oxazoline) arms, the relationship between the G_T and the number of poly(2-oxazoline) arms can be deduced, Figure 80.

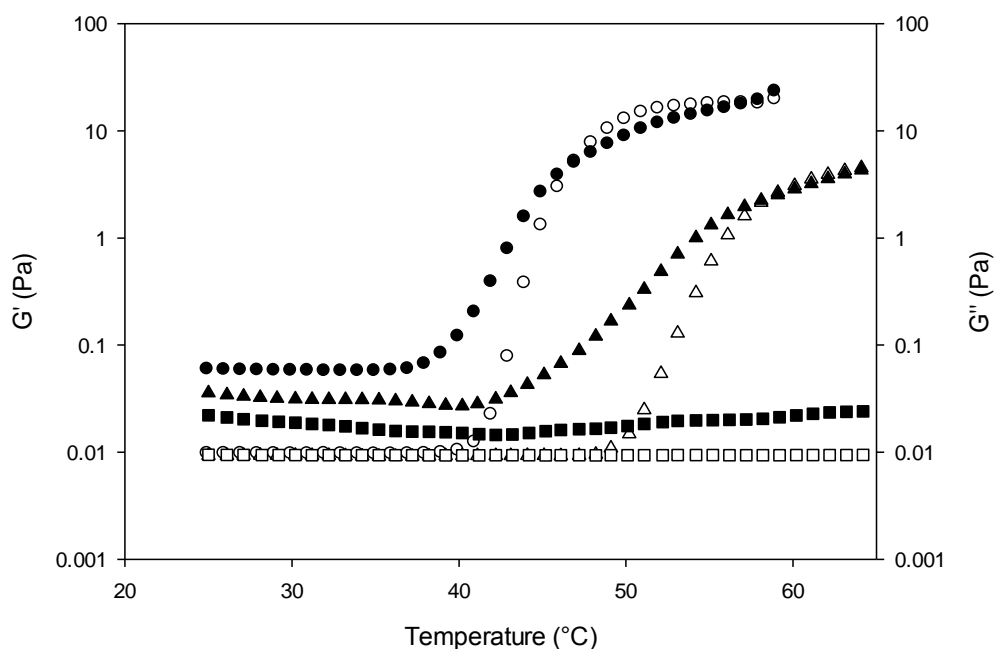


Figure 80: Thermogelling behaviour of TG-I-A to TG-I-C
A 4% by weight solution was used. G' (open) and G'' (filled). TG-I-A (circle) TG-I-B (triangle), TG-I-C (square)

For TG-I-A - C we see a clear relationship between the amount of poly(2-oxazoline) added and the gelation properties (see Table 15). We find that G_T decreases as the amount of poly(2-oxazoline) added decreases. TG-I-C does not display a G_T , probably due to the number of thermoresponsive arms being too low for cross-linking to occur. The gelation temperature for TG-I-A is 47°C and TG-I-B 58°C which are too high to be potentially useful for biological applications.

6.4.4.2 Lowering the Gelation Temperature Via Copolymerisation

To lower the temperature to an acceptable range we decided to use the co-polymer of *i*PrOx and *n*BuOx which was previously shown in Chapter 2 to have a dramatically reduced T_{cp} . Figure 81 below shows a representation of the thermoresponsive gelation of polymers containing three poly(2-oxazoline) arms containing different amounts of *n*BuOx.

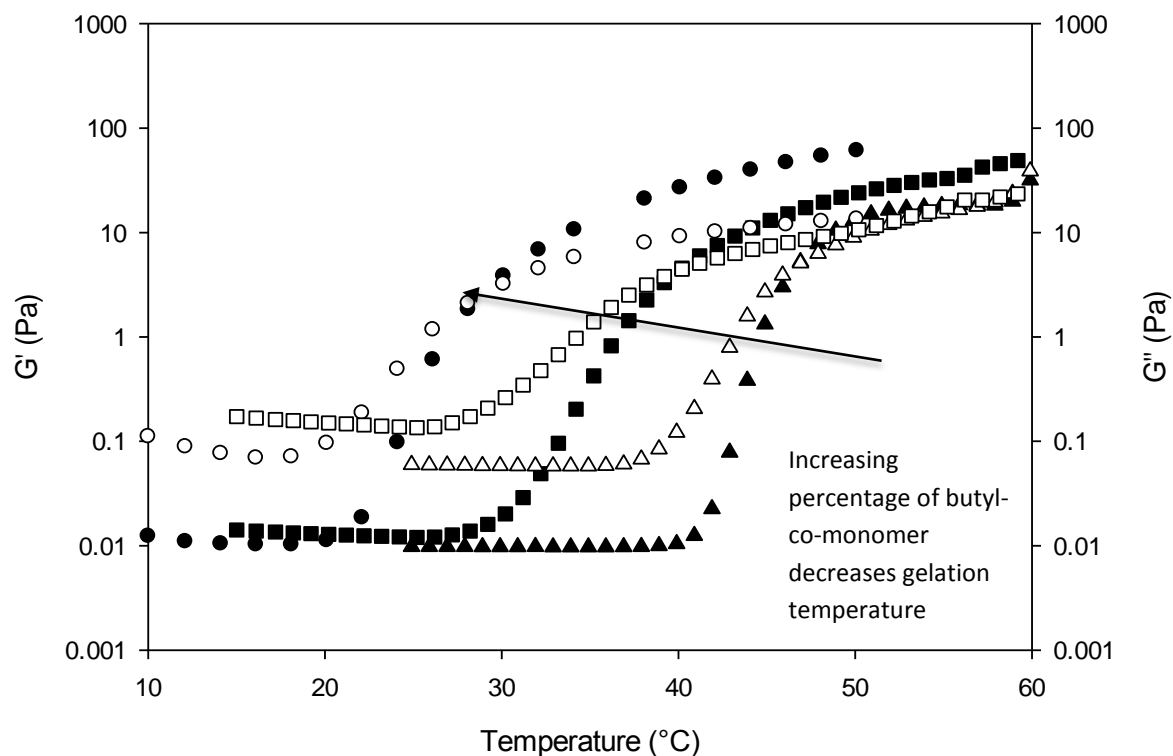


Figure 81: Thermogelation of TG-I-A, TG-27.5-A and TG-35-A
A 4% by weight solution in water. G'' (open) and G' (filled). TG-I-A (triangle), TG-27.5-A (square), TG-35-A (circle)

By incorporating more of the hydrophobic monomer into the gelling polymer the G_T has successfully been lowered.

| Polymer | G_T (°C) | T_{cp} of arms (°C) | Difference (°C) |
|-----------|------------|-----------------------|-----------------|
| TG-I-A | 49.1 | 38.5 | 10.6 |
| TG-27.5-A | 40.2 | 23 | 17.2 |
| TG-35-A | 29 | 13.1 | 15.9 |

Table 16: Comparison between T_{cp} and G_T

As anticipated we observed an increase from the T_{cp} of the arms to the G_T of the corresponding thermogelling brush polymers as proposed in Section 6.3.2. In the case of TG-27.5-A, the T_{cp} of the poly(2-oxazoline) arms, $PiPrOx-nBuOx-NH_2-1$, was 23°C. After coupling to CMC the G_T , which is effectively the T_{cp} of the thermogelling material is now 40.2°C. This is now above the temperature useful for biological applications. TG-35-A however is within the range even though the T_{cp} has increased by about 15°C. This demonstrates control can be achieved even when the T_{cp} of the original poly(2-oxazoline) arms changes by a large amount.

6.4.5 Influence of Concentration on the Gelation Temperature

Once control over the G_T had been demonstrated, the reaction was scaled up producing a larger amount of gelling polymer. We had previously synthesised batches of around 50mg so the

Thermogelling Poly(2-oxazoline)s synthesis was scaled up by a factor of 10 to produce around 500mg of gelling polymer, TG-33-A. This then allowed further investigation into the properties of this novel thermogelling material.

The effect of concentration on the gelation transition was initially investigated. Five samples were made up from 2% (w/v) up to 10% (w/v). The results of the rheological studies are shown in Table 17

| Weight % | Calc conc. (μM) | G_T ($^{\circ}\text{C}$) |
|----------|------------------------------|------------------------------|
| 10% | 4.15 | 20.1 |
| 8% | 3.32 | 23 |
| 6% | 2.49 | 26 |
| 4% | 1.66 | 29 |
| 2% | 0.83 | No gelation |

Table 17: Properties of TG-33-A at different concentrations

We see an increase in the G_T as the thermogel decreases in concentration. This can be observed clearly in Figure 82.

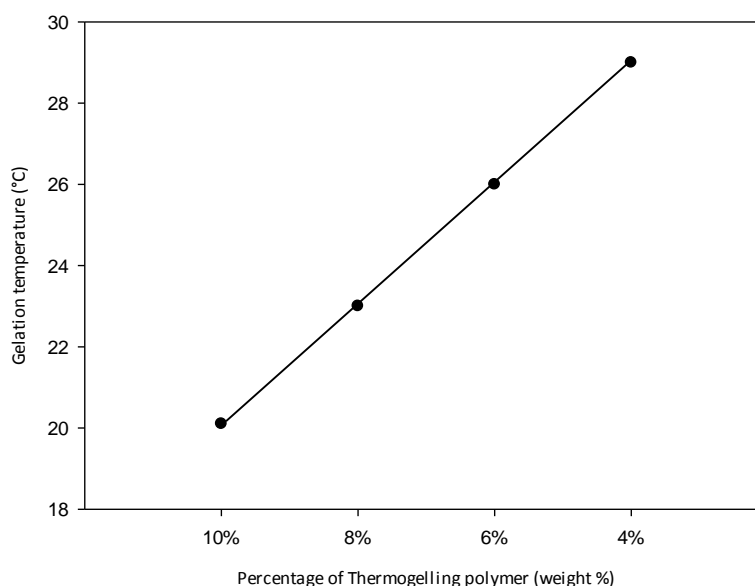


Figure 82: Relationship between gelation temperature and thermogel concentration

This is analogous to the observed trend for poly(2-oxazoline)'s T_{cp} concentration dependency as demonstrated in Chapter 1. The G_T of these polymers increases as the concentration decreases. Gelation was not observed for the 2% sample which could possibly be due to the sample reaching a critical concentration of poly(2-oxazoline) arms. If there are not enough arms to link together then the sample does not gel. This point may lie between 4-2% for this specific system.

For all the samples we see an increase of around 100 times in the complex viscosity. The trend in increasing viscosity can be seen if we plot the complex viscosity as a function of temperature for the 2%-8% samples, Figure 83.

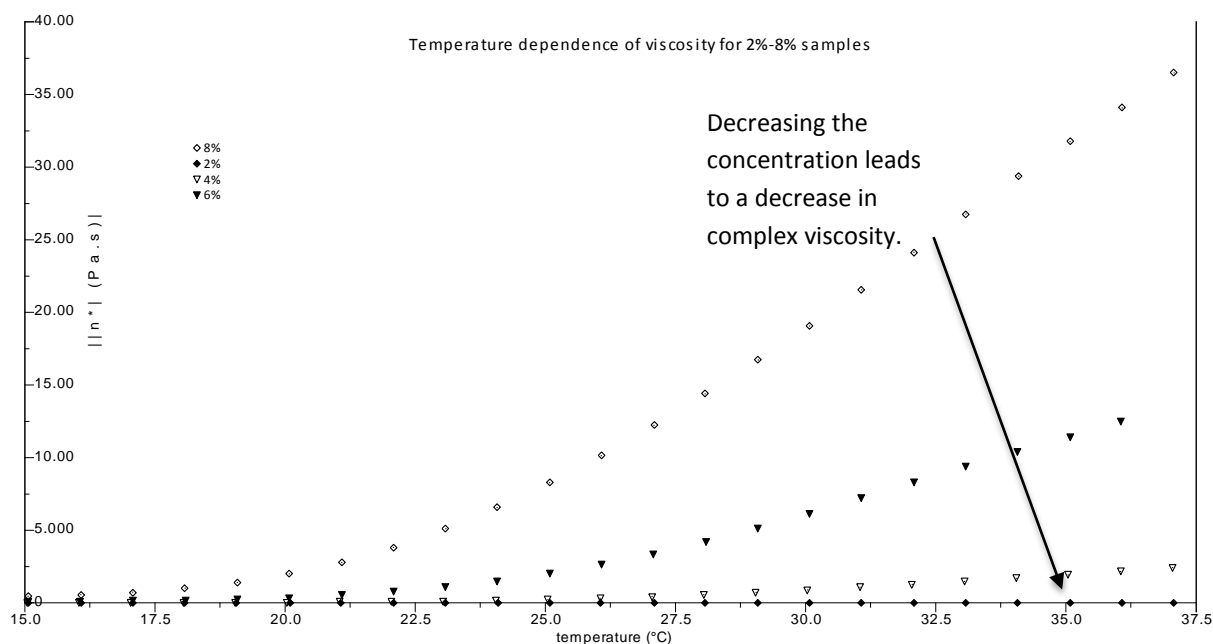


Figure 83: Complex viscosity of TG-33-A at different concentrations

The 10% sample displayed a lower viscosity than the 8% therefore not conforming to the trend. This could be because of the polymer solution becoming too viscous to allow the poly(2-oxazoline) arms to become entangled, lowering the amount of cross-linking and thereby lowering the viscosity.

6.4.6 Stability

So far we have studied the polymer in solution at pH-7 which is the natural pH of the polymer. By holding the gel above its gelation temperature for prolonged periods of time we can study whether the polymer degrades. We propose that this is due to the hydrolysis of the amide linker between the poly(2-oxazoline) arms and the CMC backbone as has been observed for similar materials²²⁸. The gelation temperature and G' were monitored after holding TG-33-A above its gelation temperature for periods up to two weeks, Figure 84.

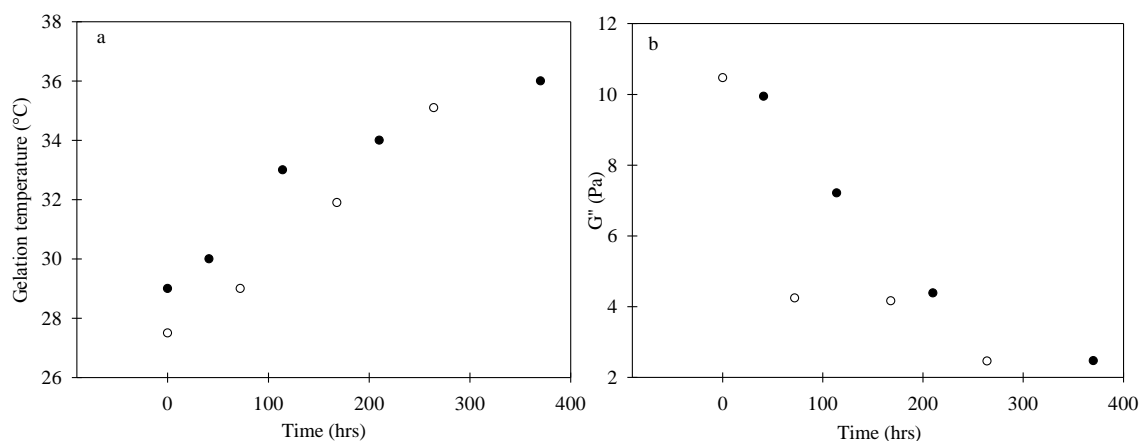


Figure 84: Time dependent degradation of TG-33-A at two pH
Using a 4% w/w solution. Change in gelation temperature (a) and G' (b) at 37 °C, for pH 7 (○) and pH 3 (●)

At both pH 3 and 7 we observed a change in both gelation temperature and G' over time. As the samples were held for longer periods of time, the gelation temperature increased and G' decreased. This is consistent with the expected breakdown of the polymer. If the thermogels are degrading, we would expect both the gelation temperature to increase and the gels to lose their mechanical strength, in a manner analogous to the concentration dependence observed previously. Although degradation occurs, it appears to be a slow process. In the time frame investigated here TG-33-A remained gelled and mechanically stable at 37 °C after two week. No appreciable difference in the degradation behaviour of TG-33-A was observed at pH 7 or pH 3.

The behaviour of one sample of TG-33-A at pH 12 (4% w/v) was briefly investigated. At this value we observed an increase in gelation temperature to from 29 °C to 47 °C. This was attributable to deprotonation of the carboxylic acid groups at pH 12 which results in repulsion between the cellulose units, thereby inhibiting gelation and entanglement, a phenomenon which has been observed for similarly charged thermogelling polymers²¹⁵.

6.5 Application in Tissue Engineering

6.5.1 Overview

As discussed in the Introduction the main application of thermogels are as injectable, drug delivery materials^{136, 216, 221, 228-231}. For the poly(2-oxazoline) thermogels a different application was investigated, namely cellular engineering as discussed in the following section.

6.5.2 Modelling Tissue

To create a tissue model in the laboratory multiple cell types are required. Combining different cell types to create model tissue is far more complex than simply combining cells together. Apart from laboratory grown cells generally requiring different growth factors and conditions in the cell media, one of the main issues is the cells competing with each other when first added to a tissue culture dish. This leads to one cell type becoming dominant and prevents formation of any tissue-like structure.

For the model investigated two cell types were studied; human bronchial epithelial cells (16HBE); and human foetal lung fibroblast cells (MRC5). As discussed in chapter 3 these cells are involved in creating the barrier in airways in the lung. The fibroblasts are the structural component with the epithelial cells creating a membrane-like barrier. Currently models using these two cell types are grown in transwells. The transwell allows the top (airway) and bottom (blood vessel) to be differentiated thereby mimicking the airway. One major constraint is that the models currently used have to physically separate the two cell types to prevent any competition between the cells, Figure 85.

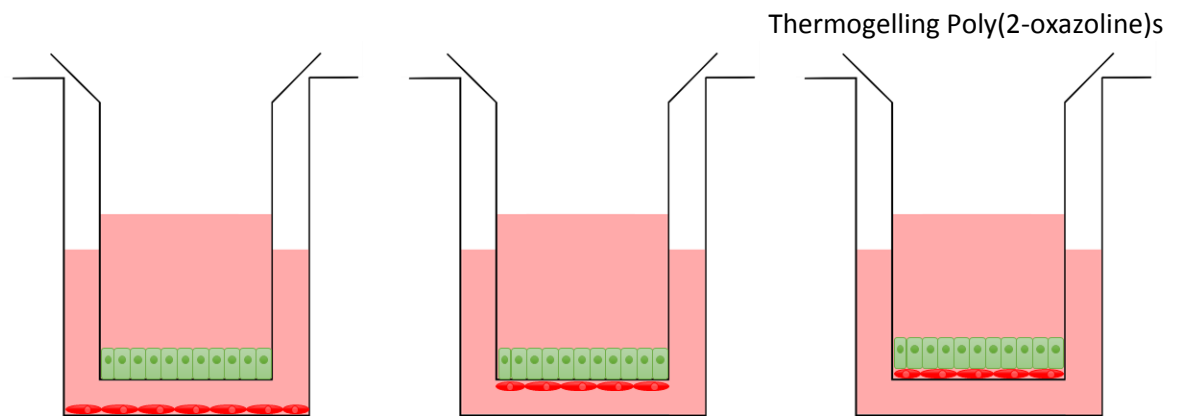


Figure 85: Graphic of the different methods of co-culturing cells currently used
Non-contact co-culture with fibroblast (red) on the bottom and epithelial (green) in the transwell (left). Membrane co-culture with the fibroblasts and epithelial cells separated by a transwell membrane (center). Ideal situation with both cells in contact but currently not possible using conventional methods (right)

It was hoped that, by using the thermogel as an intermediate substrate, the cells can be introduced together and will allow two layers to form instead. Instead of adding individual cells together the thermogel will be used to allow the epithelial cells to form larger aggregates. These larger aggregates, when added to an already confluent layer of fibroblasts, would spread out and form the second sheet. The advantage of using the thermogel would be that it enables the initial epithelial aggregation to occur without the cells adhering to the substrate they are sitting on which would otherwise prevent this method from being possible. Any excess thermogel could be removed by dissolution into the cell media by cooling the media briefly. The method is illustrated below (Figure 86).

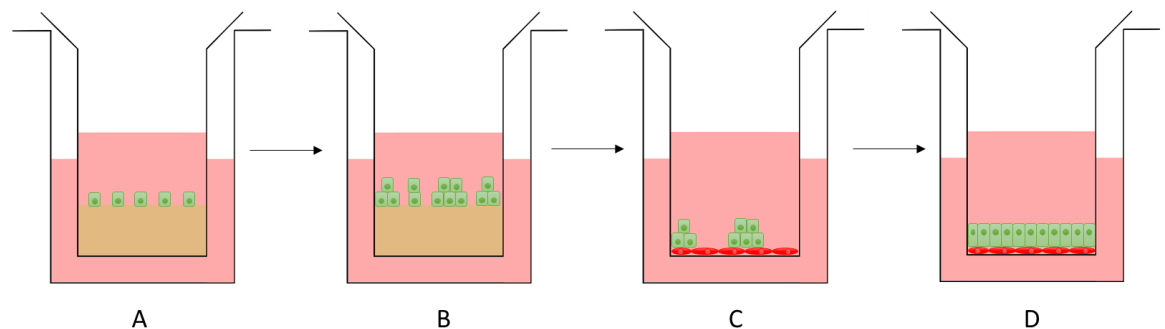


Figure 86: Method of co-culture using a thermogel
Epithelial cells are added to thermogel (A). After two hours aggregates have formed (B). These are transferred to a confluent layer of fibroblast cells (C). The gel aggregates form a cell sheet over the fibroblasts (D)

6.5.3 Toxicity

To assess the toxicity of the thermogel it was incubated with the epithelial cells for different periods of time. The cells were then stained to highlight the dead cells. The cells were seeded onto the bottom of a cell culture substrates and then covered with the thermogel. This was because the cells were difficult to image when on top of the thermogel as a result of the uneven

Thermogelling Poly(2-oxazoline)s
surface of the gel. Figure 877 below shows the percentage of dead cells found over a period of 24 hours.

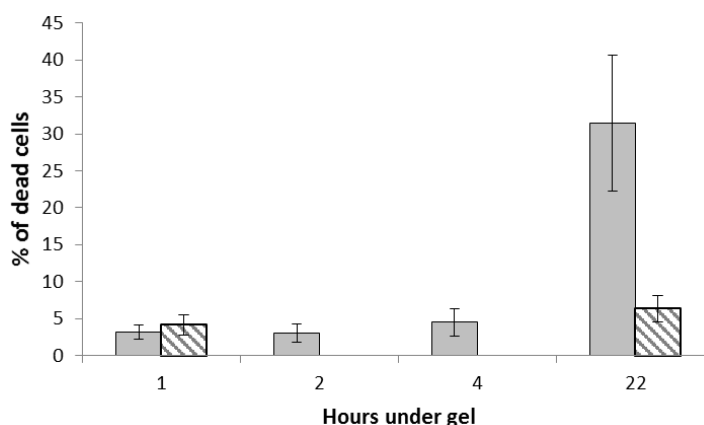


Figure 87: Toxicity of poly(2-oxazoline) thermogel over time
Thermogel coated cells (solid), control (dashed)

Over a period of 24 hours the thermogel appears to be reasonably toxic killing around a third of cells. The thermogel material should not in itself be toxic. Toxicity could be due to several factors, one of which arises from impurities in the gel killing cells. However if this was the case cells would begin to die immediately after their addition, after four hours there does not seem to be a significant amount of dead cells relative to one hour. Another potential issue may be suffocation of the cells. If the nutrients in the media cannot diffuse fast enough through the gel to supply the cells this could cause the cells to die. As the actual application requires the cells to be in contact with the gel for only two hours there would be no issues arising from the toxicity of the gel in this particular case.

6.5.4 Creating Tissue Models

Cells which had been genetically modified to express a green fluorescent protein (16HBE cells) and a red fluorescent protein (MRC5 cells) were kindly provided by Angela Tait at Southampton General Hospital. This made them easier to image without the need for a cell staining step. Once the epithelial cells were added to the fibroblasts they were imaged for up to five days.

The cells were imaged using a time-lapse system which allows a video to be compiled from the frames. The green aggregates can be seen spreading out in a process called plithotaxis (which is a migratory behaviour displayed by groups of cells), Figure 88. This behaviour is the key difference between adding cell aggregates or individual cells. Without plithotaxis the cell sheets will not form and instead the cells will burrow through the fibroblast layer.

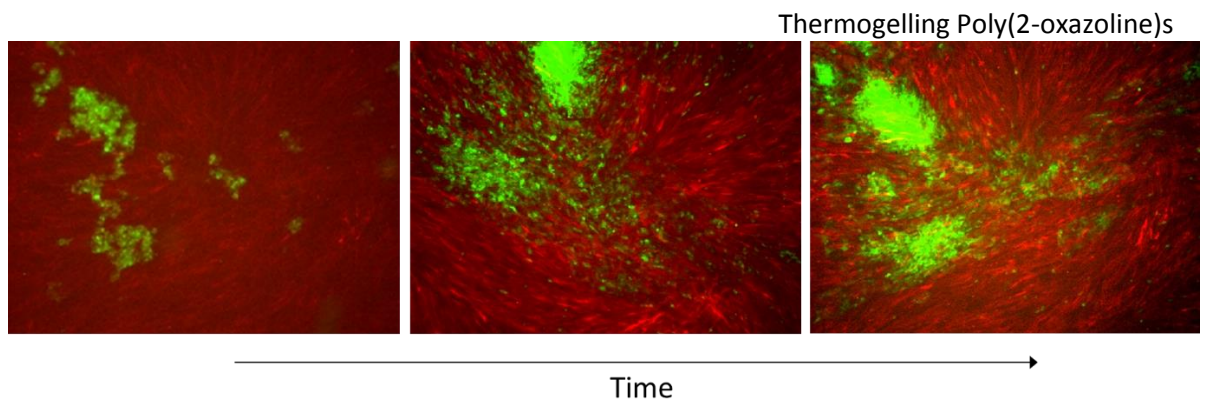


Figure 88: Fluorescent microscopy of co-cultures
Imaged using an optical microscope at 10x magnification. MRC5 cells (5×10^3) were loaded with Cell Tracker Orange (red) and 16HBE cells (5×10^3) stably transfected with GFP (green) at different times from 0 days (left) to three days (right)

Although in the images it appears that cells were migrating over the fibroblasts, confirmation of the presence of two layered sheets was obtained using confocal microscopy to produce a 'z-stack' image. As is implied in the name, images of the cell sheet are taken as the focus is adjusted through the z-plane of the sheet (vertically) at regular intervals. This allows a cross-sectional image of the cell sheets to be generated, Figure 89.

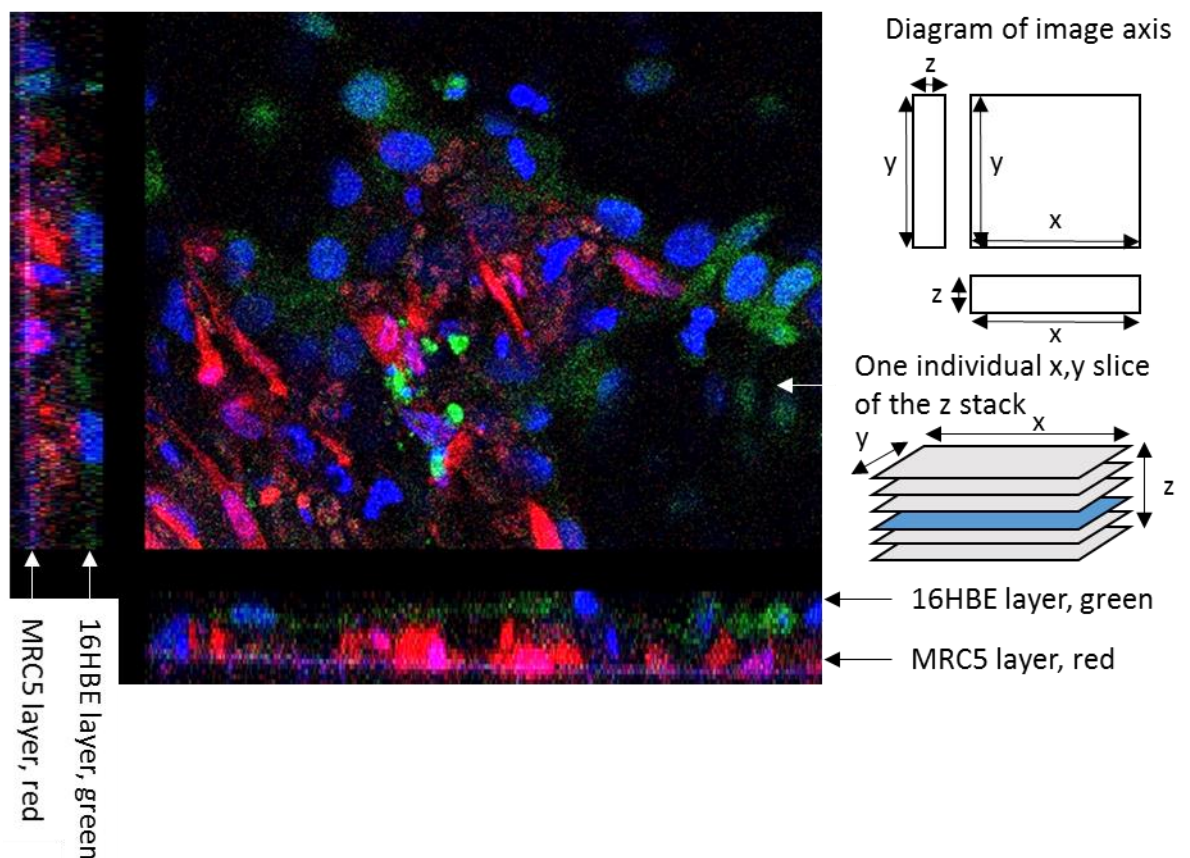


Figure 89: Confocal microscope image of co-cultured cell sheet
The two vertical cross sections of the main image (x,z and y,z images) show the two layers of cells (red and green) on top of each other. The nuclei (blue) are distributed between both layers as expected.

The confocal image clearly shows the two layers of the sheets with the red layer of fibroblasts on the bottom and the green layer of epithelial cells on top confirming the synthesis of a multi-layered cell sheet.

This is a potentially significant discovery which could have applications in many areas of tissue engineering not just with the specific case here. The method is simple and should be adaptable for more than two cell types. Many obstacles still lay ahead with the development of the method and characterisation of the sheets behaviour compared with other conventional methods. It is worth noting that the same results have been achieved using an acoustic levitation device instead of the thermogel material in a parallel study associated with this work.

6.5.5 Summary

In summary we have successfully demonstrated the synthesis of a novel CMC and poly(2-oxazoline) thermogelling brush co-polymer. We have characterised it's behaviour and tuned the structure and properties of this polymer to be useful in a biological applicaton, tissue engineering. We have then demonstrated its potential as a biologically relevant material by producing multi-layered cell sheets, something which is difficult to achieve conventionally and has never been demonstrated using a thermogelling material.

6.6 Second Generation Triblock Poly(2-oxazoline) Thermogels

As discussed, although the cellulose-based thermogels have potential for further development, the material itself has drawbacks.

- The amount of poly(2-oxazoline) required to make a few grams of thermogelling polymer is very uneconomical.
- The gelling solutions are very viscous when in the liquid state due to the topology of the thermogelling polymers.
- There is poor control over the carboxymethylcellulose backbone in terms of mass and PDI.
- It is difficult to prepare the material reproducibly.

6.6.1 Overview

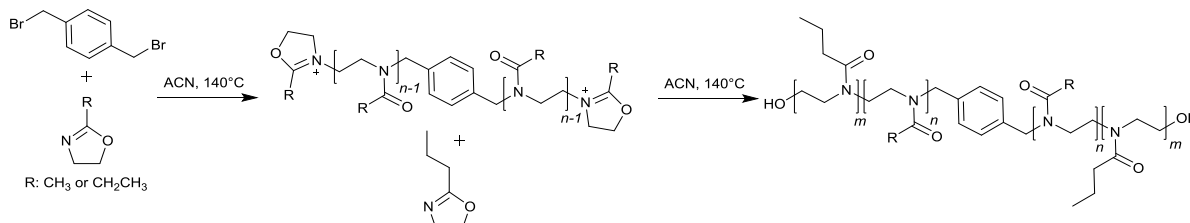
Since most of the issues arose from the use of CMC it was desirable to replace the CMC backbone with another polar moiety. It was anticipated that using either the methyl or ethyl 2-oxazoline instead of the CMC would provide sufficient polarity to form the gel. Based on similar PEG²³² and PNiPAAm^{233, 234} work a BAB triblock structure was adopted, in which the B blocks was the thermoresponsive cross-linking moiety and the A block was the polar moiety.

6.6.2 Proof of Principle

The following body of work was carried out in collaboration with Prof Richard Hoogenboom and Bart Verbreken at the University of Ghent. All the work unless noted was carried out by myself.

6.6.2.1 Synthesis

An initial proof of principle was attempted using 2-*n*-propyl-2-oxazoline (*n*PrOx) and varying the core with either MeOx or EtOx according to Scheme 20.



Scheme 20: Synthesis of a BAB triblock polymer with either a methyl or ethyl core

*n*PrOx was used as opposed to *i*PrOx as the polymer has a lower LCST of around 25°C⁵. The dibromo initiator was initially used, however one limitation of this was that the polymerisation of PMeOx is mainly ionic and the P*n*PrOx segment more covalent. This means that the propagation step with P*n*PrOx is much slower with this initiator than with a triflate or tosylate.

Consequently longer reaction times were required. The two polymers were characterised and the results displayed in Table 17.

| Sample Name | Sec Results | | | Calculated Repeating units | | | | |
|--|-------------|-------|------|----------------------------|---------------|---------|---------|-----|
| | Mn | Mw | PDI | MeOx | <i>n</i> PrOx | B block | A block | Dp |
| P <i>n</i> PrOx ₁₂ -PMeOx ₁₀₉ -P <i>n</i> PrOx ₁₂ | 27960 | 24577 | 1.45 | 109 | 24 | 12 | 109 | 301 |
| | | | | EtOx | <i>n</i> PrOx | B block | A block | |
| P <i>n</i> PrOx ₁₄ -PEtOx ₁₂₅ -P <i>n</i> PrOx ₁₄ | 33000 | 23888 | 1.27 | 125 | 28 | 14 | 125 | 327 |

Table 18: BAB triblock polymers with a methyl and ethyl core

It was observed from the SEC traces that a relatively high polydispersity was obtained along with some extra 'shoulder' peaks. It is proposed that these shoulder peaks correspond to polymer chains which have prematurely terminated leaving a B, BA and BAB polymer peak with a fourth peak at the lowest retention time corresponding to longer oligomers from chain transfer reactions.

6.6.2.2 Rheological characterisation

To test the potential thermogelling properties of these materials rheological characterisation was undertaken. The results are displayed in Figure 90.

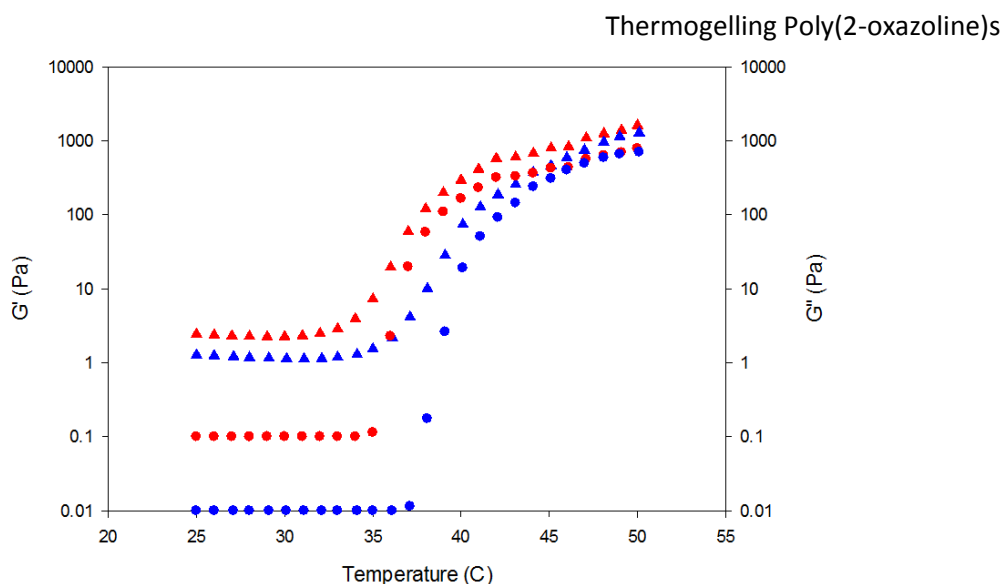


Figure 90: Thermothickening behaviour of $PnPrOx_{12}$ - $PMeOx_{109}$ - $PnPrOx_{12}$ and $PnPrOx_{14}$ - $PEtOx_{125}$ - $PnPrOx_{14}$ $PnPrOx_{12}$ - $PMeOx_{109}$ - $PnPrOx_{12}$ (circle) and $PnPrOx_{14}$ - $PEtOx_{125}$ - $PnPrOx_{14}$ (triangle) with G' in blue and G'' in red. 40% w/w in water

From the rheological characterisation thermothickening behaviour but not gelation was observed. Both G' and G'' increase indicating an increase in viscosity. However the characteristic crossover of G' and G'' is absent.

Visually the two materials behave differently. $PnPrOx_{12}$ - $PMeOx_{109}$ - $PnPrOx_{12}$ stays clear upon heating while $PnPrOx_{14}$ - $PEtOx_{125}$ - $PnPrOx_{14}$ becomes opaque. This is possibly due to the more hydrophobic character of $PEtOx$ which is causing a more pronounced phase separation leading to polymer micro-domain formation. These micro-domains scatter light leading to the opaque look. The more hydrophilic $PMeOx$ may not form these.

This provided an encouraging insight into the behaviour of poly(2-oxazoline)s with a BAB structure. It was anticipated that adjusting the structure would facilitate the formation of a gel as opposed to the thermothickening behaviour observed.

6.6.3 Development of Novel Thermogelling Poly(2-oxazoline)s

To develop the poly(2-oxazoline) thermogelling polymers it was decided to optimise the polymers using the $PMeOx$ core only. For biological applications it would be desirable to develop a colourless, transparent material which only appeared to occur with the $PMeOx$ -cored polymers. Further development would be focussed on adjusting the thermoresponsive B blocks by changing the length and the composition. The two structures focussed on are shown in Figure 91.

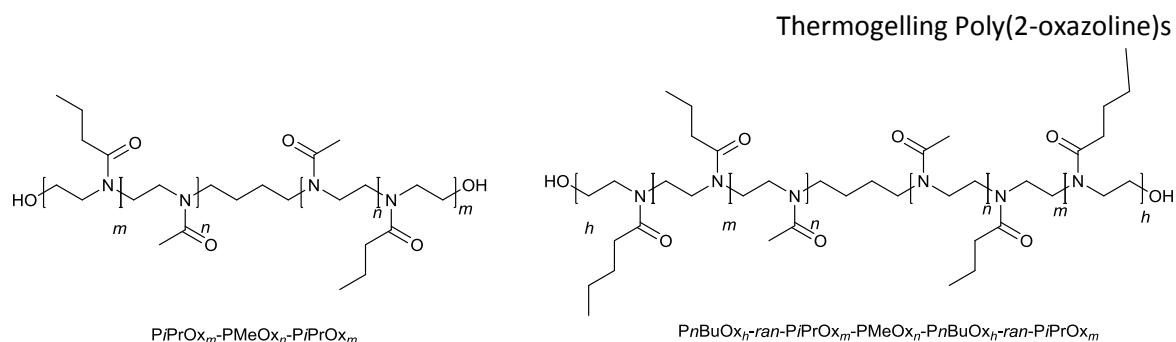


Figure 91: BAB triblock copolymers with a butane core

The dibromo-initiator was replaced with a butanedinitrile initiator since nitriles, being more reactive, display faster initiation and also facilitate *PnPrOx* and *PnBuOx* propagation. This initiator was kindly provided by Bart Verbraken in Prof Hoogenboom's group. To elucidate the influence of the BAB architecture on thermogelation a range of materials were produced. Three parameters were varied:

- The length of the thermogelling B-block.
- The inclusion of the more hydrophobic *nBuOx* monomer into the B block.
- The length of the hydrophilic A-block.

6.6.3.1 Characterisation

These polymers were characterised using SEC and NMR to obtain an approximation of the structure and relative amounts of the A and B blocks. The results of the analysis of the synthesised samples are summarised below (Table 19).

| Sample Name | Sec Results | | | Calculated Repeating units | | | | | |
|--|----------------|----------------|------|----------------------------|-------|-------|---------|---------|-----|
| | M _n | M _w | PDI | MeOx | nPrOx | nBuOx | B block | A block | Dp |
| PnPrOx ₂₄ -PMeOx ₁₃₆ -PnPrOx ₂₄ | 16835 | 24577 | 1.45 | 68 | 24 | - | 24 | 136 | 184 |
| PnPrOx ₂₈ -PMeOx ₁₁₇ -PnPrOx ₂₈ | 16408 | 23888 | 1.46 | 59 | 28 | - | 28 | 117 | 145 |
| PnPrOx ₄₁ -PMeOx ₈₄ -PnPrOx ₄₁ | 16381 | 27388 | 1.67 | 42 | 41 | - | 41 | 84 | 125 |
| PnPrOx ₅₅ -PMeOx ₈₆ -PnPrOx ₅₅ | 19496 | 30056 | 1.54 | 43 | 55 | - | 55 | 86 | 141 |
| PnPrOx ₆₆ -PMeOx ₈₂ -PnPrOx ₆₆ | 21671 | 31553 | 1.46 | 41 | 66 | - | 66 | 82 | 148 |
| PnPrOx ₆₂ -PMeOx ₆₄ -PnPrOx ₆₂ | 19117 | 28071 | 1.47 | 32 | 62 | - | 62 | 64 | 126 |
| PnPrOx ₄₈ -PMeOx ₂₀ -PnPrOx ₄₈ | 12846 | 16829 | 1.31 | 10 | 48 | - | 48 | 20 | 68 |
| PnPrOx ₄₆ -PMeOx ₅₂ -PnPrOx ₄₆ | 14739 | 21285 | 1.44 | 26 | 46 | - | 46 | 52 | 98 |
| PnPrOx ₅₄ -PMeOx ₇₂ -PnPrOx ₅₄ | 18299 | 29561 | 1.62 | 36 | 54 | - | 54 | 72 | 126 |
| PnPrOx ₆₁ /PnBuOx _{4.5} PMeOx ₆₂ | 13529 | 20969 | 1.55 | 62 | 61 | 4.5 | 66 | 62 | 194 |
| PnPrOx ₆₁ /PnBuOx _{4.5} | | | | | | | | | |
| PnPrOx ₆₃ /PnBuOx _{7.5} PMeOx ₅₇ | 13447 | 21515 | 1.60 | 57 | 63 | 7.5 | 70 | 57 | 198 |
| PnPrOx ₆₃ /PnBuOx _{7.5} | | | | | | | | | |
| PnPrOx ₅₄ /PnBuOx ₉ PMeOx ₅₁ | 12778 | 20801 | 1.63 | 51 | 54 | 9 | 63 | 51 | 178 |
| PnPrOx ₅₄ /PnBuOx ₉ | | | | | | | | | |
| PnPrOx ₄₉ /PnBuOx _{10.5} PMeOx ₄₃ | 11818 | 19811 | 1.68 | 43 | 49 | 10.5 | 60 | 43 | 163 |
| PnPrOx ₄₉ /PnBuOx _{10.5} | | | | | | | | | |
| PnPrOx ₅₄ /PnBuOx _{6.5} PMeOx ₆₄ | 13343 | 21960 | 1.65 | 64 | 54 | 6.5 | 61 | 64 | 185 |
| PnPrOx ₅₄ /PnBuOx _{6.5} | | | | | | | | | |
| PnPrOx ₆₁ /PnBuOx _{11.5} PMeOx ₈₁ | 16691 | 23990 | 1.44 | 81 | 61 | 11.5 | 73 | 81 | 226 |
| PnPrOx ₆₁ /PnBuOx _{11.5} | | | | | | | | | |

Table 19: Characterisation of a range of BAB triblock co-polymers

All the polymers suffered from quite high polydispersity which is proposed to be caused by chain termination before the block co-polymers are formed. These different terminated polymers can be observed in the SEC trace, Figure 92.

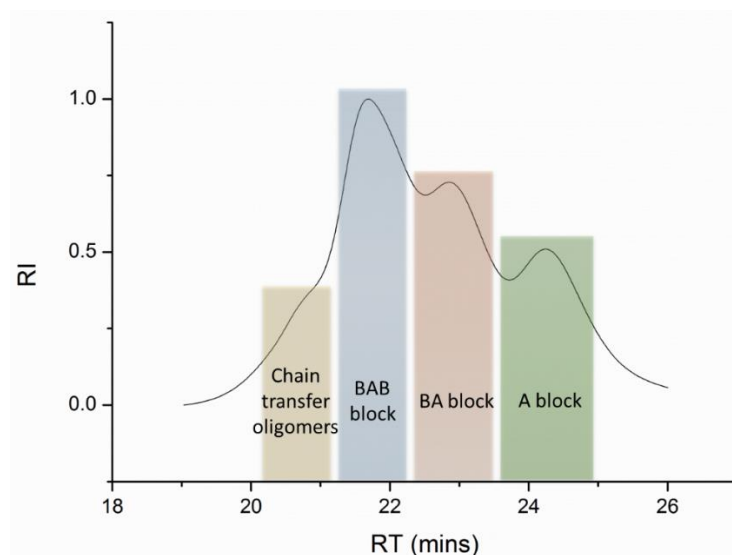


Figure 92: Different co-polymers observed in the SEC trace for PnPrOx₆₁/PnBuOx_{4.5}PMeOx₆₂PnPrOx₆₁/PnBuOx_{4.5}

Shorter retention time (RT) means larger polymers as they interact with the column less. The mixture of different polymer structures is difficult to prevent as chain termination often increases when another monomer is introduced.

6.6.4 Visual Confirmation of Gelation

As with the CMC based gels the first step to check gelation was by visual confirmation, Figure 93.



Figure 93: Visual confirmation of thermogelation of $PnPrOx_{62}$ - $PMeOx_{64}$ - $PnPrOx_{62}$
Cold (left) heated (right)

The gels appeared to be more gel-like than the previous CMC gels, indeed by using a spatula the gel could be broken up and scooped out without liquefying, something which was not possible using the CMC-based gels.

6.7 Gelation Properties

The materials were characterised using the same methodology as the first generation thermogels.

6.7.1 Reversible Gelation

The first step involved characterising the materials to make sure that the thermogelation was indeed reversible. By monitoring G' and G'' over a heating and cooling cycle any hysteresis or difference between the two could be determined, Figure 94.

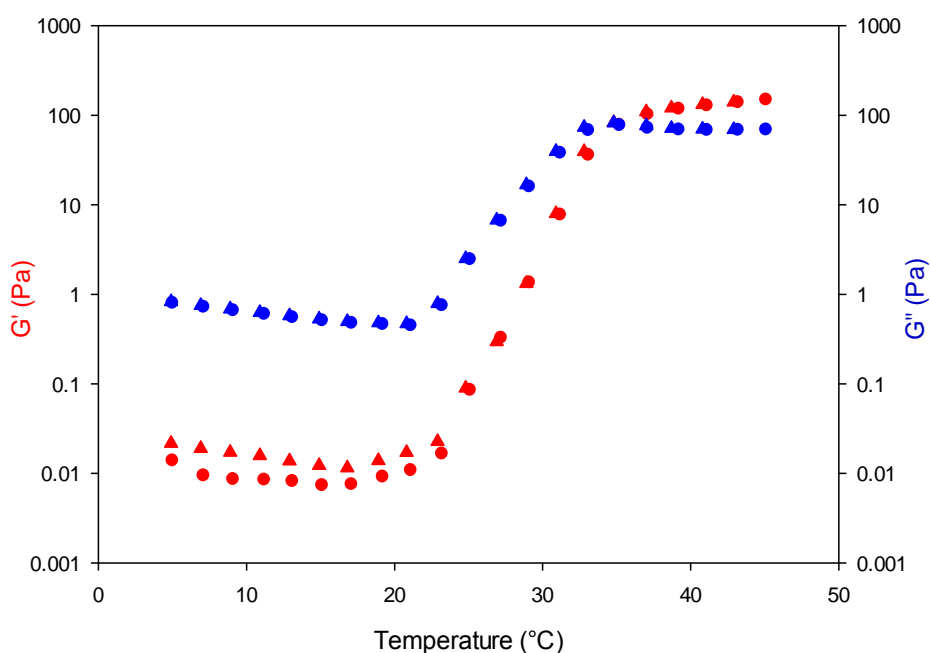


Figure 94: Heating and cooling cycle for $PnPrOx_{66}$ - $PMeOx_{82}$ - $PnPrOx_{66}$
 G' (red) and G'' (blue). Heating (triangle) and cooling (circle)

Figure 94 demonstrates that the materials display reversible gelation. As anticipated no hysteresis was observed for any sample. This is explained by the absence of hydrogen bond donors on poly(2-oxazoline)s preventing hydrogen bonding above the G_T . This is in contrast to the CMC based thermogels which display a hysteresis due to the hydrogen bond donor/acceptor properties of the CMC and the poly(2-oxazoline)s.

6.7.2 Effect of Concentration

The effect of concentration was then examined using $PnPrOx_{62}$ - $PMeOx_{64}$ - $PnPrOx_{62}$. One of the parameters used to characterise the behaviour of these materials was the complex modulus ($|G^*|$). This is a measure of the resistance to deformation of the material regardless of whether the deformation is recoverable or not. This parameter is particularly relevant in the case of cells as it has been shown that cells behave differently depending on the stiffness of the substrate. Potentially the thermogels will still allow the cells to be introduced together regardless of whether or not they actually gel, as long as the material has a high enough complex modulus.

Out of the five concentrations tested three were thermogelling, the 15%, 20% and 30% samples. Unexpectedly all were observed to gel at 39°C. This is in contrast to the CMC-based thermogels which had a G_T which was dependent on the concentration. It appeared that these materials may not display a G_T which is dependent on the concentration.

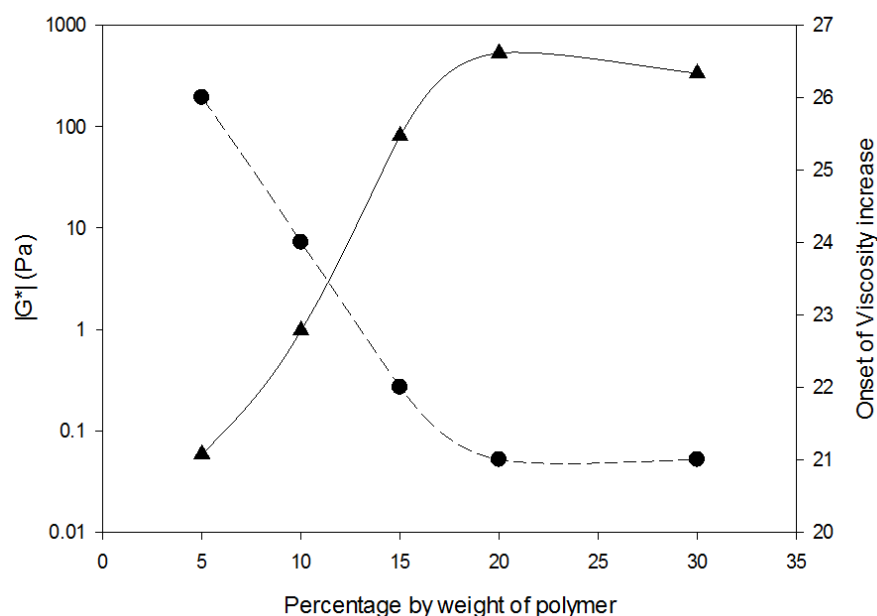


Figure 95: Dependence of the complex modulus at 37°C and onset of viscosity of $PnPrOx_{62}$ - $PMeOx_{64}$ - $PnPrOx_{62}$. Complex modulus (solid line) and the onset of the viscosity increase (dashed line)

From the analysis of the polymer solutions of different concentrations two main trends were observed based on the complex modulus and the onset of an increase in viscosity, Figure 95. The complex modulus was observed to increase logarithmically with an increase in concentration.

This trend however seems to plateau at a certain concentration. This is possibly due to the gels being unable to form such a structured and stiff network as a result of a higher degree of entanglement of the polymers before gelation.

The onset of the viscosity increase was observed to follow the same trend. This can also be explained in terms of polymer entanglement in an analogous way to the dependence of the T_{cp} on concentration. By increasing the concentration of polymers in the solution the degree of entanglement of the polymers increases. This means less water is required to be desolvated and hence a lower temperature is needed to start the thermogelation process. The plateau again could be the result of a saturation point of entanglement being reached.

Potentially the results from the concentration dependence are quite useful. Further work needs to be done but if the gelation temperature does not change with concentration whereas the complex modulus does then this offers a very simple approach for adjusting the stiffness of the gelled material by only adjusting the concentration.

6.7.3 Influence of *n*BuOx

The influence of the inclusion of *n*BuOX was then investigated. It was anticipated that the inclusion of the more hydrophobic monomer would lower the G_T . Although the co-polymer materials did not gel in the range investigated, the onset of the viscosity increase demonstrates the influence of the inclusion on *n*BuOx, Figure 96.

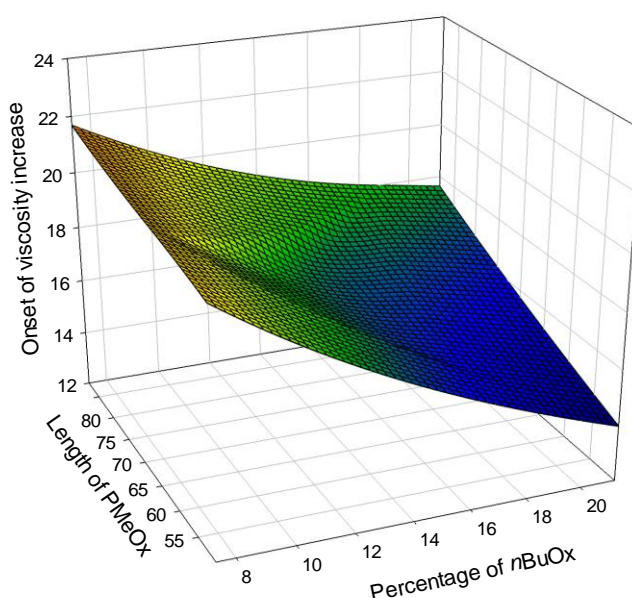


Figure 96: The dependence of the onset of the viscosity increase against the length of PMeOx and the percentage of the *n*BuOx included in the thermoresponsive B blocks

The onset of the viscosity increase is clearly dependent on the percentage of *n*BuOx present as would be expected. There is also a trend depending on the length of the PMeOx A block. This is not such a strong influence because the blocks are separate but the expected increase in the onset temperature is observed for a longer PMeOx block.

The second parameter investigated was the influence of *n*BuOx content on the complex modulus, Figure 97.

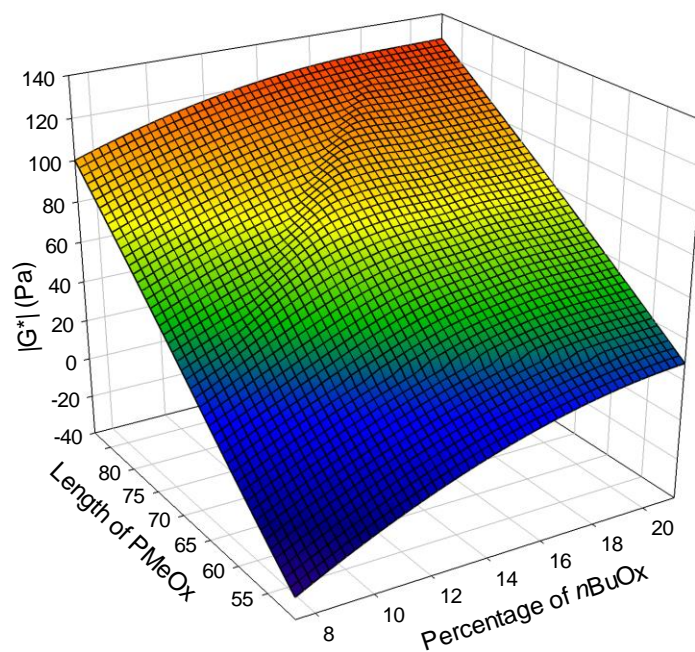


Figure 97: Influence of the length of the PMeOx block and the percentage of *n*BuOx in the thermoresponsive block on the complex viscosity at 37°C

The complex modulus at 37°C increases as the percentage of *n*BuOx. This can be attributed to the relationship between the complex modulus at 37°C and the onset of viscosity. It would be anticipated that an earlier onset of the viscosity increase would lead to a more viscous solution when comparing the complex modulus at a fixed temperature. The complex modulus was also observed to increase as the length of PMeOx increases. This is difficult to explain as it would be anticipated that increasing the A block would increase the distance between cross-linking domains. This in turn would potentially make a less stiff gel. It appears, certainly in the length range investigated here, that increasing the length increases the resistance to deformity.

There is also a slight increase in the complex viscosity as the *n*BuOx content increases. This could be due to the onset temperature being lower for the higher amounts of *n*BuOx leading to the complex viscosity being higher at 37°C as it has a wider temperature range in which to increase.

6.7.4 Influence of the Relative Lengths of the A and B Blocks

Finally the influence of the relative lengths of the A and B blocks was investigated. Data for this was less reliable than the other materials possibly due to the high polydispersity and complex mixture of polymer structures. Overall general trends could still be observed, Figure 98.

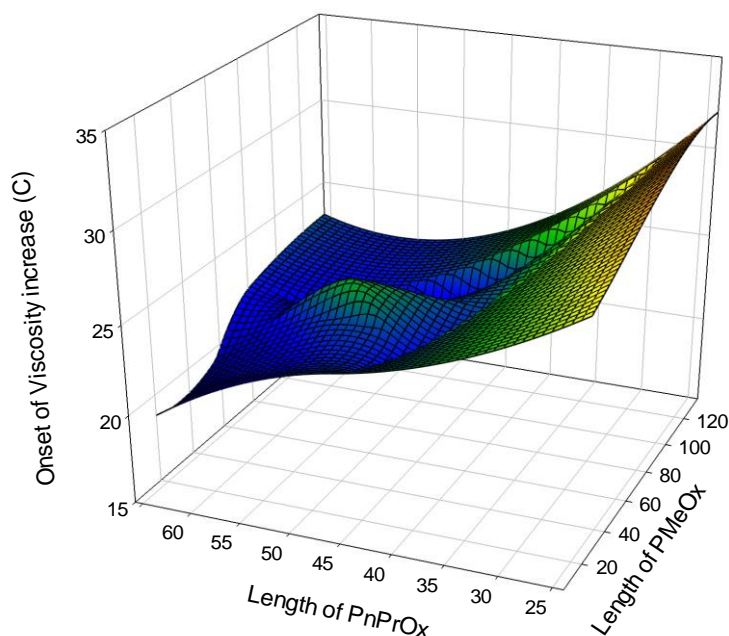


Figure 98: Dependence of the onset of viscosity on the length of the A and B blocks

When investigating the onset of viscosity increase an anticipated trend is observed. With decreasing B block the onset of viscosity increases. This can be attributed to the increased hydrophilic character of the polymer causing the onset to be higher. A similar but not so dramatic change occurs as the A block length is increased but this appears to be less significant.

The dependence of the complex viscosity was then explored. The results from this were less conclusive again because of the polydispersity and mixture of structures present, Figure 99.

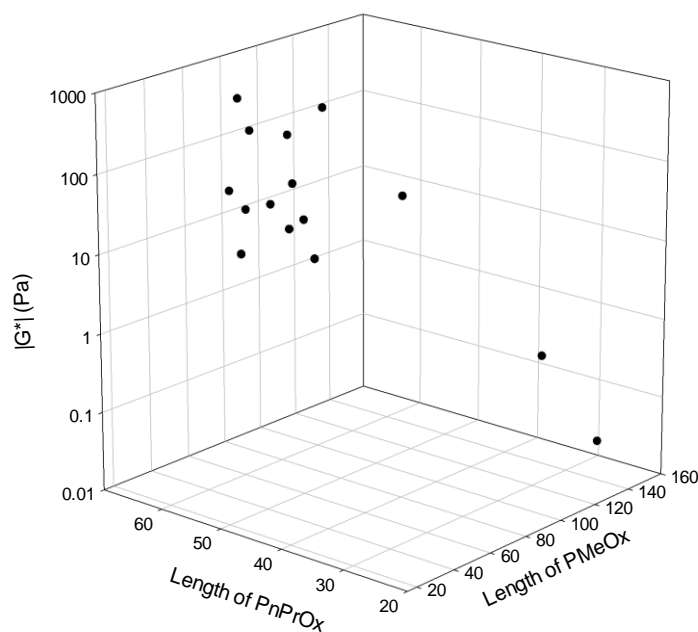


Figure 99: Dependence of the complex modulus on the length of the B and A blocks

It was observed that the complex modulus increases as length of *PnPrOx* increases. Presumably as a result of the formation of more or stronger cross-linking domains. The influence of the A block is more difficult to infer. It is anticipated that an increase in the length of *PMeOx* would affect the stiffness however further work needs to be done to determine this.

6.7.5 Summary

In summary novel BAB triblock polymers have been synthesised. The behaviour of these materials has been investigated and some of the structural influencing factors have been determined. Further work needs to be undertaken to develop more well-defined polymers which in turn should lead to more accurate analysis of the structural effects of the polymer architecture.

6.8 Conclusion

In conclusion, we have successfully demonstrated the first synthesis two types of poly(2-oxazoline)-based thermogelling polymers.

The first CMC-based thermogelling polymer was characterised using rheology and the G_T was adjusted to lie in the range suitable for biological applications. The potential for this type of material to be used in tissue engineering has been demonstrated. Successfully creating a multi-layered cell sheet, something which before this method was developed had been a very difficult proposition using current techniques.

In view of several limitations of the CMC-based thermogels, a new BAB triblock co-polymer was developed which removed the need for the inclusion of the cellulose. These new materials

allowed much more defined polymers to be synthesised and their rheological properties to be characterised which resulted in tentative structure-gelation behaviour relationships being elucidated.

Chapter 7 Summary of Work

In summary, poly(2-oxazoline)s have been successfully synthesised and control over the T_{cp} has been demonstrated. Further functionalization of these polymers via termination, initiation and co-polymerisation has been investigated. In particular a novel adamantane moiety has been introduced via initiation. This has potentially interesting applications for self-assembled supramolecular architectures.

Three general applications of these materials have been investigated: thermogelling polymers; cell growth substrates; and anti-fouling surfaces.

We have successfully grafted poly(2-oxazoline)s onto glass surfaces and have investigated how cells interact with these surfaces finding that *PiPrOx* provides the best surfaces for selectively growing 16HBE cells. This has led to the development of cell-selective surfaces, allowing 16HBE cells to be selectively grown over MRC5 cells.

We have also synthesised the first reported thermogelling polymers based on poly(2-oxazoline) polymers. The first generation involved grafting poly(2-oxazoline) chains to CMC. We then demonstrated control over the T_{cp} using a copolymer of *PiPrOx* and *PnBuOx* to produce polymers which gel at biologically relevant temperatures have investigated their gelation properties. We have then developed a new BAB triblock thermogelling material which has shown several advantages over the CMC based material, including having more defined structure and the ability to easily scale up production onto the gram scale. These benefits were successfully demonstrated and a preliminary investigation of the gelation behaviour has been undertaken.

Finally, *PMeOx* surfaces were synthesised and their anti-fouling behaviour was characterised. The behaviour of these surfaces was found be heavily dependent on the manner in which bacteria are forced to come into contact with the surface.

Chapter 8 Future Work

The projects and applications discussed in this thesis were developed without any previous work being undertaken in the group. As such, the reported results and materials are still in the early stages of development. The next steps required for further development are discussed below.

For the cell selective surfaces, future work would focus on investigating how the polymers attached to the glass surfaces could be functionalised further to increase cell selectivity. This could be achieved by incorporating a reactive moiety onto the polymer chain and reacting the surfaces with, perhaps, a protein or shorter peptide, which potentially would increase selectivity.

Additional applications for these surfaces would be enabled by the development of thermoresponsive surfaces. These should allow the surfaces to release a sheet of cells when submitted to a change in temperature. This was attempted during this PhD, however, no thermoresponsive behaviour was ever observed; this is assumed to be due to the low density of the polymer chains on the surface. A possible approach would be to adopt the methodology used in section 4.2, whereby the polymer chains are terminated with the glass-reactive silane before addition to the surface. This may result in a much denser coating of polymer being achieved when the polymers are grafted to the surface.

For the next generation of cell selective surfaces, based on β -cyclodextrin and adamantane complexation, cell compatibility work should be undertaken. The results for the glass surfaces could then be compared with the transwell based surfaces. This methodology could also lead to the development of thermoresponsive surfaces, which could also be investigated.

Further work also needs to be undertaken with the new generation of thermogelling polymers. The main issue is the high polydispersity of the triblock polymers. This should be overcome to some extent by using a different initiator. A potential alternative is to use a nosylate or an alkyl halide, as was used in the proof of principle polymers, in place of the triflate. Unfortunately, the synthetic methodology of having two steps in the polymerisation will always increase the extent of polydispersity. A possible way to combat this would be to synthesise a gradient polymer, which would include a core of PMeOx with statistically more P*n*PrOx at either end of the polymer. Optimisation would have to be undertaken to make the polymers thermoresponsive and incorporation of PMeOx monomers into the P*n*PrOx chain will inevitably lead to higher T_{cp} temperatures. It is anticipated that the inclusion of some *n*BuOx will solve any issues with a high T_{cp} .

The cell compatibility of the new generation of thermogelling polymers needs to be assessed and their application to creating cell sheets also needs to be investigated. It is anticipated that they

will work better than the first generation, as they appear to form stiffer gels, which should lead to better aggregates forming.

Finally, the bacterial capture devices require more work. There is potential to create a non-adhesive PMeOx surface which could be synthesised using a reactive initiator containing an alkyne moiety. The non-adhesive surface could then be easily functionalised using 'click' chemistry to introduce antibodies to the surface. This should create two areas which bacteria adhere to and also non-antibody coated areas which are antifouling. This type of material would have applications in several areas such as cell patterning.

Chapter 9 Experimental Details

9.1 General Experimental Details

9.1.1 Lab book

For this work an online lab-book was used to record all experimental work. For members of the University of Southampton go to <http://blogs.chem.soton.ac.uk> and, using the usual University log-in, the lab-book can be viewed. Alternatively a copy of the lab book contents in HTML format is contained on the CD at the end of this thesis.

9.1.2 Materials

Commercially available compounds were obtained from Sigma-Aldrich at the highest grade possible and were used as supplied without further purification. Common solvents were obtained from Fisher Chemical and were HPLC grade. Acetonitrile was freshly distilled over calcium hydride prior to use in polymerisation reactions. Ethanol used in the surface modifications was freshly distilled over calcium sulphate. Glass used in the surface modifications were obtained from Fisher Scientific and were standard glass coverslips cut to the required size.

9.1.3 Equipment

Contact angle goniometry was performed using a Kruss DSA 100 drop-shape analyser running SMARTDROP contact angle software²³⁵ on a Windows PC. The most suitable drop-fitting method used depended on how hydrophobic or hydrophilic the substrate was and a drop volume of 1 μ L of deionised H₂O was used. The glass used for surface functionalization was clear while borosilicate glass coverslips purchased from fisher scientific.

Image analysis was undertaken with ImageJ²³⁶ on a windows PC. Particle analysis was carried out using the particle counter which comes with the software.

T_{cp} determination using transmission measurements was carried out using a Shimadzu recording spectrophotometer UV-1601 connected to a Windows PC running UVPC version 3.5²³⁷. A pump and a heater/stirrer plate were attached via tubing to the spectrometer to allow the samples to be heated and cooled. Transmission was monitored at 550nm and the T_{cp} was recorded once transmission had dropped by 20%.

T_{cp} determination using fluorescence spectrometry was carried out using a Cary Eclipse fluorescence spectrometer equipped with a four sample heating block.

Centrifuging was performed using an Eppendorf centrifuge 5702 (0 - 4400 rpm) at room temperature.

IR spectra were collected using a Nicolet 380 FT-IR spectrometer incorporating a SmartOrbit golden gate attenuated total reflection (ATR) attachment. Polymers were dissolved in DCM and a drop was added to the spectrometer and allowed to dry before a spectra was collected.

NMR spectra were collected on a Bruker-400MHz NMR spectrometer and reprocessed using ACD labs 2014 NMR manager software²³⁸.

Microwave reactions were performed using a CEM discover microwave reactor equipped with an autoloader. This was connected to a Windows PC running CEM discover software.

Fluorescent images of cells and surfaces were taken using a Leica DMI 6000B microscope and processed using Leica software²³⁹ on a Windows PC.

Rheological measurements were carried out using a TA Instruments Discovery Series Rheometer.

SEC measurements were carried out by Rob Hanson at the University of Sheffield and by myself at the University of Ghent.

X-ray crystallographic data was obtained by the University of Southampton crystallography service. The data was collected and the crystal structure was solved by Dr Peter Horton (University of Southampton).

XPS measurements were carried out using a ThermoFisher ME17 Thetraprobe XPS system with a monochromatic Al X-ray source, set to a 400µm spot size. The scan count was 5 scans for the overview spectra and 20 scans for the elemental binding energy spectra. Deconvolution of the spectra was performed in Excel by fitting the data to multiple Gaussian bands, reducing the residual square to a minimum. The excel spreadsheet was kindly provided by Dr Nick Alderman.

9.1.4 Cell methods

9.1.4.1 Cell culture

16HBE 14o- (referred to as 16HBE, a gift from Professor D.C. Gruenert, San Fransisco, USA) were cultured in modified Eagle's medium (MEM) plus Glutamax supplemented with 10% heat-inactivated foetal bovine serum (FBS) and penicillin (50 IU/ml)/streptomycin (20 µg/ml). MRC5 fibroblasts were cultured in Dulbecco's MEM (DMEM) supplemented with 10% FBS and penicillin (50 IU/ml)/streptomycin (20 µg/ml), l-glutamine (2 mM), sodium pyruvate (1 mM), and non-essential amino acids (1 mM). In some experiments, 16HBE cells that had been stably transfected with a GFP reporter were used. These were generated by transfection with TransIT-2020[®] transfection reagent (7.5 µl; Mirus Bio, Madison, USA) containing GFP plasmid (pEGFP-N1; 2.5 µg, Clontech, California, USA) in Opti-MEM medium (250ul). After 48 h, selection medium containing G418 (600 µg/ml) was added and maintained until cells stably expressing GFP were obtained.

Once the majority of cells were GFP-labelled, the G418 concentration was reduced to 200 µg/ml and cells were FACS sorted using FACSaria (BD biosciences, New Jersey, USA).

9.1.4.2 Cell adhesion assay

To create wells on the functionalised glass coverslips, autoclaved cloning rings (6.4 mm diameter, Sigma–Aldrich) were attached to polymer-coated glass coverslips using silicon grease (Sigma–Aldrich) and then placed into a 6 well plate or attached to a glass slide ready for cell culture. A single cell suspension of 16HBE or MRC5 cells was prepared by trypsinisation and incubated with Calcein AM for 0.5 h in the dark at room temperature. The cells were then washed 3X by centrifugation to remove excess dye. The Calcein AM stained cells (1×10^4) were added to the cloning rings and incubated for 1 h before the cloning rings were removed and the petri dish was flooded with media. The dish was then gently agitated to remove non-adherent cells, the medium removed and the slide imaged at 5X magnification (Leica DMI 6000B, with heated chamber). The number of adherent cells were counted using Image J software.

9.1.4.3 Cell motility assay

Initial experiments were carried out to optimise the density of cells needed to allow attachment of single cells. After 1 h, the wells were washed to remove non-adherent cells and cell motility was monitored using time-lapse microscopy with images taken at 10 min intervals over a 17 h period. The movements of 10 cells per well were monitored and the distance travelled was measured using Image J software with the mtrackj plugin.

9.1.4.4 Immunofluorescent staining

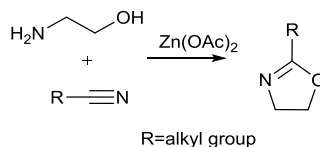
Cells were initially seeded at 1×10^5 and grown for 5 days within the cloning rings. The cells were then fixed in 4% paraformaldehyde. 16HBE cells were immunofluorescently stained for the tight junction protein, zona-occludin-1 (ZO-1), using an anti-ZO-1 mouse IgG1 antibody conjugated to Alexa 647[®] (Innova Bioscience, Cambridge, UK). The actin cytoskeleton of MRC5 cells was immunofluorescently stained using Acti-stain™ 555 fluorescent phalloidin (cytoskeleton, Inc, Denver, USA). Cell nuclei were visualised using DAPI contained in Prolong Gold mounting solution before being visualised by confocal microscopy (Leica SP5 laser scanning confocal microscope).

9.1.4.5 Cell adhesion and selectivity

MRC5 cells (5×10^3) were loaded with Cell Tracker Orange and 16HBE cells (5×10^3) stably transfected with GFP were seeded together within a cloning ring. Following 1 h incubation, the cloning ring was removed and cells washed gently to remove non-adherent cells. The medium was replaced and the cells were grown for 2 days before being imaged at 5X magnification; cell numbers were counted using Image J and the cell counter plugin.

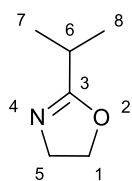
9.2 Synthesis and Cloud Point Control

9.2.1 Generic 2-alkyl-2-oxazoline Procedure



The nitrile (2.22M), ethanolamine (163ml, 2.66M) and zinc acetate (24g, 0.111M) were stirred for 20hrs at 130°C. The crude yellow oil was then distilled to yield a colourless oil, 2-alkyl-2-oxazoline. Key data for each preparation are summarised below.

9.2.1.1 2-isopropyl-2-oxazoline



Mw: 113.16

Distilled at 50°C under vacuum (lit⁴: 40°C at 16mbar)

Yield: 175g (70%)

Appearance: colourless oil

¹H NMR (CDCl₃, δ/ppm):

1.19 (d, *J*=6.9 Hz, 6H, H_{7,8}), 2.56 (spt, *J*=6.9 Hz, 1H, H₆), 3.81 (t, *J*=9.7 Hz, 2H, H₅), 4.22 (t, *J*=9.3 Hz, 2H, H₁).

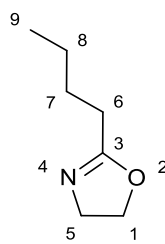
¹³C NMR (CDCl₃, δ/ppm):

19.7 (C_{7,8}), 28.1 (C₆), 54.3 (C₅), 67.2 (C₁), 172.6 (C₃).

IR (ν/cm⁻¹):

2971-2880 (C-H), 1663 (N=C), 1142 (C-O).

9.2.1.2 2-butyl-2-oxazoline



Mw: 127.18

Distilled twice at 70°C under vacuum. (Lit⁴: 56°C at 10mbar)

Yield: 100g (40%)

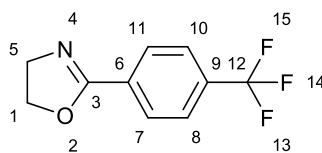
Appearance: colourless oil

¹H NMR (CDCl₃, δ/ppm): 0.91 (t, *J*=7.33 Hz, 3H, H₉), 1.36 (dq, *J*=15.03, 7.28 Hz, 2H, H₈), 1.60 (dt, *J*=15.41, 7.45 Hz, 2H, H₇), 2.26 (t, *J*=7.58 Hz, 2H,), 3.80 (t, *J*=9.60 Hz, 2H, H₅), 4.20 (t, *J*=9.35 Hz, 2H, H₁).

¹³C NMR (CDCl₃, δ/ppm): 13.7 (C₉), 22.3 (C₈), 27.6 (C₇), 28.0 (C₆), 54.3 (C₅), 67.0 (C₁), 168.6 (C₃).

IR (ν/cm⁻¹): 2971-2880 (C-H), 1663 (N=C), 1142 (C-O).

9.2.1.3 2-(4-(trifluoromethyl)phenyl)-2-oxazoline



Mw: 215.18

Recrystallized from the minimum amount of boiling hexane

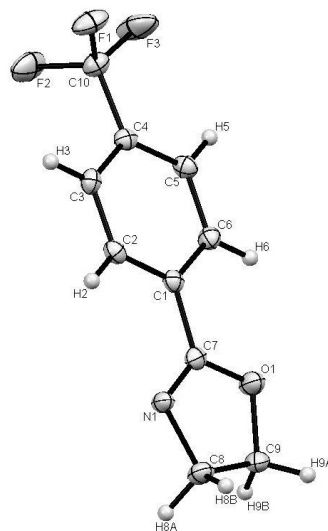
Yield: 75%

^1H NMR (CDCl_3 , δ/ppm): 4.05 (t, $J=8.42$ Hz, 2H, H_1), 4.42 (t, $J=8.42$ Hz, 2H, H_5), 7.63 (t, $J=8.05$ Hz, 2H, $\text{H}_{7,11}$), 8.02 (t, $J=8.05$ Hz, 2H,).

^{13}C NMR (CDCl_3 , δ/ppm): 55.0 (C_5), 67.8 (C_1), 123.5 (q, $J=270.90$ Hz C_{12}), 125.2 (q, $J=3.69$ Hz $\text{C}_{10,8}$), 128.4 ($\text{C}_{7,11}$), 131.0 (C_6), 137.7 (q, $J=32.1$ Hz C_9), 163.4 (C_3).

^{19}F NMR (CDCl_3 , δ/ppm): -63.2 (s, $\text{F}_{13,14,15}$)

X-ray
crystallography:



| | | |
|---|-------------------------------|--|
| $\text{C}_{12}\text{H}_{13}\text{NNaO}_{3.5}\text{S}$ | $a = 42.206(4) \text{ \AA}$ | $T = 100(2) \text{ K}$ |
| $M = 282.28 \text{ g mol}^{-1}$ | $b = 5.6362(6) \text{ \AA}$ | $\beta = 0.71075 \text{ \AA}$ |
| Monoclinic, space group Cc | $c = 10.7750(11) \text{ \AA}$ | $\mu(\text{Mo-K}\alpha) = 0.299 \text{ mm}^{-1}$ |
| $V = 2481.4(5) \text{ \AA}^3$ | $\beta = 104.511(7)$ | $0.15 \times 0.08 \times 0.01 \text{ mm}$ |
| $Z = 8$ | | |
| $R_1 = 0.0743$ | | |

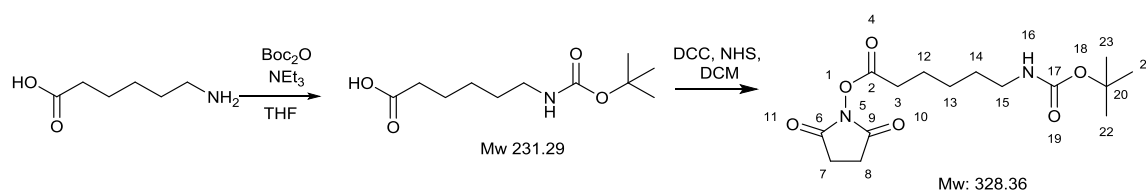
MS (ES^+ , ACN, m/z): 216.1 (100%, $[\text{M}+\text{H}]^+$).

9.2.2 2-BOC-2-Oxazoline Synthesis

The BOC-2-oxazoline was synthesised in several steps (section 9.2.2.1-9.2.2.3) and as such the material was not purified further than the precipitate until after the final reaction. This approach follows the methodology published in the literature^{141, 144}.

The synthetic route was adapted from published literature^{145, 235}.

9.2.2.1 BOC protection and succinimide formation^{145, 240145, 239145, 238145, 236145, 237145, 236145, 235}

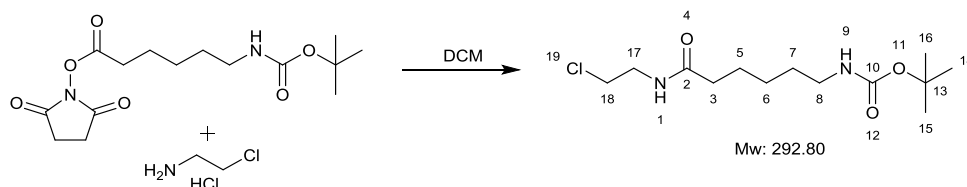


To a solution of 6-aminohexanoic acid (20.0g, 152 mmol) in dioxane/H₂O (300ml, 2:1) cooled to 0°C were added, 2M NaOH (77ml, 6.09g, 152mmol) and di-tert-butyl dicarbonate (36.6g, 152 mmol). The resulting mixture was then warmed to room temperature and left for 3 hours. The dioxane was then removed under vacuum and the aqueous solution was washed with ethyl acetate. The water layer was acidified to pH 2 using 2M HCl and extracted with fresh ethyl acetate to remove the product. The ethyl acetate was removed under reduced pressure yielding a white powder. TLC (ethyl acetate) showed mainly one product. The white powder was dissolved in 250ml of DCM and cooled to 0°C. N-hydroxysuccinimide (26.2g, 228mmol) and *N,N'*-dicyclohexylcarbodiimide (37.6g, 182mmol) were added and the reaction was left to stir for 30 min. The reaction mixture was then warmed to room temperature and left overnight. The mixture was then concentrated under vacuum and diethyl ether (400ml) was added. Vigorous stirring afforded a precipitate which was filtered yielding the intermediate product as a white powder (38.62g, 94%) which was used without further purification).

The NMR was consistent with published data²⁴¹⁻²⁴³.

| | |
|---|--|
| ¹ H NMR (CDCl ₃ , δ/ppm): | 1.45 (m, 13H, H _{13,14,21,22,23}), 1.73 (quin, <i>J</i> = 7.5 Hz, 2H, H ₁₂), 2.58 (t, <i>J</i> = 7.3 Hz, 2H, H ₇ or 8), 2.80 (m, 4H, H ₇ or 8, 3), 3.08 (m, 2H, H ₁₅), 4.65 (br. s, 1H, H ₁₆). 6.43 (br. s, 0.15H, COOH (starting material)) |
| IR (ν/cm ⁻¹): | 3386 (N-H stretch [amide]), 2870-2990 (C-H), 1726 (C=O), 1690 (C=O [amide]), 1169-1250 (C-O, C-N), 1513 (N-H bend [amide]). |
| MS (ES ⁺ , ACN, <i>m/z</i>): | 351.1 (24.7%, [M+Na] ⁺), 329.1 (2.6%, [M+H] ⁺). |

9.2.2.2 Chloroamine Substitution



As adapted from a published procedure¹⁴⁴. 2-Chloroethylamine hydrochloride (27.28g, 235mmol) and NaOH (9.41g, 235mmol) were dissolved in water (200ml). The succinimide-protected ester (38.62g, 117mmol) in DCM (400ml) was then added drop-wise while vigorously stirring. The mixture was left stirring overnight. The DCM layer was then separated and washed water (2 x 200ml), dried using MgSO₄ and concentrated to yield a white powder. This was then washed using ether:hexane 50/50 and filtered yielding a white powder (29.28g, 85%) which was used without further purification)

NMR data was consistent with published literature¹⁴¹.

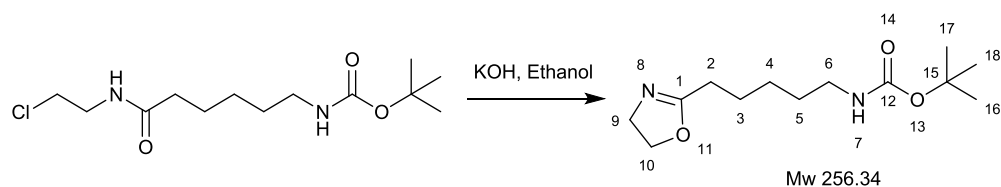
¹H NMR (CDCl₃, δ/ppm): 1.45 (m, 13H, H_{14,15,16,6,7}), 1.62 (quin, *J*=7.5 Hz, 2H, H₅), 2.18 (t, *J*=7.5 Hz, 2H, H₃), 3.06 (m, 2H, H₈), 3.56 (m, 4H, H_{17,16}), 4.68 (br. s, 1H, H₉), 6.29 (br. s, 1H, H₁).

¹³C NMR (CDCl₃, δ/ppm): 25.1 (C₇), 26.2 (C₆), 28.3 (C_{14,15,16}), 29.6 (C₇), 36.2 (C₃), 40.2 (C₈), 41.1 (C₁₈), 43.8 (C₁₇), 78.9 (C₁₃), 155.9 (C₁₀), 173.1 (C₂).

IR (ν/cm⁻¹): 3339 (N-H stretch [amide]), 2870-2985 (C-H), 1656 (C=O [amide]), 1688 (C=O [amide]), 1169-1250 (C-O, C-N), 1522 (N-H bend [amide]), 651 (C-Cl).

MS (ES⁺, ACN, *m/z*): 315.2 (100.0 %, [M+Na]⁺)¹⁴¹

9.2.2.3 Ring Closure

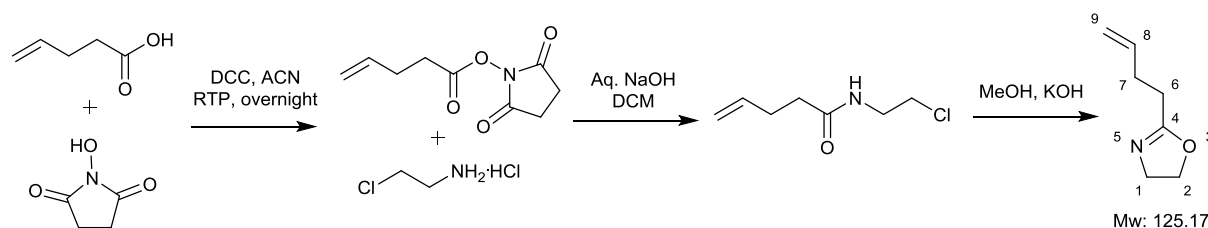


BOC-Cl (20g, 68.3mmol) was dissolved in dry ethanol (100ml). KOH (11g, 196mmol) dissolved in dry ethanol (150ml) was then added and the solution was heated to 70°C. This was cooled after 2hrs and left stirring overnight. The cloudy solution was then filtered and concentrated. It was then re-dissolved in DCM, cooled in a refrigerator and filtered to remove excess KCl. This process was repeated and the resulting solution was concentrated to yield orange oil. The oil was then purified by graded elution column chromatography using diethyl ether and increasing MeOH content from 0% up to 6% (TLC using diethyl ether/MeOH 5%). This afforded the BOC-Oxazoline as a colourless oil (4.09g, 23%).

The analysis was consisted with published literature¹⁴⁴.

| | |
|--|--|
| ¹ H NMR (CDCl ₃ , δ/ppm): | 1.43 (m, 13H, H _{17,18,16,4,5}), 1.65 (quin, <i>J</i> =7.6 Hz, 2H, H ₃), 2.27 (t, <i>J</i> =7.3 Hz, 2H, H ₂), 3.12 (m, 2H, H ₆), 3.82 (t, <i>J</i> =9.1 Hz, 2H, H ₄), 4.22 (t, <i>J</i> =9.6 Hz, 2H, H ₁₀), 4.61 (br. s, 1H, H ₇). |
| ¹³ C NMR (CDCl ₃ , δ/ppm): | 25.6 (C ₄), 26.3 (C ₅), 27.8 (C ₂), 28.4 (C _{16,17,18}), 29.6 (C ₅), 40.3 (C ₆), 54.4 (C ₉), 67.2 (C ₁₀), 79.0 (C ₁₅), 155.9 (C ₁₂), 168.4 (C ₁). |
| IR (ν/cm ⁻¹): | 3340 (N-H stretch [amide]), 2863-2975 (C-H), 1694 (C=O [amide]), 1665 (C=N), 1160-1250 (C-O, C-N), 1522 (N-H bend [amide]). |
| MS (ES ⁺ , ACN, <i>m/z</i>): | 257.2 (51%, [M+H] ⁺), 279.1 (25%, [M+Na] ⁺). |

9.2.3 2-3-(Butenyl)-2-oxazoline



4-Pentenoic acid (10.2ml, 0.1mol) and *N*-hydroxysuccinimide (11.5g, 0.1mol) were added to a stirred solution of DCC (20.6g, 0.1mol) and acetonitrile (1L). The reaction was stirred at room temperature for 18 hours, during which time a white precipitate formed. The reaction mixture was then cooled on ice for 10 minutes and filtered. The resulting solution was concentrated to yield a crude oil (20g). This oil was then dissolved in dry dichloromethane (500ml) and was added drop-wise to a vigorously stirred solution of 2-chloroethylamine hydrochloride (23.662g, 0.204mol) and NaOH (8.16g, 0.204mol) in deionized water (220ml). After stirring overnight the organic layer was separated and washed with deionised water twice before being concentrated under vacuum. The resulting oil was then dissolved in dry MeOH (15ml) and to this was added drop-wise KOH (5.21g 0.093mol) in dry MeOH (50ml). After addition the solution was heated to 70°C overnight. The resulting KCl precipitate was filtered off and the solution was reduced to an oil under vacuum. The yellow solution was distilled at reduced pressure to give 2-3-(butenyl)-2-oxazoline as a colourless liquid (4.6g, 37%).

Analysis was consistent with published literature¹⁴⁴

¹H NMR (CDCl₃, δ/ppm): 2.16 (m, 4H, H₆, γ), 3.60 (t, *J*=9.2 Hz, 2H, H₂), 4.01 (t, *J*=9.2 Hz, 2H, H₁), 4.82 (m, 2H, H₉), 5.63 (m, 1H, H₈).

¹³C NMR (CDCl₃, δ/ppm): 26.8 (C₇), 29.4 (C₆), 53.7 (C₁), 66.7 (C₂), 114.9 (C₉), 136.3 (C₈), 167.5 (C₄).

MS (ES⁺, ACN, *m/z*): 166.2 (86%, [M+ACN]), 167.1 (52%, [M+ACN+H]⁺).

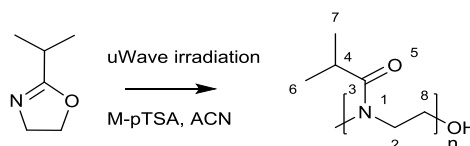
9.2.4 Generic Polymerisation Method

Unless mentioned otherwise, every polymerisation proceeded as follows.

Dry 2-oxazoline was added up to a volume of 1 ml. Freshly distilled dry acetonitrile (2ml) and dry methyl-*p*-toluenesulphonate (amount adjusted for polymer length, calculated from moles of monomer divided by moles of initiator) in a dry microwave tube. The tube was flushed with nitrogen and the vial was capped and subjected to microwave irradiation (135°C, ramp, reaction time 15 min). 1.1eq (molar) of the terminating agent was added together with triethylamine (0.01ml) and left at 60°C overnight in a sand bath. The polymer was then concentrated under vacuum until a solid foam formed. It was then re-dissolved in DCM and precipitated into ice-cold diethyl ether or, in the case of *PiPrOx* and *PnBuOx* in ice cold diethyl ether:hexane 3:1. The precipitate was then filtered and if necessary re-dissolved in DCM and precipitated again. The polymer was then dried overnight in a desiccator under vacuum. This yielded the polymer as a white powder (except when a dye was attached).

NMR data is reported following the usual conventions in which proton NMR spectra are reported with non-fractional integral values for one co-polymer component. This inevitably leads to fractional integral values for other components. This follows literature convention.

9.2.5 Poly(2-isopropyl-2-oxazoline) Lengths



| Polymer | <i>i</i> PrOx | | M-pTSA | | ACN (ml) | Estimated length |
|----------|---------------|-------|--------|-------|----------|------------------|
| | ml | mmol | μl | mmol | | |
| PiPrOx-1 | 1 | 8.660 | 8.7 | 0.058 | 2 | 150 |
| PiPrOx-2 | 1 | 8.660 | 5.2 | 0.035 | 2 | 250 |
| PiPrOx-3 | 1 | 8.660 | 4.4 | 0.029 | 2 | 300 |
| PiPrOx-4 | 1 | 8.660 | 3.7 | 0.025 | 2 | 350 |
| PiPrOx-5 | 1 | 8.660 | 3.3 | 0.022 | 2 | 400 |
| PiPrOx-6 | 1 | 8.660 | 2.6 | 0.017 | 2 | 500 |

Table 20: Quantities used to synthesise PiPrOx-1 to 6

¹H NMR (CDCl₃, δ/ppm):1.05 (br. s, 6H, H_{7,6}), 2.75 (m, 1H, H₄), 3.45 (br. s, 4H, H_{2,8}).IR (ν/cm⁻¹):

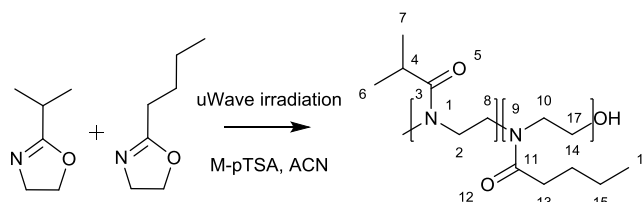
2969 (C-H), 1627 (C=O).

SEC :

| Polymer | Mw | Mn | PDI |
|----------|-------|-------|------|
| PiPrOx-1 | 13559 | 15469 | 1.14 |
| PiPrOx-2 | 24888 | 28027 | 1.13 |
| PiPrOx-3 | 30604 | 33110 | 1.08 |
| PiPrOx-4 | 36346 | 39454 | 1.09 |
| PiPrOx-5 | 39947 | 48138 | 1.21 |
| PiPrOx-6 | 53818 | 60948 | 1.13 |

Table 21: SEC analysis of PiPrOx-1 to 6

9.2.6 Poly(2-isopropyl-2-oxazoline)-co-(2-butyl-2-oxazoline)



| Polymer | <i>i</i> PrOx | | <i>n</i> BuOx | | M-pTSA | | ACN (ml) | Estimated length |
|-------------------------|---------------|-------|---------------|-------|---------------|-------|----------|------------------|
| | μl | mmol | μl | mmol | μl | mmol | | |
| PiPrOx- <i>n</i> BuOx-1 | 931 | 8.063 | 55 | 0.432 | 8.7 | 0.084 | 2 | 150 |
| PiPrOx- <i>n</i> BuOx-2 | 882 | 7.638 | 110 | 0.865 | 8.7 | 0.084 | 2 | 150 |
| PiPrOx- <i>n</i> BuOx-3 | 784 | 6.790 | 220 | 1.730 | 8.7 | 0.084 | 2 | 150 |
| PiPrOx- <i>n</i> BuOx-4 | 686 | 5.941 | 330 | 2.594 | 8.7 | 0.084 | 2 | 150 |
| PiPrOx- <i>n</i> BuOx-5 | 588 | 5.092 | 441 | 3.467 | 8.7 | 0.084 | 2 | 150 |

Table 22: Quantities used to synthesise PiPrOx-*n*BuOx-1 to 5

^1H NMR (CDCl_3 , δ/ppm): 0.9 (br. s, 1H, H_{16}), 1.09 (br. s, 5H, $\text{H}_{7,6}$), 1.32 (br. s, 0.75H, H_{15}), 1.57 (br. s, 0.6H, H_{14}), 2.26 (br. s, 0.9H, H_{13}), 2.75 (br. s, 0.9H, H_4), 3.43 (br. s, 4H, $\text{H}_{2,8,10,17}$).

IR (v/cm^{-1}): 2969 (C-H), 1627 (C=O).

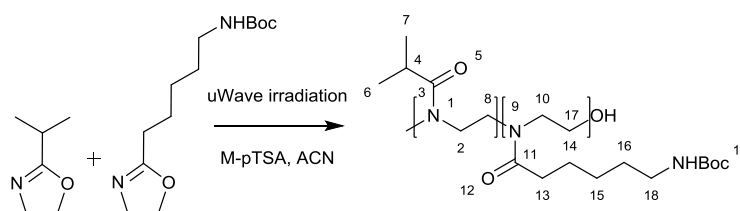
GPC :

| Polymer | Mw | Mn | PD |
|-------------------------|-------|-------|------|
| PiPrOx- <i>n</i> BuOx-1 | 25256 | 14649 | 1.72 |
| PiPrOx- <i>n</i> BuOx-2 | 24026 | 14788 | 1.62 |
| PiPrOx- <i>n</i> BuOx-3 | 23735 | 13587 | 1.74 |
| PiPrOx- <i>n</i> BuOx-4 | 22950 | 13466 | 1.7 |
| PiPrOx- <i>n</i> BuOx-5 | 20282 | 12298 | 1.64 |

Table 23: SEC analysis of PiPrOx-*n*BuOx-1 to 5

9.2.7 Poly(2-isopropyl-2-oxazoline)-co-(2-pentan-1-amine-2-oxazoline)

9.2.7.1 Synthesis



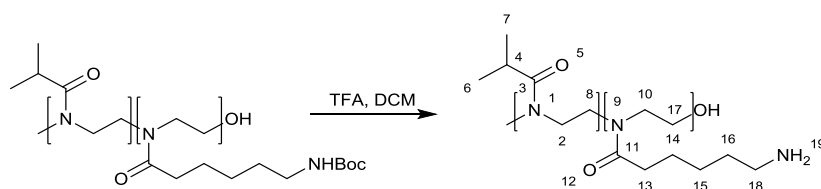
| Polymer | iPrOx | | BOCOx | | M-pTSA | | ACN (ml) | Estimated length |
|--------------|---------------|-------|---------------|-------|---------------|-------|----------|------------------|
| | μl | mmol | μl | mmol | μl | mmol | | |
| PiPrOx-BOC-1 | 662 | 5.965 | 153 | 0.597 | 30 | 0.131 | 2 | 50 |
| PiPrOx-BOC-2 | 662 | 5.965 | 31 | 0.119 | 9 | 0.041 | 2 | 150 |
| PiPrOx-BOC-3 | 662 | 5.965 | 31 | 0.119 | 9 | 0.041 | 2 | 150 |

Table 24: Quantities used to synthesise PiPrOx-BOC-1 to 3

^1H NMR (CDCl_3 , δ/ppm): 1.11 (br. s., 5H, $\text{H}_{7,6}$), 1.55 (m, 1.43H, $\text{H}_{\text{BOC},14,15,16}$), 2.35 (s, 0.32H, H_{13}), 2.84 (br. s, 1H, H_4), 3.11 (s, 0.11H, H_{18}), 3.42 (m, 4H, $\text{H}_{2,8,10,17}$), 4.86 (m, 0.1H, H_{19})

IR (v/cm^{-1}): 2870-2970 (C-H), 1633 (C=O).

9.2.7.2 Deprotection



Generic Method

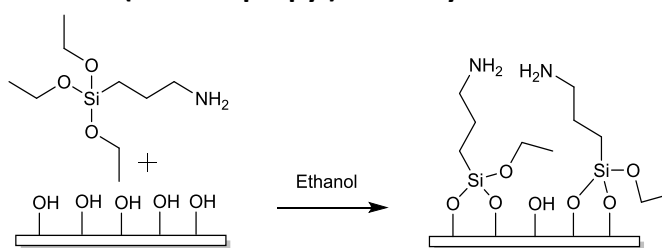
BOC-protected polymer (500mg) was dissolved in DCM (1ml). TFA (1ml) was then added and the solution was stirred for 3 hours. The solution was then added drop-wise to an excess of diethyl ether (200ml) and the precipitate was isolated by filtration yielding the unprotected poly(2-oxazoline) in quantitative yield.

^1H NMR (CDCl_3 , δ/ppm): 1.11 (br. s., 5H, $\text{H}_{7,6}$), 1.55 (m, 1.33H, $\text{H}_{14,15,16}$), 2.35 (s, 0.33H, H_{13}), 2.76 (br. s, 1H, H_4), 3.11 (s, 0.1H, H_{18}), 3.49 (m, 4H, $\text{H}_{2,8,10,17}$), 8.12 (m, 0.1H, H_{19})

IR (v/cm^{-1}): 2870-2970 (C-H), 1633 (C=O), 752 (NH_2).

9.3 Cell Selective Surfaces

9.3.1 Generic method for (3-aminopropyl)triethoxysilane Coated Slides



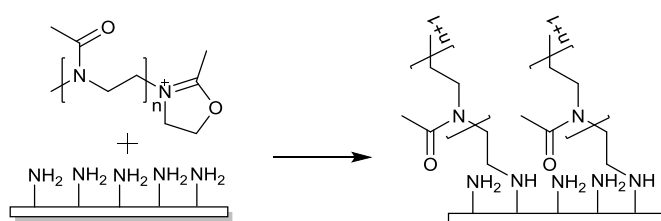
Glass coverslips were cut to size using a diamond-tipped pen, approximately 1cm x 2cm. These were then put into a solution of concentrated sulphuric acid:hydrogen peroxide 3:1 v/v.

[CAUTION: reacts vigorously with any organic compounds, keep well away from sources of organic chemicals]. After 1 hour the slides were washed with copious amounts of water followed by ethanol. Each individual slide was then immersed in a solution of (3-aminopropyl)triethoxysilane (38 μ l) in freshly distilled ethanol (5ml) in a medium vial and capped for 1 hour. The slides were removed and washed with copious amounts of ethanol before being placed in a clean vial and heated to 80°C for a further hour. The amine-coated slides were then ready for use.

Contact angle (average of 76 droplets):¹⁸⁹ $55 \pm 4^\circ$

9.3.2 Generic Methods for Poly(2-alkyl-2-oxazoline) Glass Coverslip Attachment

9.3.2.1 PMeOx Coated Slides



Batch Preparation

For each batch a polymer stock solution was used with the amounts described in the following paragraph. This was distributed into microwave vials, 3ml each.

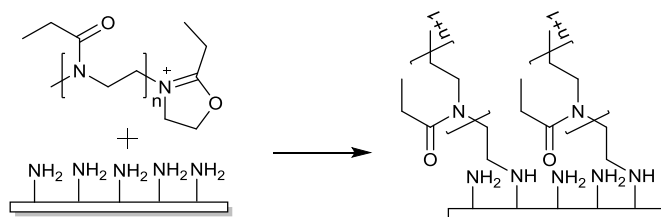
Acetonitrile (44ml), 2-methyl-2-oxazoline (22ml, 259.81mmol) and methyl *p*-toluenesulfonate (0.261ml, 1.73mmol) were thoroughly mixed, and then split into aliquots (3ml), each in a microwave vial. 24 microwave vials were obtained. Each vial was subjected to microwave irradiation for 15 min (ramp time 20 min; 135°C; 130 psi).

Surface Attachment

Each crude polymer solution was split into two portions (2 x 1.5 ml) and to each portion was added triethylamine (0.030 ml) and acetonitrile (1.5 ml). An amine-coated slide was then added and the reaction mixture was left overnight at 60°C. The glass slide was then removed, rinsed with ethanol, and dried under a stream of nitrogen.

Contact angle (average of 62 droplets): $26 \pm 3.6^\circ$

9.3.2.2 PEtOx Coated Slides



Batch Preparation

For each batch a polymer stock solution was used with the amounts described in the following paragraph. This was distributed into microwave vials, 3ml each.

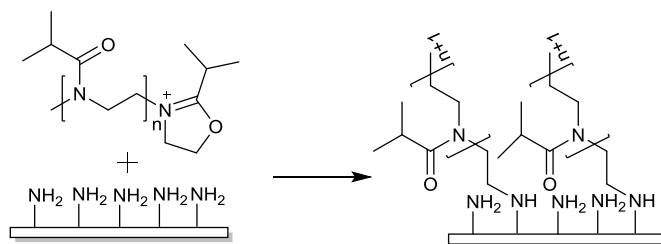
Acetonitrile (44ml), 2-ethyl-2-oxazoline (26.22ml, 259.8mmol) and methyl *p*-toluenesulfonate (0.261ml, 1.73mmol) were thoroughly mixed, and then split into aliquots (3ml), each in a microwave vial. 24 microwave vials were prepared. Each vial was subjected to microwave irradiation for 15 min (ramp time 20 min; 135°C; 130 psi).

Surface attachment

Each crude polymer solution was split into two portions (2 x 1.5 ml) and to each portion were added triethylamine (0.030 ml) and acetonitrile (1.5 ml). An amine-coated slide was then added and the reaction mixture was left overnight at 60°C. The glass slide was then removed, rinsed with ethanol, and dried under a stream of nitrogen.

Contact angle (average of 40 droplets): $52 \pm 2.2^\circ$

9.3.2.3 PiPrOx Coated Slides



Batch Preparation

For each batch a polymer stock solution was used with the amounts described in the following paragraph. This was distributed into microwave vials, 3ml each.

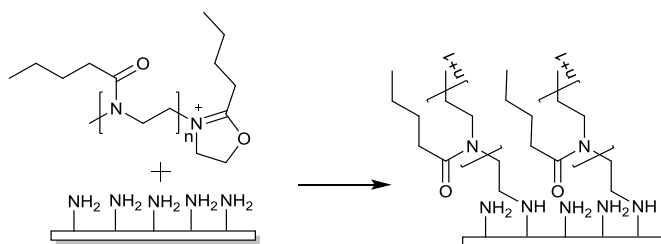
Acetonitrile (44ml), 2-isopropyl-2-oxazoline (31.07ml, 259.8mmol) and methyl *p*-toluenesulfonate (0.261ml, 1.73mmol) were thoroughly mixed, and then split into aliquots (3ml), each in a microwave vial. 24 aliquots were prepared. Each vial was subjected to microwave irradiation for 15 min (ramp time 20 min; 135°C; 130 psi).

Surface Attachment

Each crude polymer solution was split into two portions (2 x 1.5 ml) and to each portion were added triethylamine (0.030 ml) and acetonitrile (1.5 ml). An amine-coated slide was then added and the reaction mixture was left overnight at 60°C. The glass slide was then removed, rinsed with ethanol, and dried under a stream of nitrogen.

Contact angle (average of 38 droplets): $60 \pm 2.1^\circ$

9.3.2.4 PnBuOx Coated Slides



Batch Preparation

For each batch a polymer stock solution was used with the amounts described in the following paragraph. This was distributed into microwave vials, 3ml each.

Acetonitrile (44ml), 2-butyl-2-oxazoline (35.91ml, 259.8mmol) and methyl *p*-toluenesulfonate (0.261ml, 1.73mmol) were thoroughly mixed, and then split into aliquots (3ml), each in a microwave vial. 24 aliquots were prepared. Each vial was subjected to microwave irradiation for 15 min (ramp time 20 mins 135°C; 130 psi).

Surface Attachment

Each crude polymer solution was split into two portions (2 x 1.5 ml) and to each portion were added triethylamine (0.030 ml) and acetonitrile (1.5 ml). An amine-coated slide was then added and the reaction mixture was left overnight at 60°C. The glass slide was then removed, rinsed with ethanol, and dried under a stream of nitrogen.

Contact angle (average of 40 droplets): $75 \pm 5.8^\circ$

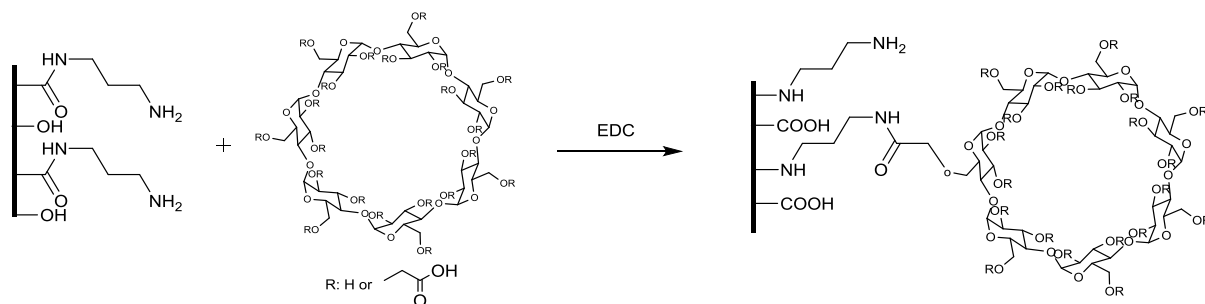
9.3.3 Aminolysis of Polycaprolactone (PCL)

PCL sheets were cast from a 10% by weight solution in dioxane of PCL. These were cut up into 1cmx2cm sheets. 1,3-Diaminopropane (210 μ L) was added to the solvent either methanol, ethanol, isopropanol (5ml) to make a 0.5M solution of diamine. The PCL sheets were then added to this solution for different periods of time (from 1 min to 22 min) at 35°C. These were removed, rinsed with water and left to soak in water for at least 2 hours before drying. They were then added to 2ml of ninhydrin solution (0.1M in ethanol) and heated to 80°C for 30min. Dioxane (8ml) was then added to dissolve the PCL sheets. The solutions were then analysed using UV-Vis to calculate the concentration of primary amines based on the conversion of ninhydrin by comparison to a calibration sample.

9.3.4 Aminolysis of Polyethylene terephthalate (PET)

35% by weight solution of ethylenediamine in MeOH was prepared and heated to 50°C. Transwell inserts were added for different periods of time. They were then characterised using orange II dye to assess amine content.

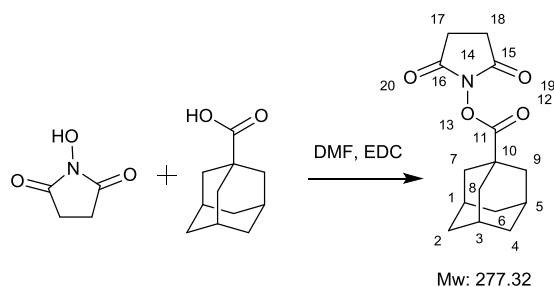
9.3.5 Carboxymethyl- β -cyclodextrin-Functionalization of Amine Surfaces



To water (2ml) was added EDC (10mg) and carboxymethyl- β -cyclodextrin (10mg). This mixture was left for one hour. The solution was then adjusted to pH 5 using dilute HCl and the aminolysed surface was then placed in the solution and left overnight at room temperature. The slides were then washed with copious amounts of water and soaked in water for 30min to remove unbound carboxymethyl- β -cyclodextrin.

9.3.6 Adamantane-Functionalization of Amine Surface

9.3.6.1 Synthesis of 1-adamantane-N-hydroxysuccinimide



1-Adamantanecarboxylic acid (3.6g, 0.020 mol), N-(3-Dimethylaminopropyl)-N'-ethylcarbodiimide hydrochloride (3.83g, 0.020 mol) and N-Hydroxysuccinimide (2.53g, 0.022 mol) were added to DMF (80ml) and stirred overnight. Approximately half the DMF was evaporated and water (40ml) was then added. The white precipitate was then filtered, washed several times with more water and dried for several days under vacuum to yield a white powder (2.87g, 50%).

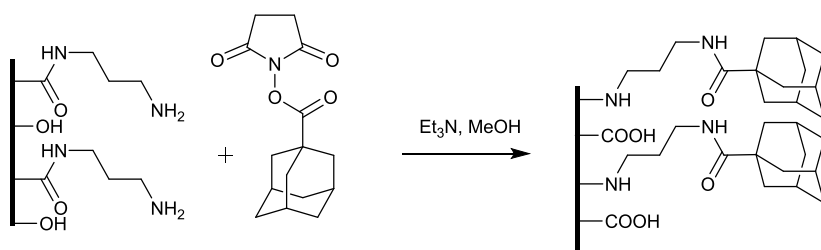
NMR data is consistent with published literature²⁴⁴.

¹H NMR (CDCl₃, δ/ppm): 1.77 (m, 6H, H_{2,4,8}), 2.09 (m, 9H, H_{1,3,5,7,8,9}), 2.83 (m, 4H, H_{17,18})

¹³C NMR (CDCl₃, δ/ppm): 25.9 (C_{17,18}), 27.9 (C_{1,3,5}), 36.5 (C_{2,4,8}), 38.7 (C_{7,8,9}), 38.1 (C₁₀), 169.0 (C_{14,15}), 170.9 (C₁₁)

IR (ν/cm⁻¹): 2903 (C-H), 1738, 1776, 1798 (C=O).

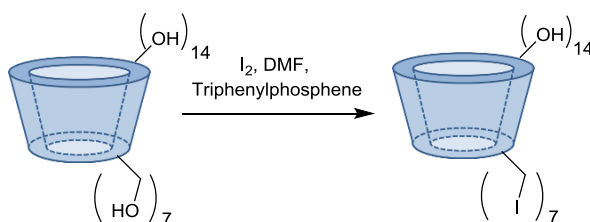
9.3.6.2 Functionalization of amine surface



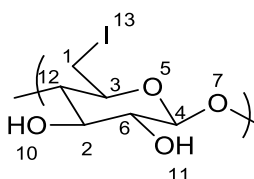
To Adamantane-n-hydroxysuccinimide (10mg) and triethylamine (10μl) in methanol (5ml) was added an aminolysed PCL slide. The slide was left overnight and was removed and washed with copious amounts of methanol followed by water and dried.

9.3.7 Synthesis of β -cyclodextrin Initiated Polymers

9.3.7.1 β -cyclodextrin Iodination



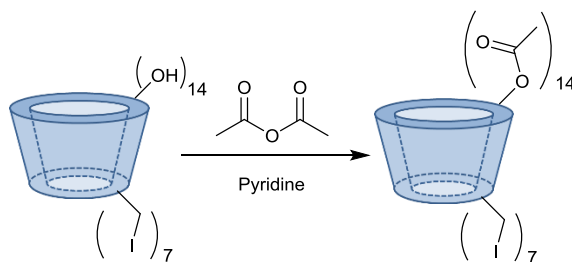
Triphenylphosphine (23.06g, 88 mmol) was added to DMF (90ml) and stirred at 0°C until the triphenylphosphine had dissolved. Iodine (22.34g, 88 mmol) was then added drop wise and the resulting brown solution was heated to 50°C. β -cyclodextrin (5g, 4.4 mmol) was then added and the solution was heated to 70°C and left overnight. The solution was then cooled to 0°C and sodium methoxide solution in methanol (22ml, 25% w/v) was added and the solution was stirred for a further 5 min whilst being cooled. The β -cyclodextrin was then precipitated by pouring into stirred methanol (600ml). The precipitate was then filtered and washed with methanol until the filtrate no longer washed through brown. The brown powder was then dried under vacuum overnight yielding iodinated cyclodextrin (6.67g, 80%).



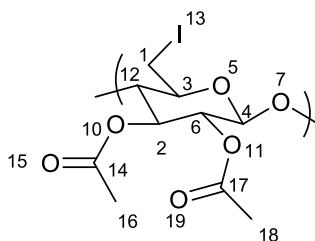
The analysis is consisted with published literature¹⁵³.

| | |
|---|---|
| ^1H NMR (DMSO d_6 , δ /ppm): | 3.35 (m, 3H, $\text{H}_{1,12}$), 3.61 (m, 2H, $\text{H}_{3,4}$), 3.81 (m, 1H, H_2), 4.98 (m, 1H, H_4), 5.90 (s, 1H, H_{11} or H_{12}), 6.03 (s, 1H, H_{11} or H_{12}) |
| ^{13}C NMR (DMSO d_6 , δ /ppm): | 9.5 (C_1), 70.9 (C_6), 71.9 (C_3), 72.2 (C_2), 85.9 (C_{12}), 102.1 (C_4) |
| IR (ν/cm^{-1}): | 3324 (O-H), 2912 (C-H), 1033 (C-O), 583 (C-I). |

9.3.7.2 Acetylation



Iodo- β -cyclodextrin (1 g, 0.525 mmol), acetic anhydride (77.7 mL, 9.23 mmol), pyridine (5 mL, 62 mmol), and 4-dimethylaminopyridine (14 mg, 0.11 mmol) were mixed under nitrogen. The solution was left stirring for 72 hrs. The mixture was then poured into ice water (40 mL) and vigorously stirred under ice. The precipitate was then filtered and recrystallised in methanol. The product (1.23 g), was filtered and dried under vacuum.



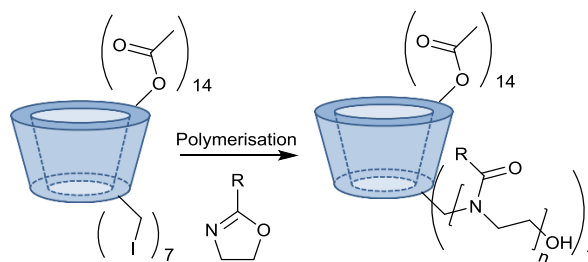
The analysis is consistent with published literature¹⁵³.

^1H NMR (CDCl_3 , δ/ppm): 2.04 (s, 3H, H_{16}), 2.09 (s, 3H, H_{18}), 3.61 (m, 2H, H_1), 3.79 (m, 2H, $\text{H}_{12,3}$), 4.83 (m, 1H, H_4), 5.11 (m, 1H, H_6), 5.24 (m, 1H, H_2)

^{13}C NMR (CDCl_3 , δ/ppm): 7.9 (C_1), 20.7 ($\text{C}_{16,18}$), 70.1 (C_6), 70.2 (C_2), 70.4 (C_3), 80.4 (C_{12}), 96.5 (C_4), 169.4 (C_{19}), 170.6 (C_{20})

IR (ν/cm^{-1}): 2953 (C-H), 1745 (C=O), 1033 (C-O), 1213, 1027 (C-O), 599 (C-I).

9.3.7.3 Polymerisation



Polymer solutions (containing either methyl, ethyl or isopropyl-2-oxazoline) were subjected to microwave irradiation as described in section 0. One sample containing 2-methyl-2-oxazoline was quenched with rhodamine B (120mg) and triethylamine (10 μ l). Three samples containing methyl, ethyl and isopropyl-2-oxazoline were quenched using water. Each of these samples was then concentrated to a foam, dissolved in a small amount of DCM (approx. 1ml) and precipitated in ether (*i*PrOx ether:hexane) (100ml) to yield the polymers.

| Sample | Monomer | | | Initiator | | [M]:[I] | Yield (%) |
|--------------------|---------------|----|------|-----------|-------|---------|-----------|
| | 2-oxazoline | MI | mmol | mg | mmol | | |
| CD-PMeOx | MeOx | 1 | 11.8 | 84 | 0.033 | 51 | 86 |
| CD-PMeOx-R | MeOx | 1 | 11.8 | 84 | 0.033 | 51 | 79 |
| CD-PEtOx | EtOx | 1 | 9.9 | 71 | 0.028 | 51 | 92 |
| CD-P <i>i</i> PrOx | <i>i</i> PrOx | 1 | 8.4 | 60 | 0.024 | 50 | 72 |

Table 25: Quantities used to synthesise β -cyclodextrin initiated polymers

CD-PMeOx

^1H NMR (CDCl_3 , δ/ppm): 1.98 (m, 0.07H), 2.11 (m, 3H), 3.45 (m, 4H)

CD-PMeOx-R

^1H NMR (CDCl_3 , δ/ppm): 1.95 (m, 0.08H), 2.11 (m, 3H), 3.45 (m, 4H)

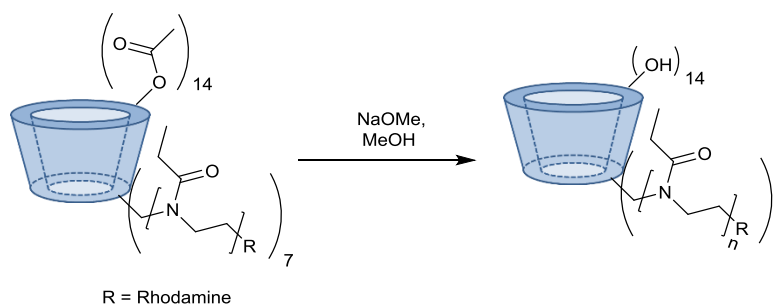
CD-PEtOx

^1H NMR (CDCl_3 , δ/ppm): 1.09 (m, 3H), 2.04 (m, 0.13H), 2.34 (m, 2H), 3.44 (m, 4H)

CD-P*i*PrOx

^1H NMR (CDCl_3 , δ/ppm): 1.01 (m, 3H), 2.08 (m, 0.39H), 2.78 (m, 2H), 3.45 (m, 4H)

9.3.7.4 Deacetylation



Following a published method¹⁹⁷. CD-PMeOx-R (500mg) was dissolved in methanol (5ml) followed by the addition of sodium methoxide (0.5ml, 25% in methanol). The mixture was stirred at room temperature for 2 hours before being quenched with water (0.5ml). The solution was concentrated to a foam making sure excess water was removed and redissolved in DCM and cooled. The mixture was filtered through a celite plug to remove excess sodium methoxide and concentrated to yield deacetylated CD-PMeOx-R (429mg).

NMR shows the loss of the acetate CH_3 .

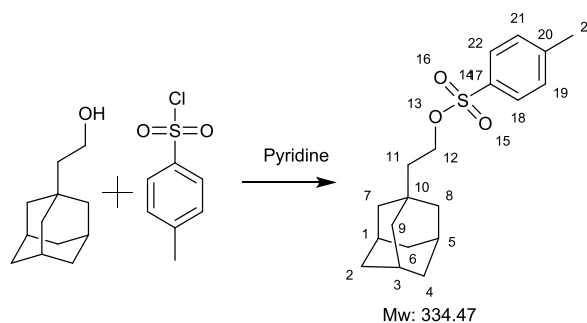
CD-PMeOx-R

^1H NMR (CDCl_3 , δ/ppm):

2.11 (m, 3H), 3.45 (m, 4H)

9.3.8 2-(1-Adamantyl)ethyl p-toluenesulfonate initiator

9.3.8.1 Synthesis



To a cooled suspension of TsCl (1.37g, 0.0072mmol) in pyridine (4ml), 1-adamantane-ethanol (1g, 5.5mmol) was added in portions. The mixture was left overnight in the fridge. It was diluted with water (20ml) and extracted with DCM (3x30ml). The DCM was washed three times with 6M HCl and dried using MgSO_4 . The DCM was concentrated to yield a clear oil which was columned (DCM:MeOH) 1%-5% MeOH. This yielded the product as a colourless oil (1.14g, 47%).

Analysis of the compound is consisted with literature¹⁹⁶.

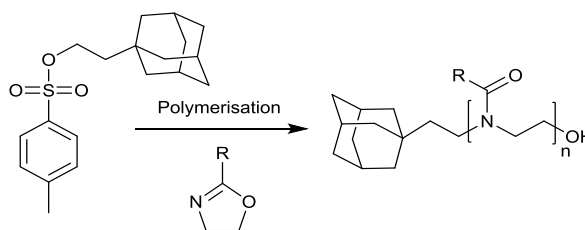
^1H NMR (CDCl_3 , δ/ppm): 1.45 (m, 8H, $\text{H}_{7,9,8}$), 1.50-1.75 (m, 6H, $\text{H}_{2,6,4,11}$), 1.92 (br. s, 3H, $\text{H}_{1,3,5}$), 2.46 (s, 3H, H_{23}), 4.10 (t, $J=7.3$ Hz, 2H, H_{12}), 7.36 (t, $J=8.1$ Hz, 2H, $\text{H}_{21,19}$), 7.80 (d, $J=8.4$ Hz, 2H, $\text{H}_{18,22}$).

^{13}C NMR (CDCl_3 , δ/ppm): 21.2 (C_{23}), 28.0 ($\text{C}_{1,3,5}$), 31.3 (C_{10}), 36.4 ($\text{C}_{2,4,6}$), 41.9 ($\text{C}_{7,9,8}$), 42.0 (C_{11}), 66.9 (C_{12}), 127.45 ($\text{C}_{18,20}$), 129.3 ($\text{C}_{19,21}$), 132.9 (C_{17}), 144.2 (C_{20}).

IR (ν/cm^{-1}): 2840-2900 (C-H), 1358 & 1172 (S=O).

MS (ES^+ , ACN, m/z): 357.2 (11%, $[\text{M}+\text{Na}]^+$).

9.3.8.2 Polymerisation



This used the general polymerisation method discussed previously in section 0. The quantities used are shown in Table 26. After polymerisation, methanolic KOH was added to vials and the mixture was heated to 80°C overnight. The 2-ethyl-2-oxazoline polymer was repeated and quenched with rhodamine 6G (100mg) and trimethylamine (10µl). The four samples were then added to DCM (20ml) and filtered. The DCM was evaporated and the foamy polymer dissolved in DCM. The polymers were precipitated in diethyl ether (*i*PrOx, 1:3 hexane:ether).

| Monomer | | | Initiator | | [M]:[I] |
|---------------|----|------|-----------|------|---------|
| 2-oxazoline | ml | Mmol | mg | mmol | |
| MeOx | 1 | 11.8 | 79 | 0.24 | 50 |
| EtOx | 1 | 9.9 | 66 | 0.20 | 50 |
| <i>i</i> PrOx | 1 | 8.4 | 56 | 0.17 | 50 |

Table 26: Quantities used to synthesise adamantane initiated polymers.

Because of the large size of the polymers (see SEC data, Table 27) the end groups were not visible on the NMR spectrum.

Ad-PMeOx

¹H NMR (CDCl₃, δ/ppm): 2.11 (m, 3H), 3.46 (m, 4H)

Ad-PEtOx

¹H NMR (CDCl₃, δ/ppm): 1.12 (m, 3H), 2.37 (m, 2H), 3.46 (m, 4H)

Ad-PEtOx-R

¹H NMR (CDCl₃, δ/ppm): 1.13 (m, 3H), 2.34 (m, 2H), 3.48 (m, 4H)

Ad-P*i*PrOx

¹H NMR (CDCl₃, δ/ppm): 1.11 (m, 6H), 2.77 (m, 1H), 3.47 (m, 4H)

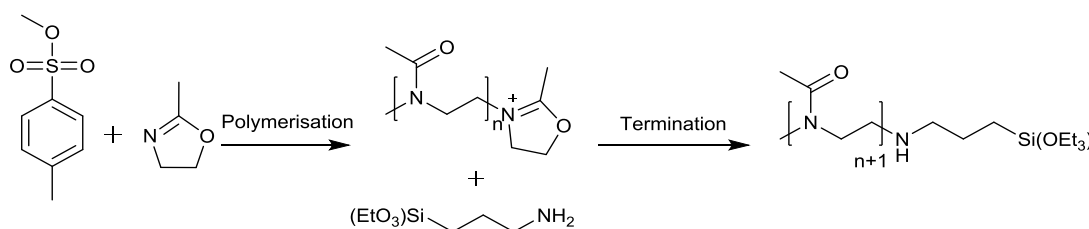
SEC:

| Polymer | Mw | Mn | PD |
|--------------------|-------|-------|------|
| Ad-PMeOx | 32229 | 25381 | 1.26 |
| Ad-PEtOx | 32257 | 26007 | 1.24 |
| Ad-PEtOx-R | 38012 | 32577 | 1.16 |
| Ad-P <i>i</i> PrOx | 33730 | 30158 | 1.19 |

Table 27: SEC analysis of adamantane initiated polymers.

9.4 Antifouling Surfaces

9.4.1 PMeOx-Silane Terminated Polymers



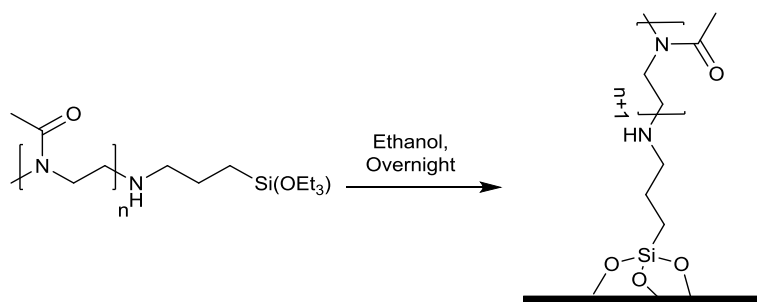
Acetonitrile (2 ml), 2-methyl-2-oxazoline (1 ml) and methyl p-toluenesulfonate (0.028 ml) was added to 6 microwave vials. Each vial was subjected to microwave irradiation for 15 mins (135°C).

To the crude polymer solution was then added triethylamine (0.010 ml) and (3-aminopropyl)triethoxysilane (0.049ml) and the solutions were then stirred at 60°C overnight. The solutions were combined and concentrated under vacuum. They were then dissolved in DCM (20ml) and the product was precipitated by pouring into cold diethyl ether (500ml). The white precipitate was filtered and dried under vacuum overnight (0.79g, 79%). The polymer was used immediately to prevent the silane reacting with moisture in the atmosphere.

^1H NMR (CDCl_3 , δ/ppm): 2.08 (m, 3H), 3.02 (m, 0.05H), 3.44 (m, 4H)

The Dp was estimated to be approx. 50 by comparison of the end group methyl at 3.02 ppm and the backbone peaks at 2.08 ppm and 3.44ppm.

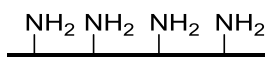
9.4.2 Surface Functionalization of PMeOx



Poly(2-methyl-2-oxazoline) terminated with a silane (1g) was dissolved in freshly distilled ethanol (50ml) and put in a centrifuge tube. A thoroughly cleaned glass slide (Piranha solution, 1hr) which had been rinsed in ethanol was then added. The solution was stirred for 24hr at which point the glass slide was removed and rinsed with copious amounts of ethanol, water and ethanol and left to dry for 10min in an oven).

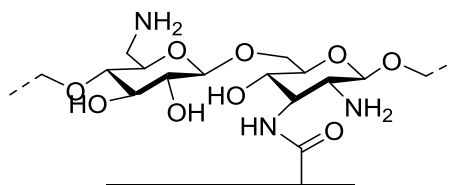
9.5 Bacterial Capture Device

9.5.1 Amine Surface Synthesis



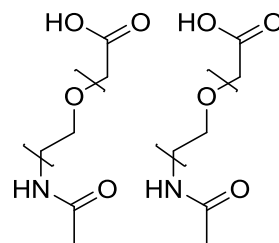
A piranha-solution cleaned glass slide was immersed for 1hr in (3-aminopropyl)triethoxysilane (1ml) in ethanol (50ml). It was then rinsed with ethanol and dried in an oven for 1hr.

9.5.2 Chitosan Surface Synthesis



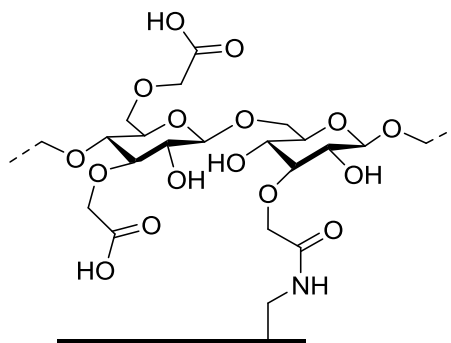
A piranha-solution cleaned glass slide was immersed for 1hr in methyl 3-(trimethoxysilyl)propionate (1ml) in ethanol (50ml). Rinsed with ethanol and water before being immersed in 2M HCl at 80°C for 2hrs. EDC (0.4M) (6.2mg in 0.1ml of 2-ethanesulfonic acid (MES) buffer) and Sulfo-NHS (0.1M) (2.7mg in 0.1ml in MES buffer) were added to the coating for 15min before rinsing with PBS and Chitosan (10mg in 1ml) was then added to the slide and left in the fridge overnight. The slide was then rinsed with PBS.

9.5.3 Carboxylated PEG Surface Synthesis



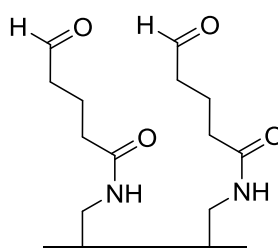
A piranha-solution cleaned glass slide was immersed for 1hr in methyl 3-(trimethoxysilyl)propionate (1ml) in ethanol (50ml). The slide was rinsed with ethanol and water before being immersed in 2M HCl at 80°C for 2hrs. After rinsing with PBS, EDC (0.4M) (6.2mg in 0.1ml in MES buffer) and Sulfo-NHS (0.1M) (2.7mg in 0.1ml in MES buffer) were added to the coating for 15min before rinsing with PBS. PEG (0.01M) (0.18ml PBS, CA(PEG) (10μl), MA(PEG) (10μl)) were then added and the mixture was then left overnight in a refrigerator. The slide was rinsed with MES buffer and then EDC (0.4M) (6.2mg in 0.1ml in MES buffer) and Sulfo-NHS (0.1M) (2.7mg in 0.1ml in MES buffer) were added to the coating for 15min before rinsing with PBS.

9.5.4 Carboxymethylcellulose Surface Synthesis



A piranha-solution cleaned glass slide was immersed for 1hr in (3-aminopropyl)triethoxysilane (1ml) in ethanol (50ml). The slide was rinsed with ethanol and dried in an oven for 1hr. Meanwhile, to a CMC solution (10mg in 1ml of MES) was added EDC (0.4M) (6.2mg in 0.1ml MES) and Sulfo-NHS (0.1M) (2.7mg in 0.1ml MES) and left for 15 min. The activated CMC solution was then added to the amine coated slide overnight at 4°C. The slide was then rinsed with PBS followed by rinsing with MES buffer before a solution of EDC (0.4M) (6.2mg in 0.1ml MES) and Sulfo-NHS (0.1M) (2.7mg in 0.1ml MES) were added for 15 min. The slide was then rinsed with PBS.

9.5.5 Glutaraldehyde Surface Synthesis

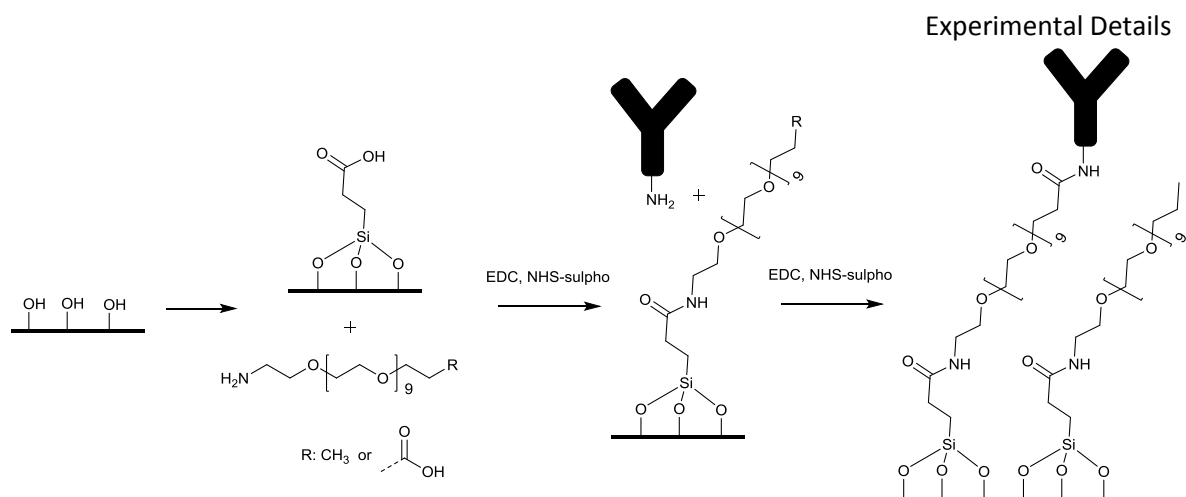


A piranha-solution cleaned glass slide was immersed for 1hr in (3-aminopropyl)triethoxysilane (1ml) in ethanol (50ml). The slide was rinsed with ethanol and dried in an oven for 1hr. A 2% solution of glutaraldehyde in PBS was then added to the surface and left for 1hr before being rinsed with PBS.

9.5.6 Antibody Functionalization

A fluorescein-labelled antibody (Anti-E. coli antibody (FITC), 0.2mg/ml) diluted with a PBS solution (PBS, pH 7, Tween-20 (0.01% w/v), BSA (1% w/v)) was added to the five surfaces described in sections 9.5.19.5.5. The slides were then left overnight in a refrigerator before being rinsed with PBS. The slides were then used immediately to prevent the antibodies deactivating. E. coli bacteria were used for the attachment and detection.

9.5.7 PEG Surfaces of Different Carboxylated PEG

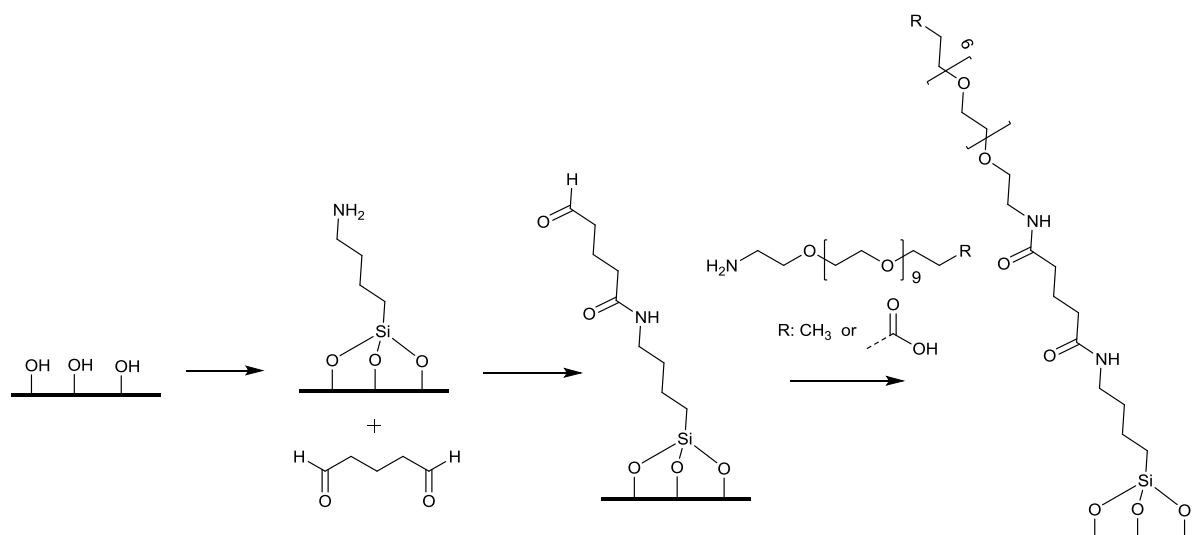


A piranha-cleaned glass slide was immersed for 1 hour in methyl 3-(trimethoxysilyl)propionate (1ml) in ethanol (50ml). The slide was rinsed with ethanol and water before being immersed in 2M HCl at 80°C for 2 hours. EDC (0.4M) (6.2mg in 0.1ml MES buffer) and Sulfo-NHS (0.1M) (2.7mg in 0.1ml MES buffer) were added to the coating for 15min before rinsing with PBS.

From two stock solutions containing CA(PEG) 0.1M (100mg in 2.3ml dry DMSO) and MA(PEG) 0.1M (100mg in 2.3ml dry DMSO) several different percentages of CA(PEG)-containing solutions were made (10%, 30%, 50%, 70%, 90%). This was achieved by mixing the two PEG stock solutions together to make the desired ratio, the combined volume of the PEG solutions came to 20µl and to this was added PBS (180µl). For example, a 30% solution of CA(PEG) would contain 6µl of CA(PEG) stock solution, 14µl of MA(PEG) stock solution and 180µl of PBS. These solutions were added to the activated glass slide surfaces and left for a period of 2 hours.

The slide was then rinsed with MES buffer and a solution containing EDC (0.4M) (6.2mg in 0.1ml MES buffer) and Sulfo-NHS (0.1M) (2.7mg in 0.1ml MES buffer) was added to the coating for 15 min before rinsing with PBS. The surface was cleaned with PBS and a fluorescein-labelled antibody (Anti-E. coli antibody (FITC), 0.2mg/ml) diluted with a PBS solution (PBS, pH 7, Tween-20 (0.01% w/v), BSA (1% w/v) was then added and the slide was left overnight in a refrigerator.

9.5.8 Glutaraldehyde Modification of PEG Surface Attachment



A piranha-cleaned glass slide was immersed for 1 hour in (3-aminopropyl)triethoxysilane (1ml) in ethanol (50ml). It was then rinsed with ethanol and then dried in an oven at 80°C for 1 hour. A 2% solution of glutaraldehyde in PBS was then added to the surface which was then left for 1 hour before rinsing with PBS.

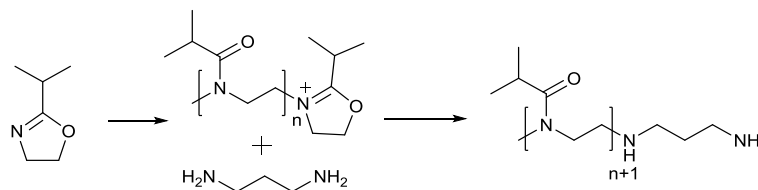
From two stock solutions containing CA(PEG) 0.1M (100mg in 2.3ml dry DMSO) and MA(PEG) 0.1M (100mg in 2.3ml dry DMSO) several different percentages of CA(PEG)-containing solutions were made (10%, 30%, 50%, 70%, 90%). This was achieved by mixing the two PEG stock solutions together to make the desired ratio, the combined volume of the PEG solutions came to 20μl and to this was added PBS (180μl). For example, a 30% solution of CA(PEG) would contain 6μl of CA(PEG) stock solution, 14μl of MA(PEG) stock solution and 180μl of PBS. These solutions were added to the activated glass slide surfaces and left for a period of 2 hours.

The slide was rinsed with MES and EDC (0.4M) (6.2mg in 0.1ml MES) and Sulfo-NHS (0.1M) (2.7mg in 0.1ml MES) was added to the coating for 15 min before rinsing with PBS. The surface was cleaned with PBS and a fluorescein-labelled antibody (Anti-E. coli antibody (FITC), 0.2mg/ml) diluted with a PBS solution (PBS, pH 7, Tween-20 (0.01% w/v), BSA (1% w/v) was added and the slide was left overnight in a refrigerator. Excess antibody was removed by rinsing with PBS.

9.6 Thermogelling Polymers

9.6.1 Thermoresponsive Polymer Arms

9.6.1.1 Synthesis of P*i*PrOx-NH₂-1



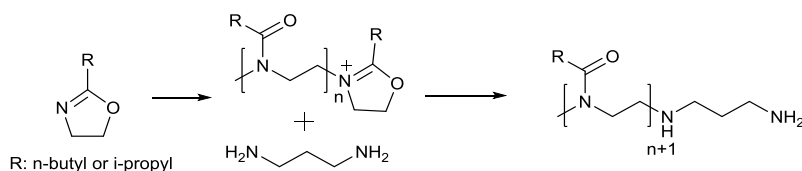
Two solutions containing; acetonitrile (2ml), 2-isopropyl-2-oxazoline (1ml, 8.3mmol) and methyl *p*-toluenesulfonate (0.0032ml, 0.021mmol) were added to two microwave vials. Each vial was subjected to microwave irradiation for 15 min (ramp time 20 min; 135°C; 130 psi).

Triethylamine (10μl) and diaminopropane (100μl) were then added and the solutions were heated to 60°C overnight. The samples were then combined and dialysed for 3 days in deionised water. The water was changed twice a day. The samples were then freeze-dried leaving amine end-capped poly(2-isopropyl-2-oxazoline), 1.87g (94%).

¹H NMR (CDCl₃, δ/ppm): 1.05 (br. s, 6H, H_{10,9}), 2.75 (m, 1H, H₇), 3.45 (br. s, 4H, H_{3,4}).

IR (ν/cm⁻¹): 2969 (C-H), 1627 (C=O).

GPC : Mw: 44555 Da
Mn: 39854 Da
PDI: 1.11

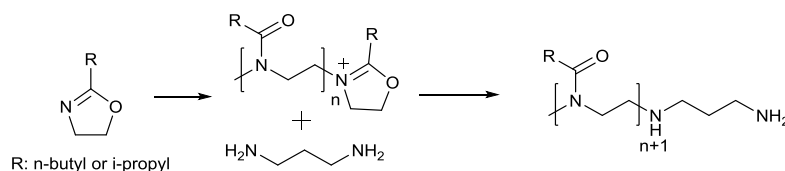
9.6.1.2 Synthesis of PiPrOx-*n*BuOx-NH₂-1

A stock solution containing acetonitrile (12ml), 2-isopropyl-2-oxazoline (4.704ml, 42.41mmol), 2-butyl-2-oxazoline (1.32ml 10.37mmol) and methyl *p*-toluenesulfonate (52.2 μ l, 0.23mmol) was prepared. The stock solution (5ml) was added to each of five microwave vials. Each vial was subjected to microwave irradiation for 15 min (ramp time 20 min; 135°C). Triethylamine (10 μ l) and diaminopropane (100 μ l) were then added to each solution and the solutions were heated to 60°C overnight. The samples were then combined and dialysed for 3 days in deionised water. The water was changed twice a day. The samples were then freeze dried to remove the water leaving amine end-capped poly(2-isopropyl-2-oxazoline)-co-(2-butyl-2-oxazoline) PiPrOx-*n*BuOx-NH₂-1 (5.23g, 87%).

¹H NMR (CDCl₃, δ /ppm): 0.9 (br. s, 1H), 1.09 (br. s, 5H), 1.32 (br. s, 0.75H), 1.57 (br. s, 0.6H), 2.26 (br. s, 0.9H), 2.75 (br. s, 0.9H), 3.43 (br. s, 4H).

IR (ν /cm⁻¹): 2969 (C-H), 1627 (C=O).

GPC : Mw: 26631 Da
Mn: 16066 Da
PDI: 1.65

9.6.1.3 Synthesis of PiPrOx-*n*BuOx-NH₂-2

A stock solution containing; acetonitrile (12ml), 2-isopropyl-2-oxazoline (4.116ml, 37.11mmol), 2-butyl-2-oxazoline (1.98ml 15.6mmol) and methyl *p*-toluenesulfonate (52.2 μ l, 0.23mmol) was prepared. The stock solution (5ml) was added to each of five microwave vials. Each vial was subjected to microwave irradiation for 15 mins (ramp time 20 mins; 135°C). Triethylamine (10 μ l) and diaminopropane (100 μ l) were then added to each solution and the solutions were heated to 60°C overnight. The samples were then combined and dialysed for 3 days in deionised water. The water was changed twice a day. The samples were then freeze dried to remove the water leaving amine end-capped poly(2-isopropyl-2-oxazoline)-co-(2-butyl-2-oxazoline) PiPrOx-*n*BuOx-NH₂-2 (5.89g, 97%).

¹H NMR (CDCl₃, δ /ppm):

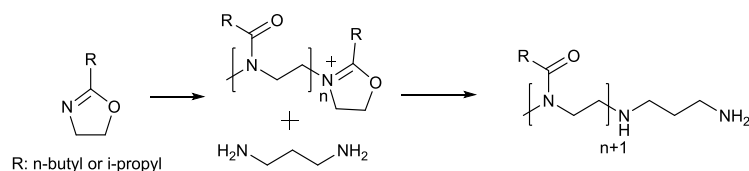
0.9 (br. s, 1H), 1.09 (br. s, 5H), 1.32 (br. s, 0.75H), 1.57 (br. s, 0.6H), 2.26 (br. s, 0.9H), 2.75 (br. s, 0.9H), 3.43 (br. s, 4H).

IR (ν /cm⁻¹):

2969 (C-H), 1627 (C=O).

GPC :

Mw: 28115 Da
Mn: 17182 Da
PDI: 1.63

9.6.1.4 Synthesis of PiPrOx-nBuOx-NH₂-3

A stock solution of 2-isopropyl-2-oxazoline (17.15ml, 0.154mol), acetonitrile (50 ml), 2-butyl-2-oxazoline (8.26ml, 0.064) and methyl p-toluenesulfonate (217 μ l, 0.944mmol) was made up. 24 microwave vials were each filled with 3ml of the stock solution. These were then subjected to microwave irradiation for 15min (ramp time 20 min, 135°C). The vials were then uncapped and 1,3 diaminopropane (100 μ l) and triethylamine (10 μ l) were then added to each sample. These samples were capped and heated to 60°C overnight. The samples were then combined and concentrated under vacuum, re-dissolved in chloroform and precipitated in 2L of 3:1 (v/v) diethyl ether:hexane. After filtration a white polymer was obtained which was left to dry under vacuum yielding 17.87g (71%) of co-polymer.

¹H NMR (CDCl₃, δ /ppm):

0.9 (br. s, 1H), 1.09 (br. s, 5H), 1.32 (br. s, 0.75H), 1.57 (br. s, 0.6H), 2.26 (br. s, 0.9H), 2.75 (br. s, 0.9H), 3.43 (br. s, 4H).

IR (ν /cm⁻¹):

2969 (C-H), 1627 (C=O).

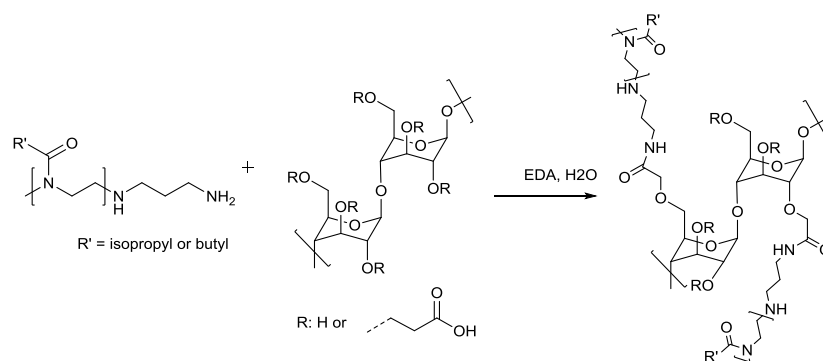
GPC :

Mw: 35212 Da
Mn: 42243 Da
PDI: 1.19

9.6.2 Thermogelling Polymers

All of the gelling polymers described below were synthesised via the same method with different amounts of smarting materials added (unless specified).

9.6.2.1 Generic Coupling Method for The Preparation of Thermogelling (TG-*n*) polymers



Where $n = 1$ (R = isopropyl), 25.7 (R = isopropyl or butyl), 35 (R = isopropyl or butyl), 33 (R = isopropyl or butyl). The number denotes the percentage of *n*BuOx content on the polymer arms

Carboxymethylcellulose (50mg, av. mw 90000) was dissolved in distilled water (5ml). EDC (50mg) was then added to the solution which was then left overnight in a refrigerator. One or two drops of 2M HCl was added to adjust the pH to 5.5. The relevant amount of amine-capped poly(2-oxazoline) pre-dissolved in water (approx. 5ml) was added and the mixture was stirred at room temperature overnight. The solution was then concentrated under vacuum or freeze dried to remove most of the water. A large excess of methanol (approx. 50ml) was then added. The precipitate was centrifuged and washed twice with methanol, re-dispersing and centrifuging each time and then dried under vacuum to yield approximately 50mg of thermogelling polymer.

9.6.2.2 Thermogelling Polymer Analysis

TG-I

PiPrOx-NH₂-1 arm amounts:

| | Amount (g) | μmoles | Water removal |
|---------------|------------|--------|---------------|
| TG-I-A | 0.990 | 2.48 | Freeze drying |
| TG-I-B | 0.495 | 1.24 | Freeze drying |
| TG-I-C | 0.165 | 0.41 | Freeze drying |

Table 28: Quantities of PiPrOx-NH₂-1 used to synthesise TG-I thermogelling polymers

Elemental analysis was not performed on these polymers. Percentage yields were not calculated as the product Mw was not known. The amount of polymer collected was approximately the weight of CMC added i.e. around 50mg.

TG-27.5

PiPrOx-*n*BuOx-NH₂-1 arm amounts:

| | Amount (g) | μmoles | Water removal |
|------------------|------------|--------|---------------|
| TG-27.5-A | 1.135 | 7.07 | Vacuum |
| TG-27.5-B | 0.568 | 3.53 | Vacuum |
| TG-27.5-C | 0.284 | 1.77 | Vacuum |
| TG-27.5-D | 0.189 | 1.18 | Vacuum |

Table 29: Quantities of PiPrOx-*n*BuOx-NH₂-1 used to synthesise TG-27.5 thermogelling polymers

Percentage yields were not calculated as the product Mw was not known. The amount of polymer collected was approximately the weight of CMC added i.e. around 50mg.

Elemental analysis

The elemental analysis demonstrates the presence of poly(2-oxazoline) arms by the nitrogen content which would not be present in the CMC alone. We find the highest nitrogen content in TG-27.5-A which has the highest amount of PiPrOx-*n*BuOx-NH₂-1 added to it. There appears to be very little difference in the nitrogen content of the other three samples.

| | | C | H | N | O |
|------------------|------------------|----------|----------|----------|----------|
| TG-27.5-A | % Found 1 | 43.79 | 6.74 | 4.38 | - |
| | % Found 2 | 44.02 | 6.51 | 4.44 | - |
| | Average | 43.91 | 6.63 | 4.41 | 45.06 |
| TG-27.5-B | | C | H | N | O |
| | % Found 1 | 42.37 | 6.31 | 3.75 | - |
| | % Found 2 | 42.43 | 6.22 | 3.82 | - |
| | Average | 42.40 | 6.27 | 3.79 | 47.55 |
| TG-27.5-C | | C | H | N | O |
| | % Found 1 | 42.29 | 6.36 | 4.01 | - |
| | % Found 2 | 42.32 | 6.41 | 3.99 | - |
| | Average | 42.31 | 6.39 | 4.00 | 47.31 |
| TG-27.5-D | | C | H | N | O |
| | % Found 1 | 43.07 | 6.34 | 4.06 | - |
| | % Found 2 | 42.91 | 6.12 | 4.07 | - |
| | Average | 42.99 | 6.23 | 4.07 | 46.72 |

Table 30: Elemental analysis results of the TG-27.5 thermogelling polymers

TG-35

PiPrOx-*n*BuOx-NH₂-2 arm amounts:

| | Amount (g) | μmoles | Water removal |
|----------------|------------|--------|---------------|
| TG-35-A | 1.142 | 5.34 | Vaccum |
| TG-35-B | 0.571 | 2.67 | Vaccum |
| TG-35-C | 0.285 | 1.33 | Vaccum |
| TG-35-D | 0.190 | 0.89 | Vaccum |

Table 31: Quantities of PiPrOx-*n*BuOx-NH₂-2 used to synthesise the TG-35 series of thermogelling polymers

Percentage yields were not calculated as the product Mw was not known. The amount of polymer collected was approximately the weight of CMC added i.e. around 50mg.

Elemental analysis

As anticipated the amount of nitrogen found in the thermogelling samples decreases as the amount of PiPrOx-*n*BuOx-NH₂-2 added into the coupling reaction decreases. TG-35-A containing the highest amount of nitrogen and TG-35-D containing the least.

| | | C | H | N | O |
|----------------|------------------|----------|----------|----------|----------|
| TG-35-A | % Found 1 | 46.15 | 7.43 | 5.79 | - |
| | % Found 2 | 45.98 | 7.32 | 5.83 | - |
| | Average | 46.07 | 7.38 | 5.81 | 40.75 |
| | | | | | |
| | | C | H | N | O |
| TG-35-B | % Found 1 | 46.44 | 7.33 | 4.92 | - |
| | % Found 2 | 46.27 | 7.01 | 5.03 | - |
| | Average | 46.36 | 7.17 | 4.98 | 41.50 |
| | | | | | |
| | | C | H | N | O |
| TG-35-C | % Found 1 | 44.34 | 6.56 | 4.15 | - |
| | % Found 2 | 43.98 | 6.49 | 4.09 | - |
| | Average | 44.16 | 6.53 | 4.12 | 45.20 |
| | | | | | |
| | | C | H | N | O |
| TG-35-D | % Found 1 | 43.83 | 6.58 | 3.98 | - |
| | % Found 2 | 44.01 | 6.83 | 3.97 | - |
| | Average | 43.92 | 6.71 | 3.98 | 45.40 |

Table 32: Elemental analysis results of the TG-35 thermogelling polymers

TG-33

PiPrOx-*n*BuOx-NH₂-3 arm amounts:

| | Amount (g) | μmoles | Water removal |
|----------------------------|------------|--------|---------------|
| TG-33-A[†] | 12.000 | 34.08 | Freeze drying |

Table 33: Quantity of PiPrOx-*n*BuOx-NH₂-3 used to synthesise TG-33-A.

[†]CMC (400mg) dissolved in 40ml water, EDC (400mg). Polymer added in 50ml water.

Yielded 596mg of TG-33-A.

Elemental analysis

A relatively high amount of nitrogen was found in TG-33-A (comparable to that of TG-35-A). This indicates comparable coupling efficiency to that of the previous samples.

| | | C | H | N | O |
|----------------|------------------|-------|------|------|-------|
| TG-33-A | % Found 1 | 45.15 | 7.31 | 5.08 | - |
| | % Found 2 | 45.78 | 7.75 | 5.21 | - |
| | Average | 45.47 | 7.53 | 5.15 | 41.86 |

Table 34: Elemental analysis results for TG-33-A

9.6.3 Cell Work**9.6.3.1 Seeding 16HBE Cells on Top of Thermogels**

A solution of TG-33-A (6% w/w, 100μl) in 16HBE medium was added under 16HBE medium (100μl) into a 96 well plate and centrifuged (300g for 5 minutes) to reduce any meniscus that was formed. This was then incubated at 37°C for 30 minutes. 16HBE cells (3x10⁵ in 50μl of 16HBE medium) were gently added to the medium covering the gel layer. The cells were then incubated for 2 hours at 37°C. The cell aggregates that had formed were then captured using a wide bore pastette and placed onto a transwell containing a confluent layer of MRC5 cells.

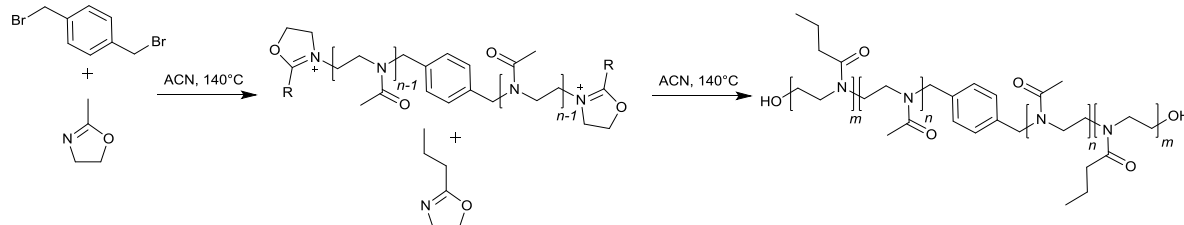
9.6.3.2 Creating Multi-Layered Cell Sheets

3x10⁴ MRC5 cells were seeded on to a transwell and allowed to achieve confluence. The 16HBE cell aggregates were then gently added to the transwell and the media replaced after two hours. Within 1 hour the aggregates could be seen to be anchoring themselves to the MRC5 later.

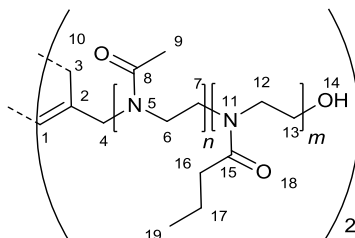
9.7 Second Generation BAB Triblock Copolymers

9.7.1 Proof of Principle Polymers

9.7.1.1 PnPrOx-PMeOx-PnPrOx



To a 20 ml microwave vial were added acetonitrile (9.34 ml), 2-methyl-2-oxazoline (3.38 ml 0.04 mol) and α,α' -dibromo-*p*-xylene (105 mg, 0.8 mmol). This was then heated to 140°C for 8 minutes in a microwave reactor. Once cool 2-*n*-propyl-2-oxazoline (2.26 ml, 0.02 mol) was added and the solution was heated to 140°C for 41 minutes. To terminate the polymer saturated KOH in methanol (100 μ l) was added and the solution was stirred for 30min. The solution was diluted with dichloromethane (approx. 20ml) and added dropwise to vigorously stirred, ice cold, diethyl ether (400 ml). The precipitate was then filtered yielding PnPrOx-PMeOx-PnPrOx as a white powder.



^1H NMR (CDCl_3 , δ/ppm):

0.94 (br. s, 0.89H, H_{19}), 1.64 (br. s, 0.61H, H_{17}),
2.11 (br. m, 2.97H, $\text{H}_{9,16}$), 3.45 (br. s, 4H,
 $\text{H}_{6,7,12,13}$).

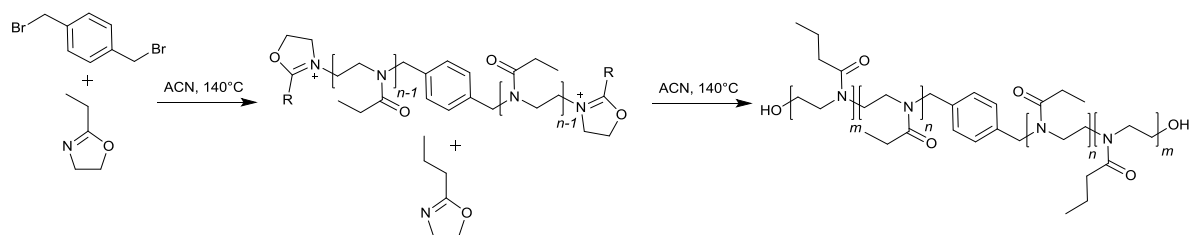
SEC:

M_n : 27960

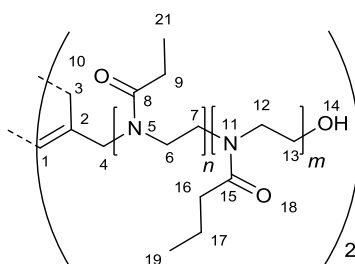
M_w : 24577

PDI: 1.45

9.7.1.2 PnPrOx-PEtOx-PnPrOx



To a 20 ml microwave vial was added acetonitrile (8.79 ml), 2-ethyl-2-oxazoline (3.94 ml 0.04 mol) and α,α' -dibromo-*p*-xylene (105 mg, 0.8 mmol). This was heating to 140°C for 12 minutes in a microwave reactor. Once cool 2-*n*-propyl-2-oxazoline (2.26 ml, 0.02 mol) was added and the solution was heated to 140°C for 41 minutes. To terminate the polymer saturated KOH in methanol (100 μ l) was added and the solution was stirred for 30min. The solution was diluted with dichloromethane (approx. 20ml) and added dropwise to vigorously stirred, ice cold, diethyl ether (400 ml). The precipitate was then filtered yielding PnPrOx-PEtOx-PnPrOx as a white powder.



^1H NMR (CDCl_3 , δ/ppm):

0.93 (br. s, 0.95H, H_{19}), 1.11 (br. s, 2.09H, H_{21}),
1.64 (br. s, 0.61H, H_{17}), 2.33 (br. m, 2.1H, $\text{H}_{9,16}$),
3.44 (br. s, 4H, $\text{H}_{6,7,12,13}$).

SEC:

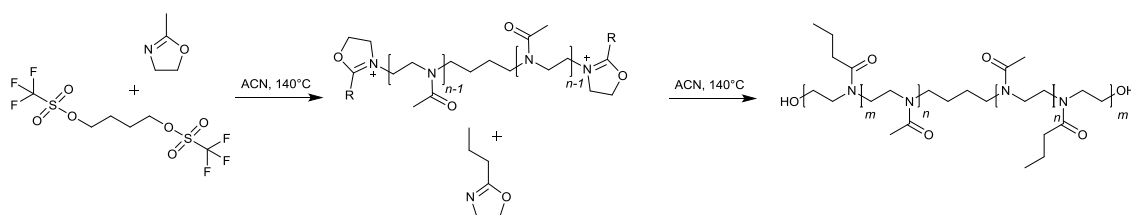
M_n : 33000

M_w : 23888

PDI: 1.27

9.7.2 Thermogelling BAB Triblock polymers

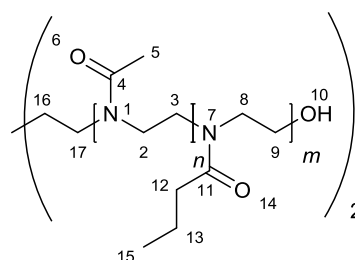
9.7.2.1 PnPrOx-MeOx-PnPrOx Polymers



General Procedure

To a 2-5 ml microwave vial was added acetonitrile, 2-methyl-2-oxazoline and butane-1,4-diyl bis(trifluoromethanesulfonate) (0.1 g ml^{-1} solution in acetonitrile). This was heated to 140°C for a predetermined amount of time (time 1) in a microwave reactor. Once cool 2-*n*-propyl-2-oxazoline was added and the solution was heated to 140°C for predetermined amount of time (time 2). To terminate the polymer saturated KOH in methanol ($100 \mu\text{l}$) was added and the solution stirred for 30min. The acetonitrile was then removed under vacuum to yield the PnPrOx-PMeOx-PnPrOx triblock polymer.

Analysis



^1H NMR (CDCl_3 , δ/ppm): 0.95 (br. s, 1H, H_{15}), 1.65 (br. s, 0.9H, H_{13}), 2.15 (br. m, 2.8H, $\text{H}_{12,5}$), 3.46 (br. s, 4H, $\text{H}_{2,3,8,9}$).

SEC:

| Sample Name | Sec Results | | |
|--|-------------|-------|------|
| | M_n | M_w | PDI |
| PnPrOx ₂₄ -PMeOx ₁₃₆ -PnPrOx ₂₄ | 16835 | 24577 | 1.45 |
| PnPrOx ₂₈ -PMeOx ₁₁₇ -PnPrOx ₂₈ | 16408 | 23888 | 1.46 |
| PnPrOx ₄₁ -PMeOx ₈₄ -PnPrOx ₄₁ | 16381 | 27388 | 1.67 |
| PnPrOx ₅₅ -PMeOx ₈₆ -PnPrOx ₅₅ | 19496 | 30056 | 1.54 |
| PnPrOx ₆₆ -PMeOx ₈₂ -PnPrOx ₆₆ | 21671 | 31553 | 1.46 |
| PnPrOx ₆₂ -PMeOx ₆₄ -PnPrOx ₆₂ | 19117 | 28071 | 1.47 |
| PnPrOx ₄₈ -PMeOx ₂₀ -PnPrOx ₄₈ | 12846 | 16829 | 1.31 |
| PnPrOx ₄₆ -PMeOx ₅₂ -PnPrOx ₄₆ | 14739 | 21285 | 1.44 |
| PnPrOx ₅₄ -PMeOx ₇₂ -PnPrOx ₅₄ | 18299 | 29561 | 1.62 |

Table 35: SEC results for PnPrOx-MeOx-PnPrOx polymers

The expected Dp and calculated Dp was determined from analysis of the SEC and NMR data (Table 36). Some of the calculated values are quite far from the expected Dp. This is attributed to

the large PDI in the polymer samples causing an inaccurate reflection of the composition of the triblock polymer in the Dp. As discussed in section 0 the SEC trace of the synthesised polymers contains different species of polymer. The Mn and Mw is an average of these peaks and so does not accurately reflect the Mn and Mw of the triblock poly(2-oxazoline) only. The calculated Dp values reflect the average in the sample while the expected Dp is for a purely homogeneous solution of triblock polymer. This illustrates why polymers of lower polydispersity are required, particularly to aid characterisation of the polymer structure.

| Sample | Expected Dp | | | Calculated Dp | | |
|--|-------------|-------|-----|---------------|-------|-----|
| | MeOx | nPrOx | Dp | MeOx | nPrOx | Dp |
| PnPrOx₂₄-PMeOx₁₃₆-PnPrOx₂₄ | 50 | 25 | 75 | 68 | 24 | 92 |
| PnPrOx₂₈-PMeOx₁₁₇-PnPrOx₂₈ | 66 | 33 | 100 | 59 | 28 | 87 |
| PnPrOx₄₁-PMeOx₈₄-PnPrOx₄₁ | 67 | 67 | 134 | 42 | 41 | 83 |
| PnPrOx₅₅-PMeOx₈₆-PnPrOx₅₅ | 67 | 101 | 168 | 43 | 55 | 98 |
| PnPrOx₆₆-PMeOx₈₂-PnPrOx₆₆ | 66 | 133 | 200 | 41 | 66 | 107 |
| PnPrOx₆₂-PMeOx₆₄-PnPrOx₆₂ | 13 | 67 | 80 | 10 | 48 | 58 |
| PnPrOx₄₈-PMeOx₂₀-PnPrOx₄₈ | 40 | 67 | 107 | 26 | 46 | 72 |
| PnPrOx₄₆-PMeOx₅₂-PnPrOx₄₆ | 93 | 67 | 160 | 36 | 54 | 90 |
| PnPrOx₅₄-PMeOx₇₂-PnPrOx₅₄ | 50 | 100 | 150 | 32 | 62 | 94 |

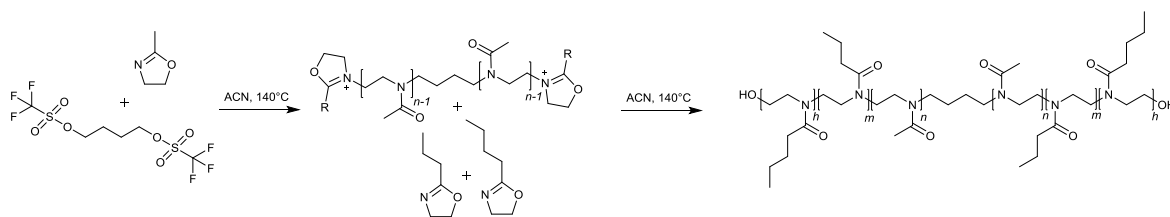
Table 36: Dp analysis of PnPrOx-MeOx-PnPrOx polymers

Samples, Amounts and Times

| Sample | Initiator (μ l) | Initiator (mmol) | MeOx (μ l) | MeOx (mmol) | nPrOx (μ l) | nPrOx (mmol) | Acetonitrile (ml) | Time 1 (min) | Time 2 (min) |
|---|-------------------------|---------------------|--------------------|----------------|---------------------|-----------------|----------------------|-----------------|-----------------|
| PnPrOx₂₄-PMeOx₁₃₆- PnPrOx₂₄ | 142 | 0.080 | 339 | 4.000 | 226 | 2.000 | 2.15 | 17 | 28 |
| PnPrOx₂₈-PMeOx₁₁₇- PnPrOx₂₈ | 106 | 0.060 | 339 | 4.000 | 226 | 1.997 | 2.29 | 17 | 27 |
| PnPrOx₄₁-PMeOx₈₄- PnPrOx₄₁ | 79 | 0.045 | 254 | 2.984 | 339 | 2.996 | 2.29 | 23 | 36 |
| PnPrOx₅₅-PMeOx₈₆- PnPrOx₅₅ | 63 | 0.036 | 203 | 2.385 | 407 | 3.597 | 2.30 | 29 | 45 |
| PnPrOx₆₆-PMeOx₈₂- PnPrOx₆₆ | 53 | 0.030 | 169 | 1.986 | 452 | 3.994 | 2.30 | 35 | 54 |
| PnPrOx₆₂-PMeOx₆₄- PnPrOx₆₂ | 132 | 0.075 | 84 | 0.987 | 565 | 4.993 | 2.17 | 14 | 22 |
| PnPrOx₄₈-PMeOx₂₀- PnPrOx₄₈ | 99 | 0.056 | 190 | 2.232 | 424 | 3.747 | 2.25 | 19 | 29 |
| PnPrOx₄₆-PMeOx₅₂- PnPrOx₄₆ | 66 | 0.037 | 296 | 3.478 | 282 | 2.492 | 2.33 | 28 | 44 |
| PnPrOx₅₄-PMeOx₇₂- PnPrOx₅₄ | 354 | 0.200 | 847 | 9.952 | 2260 | 19.972 | 11.50 | 34 | 54 |

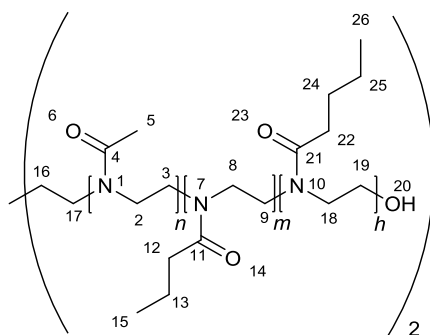
Table 37: Quantities used to synthesise the PnPrOx-MeOx-PnPrOx series of polymers

9.7.2.2 PnPrOx/PnBuOx-PMeOx-PnPrOx/PnBuOx Polymers



To a 2-5 ml microwave vial was added acetonitrile, 2-methyl-2-oxazoline and butane-1,4-diyl bis(trifluoromethanesulfonate) (0.1 g ml^{-1} solution in acetonitrile). This was heated to 140°C for a predetermined amount of time (time 1) in a microwave reactor. Once cool 2-*n*-propyl-2-oxazoline and 2-*n*-butyl-2-oxazoline were added and the solution was heated to 140°C for a predetermined amount of time (time 2). To terminate the polymer saturated KOH in methanol ($100 \mu\text{l}$) was added and the solution was stirred for 30min. The acetonitrile was then removed under vacuum to yield the PnPrOx/PnBuOx-PMeOx-PnPrOx/PnBuOx triblock polymer.

Analysis



^1H NMR (CDCl_3 , δ/ppm):

0.95 (br. s, 1.5H, $\text{H}_{15, 26}$), 1.34 (br. s, 0.07H, H_{25}),
1.64 (br. s, 1H, $\text{H}_{24,13}$), 2.17 (br. m, 2.7H,
 $\text{H}_{12,5,22}$), 3.45 (br. s, 4H, $\text{H}_{2,3,8,9,18,19}$).

SEC:

| Sample Name | Sec Results | | |
|---|-------------|-------|------|
| | M_n | M_w | PDI |
| PnPrOx ₆₁ /PnBuOx _{4.5} PMeOx ₆₂ PnPrOx ₆₁ /PnBuOx _{4.5} | 13529 | 20969 | 1.55 |
| PnPrOx ₆₃ /PnBuOx _{7.5} PMeOx ₅₇ PnPrOx ₆₃ /PnBuOx _{7.5} | 13447 | 21515 | 1.60 |
| PnPrOx ₅₄ /PnBuOx ₉ PMeOx ₅₁ PnPrOx ₅₄ /PnBuOx ₉ | 12778 | 20801 | 1.63 |
| PnPrOx ₄₉ /PnBuOx _{10.5} PMeOx ₄₃ PnPrOx ₄₉ /PnBuOx _{10.5} | 11818 | 19811 | 1.68 |
| PnPrOx ₅₄ /PnBuOx _{6.5} PMeOx ₆₄ PnPrOx ₅₄ /PnBuOx _{6.5} | 13343 | 21960 | 1.65 |
| PnPrOx ₆₁ /PnBuOx _{11.5} PMeOx ₈₁ PnPrOx ₆₁ /PnBuOx _{11.5} | 16691 | 23990 | 1.44 |

Table 38: SEC results for the PnPrOx/PnBuOx-PMeOx-PnPrOx/PnBuOx series of polymers

The calculated Dp (Table 39) for this series of polymers does not match up exactly with the expected Dp. However, these samples do appear to correspond more closely than the previous

samples. The high PDI of these samples means that the calculated values will not correspond to that of the Dp for the triblock polymers only.

| Sample | Expected Dp | | | | Calculated Dp | | | |
|---------------------------------------|-------------|-------|-------|-----|---------------|-------|-------|-----|
| | MeOx | nPrOx | nBuOx | Dp | MeOx | nPrOx | nBuOx | Dp |
| $PnPrOx_{61}/PnBuOx_{4.5}PMeOx_{62}$ | 52 | 49 | 3 | 104 | 62 | 61 | 5 | 97 |
| $PnPrOx_{63}/PnBuOx_{7.5}PMeOx_{57}$ | 52 | 47 | 5 | 104 | 57 | 63 | 8 | 99 |
| $PnPrOx_{54}/PnBuOx_9PMeOx_{51}$ | 52 | 44 | 8 | 104 | 51 | 54 | 9 | 89 |
| $PnPrOx_{49}/PnBuOx_{10.5}PMeOx_{43}$ | 52 | 42 | 10 | 104 | 43 | 49 | 11 | 82 |
| $PnPrOx_{54}/PnBuOx_{6.5}PMeOx_{64}$ | 52 | 46 | 8 | 106 | 64 | 54 | 7 | 92 |
| $PnPrOx_{61}/PnBuOx_{11.5}PMeOx_{81}$ | 50 | 42 | 7 | 99 | 81 | 61 | 12 | 113 |

Table 39: Dp analysis for the $PnPrOx/PnBuOx$ - $PMeOx$ - $PnPrOx/PnBuOx$ series of polymers

| Sample | Initiator (μ l) | Initiator (mmol) | MeOx (μ l) | MeOx (mmol) | nPrOx (μ l) | nPrOx (mmol) | nBuOx (μ l) | nBuOx (mmol) | Acetonitrile (ml) | Time 1 (min) | Time 2 (min) |
|---|-------------------------|---------------------|--------------------|----------------|---------------------|-----------------|---------------------|-----------------|----------------------|-----------------|-----------------|
| PnPrOx₆₁/PnBuOx_{4.5}PMeO x₆₂PnPrOx₆₁/PnBuOx_{4.5} | 102 | 0.058 | 254 | 2.984 | 285 | 2.519 | 22 | 0.173 | 2.32 | 24 | 36 |
| PnPrOx₆₃/PnBuOx_{7.5}PMeO x₅₇PnPrOx₆₃/PnBuOx_{7.5} | 102 | 0.058 | 254 | 2.984 | 305 | 2.695 | 38 | 0.299 | 2.29 | 24 | 36 |
| PnPrOx₅₄/PnBuOx₉PMeOx₅ ₁PnPrOx₅₄/PnBuOx₉ | 102 | 0.058 | 254 | 2.984 | 285 | 2.519 | 61 | 0.480 | 2.27 | 24 | 36 |
| PnPrOx₄₉/PnBuOx_{10.5}PMeO x₄₃PnPrOx₄₉/PnBuOx_{10.5} | 102 | 0.058 | 254 | 2.984 | 271 | 2.395 | 76 | 0.598 | 2.26 | 24 | 36 |
| PnPrOx₅₄/PnBuOx_{6.5}PMeO x₆₄PnPrOx₅₄/PnBuOx_{6.5} | 70 | 0.359 | 2 | 17.906 | 2 | 15.907 | 357 | 2.807 | 2.94 | 24 | 30 |
| PnPrOx₆₁/PnBuOx_{11.5}PMeO x₈₁PnPrOx₆₁/PnBuOx_{11.5} | 531 | 0.300 | 1 | 14.922 | 1 | 12.549 | 305 | 2.398 | 12.00 | 23 | 36 |

Table 40: Quantities used to synthesise the PnPrOx/PnBuOx-PMeOx-PnPrOx/PnBuOx series of polymers

Chapter 10 List of References

1. R. Hoogenboom, *Angewandte Chemie International Edition*, 2009, **48**, 7978-7994.
2. R. Hoogenboom, *Macromolecular Chemistry and Physics*, 2007, **208**, 18-25.
3. M. Bauer, C. Lautenschlaeger, K. Kempe, L. Tauhardt, U. S. Schubert and D. Fischer, *Macromolecular Bioscience*, 2012, **12**, 986-998.
4. S. Huber and R. Jordan, *Colloid Polym Sci*, 2007, **286**, 395-402.
5. R. Hoogenboom, H. M. L. Thijs, M. J. H. C. Jochems, B. M. van Lankvelt, M. W. M. Fijten and U. S. Schubert, *Chem. Commun.*, 2008, 5758-5760.
6. H. Staudinger, *From Organic Chemistry to Macromolecules*, Wiley Interscience, 1970.
7. R. Hoogenboom, H. M. L. Thijs, D. Wouters, S. Hoeppener and U. S. Schubert, *Macromolecules*, 2008, **41**, 1581-1583.
8. R. Hoogenboom, M. W. M. Fijten, H. M. L. Thijs, B. M. van Lankvelt and U. S. Schubert, *Designed Monomers & Polymers*, 2005, **8**, 659-671.
9. I. Cambell, *Introduction to Synthetic Polymers*, Oxford University Press, 2000.
10. IUPAC, *Pure Appl. Chem.*, 1976, **48**, 373-386.
11. E. S. Wilks, *Macromolecular Nomenclature Note No. 18*,
www.polyacs.org/uploaded/files/mnn18.pdf.
12. H.-J. W. H-W. Engels, M. Pieroth, W. Hofmann, K-H. Menting, T. Mergenhagen, R. Schmoll, S. Uhrlandt, *Ullmann's Encyclopedia of Industrial Chemistry 2004*, Wiley-VCH.
13. W. F. Busse and R. Longworth, *Journal of Polymer Science*, 1962, **58**, 49-69.
14. J. D. Ferry, *Viscoelastic Properties of Polymers*, Wiley, New York, 1980.
15. D. Astruc, E. Boisselier and C. Ornelas, *Chemical Reviews*, 2010, **110**, 1857-1959.
16. F. Wiesbrock, R. Hoogenboom, M. A. M. Leenen, M. A. R. Meier and U. S. Schubert, *Macromolecules*, 2005, **38**, 5025-5034.
17. T. P. D. Krzysztof Matyjaszewski, *Handbook of Radical Polymerization*, Wiley.
18. J. You, G. Li and Z. Wang, *Organic & Biomolecular Chemistry*, 2012, **10**, 9481-9490.
19. J. M. G. A. Cowie, V., *Polymers: Chemistry and Physics of Modern Materials*, CRC Press, 2008.
20. M. E. L. Rogers, T. E. Turners, S. R., *Synthetic methods in step-growth polymers*, Wiley-Interscience.
21. R. J. Y. C. Hall, *Introduction to Polymers*, 1987.
22. R. Grubbs and W. Tumas, *Science*, 1989, **243**, 907-915.
23. O. W. Webster, *Science*, 1991, 8877.
24. M. Krzysztof, *Current Opinion in Solid State and Materials Science*, 1996, **1**, 769-776.
25. T. E. Patten and K. Matyjaszewski, *Adv. Mater.*, 1998, **10**, 901-915.
26. D. Greszta, D. Mardare and K. Matyjaszewski, *Macromolecules*, 1994, **27**, 638-644.
27. R. P. N. Veregin, M. K. Georges, P. M. Kazmaier and G. K. Hamer, *Macromolecules*, 1993, **26**, 5316-5320.
28. A. Goto and T. Fukuda, *Progress in Polymer Science*, 2004, **29**, 329-385.
29. K. Matyjaszewski, *Macromolecules*, 1999, **32**, 9051-9053.
30. W. A. Braunecker and K. Matyjaszewski, *Progress in Polymer Science*, 2007, **32**, 93-146.
31. H. Fischer, *Chemical Reviews*, 2001, **101**, 3581-3610.
32. W. Tang, T. Fukuda and K. Matyjaszewski, *Macromolecules*, 2006, **39**, 4332-4337.
33. W. Tang, N. V. Tsarevsky and K. Matyjaszewski, *Journal of the American Chemical Society*, 2006, **128**, 1598-1604.
34. G. Odian, *Principles of Polymerisation*, Wiley-Interscience, 2004.
35. S. Penczek, M. Cypryk, A. Duda, P. Kubisa and S. Słomkowski, *Progress in Polymer Science*, 2007, **32**, 247-282.
36. S. Kobayashi and H. Uyama, *Journal of Polymer Science Part A: Polymer Chemistry*, 2002, **40**, 192-209.

37. M. Heskins and J. E. Guillet, *Journal of Macromolecular Science: Part A - Chemistry*, 1968, **2**, 1441-1455.
38. S. Cammas, K. Suzuki, C. Sone, Y. Sakurai, K. Kataoka and T. Okano, *J. Controlled Release*, 1997, **48**, 157-164.
39. J. E. Chung, M. Yokoyama, M. Yamato, T. Aoyagi, Y. Sakurai and T. Okano, *J. Controlled Release*, 1999, **62**, 115-127.
40. M. Kurisawa, M. Yokoyama and T. Okano, *J. Controlled Release*, 2000, **69**, 127-137.
41. N. Takeda, E. Nakamura, M. Yokoyama and T. Okano, *J. Controlled Release*, 2004, **95**, 343-355.
42. M. Matsukata, T. Aoki, K. Sanui, N. Ogata, A. Kikuchi, Y. Sakurai and T. Okano, *Bioconjugate Chemistry*, 1996, **7**, 96-101.
43. A. Chilkoti, G. Chen, P. S. Stayton and A. S. Hoffman, *Bioconjugate Chemistry*, 1994, **5**, 504-507.
44. C. Yu, S. Mutlu, P. Selvaganapathy, C. H. Mastrangelo, F. Svec and J. M. J. Fréchet, *Analytical Chemistry*, 2003, **75**, 1958-1961.
45. R. Pelton, *Adv. Colloid Interface Sci.*, 2000, **85**, 1-33.
46. R. M. P. da Silva, J. F. Mano and R. L. Reis, *Trends Biotechnol.*, 2007, **25**, 577-583.
47. M. A. Cooperstein and H. E. Canavan, *Langmuir*, 2009, **26**, 7695-7707.
48. K. Nagase, J. Kobayashi and T. Okano, *Journal of The Royal Society Interface*, 2009, **6**, S293-S309.
49. H. G. Schild, *Progress in Polymer Science*, 1992, **17**, 163-249.
50. Z. M. O. Rzaev, S. Dinçer and E. Piskin, *Progress in Polymer Science*, 2007, **32**, 534-595.
51. R. Liu, P. De Leonardis, F. Celliesi, N. Tirelli and B. R. Saunders, *Langmuir*, 2008, **24**, 7099-7106.
52. G. Masci, M. Diociaiuti and V. Crescenzi, *Journal of Polymer Science Part A: Polymer Chemistry*, 2008, **46**, 4830-4842.
53. R. N. Zuckermann, J. M. Kerr, S. B. H. Kent and W. H. Moos, *Journal of the American Chemical Society*, 1992, **114**, 10646-10647.
54. M. Sisido, Y. Imanishi and T. Higashimura, *Die Makromolekulare Chemie*, 1977, **178**, 3107-3114.
55. H. R. Kricheldorf, C. von Lossow and G. Schwarz, *Macromolecular Chemistry and Physics*, 2004, **205**, 918-924.
56. J. Chai, G. Liu, K. Chaicharoen, C. Wesdemiotis and L. Jia, *Macromolecules*, 2008, **41**, 8980-8985.
57. L. Jia, H. Sun, J. T. Shay, A. M. Allgeier and S. D. Hanton, *Journal of the American Chemical Society*, 2002, **124**, 7282-7283.
58. H. Sun, J. Zhang, Q. Liu, L. Yu and J. Zhao, *Angewandte Chemie International Edition*, 2007, **46**, 6068-6072.
59. D. Zhang, S. H. Lahasky, L. Guo, C.-U. Lee and M. Lavan, *Macromolecules*, 2012, **45**, 5833-5841.
60. M. C. Woodle, C. M. Engbers and S. Zalipsky, *Bioconjugate Chemistry*, 1994, **5**, 493-496.
61. S. Zalipsky, C. B. Hansen, J. M. Oaks and T. M. Allen, *J. Pharm. Sci.*, 1996, **85**, 133-137.
62. F. Wiesbrock, R. Hoogenboom, C. H. Abeln and U. S. Schubert, *Macromolecular Rapid Communications*, 2004, **25**, 1895-1899.
63. V. de la Rosa, *J. Mater. Sci.: Mater. Med.*, 2014, **25**, 1211-1225.
64. A. Levy and M. Litt, *Journal of Polymer Science Part B: Polymer Letters*, 1967, **5**, 881-886.
65. T. Kagiya, S. Narisawa, T. Maeda and K. Fukui, *Journal of Polymer Science Part B: Polymer Letters*, 1966, **4**, 441-445.
66. W. Seeliger, E. Aufderhaar, W. Diepers, R. Feinauer, R. Nehring, W. Thier and H. Hellmann, *Angewandte Chemie*, 1966, **78**, 913-927.
67. D. A. Tomalia and D. P. Sheetz, *Journal of Polymer Science Part A-1: Polymer Chemistry*, 1966, **4**, 2253-2265.
68. K. Aoi and M. Okada, *Progress in Polymer Science*, 1996, **21**, 151-208.

69. R. Hoogenboom, M. W. M. Fijten, R. M. Paulus, H. M. L. Thijs, S. Hoepfener, G. Kickelbick and U. S. Schubert, *Polymer*, 2006, **47**, 75-84.
70. R. Hoogenboom, H. M. L. Lambermont-Thijs, M. J. H. C. Jochems, S. Hoepfener, C. Guerlain, C.-A. Fustin, J.-F. Gohy and U. S. Schubert, *Soft Matter*, 2009, **5**, 3590.
71. C. Diehl and H. Schlaad, *Macromolecular Bioscience*, 2009, **9**, 157-161.
72. R. Obeid, F. Tanaka and F. M. Winnik, *Macromolecules (Washington, DC, U. S.)*, 2009, **42**, 5818-5828.
73. R. Weberskirch, J. Preuschen, H. W. Spiess and O. Nuyken, *Macromolecular Chemistry and Physics*, 2000, **201**, 995-1007.
74. R. Obeid, E. Maltseva, A. F. Thunemann, F. Tanaka and F. M. Winnik, *Macromolecules (Washington, DC, U. S.)*, 2009, **42**, 2204-2214.
75. G. Volet, V. Chanthavong, V. Wintgens and C. Amiel, *Macromolecules*, 2005, **38**, 5190-5197.
76. R. Jordan, K. Martin, H. J. Räder and K. K. Unger, *Macromolecules*, 2001, **34**, 8858-8865.
77. M. W. M. Fijten, C. Haensch, B. M. van Lankvelt, R. Hoogenboom and U. S. Schubert, *Macromolecular Chemistry and Physics*, 2008, **209**, 1887-1895.
78. S. Huber, N. Hutter and R. Jordan, *Colloid Polym. Sci.*, 2008, **286**, 1653-1661.
79. J.-S. Park, Y. Akiyama, Y. Yamasaki and K. Kataoka, *Langmuir*, 2007, **23**, 138-146.
80. R. Luxenhofer, G. Sahay, A. Schulz, D. Alakhova, T. K. Bronich, R. Jordan and A. V. Kabanov, *J. Controlled Release*, 2011, **153**, 73-82.
81. M. Miyamoto, K. Naka, M. Tokumizu and T. Saegusa, *Macromolecules*, 1989, **22**, 1604-1607.
82. R. Weberskirch and O. Nuyken, *Journal of Macromolecular Science, Part A*, 1999, **36**, 843-857.
83. K. Kempe, A. Vollrath, H. W. Schaefer, T. G. Poehlmann, C. Biskup, R. Hoogenboom, S. Hornig and U. S. Schubert, *Macromolecular Rapid Communications*, 2010, **31**, 1869-1873.
84. J.-S. Park, Y. Akiyama, F. M. Winnik and K. Kataoka, *Macromolecules*, 2004, **37**, 6786-6792.
85. B. Ilkgul, D. Gunes, O. Sirkecioglu and N. Bıcak, *Tetrahedron Letters*, 2010, **51**, 5313-5315.
86. K. Hioki, Y. Takechi, N. Kimura, H. Tanaka and M. Kunishima, *Chem. Pharm. Bull.*, 2008, **56**, 1735-1737.
87. K. Kempe, M. Lobert, R. Hoogenboom and U. S. Schubert, *J. Comb. Chem.*, 2009, **11**, 274-280.
88. I. Mohammadpoor-Baltork, M. Moghadam, S. Tangestaninejad, V. Mirkhani and S. F. Hojati, *Catal. Commun.*, 2008, **9**, 1153-1161.
89. P. Zhou, J. E. Blubaum, C. T. Burns and N. R. Natale, *Tetrahedron Letters*, 1997, **38**, 7019-7020.
90. Q. Xu and Z. Li, *Tetrahedron Letters*, 2009, **50**, 6838-6840.
91. A. J. Phillips, Y. Uto, P. Wipf, M. J. Reno and D. R. Williams, *Org. Lett.*, 2000, **2**, 1165-1168.
92. B. P. Bandgar and S. S. Pandit, *Tetrahedron Letters*, 2003, **44**, 2331-2333.
93. A. Cevallos, R. Rios, A. Moyano*, M. A. Pericàs and A. Riera, *Tetrahedron: Asymmetry*, 2000, **11**, 4407-4416.
94. C. O. Kangani and B. W. Day, *Tetrahedron Letters*, 2009, **50**, 5332-5335.
95. T. Saegusa, *Pure Appl. Chem.*, 1974, **39**, 81-97.
96. B. Pidhatika, J. Möller, V. Vogel and R. Konradi, *CHIMIA International Journal for Chemistry*, 2008, **62**, 264-269.
97. R. Konradi, B. Pidhatika, A. Mühlebach and M. Textor, *Langmuir*, 2008, **24**, 613-616.
98. B. Pidhatika, J. Möller, E. M. Benetti, R. Konradi, E. Rakhmatullina, A. Mühlebach, R. Zimmermann, C. Werner, V. Vogel and M. Textor, *Biomaterials*, 2010, **31**, 9462-9472.
99. B. Pidhatika, M. Rodenstein, Y. Chen, E. Rakhmatullina, A. Mühlebach, C. Acikgöz, M. Textor and R. Konradi, *Biointerphases*, 2012, **7**, -.
100. M. Barz, R. Luxenhofer, R. Zentel and M. J. Vicent, *Polymer Chemistry*, 2011, **2**, 1900-1918.

101. K. Knop, R. Hoogenboom, D. Fischer and U. S. Schubert, *Angewandte Chemie International Edition*, 2010, **49**, 6288-6308.
102. B. Balakrishnan, D. S. Kumar, Y. Yoshida and A. Jayakrishnan, *Biomaterials*, 2005, **26**, 3495-3502.
103. <http://www.inchem.org/documents/jecfa/jecmono/v14je19.htm>.
104. C. Assal and P. Y. Watson, *Gastrointestinal Endoscopy*, 2006, **64**, 294-295.
105. N. Stollman and H. D. Manten, *Gastrointestinal Endoscopy*, 1996, **44**, 209-210.
106. E. Brullet, A. Moron, X. Calvet, C. Frias and J. Sola, *Gastrointestinal Endoscopy*, 1992, **38**, 400-401.
107. E. Schuman and P. E. Balsam, *Gastrointestinal Endoscopy*, 1991, **37**, 411.
108. M. Ito, D. Watanabe, M. Kobayashi, Y. Tamada and Y. Matsumoto, *Contact Dermatitis*, 2006, **54**, 225-225.
109. A. A. Fisher, *Contact Dermatitis*, 1978, **4**, 135-138.
110. E. T. M. Dams, P. Laverman, W. J. G. Oyen, G. Storm, G. L. Scherphof, J. W. M. van der Meer, F. H. M. Corstens and O. C. Boerman, *J. Pharmacol. Exp. Ther.*, 2000, **292**, 1071-1079.
111. T. Ishida, R. Maeda, M. Ichihara, K. Irimura and H. Kiwada, *J. Controlled Release*, 2003, **88**, 35-42.
112. D. A. Herold, K. Keil and D. E. Bruns, *Biochem. Pharmacol.*, 1989, **38**, 73-76.
113. B. Romberg, J. M. Metselaar, L. Baranyi, C. J. Snel, R. B  nger, W. E. Hennink, J. Szebeni and G. Storm, *International Journal of Pharmaceutics*, 2007, **331**, 186-189.
114. T. Aarthi, M. S. Shaama and G. Madras, *Ind. Eng. Chem. Res.*, 2007, **46**, 6204-6210.
115. S. Morlat and J.-L. Gardette, *Polymer*, 2001, **42**, 6071-6079.
116. A. M. Afifi-Effat and J. N. Hay, *Eur. Polym. J.*, 1972, **8**, 289-297.
117. S. Han, C. Kim and D. Kwon, *Polymer*, 1997, **38**, 317-323.
118. T. G. Papaioannou, E. N. Karatzis, M. Vavuranakis, J. P. Lekakis and C. Stefanadis, *International Journal of Cardiology*, 2006, **113**, 12-18.
119. X. Zhang and S. Granick, *Macromolecules*, 2002, **35**, 4017-4022.
120. F. C. Gaertner, R. Luxenhofer, B. Blechert, R. Jordan and M. Essler, *Journal of controlled release : official journal of the Controlled Release Society*, 2007, **119**, 291-300.
121. C.-H. Wang, K.-R. Fan and G.-H. Hsiue, *Biomaterials*, 2005, **26**, 2803-2811.
122. C.-H. Wang, C.-H. Wang and G.-H. Hsiue, *J. Controlled Release*, 2005, **108**, 140-149.
123. S. Cheon Lee, C. Kim, I. Chan Kwon, H. Chung and S. Young Jeong, *J. Controlled Release*, 2003, **89**, 437-446.
124. A. Mero, G. Pasut, L. D. Via, M. W. M. Fijten, U. S. Schubert, R. Hoogenboom and F. M. Veronese, *J. Controlled Release*, 2008, **125**, 87-95.
125. I. Dimitrov, B. Trzebicka, A. H. E. M  ller, A. Dworak and C. B. Tsvetanov, *Progress in Polymer Science*, 2007, **32**, 1275-1343.
126. Y. Tachibana, M. Kurisawa, H. Uyama, T. Kakuchi and S. Kobayashi, *Chem. Commun.*, 2003, 106-107.
127. C. Zhang, L. Liao and S. Gong, *Macromolecular Chemistry and Physics*, 2007, **208**, 1122-1128.
128. E. Watanabe and N. Tomoshige, *Chemistry Letters*, 2005, **34**, 876-877.
129. Y. Iwasaki, C. Wachiralarpphaithoon and K. Akiyoshi, *Macromolecules*, 2007, **40**, 8136-8138.
130. H. Uyama and S. Kobayashi, *Chem. Lett.*, 1992, 1643-1646.
131. C. Diab, Y. Akiyama, K. Kataoka and F. M. Winnik, *Macromolecules*, 2004, **37**, 2556-2562.
132. J.-S. Park and K. Kataoka, *Macromolecules (Washington, DC, U. S.)*, 2007, **40**, 3599-3609.
133. J.-S. Park and K. Kataoka, *Macromolecules*, 2006, **39**, 6622-6630.
134. P. Lin, C. Clash, E. M. Pearce, T. K. Kwei and M. A. Aponte, *Journal of Polymer Science Part B: Polymer Physics*, 1988, **26**, 603-619.
135. D. Christova, R. Velichkova, W. Loos, E. J. Goethals and F. D. Prez, *Polymer*, 2003, **44**, 2255-2261.
136. P. Bawa, V. Pillay, Y. E. Choonara and L. C. du Toit, *Biomed. Mater.*, 2009, **4**, 022001.

137. P. Goddard, L. E. Hutchinson, J. Brown and L. J. Brookman, *J. Controlled Release*, 1989, **10**, 5-16.
138. P.-F. Caponi, X.-P. Qiu, F. Vilela, F. M. Winnik and R. V. Ulijn, *Polymer Chemistry*, 2011, **2**, 306.
139. O. Sedlacek, B. D. Monnery, S. K. Filippov, R. Hoogenboom and M. Hruby, *Macromolecular Rapid Communications*, 2012, **33**, 1648-1662.
140. H. Witte and W. Seeliger, *Justus Liebigs Annalen der Chemie*, 1974, **1974**, 996-1009.
141. S. Cesana, J. Auernheimer, R. Jordan, H. Kessler and O. Nuyken, *Macromolecular Chemistry and Physics*, 2006, **207**, 183-192.
142. M. T. Zarka, O. Nuyken and R. Weberskirch, *Chemistry – A European Journal*, 2003, **9**, 3228-3234.
143. S. Cesana, A. Kurek, M. A. Baur, J. Auernheimer and O. Nuyken, *Macromolecular Rapid Communications*, 2007, **28**, 608-615.
144. A. Gress, A. Völkel and H. Schlaad, *Macromolecules*, 2007, **40**, 7928-7933.
145. A. C. s. Biraboneye, S. b. Madonna, Y. Laras, S. Krantic, P. Maher and J.-L. Kraus, *Journal of Medicinal Chemistry*, 2009, **52**, 4358-4369.
146. M. A. Cortez and S. M. Grayson, *Macromolecules*, 2010, **43**, 4081-4090.
147. K. Kempe, R. Hoogenboom, M. Jaeger and U. S. Schubert, *Macromolecules*, 2011, **44**, 6424-6432.
148. R. Hoogenboom and U. S. Schubert, *Macromolecular Rapid Communications*, 2007, **28**, 368-386.
149. K. Kempe, C. R. Becer and U. S. Schubert, *Macromolecules*, 2011, **44**, 5825-5842.
150. R. Luxenhofer, A. Schulz, C. Roques, S. Li, T. K. Bronich, E. V. Batrakova, R. Jordan and A. V. Kabanov, *Biomaterials*, 2010, **31**, 4972-4979.
151. J. Tong, R. Luxenhofer, X. Yi, R. Jordan and A. V. Kabanov, *Mol. Pharm.*, 2010, **7**, 984-992.
152. F. Yuen and K. C. Tam, *Soft Matter*, 2010, **6**, 4613-4630.
153. G. Pereira, C. Huin, S. Morariu, V. Bennevault-Celton and P. Guégan, *Aust. J. Chem.*, 2012, **65**, 1145-1155.
154. C. J. Waschinski and J. C. Tiller, *Biomacromolecules*, 2004, **6**, 235-243.
155. R. Hoogenboom, H. M. L. Lambermont-Thijs, M. J. H. C. Jochems, S. Hoeppener, C. Guerlain, C.-A. Fustin, J.-F. Gohy and U. S. Schubert, *Soft Matter*, 2009, **5**, 3590-3592.
156. S. Halacheva, G. J. Price and V. M. Garamus, *Macromolecules*, 2011, **44**, 7394-7404.
157. V. V. Jerca, F. A. Nicolescu, R. Trusca, E. Vasile, A. Baran, D. F. Anghel, D. S. Vasilescu and D. M. Vuluga, *Reactive and Functional Polymers*, 2011, **71**, 373-379.
158. R. Takahashi, T. Sato, K. Terao, X.-P. Qiu and F. M. Winnik, *Macromolecules*, 2012, **45**, 6111-6119.
159. H. M. L. Lambermont-Thijs, J. P. A. Heuts, S. Hoeppener, R. Hoogenboom and U. S. Schubert, *Polymer Chemistry*, 2011, **2**, 313.
160. M. M. Bloksma, C. Weber, I. Y. Perevyazko, A. Kuse, A. Baumgärtel, A. Vollrath, R. Hoogenboom and U. S. Schubert, *Macromolecules*, 2011, **44**, 4057-4064.
161. G.-H. Hsiue, C.-H. Wang, C.-L. Lo, C.-H. Wang, J.-P. Li and J.-L. Yang, *International Journal of Pharmaceutics*, 2006, **317**, 69-75.
162. P.-F. Caponi and R. V. Ulijn, *Polymers*, 2012, **4**, 1399-1415.
163. T. Karstens and K. Kobs, *The Journal of Physical Chemistry*, 1980, **84**, 1871-1872.
164. B.-J. Chang, O. Prucker, E. Groh, A. Wallrath, M. Dahm and J. Rühle, *Colloids and Surfaces A: Physicochemical and Engineering Aspects*, 2002, **198-200**, 519-526.
165. M. Agrawal, J. C. Rueda, P. Uhlmann, M. Müller, F. Simon and M. Stamm, *ACS Applied Materials & Interfaces*, 2012, **4**, 1357-1364.
166. R. Jordan, K. Graf, H. Riegler and K. K. Unger, *Chem. Commun.*, 1996, **0**, 1025-1026.
167. R. Jordan and A. Ulman, *Journal of the American Chemical Society*, 1998, **120**, 243-247.
168. I. Elloumi-Hannachi, M. Yamato and T. Okano, *J. Intern. Med.*, 2010, **267**, 54-70.
169. T. Takezawa, Y. Mori and K. Yoshizato, *Nat Biotech*, 1990, **8**, 854-856.
170. N. Yamada, T. Okano, H. Sakai, F. Karikusa, Y. Sawasaki and Y. Sakurai, *Die Makromolekulare Chemie, Rapid Communications*, 1990, **11**, 571-576.

171. M. C. Morra, C., *Surface Modification of Polymeric Biomaterials*, Plenum Press, 1997.
172. Nunc, <http://www.sigmaaldrich.com/labware/labware-products.html?TablePage=103658786>.
173. H. E. Canavan, X. Cheng, D. J. Graham, B. D. Ratner and D. G. Castner, *Journal of Biomedical Materials Research Part A*, 2005, **75A**, 1-13.
174. H. E. Canavan, X. Cheng, D. J. Graham, B. D. Ratner and D. G. Castner, *Langmuir*, 2004, **21**, 1949-1955.
175. Y. V. Pan, R. A. Wesley, R. Luginbuhl, D. D. Denton and B. D. Ratner, *Biomacromolecules*, 2000, **2**, 32-36.
176. Y. G. Takei, T. Aoki, K. Sanui, N. Ogata, Y. Sakurai and T. Okano, *Macromolecules*, 1994, **27**, 6163-6166.
177. Y. G. Takei, T. Aoki, K. Sanui, N. Ogata, T. Okano and Y. Sakurai, *Bioconjugate Chemistry*, 1993, **4**, 42-46.
178. S. Kidoaki, S. Ohya, Y. Nakayama and T. Matsuda, *Langmuir*, 2001, **17**, 2402-2407.
179. T. Yakushiji, K. Sakai, A. Kikuchi, T. Aoyagi, Y. Sakurai and T. Okano, *Langmuir*, 1998, **14**, 4657-4662.
180. T. Yakushiji, K. Sakai, A. Kikuchi, T. Aoyagi, Y. Sakurai and T. Okano, *Analytical Chemistry*, 1999, **71**, 1125-1130.
181. A. Mizutani, A. Kikuchi, M. Yamato, H. Kanazawa and T. Okano, *Biomaterials*, 2008, **29**, 2073-2081.
182. N. Idota, A. Kikuchi, J. Kobayashi, Y. Akiyama, K. Sakai and T. Okano, *Langmuir*, 2005, **22**, 425-430.
183. M. A. Cooperstein and H. E. Canavan, *Langmuir*, 2010, **26**, 7695-7707.
184. M. Cole, N. Voelcker, H. Thissen and H. Griesser, *Biomaterials*, 2009, **30**, 1827-1850.
185. M. Yamato, M. Okuhara, F. Karikusa, A. Kikuchi, Y. Sakurai and T. Okano, *Journal of Biomedical Materials Research*, 1999, **44**, 44-52.
186. K. Fukumori, Y. Akiyama, Y. Kumashiro, J. Kobayashi, M. Yamato, K. Sakai and T. Okano, *Macromolecular Bioscience*, 2010, **10**, 1117-1129.
187. N. Zhang, T. Pompe, I. Amin, R. Luxenhofer, C. Werner and R. Jordan, *Macromolecular Bioscience*, 2012, **12**, 926-936.
188. F. Rehfeldt, M. Tanaka, L. Pagnoni and R. Jordan, *Langmuir*, 2002, **18**, 4908-4914.
189. C. Perruchot, M. M. Chehimi, M. Delamar, E. Cabot-Deliry, B. Miksa, S. Slomkowski, M. A. Khan and S. P. Armes, *Colloid Polym Sci*, 2000, **278**, 1139-1154.
190. S. Noel, B. Liberelle, L. Robitaille and G. De Crescenzo, *Bioconjugate Chemistry*, 2011, **22**, 1690-1699.
191. H. J. Martin, K. H. Schulz, J. D. Bumgardner and K. B. Walters, *Langmuir*, 2007, **23**, 6645-6651.
192. C. Jaime, J. Redondo, F. Sánchez-Ferrando and A. Virgili, *J. Mol. Struct.*, 1991, **248**, 317-329.
193. Y. Zhu, Z. Mao, H. Shi and C. Gao, *Sci. China Chem.*, 2012, **55**, 2419-2427.
194. T. I. Croll, A. J. O'Connor, G. W. Stevens and J. J. Cooper-White, *Biomacromolecules*, 2004, **5**, 463-473.
195. S. Noel, B. Liberelle, A. Yogi, M. J. Moreno, M. N. Bureau, L. Robitaille and G. De Crescenzo, *Journal of Materials Chemistry B*, 2013, **1**, 230-238.
196. K. Mlinarić-Majerski and T. Šumanovac Ramljak, *Tetrahedron*, 2002, **58**, 4893-4898.
197. M. Řezanka, B. Eignerová, J. Jindřich and M. Katora, *Eur. J. Org. Chem.*, 2010, **2010**, 6256-6262.
198. Z. Yang, Y. Chevolot, T. Géhin, V. Dugas, N. Xanthopoulos, V. Laporte, T. Delair, Y. Ataman-Önal, G. Choquet-Kastylevsky, E. Souteyrand and E. Laurenceau, *Langmuir*, 2013, **29**, 1498-1509.
199. S. Qin, Y. Geng, D. E. Discher and S. Yang, *Adv. Mater.*, 2006, **18**, 2905-2909.
200. S. P. Martin, R. J. Townsend, L. A. Kuznetsova, K. A. J. Borthwick, M. Hill, M. B. McDonnell and W. T. Coakley, *Biosensors and Bioelectronics*, 2005, **21**, 758-767.
201. K. Almdal, J. Dyre, S. Hvidt and O. Kramer, *Polymer Gels and Networks*, 1993, **1**, 5-17.

202. S.-k. Ahn, R. M. Kasi, S.-C. Kim, N. Sharma and Y. Zhou, *Soft Matter*, 2008, **4**, 1151-1157.
203. Y. Osada, J. Ping Gong and Y. Tanaka, *J. Macromol. Sci., Polym. Rev.*, 2004, **44**, 87-112.
204. A. S. Hoffman, *Adv. Drug Delivery Rev.*, 2002, **54**, 3-12.
205. T. Kissel, Y. Li and F. Unger, *Adv. Drug Delivery Rev.*, 2002, **54**, 99-134.
206. Y. Zhang, W. Zhu, B. Wang and J. Ding, *J. Controlled Release*, 2005, **105**, 260-268.
207. S. V. Graeter, J. Huang, N. Perschmann, M. López-García, H. Kessler, J. Ding and J. P. Spatz, *Nano Lett.*, 2007, **7**, 1413-1418.
208. L. E. Bromberg and E. S. Ron, *Adv. Drug Delivery Rev.*, 1998, **31**, 197-221.
209. P. J. Flory, *Principles of Polymer Chemistry*, 15th edn., Cornell University Press, 1992.
210. A. Silberberg, in *Polymers in Aqueous Media. Performance Through Association*, American Chemical Society, Washington, Editon edn., 1989.
211. C. Mangold, B. Obermeier, F. Wurm and H. Frey, *Macromolecular Rapid Communications*, 2011, **32**, 1930-1934.
212. J. L. J.Y. Cho, A. Gutowska, B.J. Tarasevich, Y.S. Sohn, B. Jeong, *J. Drug Del. Sci. Tech*, 2006, **16**, 71-76.
213. J. F. Pollock and K. E. Healy, *Acta Biomaterialia*, 2010, **6**, 1307-1318.
214. N. Beheshti, K. Zhu, A.-L. Kjoniksen, K. D. Knudsen and B. Nystrom, *Soft Matter*, 2011, **7**, 1168-1175.
215. E. Siband, Y. Tran and D. Hourdet, *Macromolecules*, 2011, **44**, 8185-8194.
216. J. C. Garbern, A. S. Hoffman and P. S. Stayton, *Biomacromolecules*, 2010, **11**, 1833-1839.
217. X. Yin, A. S. Hoffman and P. S. Stayton, *Biomacromolecules*, 2006, **7**, 1381-1385.
218. R. Liu, F. Cellesi, N. Tirelli and B. R. Saunders, *Polymer*, 2009, **50**, 1456-1462.
219. V. Bütün, S. P. Armes and N. C. Billingham, *Polymer*, 2001, **42**, 5993-6008.
220. T. Vermonden, N. A. M. Besseling, M. J. van Steenbergen and W. E. Hennink, *Langmuir*, 2006, **22**, 10180-10184.
221. Z. Cui, B. H. Lee, C. Pauken and B. L. Vernon, *Journal of Biomedical Materials Research Part A*, 2011, **98A**, 159-166.
222. Z. Li, X. Guo, S. Matsushita and J. Guan, *Biomaterials*, 2011, **32**, 3220-3232.
223. D. J. Overstreet, H. D. Dhruv and B. L. Vernon, *Biomacromolecules*, 2010, **11**, 1154-1159.
224. Z. Ma, D. M. Nelson, Y. Hong and W. R. Wagner, *Biomacromolecules*, 2010, **11**, 1873-1881.
225. K. L. Fujimoto, Z. Ma, D. M. Nelson, R. Hashizume, J. Guan, K. Tobita and W. R. Wagner, *Biomaterials*, 2009, **30**, 4357-4368.
226. T. G. Mezger.
227. J.-P. Chen and T.-H. Cheng, *Polymer*, 2009, **50**, 107-116.
228. S. Lü, M. Liu and B. Ni, *Chem. Eng. J.*, 2011, **173**, 241-250.
229. C. He, S. W. Kim and D. S. Lee, *J. Controlled Release*, 2008, **127**, 189-207.
230. L. Yu and J. Ding, *Chemical Society Reviews*, 2008, **37**, 1473-1481.
231. W. S. Shim, J. S. Yoo, Y. H. Bae and D. S. Lee, *Biomacromolecules*, 2005, **6**, 2930-2934.
232. P. Alexandridis and T. Alan Hatton, *Colloids and Surfaces A: Physicochemical and Engineering Aspects*, 1995, **96**, 1-46.
233. Z. Ge, Y. Zhou, Z. Tong and S. Liu, *Langmuir*, 2011, **27**, 1143-1151.
234. M. D. C. Topp, P. J. Dijkstra, H. Talsma and J. Feijen, *Macromolecules*, 1997, **30**, 8518-8520.
235. Kruss website, <http://www.kruss.de/products/contact-angle/dsa100/drop-shape-analyzer-dsa100/>.
236. ImageJ website, <http://imagej.nih.gov/ij/>.
237. Shimadzu website, <http://www.shimadzu.com/an/spectro/uv/index.html>.
238. ACD labs website, <http://www.acdlabs.com/>.
239. Leica website, <http://www.leica-microsystems.com/products/microscope-software/software-for-life-science-research/las-x/>.
240. M. B. Doughty, C. S. Chaurasia and K. Li, *Journal of Medicinal Chemistry*, 1993, **36**, 272-279.

241. S. Kitamura, H. Fukushi, T. Miyawaki, M. Kawamura, N. Konishi, Z.-i. Terashita and T. Naka, *Journal of Medicinal Chemistry*, 2001, **44**, 2438-2450.
242. Y. Song, A. Goel, V. Basrur, P. E. A. Roberts, J. A. Mikovits, J. K. Inman, J. A. Turpin, W. G. Rice and E. Appella, *Bioorg. Med. Chem.*, 2002, **10**, 1263-1273.
243. N. Gavande, H.-L. Kim, M. R. Doddareddy, G. A. R. Johnston, M. Chebib and J. R. Hanrahan, *ACS Medicinal Chemistry Letters*, 2013, **4**, 402-407.
244. S.-K. Choi, M. Mammen and G. M. Whitesides, *Journal of the American Chemical Society*, 1997, **119**, 4103-4111.